DISSERTATION

ALTERNATIVE METRICS FOR MEASURING HEATING TRENDS, WITH POSSIBLE CONNECTIONS BETWEEN THE SURFACE AND TROPOSPHERE

Submitted by

Christopher A. Davey

Graduate Degree Program in Ecology

In partial fulfillment of the requirements

For the Degree of Doctor of Philosophy

Colorado State University

Fort Collins, Colorado

Spring, 2005

COLORADO STATE UNIVERSITY

January 18, 2005

WE HEREBY RECOMMEND THAT THE **DISSERTATION** PREPARED UNDER OUR SUPERVISION BY CHRISTOPHER A. DAVEY ENTITLED ALTERNATIVE METRICS FOR MEASURING HEATING TRENDS, WITH POSSIBLE CONNECTIONS BETWEEN THE SURFACE AND TROPOSPHERE BE ACCEPTED AS FULFULLING IN PART REQUIREMENTS FOR THE DEGREE OF DOCTOR OF PHILOSOPHY

Committee on Graduate Work

Dr. Thomas J. Stohlgren

Dr Dennis S. Ojima

Dr. Richard H. Johnson

Dr. Roger A. Pielke, Sr., Advisor

Department Head/Director

ABSTRACT OF **DISSERTATION**

ALTERNATIVE METRICS FOR MEASURING HEATING TRENDS, WITH POSSIBLE CONNECTIONS BETWEEN THE SURFACE AND TROPOSPHERE

The term "global warming" has been used to describe the observed surface temperature increases during the last century. The proper use of this term, however, requires using surface heat content to monitor this aspect of the climate system. Surface observation site microclimates highlight the influence of land surface characteristics on surface heat trends. Exposure metadata should be improved. The real changes in heat content of the Earth's climate are not fully described by temperature alone. Moist enthalpy is more sensitive to surface vegetation properties and more accurately depicts surface heating than temperature. Monitoring trends in moist enthalpy, or equivalent temperature, could help explain the differences between previously observed temporal trends in surface and tropospheric temperatures. Surface heating trends have usually indicated warming with time, while tropospheric results have been mixed. Temperature and equivalent temperature trends from 1982-1997 are examined for sites in the eastern United States. Overall, surface trends show slight cooling in temperatures and slight warming in equivalent temperatures. Surface equivalent temperature trends are generally smaller in magnitude than temperature trends. Seasonally, surface trends show the most

warming in winter and the most cooling in fall. Equivalent temperature trends during the winter and fall are generally identical in sign to, and larger than, temperature trends, but opposite in sign during the spring and summer. Trend patterns vary widely, however, between individual sites. Local land cover has a large influence on heating trends. Urban sites show more warming, or less cooling, than rural sites. Tropospheric temperature and thickness trends for radiosonde data and collocated reanalysis data are examined from 1979-2001. Radiosondes compare favorably to reanalysis data. The upper troposphere indicates cooling, while the lower troposphere is neutral or slightly warming. Comparisons of tropospheric and surface trends for the eastern United States show similar seasonal patterns. Lower-tropospheric trends in the eastern United States show some cooling in the fall, providing a possible connection between the surface and troposphere. Continued work with alternative heating metrics will increase understanding of microclimate influences and surface-troposphere connections.

Christopher Aaron Davey
Graduate Degree Program in Ecology
Colorado State University
Fort Collins, CO 80523
Spring 2005

ACKNOWLEDGEMENTS

First of all, I can't give enough thanks to my Lord Jesus Christ for providing me this opportunity in the first place, and the endurance to finish! Many thanks to my advisor, Dr. Roger A. Pielke, Sr., and committee members, Drs. Dennis S. Ojima, Thomas J. Stohlgren, and Richard H. Johnson. I would like to thank Dr. Thomas Chase and his CIRES staff at the University of Colorado - Boulder, particularly Eungul Lee, for their assistance in obtaining NCEP reanalysis data. My thanks to Drs. John Christy and Benjie Norris at University of Alabama in Huntsville for their extensive help with the CARDS radiosonde dataset. Dave Swartz, thanks for the opportunity to interact with and help teach your science classes at Rocky Mountain High School for the past three years. It was quite a learning experience! Thanks go to both Odie Bliss and Dallas Staley for their valuable manuscript assistance, along with my mother, Gretchen Davey, and my grandfather, Lewis Hatfield. This dissertation was supported under the NSF fellowship program entitled "Graduate Teaching Fellows in K-12 Education (GK-12)" (GKA01-0177), the Colorado Agricultural Experiment Station Project, and the NSF GLOBE project (GEO-0222578).

TABLE OF CONTENTS

CHAPTER 1

INTRODUCTION

There is currently much interest in the possibility of inadvertent climate change caused by anthropogenic influences, particularly with respect to air temperature. Estimates of global warming generally state that surface temperatures have risen by 0.3 - 0.6 °C over the past century (Hansen and Lebedeff, 1987; Jones, 1988; IPCC, 1990; Vinnikov et al., 1990; Jones, 1994b; IPCC, 1996; IPCC, 2001). Surface data have received much attention in most of these studies. However, even in light of the above findings, can it truly be said that full-scale global warming is occurring throughout the atmosphere?

To address this question, tropospheric temperature and thickness values are compared for 1979-2001 from radiosonde observations and collocated NCEP and ERA-40 reanalysis datasets, in an effort to determine what heating trends are occurring for the troposphere as a whole. We will also investigate, and attempt to better define, surface heating/cooling trends for the period 1982-1997. The surface analysis will focus not only on air temperature but also on the heat content of near-surface atmospheric moisture.

1.1 Troposphere

It is generally unclear what the climatic change signals in the troposphere *are* exactly. Some have argued that the signals of the troposphere and the surface are "at odds", in that the surface is indicating warming while the troposphere is not (Pielke, 1998; Bengtssen et al., 1999). This reported discrepancy could be expected, since the surface and the tropospheric layers are indeed physically different quantities (Hurrell et al., 2000). However, other sources (e.g. Hansen et al., 1995) argue that these two signals are not actually at odds. Because of instrument error, signal noise, and other biases, the surface and tropospheric signals may actually be comparable to each other.

There have been a wide range of studies investigating temperature trends in the troposphere. Observational studies have been conducted using satellite data sources (e.g. Spencer and Christy, 1990; Christy and Spencer, 1995; Christy et al., 2000; Christy et al., 2003; Mears et al., 2003) and radiosonde data sources (Angell, 1988; Oort and Liu, 1993; Parker et al., 1997; Angell, 2000; Gaffen et al., 2000b). There have also been significant efforts in this area using operational forecast model data (Pielke, 1998; Chase et al., 2000; Santer et al., 2003a). The combined results from these studies are unclear as to whether tropospheric heating trends indicate warming or cooling.

Satellites have been used for monitoring tropospheric and surface temperature trends over the past few decades. One satellite series in particular that has been heavily used for temperature trend analyses is the Microwave Sounding Unit (MSU) satellite series (e.g. Spencer and Christy, 1990; Christy and Spencer, 1995; Christy et al., 2000; Christy et al., 2003; Mears et al., 2003).

Initial studies (e.g. Spencer and Christy, 1990) indicated that the troposphere was cooling over time. These initial results have been brought into question, however, by various members of the research community. In particular, there likely are problems with the data caused in part by satellite orbit drift and instrumentation changes as old satellites cease to work and new satellites are launched to take their place (Hurrell and Trenberth, 1996; Hurrell and Trenberth, 1997; Hurrell and Trenberth, 1998). Contamination of tropospheric signals by the earth's surface could also be a factor.

Newer microwave products (e.g. Christy and Spencer, 1995; Christy et al., 2003; Vinnikov and Grody, 2003; Christy and Norris, 2004) have been developed in an attempt to correct for many of these cited problems. Subsequent studies using these new satellite datasets have indicated that tropospheric temperatures may in fact only be neutral or perhaps warming slightly over time (Christy and Spencer, 1995; Christy et al., 2000; Mears et al., 2003; Christy and Norris, 2004).

Most studies of tropospheric temperature trends using operational forecast model reanalyses such as the National Centers for Environmental Prediction (NCEP) Reanalysis product have indicated that there is no statistically significant warming going on in the troposphere (Pielke, 1998; Chase et al., 2000; Pielke et al., 2001b). Some recent work has claimed, however, that NCEP indicates a warming troposphere over the past few decades, as indicated by increases in tropopause heights (Santer et al., 2003a; Santer et al., 2003b). This phenomenon may be a model response, however, and not something that is reflected by actual observations (Pielke and Chase, 2004).

In fact, similar studies performed on radiosonde data have given mixed results, at best, regarding overall tropospheric heating trends (Angell, 1988; Oort and Liu, 1993;

Parker et al., 1997; Angell, 2000; Gaffen et al., 2000b). The use of radiosonde data is one of the other remaining sources, besides satellite and reanalysis data, for observational data in the free troposphere. Radiosonde data provides more detailed vertical resolution and a longer record than satellite data currently does (Free et al., 2002). Generally, these radiosonde studies have found obvious warming at the surface and cooling in the uppermost troposphere and stratosphere, but results from most of these studies have been mixed regarding the lower and middle troposphere.

Caution must be exercised in using radiosonde data, however. These data are known to suffer from numerous inhomogeneities. Some of these inhomogeneities are caused by changes in instrumentation and observational practices (Gaffen, 1994). Others can be attributed to various environmental factors such as solar heating (Luers and Eskridge, 1998). Fortunately, many of these problems are being addressed with newer radiosonde datasets that are now available. These datasets include the Comprehensive Aerological Reference Data Set (CARDS – Eskridge et al., 1995), administered by the National Climatic Data Center (NCDC) in Asheville, North Carolina, and the Geophysical Fluid Dynamics Laboratory (GFDL) dataset (Lanzante et al., 2003a; Lanzante et al., 2003b), maintained in Princeton, New Jersey.

In summary, most of the studies reviewed here make it clear that upper tropospheric/stratospheric cooling has been occurring over the past few decades, while temperature trends in the lower troposphere remain unclear. Although some studies (e.g. Santer et al., 2003a; Santer et al., 2003b) suggest that the lower troposphere is warming, other studies (e.g. Pielke 1998; Chase et al. 2000) show that the temperature trends in the lower troposphere are neutral. In light of this dilemma over temperature trends, this

dissertation looks also at temporal trends in tropospheric thickness, which provides a measure of layer-mean temperatures and therefore will help to show whether or not the troposphere, as a whole, is warming.

Comparison studies on tropospheric temperature trends have been done between satellite and reanalysis data (Pielke, 1998; Chase et al., 2000) and satellite and radiosonde data (Christy et al., 2000; Hurrell et al., 2000). As of yet, however, no studies have compared tropospheric temperature or thickness trends between reanalysis and radiosonde datasets. This study is one such attempt, comparing radiosonde trends and trends for both the NCEP reanalyses and the European Centre for Medium-Range Weather Forecasts (ECMWF) 40-year reanalysis product (ERA-40). Tropospheric trends for 1979-2001 are investigated. The time period was selected because previous studies have indicated that warming should become most evident during this time (e.g. Chase et al., 2000). This is also a time period where global observations through the full depth of the atmosphere have been the most reliable (Bengtssen et al., 1999). For the troposphere, it is expected that in all datasets, the upper troposphere has a significant cooling trend but the lower troposphere has no significant warming or cooling.

1.2 Surface

By itself, air temperature may not provide the best measure of actual climate warming or cooling. In fact, it is difficult to accurately diagnose global surface temperature trends. Climate responses are often highly regional in nature, with a high degree of spatial variation in the magnitudes of these responses (Chase et al., 2000).

Much attention has been given to surface temperature data because of

the length of record of the surface data and since the surface is where humans conduct most of their daily activities (Hurrell et al., 2000). Yet even the surface data record should be subject to question. How much should we trust it? Caution should be exercised when stating that global surface temperature trends indicate a certain level of warming (or cooling). For starters, it is likely that the impacts of any "global" surface temperature changes would be highly regional and spatially heterogeneous in nature, due in part to terrain and surface land cover characteristics (Chase et al., 2000). Also, in spite of some claims that the current global network is adequate for measuring global land-based surface temperature trends (Jones, 1995), there are still unresolved issues about data inhomogeneity, particularly with respect to instrument siting (see Chapter 2). Many of the surface observation sites have inherent problems with instrumentation biases and changes along with microclimate and site exposure effects (Karl et al., 1995; NRC, 1999) that must be addressed before any substantial claims can be made regarding global surface trends.

These issues surrounding site microclimates make it difficult to determine the full scope of long-term warming or cooling, based solely on surface temperature observations. Other means should be employed to monitor surface heating and its trends over the last few decades. This dissertation proposes an alternate way of assessing changes over time with surface heating. The proposed metric, called the "moist enthalpy", accounts for not only surface air temperature changes but also heating of atmospheric moisture. The "moist enthalpy" is defined as

$$H = C_p T + Lq\,, \tag{1.1}$$

where C_p is the specific heat of air at constant pressure, T is the measured air temperature, L is the latent heat of vaporization, and q is the specific humidity.

In order to derive H, we must first find an expression for q. The specific humidity, q, is defined as the mass of water vapor per unit mass of moist air (Rogers and Yau, 1989) and is, under most atmospheric conditions, approximately equal to the mixing ratio (mass of water vapor per unit mass of *dry* air):

$$q = w = \frac{M_v}{M_d} = \frac{\rho_v}{\rho_d}. \tag{1.2}$$

From the ideal gas law, $\rho_v = e/R_vT$ and $\rho_d = (p - e)/R'T$, where R' and R_v are the individual gas constants for dry air and water vapor, respectively, and e is the vapor pressure. Substituting these expressions into (1.2), we obtain

$$q = \frac{eR'}{(p-e)R_v} = 0.622\frac{e}{p-e} \approx 0.622\frac{e}{p}. \tag{1.3}$$

Before proceeding, however, an expression for e needs to be obtained. Assuming the relative humidity RH (in %) is known,

$$e = e_s\frac{RH}{100}. \tag{1.4}$$

To calculate e_s, one starts with the Clausius-Clapeyron equation describing the change in saturation vapor pressure with temperature over an air/water interface. This equation is given by

$$\frac{de_s}{dT} = \frac{L}{T(\alpha_2 - \alpha_1)}, \tag{1.5}$$

where e_s is the saturation vapor pressure and α is the specific volume

$$\alpha = \frac{R_vT}{e_s}. \tag{1.6}$$

Under most atmospheric conditions, $\alpha_2 \gg \alpha_1$, so that (1.5) reduces to

$$\frac{de_s}{dT} = \frac{L}{T\alpha_2} = \frac{Le_s}{R_v T^2} \tag{1.7}$$

and is then rearranged to yield

$$\frac{de_s}{e_s} = \frac{LdT}{R_v T^2}. \tag{1.8}$$

If L is assumed to be constant with temperature, integrating (1.8) from $T_o = 273.15$ Kelvin ($e_s = 6.11$ mb at T_o) to T (and e_s) is straightforward, yielding

$$\ln\left(\frac{e_s}{6.11mb}\right) = \frac{L}{R_v}\left(\frac{1}{273.15} - \frac{1}{T}\right), \tag{1.9}$$

which can then be rearranged to obtain

$$e_s = 6.11\exp\left[\frac{L}{R_v}\left(\frac{1}{273.15} - \frac{1}{T}\right)\right]. \tag{1.10}$$

This expression is then used in (1.3) and (1.4) to obtain q. After deriving q, it is a straightforward task to determine H, using (1.1).

If RH is not known but the dewpoint temperature T_d is known, (1.10) can be used to calculate the vapor pressure e, since e is just the saturation vapor pressure when $T=T_d$. It is then possible to go immediately to (1.3) to calculate q and then use (1.1) to obtain H.

To facilitate the comparison between T and H, it is useful to calculate an effective temperature

$$T_E = \frac{H}{C_p}. \tag{1.11}$$

To explore the use of T_E as a metric for monitoring heating trends, this dissertation will initially compare annual variations in T and T_E for two surface sites situated within 60 km of each other on the high plains of Northern Colorado. This dissertation will then

extend these comparisons to look at the 1982-1997 trends in T and T_E for surface sites in the eastern half of the United States that are included in the International Surface Weather Observations (ISWO) data set (hereafter referred to as ISWO; NCDC, 1998). Special attention will be given to the different land use/land cover properties of the various sites, to see how these properties may influence the T and T_E trends.

It is proposed that equivalent temperature more accurately depicts near-surface heating trends than does near-surface air temperature alone, both globally and locally. This should hold especially at the local scales, as the equivalent temperature should be more sensitive to spatial and temporal variations in the land-cover characteristics of the surface. These characteristics include the annual cycle in vegetation greenup and senescence in the midlatitudes, along with reforestation, and the accompanying changes of tree species composition and basal areas, which have been reported over large areas in the eastern United States especially where formerly agricultural areas are being abandoned (Birdsey and Heath, 1995; Stohlgren, 2005). Areas experiencing reforestation could reasonably be expected to be retaining more surface and near-surface moisture within the newly-established forest boundary layer. These factors will influence the relationship between the temperature and equivalent temperature trends in forested areas. There are other ways in which moisture trends can influence heating trends at or near the surface, including precipitation trends with time, both in terms of spatial distribution and precipitation intensity. In response to increasing temperature, surface water bodies will also tend to experience more evaporation, which will affect near-surface moisture and thus equivalent temperature. Overall, we expect that equivalent temperature heating trends will be of the same sign as temperature-based heating trends, but larger in

magnitude, since equivalent temperature accounts for heating of surface and atmospheric moisture in addition to heating of the dry air. Locally, however, differences in this overall relationship should be expected because of variations in site exposure characteristics.

1.3 Dissertation Outline

Chapter 2 discusses issues in surface air temperature measurements regarding site microclimate and instrument exposure. We will present results from a site survey in eastern Colorado. We will then proceed to an analysis of surface heating trends in Chapters 3 and 4, comparing temperature trends with equivalent temperature trends. Chapter 3 will provide initial comparisons of annual variations of temperature and equivalent temperature for two weather observation sites near Fort Collins, Colorado. In Chapter 4, we will compare 1982-1997 trends in temperature and equivalent temperature for stations throughout the eastern half of the conterminous United States. Chapter 5 will investigate trends in temperature and thickness values in the troposphere for selected sites around the world, using both radiosonde and reanalysis datasets. Final conclusions about the initial hypotheses presented in this chapter will be given in Chapter 6, along with remarks and suggestions for further work.

CHAPTER 2

IMPLICATIONS OF SITE MICROCLIMATE ON THE ASSESSMENT OF LONG-TERM HEATING TRENDS

2.1 General Exposure Standards

For near-surface air temperature observations, it is generally desirable that the observed temperature be representative of the free-air conditions over as great an area surrounding the site as possible, at a height of about 1.5 meters above the ground surface. Ideally, the site should be level and should not be situated where there are significant local topographical variations. Any steep slopes or hollows should be avoided. The site should also be freely exposed to both sunshine and wind, which then necessitates that it not be located too close to trees, buildings, or other possible obstructions (WMO, 1996).

It thus becomes critical, whenever any potential regional change in observed air temperatures is detected, to determine conclusively how much of the detected change is explained by true larger-scale climate trends versus how much is explained by influences from land-use changes at the site exposure itself. These latter influences may include local-scale urban development around the site or changes in local vegetation characteristics. Those who are monitoring long-term climate trends must have access to

information on local-scale exposures, if this potential problem is to be adequately addressed.

We attempted to retrieve such data in the late spring and early summer of 2002 for eastern Colorado, visiting nearly all of the National Weather Service (NWS) Cooperative Network (COOP) sites in the region that measure air temperature (Davey and Pielke, 2005). We gave particular emphasis to sites in the United States Historical Climatology Network (USHCN-Karl et al., 1990). The USHCN network consists of a subset of stations from the NWS COOP network. These USHCN stations are used in the construction of homogeneous climate data reference series and in the detection and monitoring of long-term climate trends. As a group, these sites revealed a wide variety of site exposure characteristics. Many sites were located at the observers' residences. The temperature sensors, of which the vast majority are now electronic Maximum Minimum Temperature Sensor (MMTS) devices (see Figure 2.1), are often unsatisfactorily close (within 2-3 meters) to the residence building (Figure 2.2). A primary reason for this siting practice is the cost of running electricity out to the MMTS sensor. The act of locating a temperature sensor relatively close to the observer's residence or place of work reflects an effort to minimize the costs of providing electrical power to the sensor, while at the same time providing a measure of open ventilation to the sensor.

Another common situation we observed is one in which the temperature sensor is situated in a relatively open location, but the surface under and around the sensor consists of a patchwork of different land covers. Land surfaces such as lawn, asphalt, gravel, bare dirt, and concrete were frequently in close proximity to each other. Sites that met all the WMO site exposure requirements (e.g. Figure 2.3) were in the minority. The poorest

exposures were usually found at sites at which excessive vegetation growth was found around the temperature sensor (Figure 2.4) or at locally urbanized sites that were not representative of the immediately surrounding region (Figure 2.5).

Again, we should remind ourselves that the USHCN stations are a subset of the larger COOP station network. Since the criteria used to select USHCN sites usually do not address site exposure features, these sites may indeed have a range of exposures similar to the COOP network as a whole. This situation poses a potential problem in constructing long-term climate records.

2.2 Field Surveys of Site Exposure

In the late spring/early summer of 2002, we conducted a site exposure survey of nearly all of the temperature-measuring COOP stations in eastern Colorado (65 stations – Table 2.1), focusing especially on USHCN stations (Figure 2.6). The USHCN sites that were visited in this survey are:

- Boulder
- Cheyenne Wells
- Eads
- Fort Collins
- Holly
- Lamar
- Las Animas
- Rocky Fort 2SE
- Trinidad

- Wray 2E.

Temperature data from these locations were used by Pielke et al. (2000, 2002) to investigate the spatial homogeneity of climate trends in eastern Colorado. Those studies concluded that no one site adequately described multi-year trends. Our site survey offers one explanation for this problematic finding.

To complete the survey, we contacted representatives from the NWS forecast offices in Boulder, Colorado, in Pueblo, Colorado, and in Goodland, Kansas, to notify them of our work. We also contacted the observers for each of the stations before visiting them, in order to obtain permission for, and confirm, our visit. The majority of stations were surveyed in June 2002 while the stations along the northern Front Range corridor from Denver to Fort Collins, Colorado, were surveyed in July 2002.

The basic method we employed for each station in this survey is as follows: First, the latitude and longitude coordinates of each site were recorded, using a Garmin® 12XL GPS unit. These were checked against the coordinates reported in the existing metadata forms (NWS B-44 forms) for the station. Next, each station's temperature sensor and its surrounding exposure characteristics were photographically documented. Finally, a sketch was made of the temperature sensor and its site characteristics. These sketches were created in a manner similar to those that were available on NWS B-44 forms prior to the mid-1980s. We documented the location of the sensor itself, along with the locations of all the nearby features and surfaces within a radius of about 100 meters that may influence temperature readings. These items included, but were not limited to, features such as buildings, trees, and streets.

The procedure used in the photographic documentation of each site was straightforward. At each site, at least five photographs were taken. One of these photographs was a picture of the temperature sensor itself. The other four photographs illustrated the views looking out from the temperature sensor in each of the four cardinal directions (North, East, South, and West). Additional photographs were taken as necessary in order to document important site characteristics that we were unable to capture in the standard set of photographs.

2.3 USHCN Site Exposures

2.3.1 Ventilation Obstructions

The majority of USHCN sites that we visited display at least one of two recurring exposure characteristics. The first such characteristic arises from the fact that many COOP sites are situated at the observers' residences, as previously discussed. This results in the air temperature sensor being situated too closely to an obstruction, such as a building or a vegetative feature (e.g. trees or hedges).

The USHCN sites at Eads, Colorado, and Holly, Colorado, were both examples of such exposures. The Eads site (Figure 2.7) was located in a mobile-home residential neighborhood situated on the south side of the town. The MMTS temperature sensor was installed on a grass lawn on the north side of the observer's mobile home. A mixture of small trees and bushes were located about 10-15 meters to the east of the sensor, helping to shield the sensor from any influences coming from the street just east of the observer's property. The site was relatively open to the north and west, with the one exception of a 1.5-meter wood fence, about 5 meters away from the sensor, running along the north side

of the observer's property. The one primary flaw for this site was that the temperature sensor was only about 3 meters north of the north wall of the observer's mobile home. Thus, the mobile home may act as an obstruction to the sensor's ventilation under any weather regime having a southerly wind component.

The Holly USHCN site (Figure 2.8) also had the problem of a temperature sensor installed too close to the observer's home. In this case, the sensor was positioned 5 meters off the home's northeast corner. Although the spacing between the sensor and its closest obstruction was better for the Holly site than for the Eads site, the home at the Holly site was a two-story building, the height of which would likely have significant influences on the ventilation of the temperature sensor. There were also several trees 15 meters in height, positioned around the north and west sides of the observer's property, which may act to further restrict ventilation around the sensor. Fortunately, the sensor was positioned over a surface consisting of a mixture of grass and weeds.

2.3.2 Patchy Surface Covers

The second exposure situation that was commonly observed with the USHCN sites we visited was one in which the sensor itself was situated over a satisfactory surface, such as grass lawn or other natural groundcovers, and yet there were multiple types of land covers and surface materials present in the near vicinity of the sensor site. In many of these cases, the temperature sensor was situated in an open, well-ventilated location. An example of such a situation is the station at Rocky Ford 2SE (Figure 2.9). This station is located in the Arkansas River Valley, at the Colorado State University Agricultural Experiment Station just outside of Rocky Ford, Colorado. The temperature sensor shelter

was located on the east edge of a gravel driveway running north-south through the eastern half of the property. To the north, east, and south, there was a scattering of one-story buildings, interspersed with larger expanses of grass lawn and/or bare dirt. There were numerous experimental field plots, containing various crops, situated everywhere to the west of the sensor site. This was definitely an open and well-ventilated site, but the placement of the sensor over a gravel surface was a concern, as this exposure was not representative of the region as a whole. There were also a large number of different land covers and surfaces present at the site. Although the various crops grown at this site are all commonly found in the Arkansas River valley of southeast Colorado, the complex interaction of the various field plots could still have a marked influence on temperature readings at the site.

2.3.3 Ideal Exposures

There were certainly some USHCN sites in our survey that did meet the WMO air temperature exposure standards. To be specific, in addition to the temperature sensors being situated at the standard height of 1.5 meters above ground level, these sites were very open sites, allowing for ample ventilation of the temperature sensor, and the land cover under the sensor and immediately surrounding areas was relatively homogeneous.

The USHCN station in Trinidad, Colorado, was an excellent example for proper siting of air temperature sensors (Figure 2.10). This station was located at the Trinidad Power Plant, located on the east side of town on US Highway 160. The temperature sensor shelter was located in the center of a grass lawn on the power plant's east side, between the power plant building and Highway 160. There were at least 10-15 meters of

grass surface in all directions from the temperature sensor. This buffer was narrowest to the south and west, where an asphalt drive ran in front of the actual power plant building. The sensor's exposure was most open to the north and east, towards Highway 160. The only other obstruction of possible concern would be the power plant building itself. Although this building was about 10-15 meters tall, it was situated well over 25 meters to the southwest of the temperature sensor.

Another USHCN site that had good exposure characteristics was at Cheyenne Wells, Colorado (Figure 2.11). The site was quite open, especially to the south. The site was on the south edge of a small bare-dirt lot that holds various livestock pens. Scattered farm equipment was present just to the north and east of the sensor site. There were open grass fields and pasturelands to the east, south, and west.

2.3.4 Questionable Exposures

Unfortunately, there are still some sites within the USHCN group that clearly do not meet the WMO exposure criteria for temperature sensors. For sites such as these, a problem arises in the area of climate change detection with respect to air temperature. Any given detected temperature change may have a significant contribution from the idiosyncrasies of the site itself and the change may not be representative of the actual temperature changes for the surrounding region. Unless the contributions from the site exposure itself are accounted for, it becomes very difficult to develop spatially representative, long-term climate records and conduct long-term climate studies in that local area.

The USHCN site at Lamar, Colorado, was one such site. It was located in a residential mobile-home neighborhood. The properties of each of the mobile-home lots were quite small in total area, leaving little open space between the mobile homes and accompanying buildings. The weather station property we visited was no exception (Figure 2.12). The temperature sensor was located on a grass lawn on the northeast corner of the observer's property and was situated 1-2 meters off the northeast corner of the observer's home. There was only a 5-meter gap between the observer's mobile home and that of the adjacent property to the north. Hence, there were only a few meters of open space between the sensor and the neighbor's home. An air-conditioning unit was installed on the east wall of the observer's home, about 7 meters south of the temperature sensor. Beside the air-conditioning unit, just to the east of the residence, was a large deciduous tree that was about 15 meters tall. An asphalt street was situated about 4 meters to the east of the sensor. In summary, there were several site exposure factors likely working against obtaining representative temperature observations at this USHCN site.

Wray, Colorado, was another USHCN site we visited that had some questionable site exposure features (Figure 2.13). The site was located at a radio station just on the east side of town in the Republican River valley. As the valley passes through the east side of Wray, it becomes quite narrow, creating significant local topographical variations. The weather station was situated midway down the south bank of the valley, so the site was not level. Locally, the Republican River valley is also quite sinuous, thus creating an environment where air ventilation can be quite restricted under certain conditions. The temperature sensor itself was situated over a grass surface, about 4 meters away from the west side of the radio station building. There was also a large satellite dish located 3

meters to the south of the temperature sensor. These features would both likely act to restrict air ventilation from the south and east to the temperature sensor. They would also act as possible sources of artificial heating.

By far the poorest site exposure for the USHCN sites we visited, however, was observed for the site in Las Animas, Colorado (Figure 2.14). This weather station was located at the Las Animas Power Plant, on the south side of town. At one time, the weather station was located in an open field about 50 meters northwest of the power plant building. At some point in the 1980s, however, the instrumentation was moved to the southeast side of the power plant. We were not able to find documentation for this station move. At the time of our visit the temperature sensor was set up over a gravel surface at the southeast corner of the power plant's main building. A set of railroad tracks running east-west passed about 30 meters to the south of the site. Beyond the tracks, to the south, were open grass fields. Thus, the site was fairly open to the south.

Ventilation was severely obstructed to the north and west, however, where the main power plant building, about 10 meters in height, was situated only about 2 meters to the west of the temperature sensor. Additionally, an exhaust vent was located only 2 meters to the north of the sensor; any air discharges from this vent would very likely affect temperature readings at this site. There were also three short stacks situated between 3-10 meters to the north of the sensor. To the north and east there were several sheds with metal siding, along with several other metal features. In summary, this is a very poor site for measuring air temperatures. It is unknown how many sites such as this are present in the entire USHCN network. It should be clear, however, that sites such as these, which are blatantly unrepresentative of the surrounding area's climate

characteristics, should not be used for developing long-term climate reference datasets and for monitoring long-term climate change.

There were numerous examples of other minor incompatibilities with the WMO exposure standards for temperature measurements. The most common incompatibility we found relates to the actual sensor height above ground level at some locations. For those sites whose sensor heights were not standard, we never observed sensor heights less than 1.5 meters above ground level; rather, all the non-standard heights were over 1.5 meters. In fact, some sensor heights were just over 2 meters above ground level. This disparity in sensor heights highlights the need for greater care in installing the temperature sensors, to ensure that they all are positioned at the standard height above ground level and thus encourage greater compatibility among all of the USHCN stations. There were also occasional problems with localized overgrowth of vegetation around the temperature sensors. Regular maintenance of the land surface (e.g. mowing, pruning) would quickly remedy these problems.

2.4 Discussion

Based on the USHCN sites that we observed in this site survey, variations in site exposures found among USHCN sites roughly parallel the site exposure variations observed throughout the COOP network as a whole. The USHCN sites that exhibit good temperature exposure characteristics (i.e. they meet all or almost all of the WMO standards) are in the minority in the set discussed in this chapter. The majority of sites in the USHCN network will likely exhibit a mixture of good and bad exposure features. One such exposure, found at many residential stations, is that the temperature sensor, albeit

located over a representative ground surface such as a grass lawn, is too close to the observer's house (and sometimes trees and other structures). This allows the house to act as an obstruction for air ventilation around the temperature sensor. Another common mixed-exposure scenario is one in which the sensor is located in an open exposure, with plenty of ventilation, but it is located at a site where there is a variety of land surfaces present in the immediate vicinity of the sensor.

Unfortunately, there are still sites within the USHCN that have obvious poor site exposure characteristics with respect to air temperature measurements. These sites are not at all representative of their surrounding region. There may be many factors present at such sites that could work to create artificial climate trends, trends that in reality are not being observed over the region as a whole. As such, it is not advisable to use these sites in the detection of climate trends and development of long-term climate datasets. If the microclimates of other climate observing sites show similar variability in the worldwide data set of surface temperature trends, this raises questions concerning their use to assess regional and even the global changes of temperature from the historical record. Because of concerns such as these, however, the use of alternate methods for monitoring surface heating, such as with the moist enthalpy term mentioned in Chapter 1, may provide a more robust way to monitor longer-term warming/cooling trends, while at the same time accounting for more of the microclimate/exposure characteristics of each site.

Table 2.1. List of visited COOP weather observation sites in eastern Colorado.

COOP ID	NAME	COOP ID	NAME
050109	AKRON 4E	054834	LAS ANIMAS
050301	ARAPAHOE 14N	054945	LEROY 5WSW
050834	BONNY DAM 2NE	055025	LINDON 4S
050848	BOULDER	055116	LONGMONT 2ESE
050945	BRIGGSDALE	055427	MATHESON 8SE
050950	BRIGHTON 1NE	055734	MONUMENT
051121	BURLINGTON 4S	055922	NEW RAYMER
051179	BYERS 5ENE	055934	NEW RAYMER 21N
051268	CAMPO 7S	055984	NORTHGLENN
051401	CASTLE ROCK	056131	ORDWAY 2ENE
051539	CHERAW 1N	056136	ORDWAY 21N
051547	CHERRY CREEK DAM	057167	ROCKY FORD 2SE
051564	CHEYENNE WELLS	057249	ROXBOROUGH STATE PARK
051996	CROOK	057287	RUSH 1N
052220	DENVER WSFO AP	057317	RYE 1SW
052223	DENVER WATER DEPT.	057515	SEDGWICK 5S
052446	EADS	057560	SHAW 4ENE
053005	FORT COLLINS	057582	SHERIDAN LAKE
053006	FORT COLLINS 4E	057866	SPRINGFIELD 7WSW
053258	GENOA	057950	STERLING
053553	GREELEY UNC	058008	STRATTON
054076	HOLLY	058157	TACONY 10SE
054082	HOLYOKE	058429	TRINIDAD
054172	HUGO 1NW	058436	TRINIDAD LAKE
054242	IDALIA	058781	WALSENBURG
054380	JOES 2SE	058793	WALSH 1W
054388	JOHN MARTIN DAM	059243	WRAY 2E
054413	JULESBURG	059295	YUMA
054444	KARVAL		
054538	KIM 15NNE		
054546	KIM 10SSE		
054603	KIT CARSON		
054606	KIT CARSON 9NNE		
054724	LA JUNTA		
054726	LA JUNTA 20S		
054770	LAMAR		
054825	LARKSPUR 4NW		

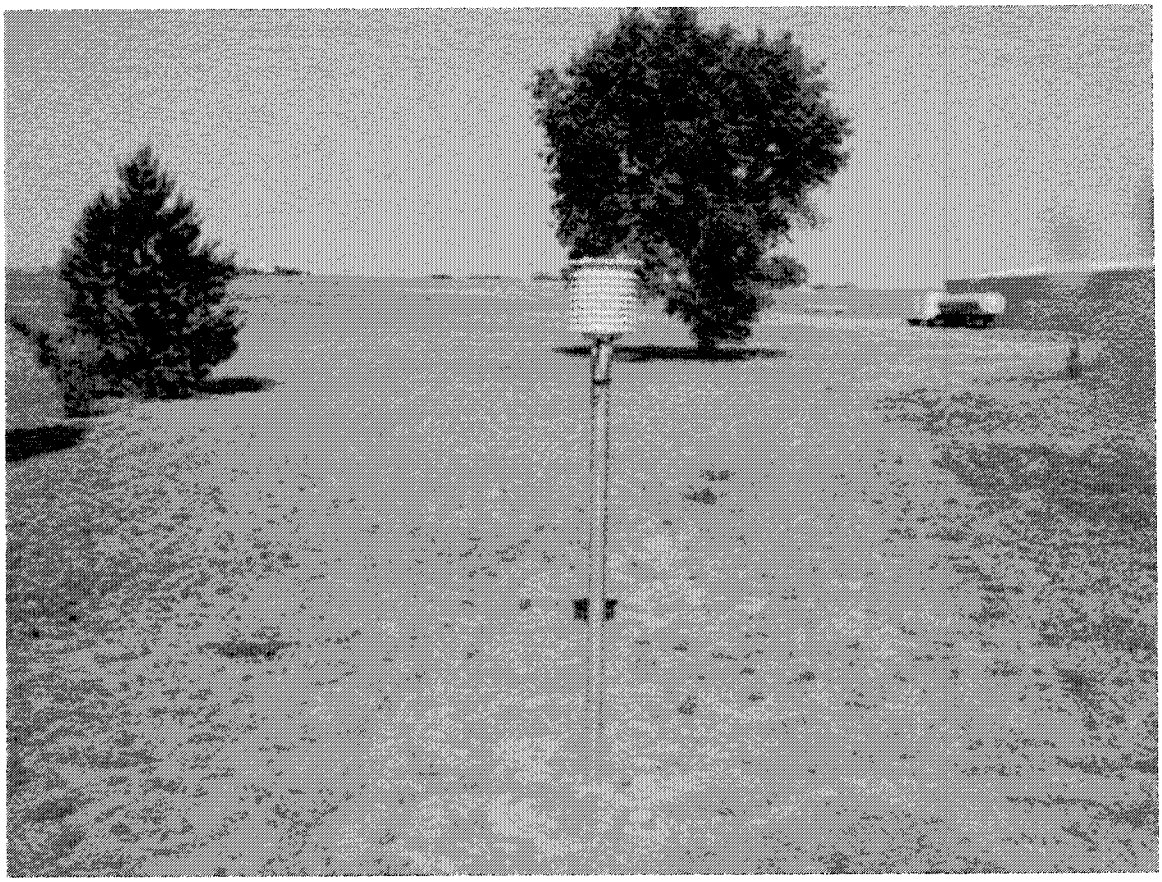

Figure 2.1. MMTS installation near Lindon, Colorado.

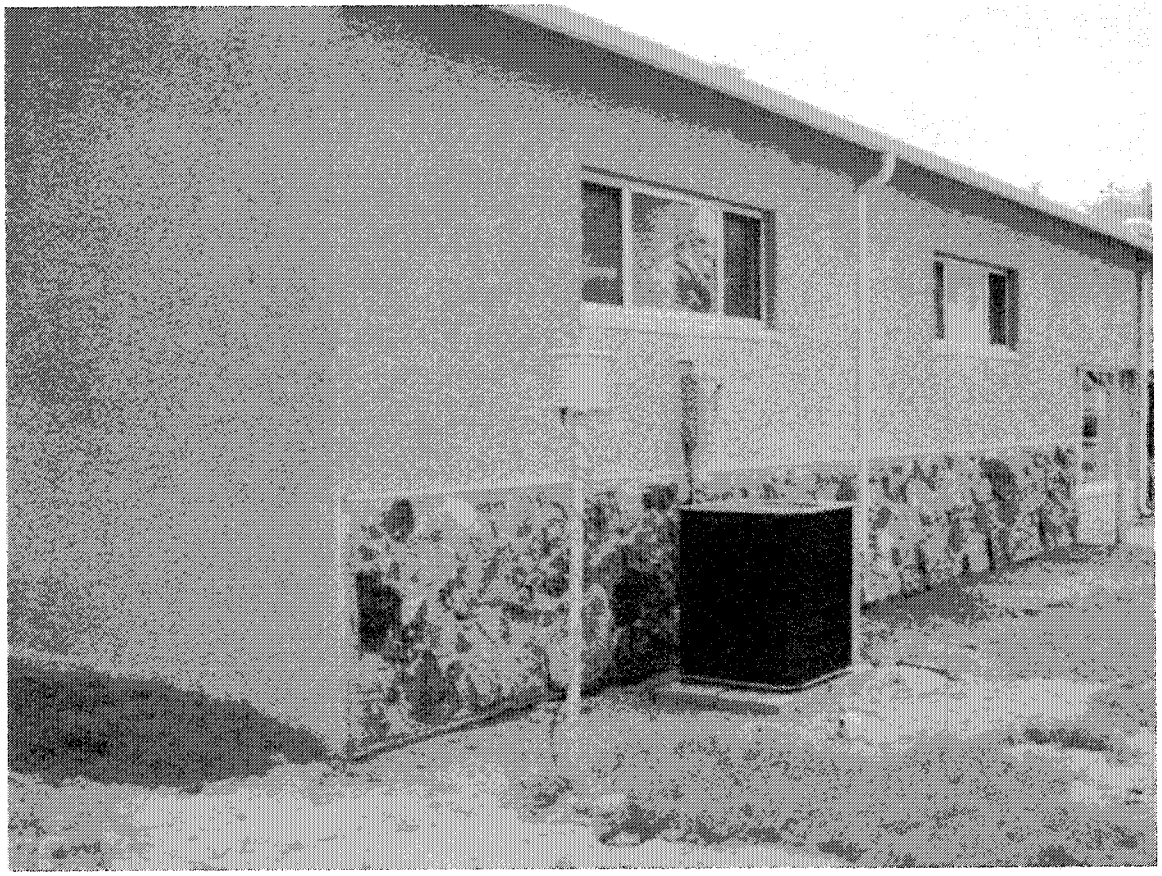

Figure 2.2. MMTS installation near John Martin Reservoir, Colorado.

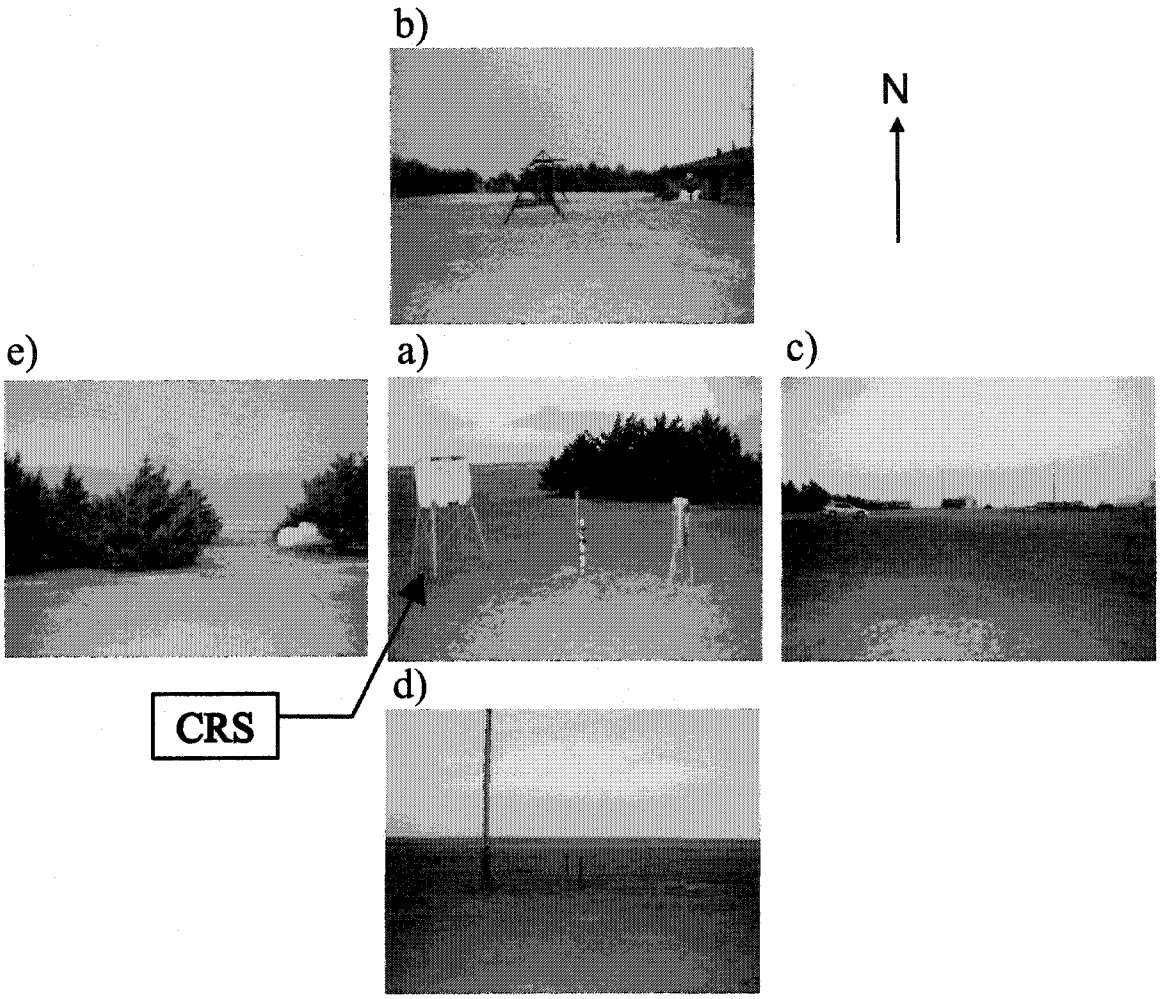

Figure 2.3. Photographs of the temperature sensor exposure characteristics of the COOP station Arapahoe 14N, near Arapahoe, Colorado. Panel a) shows the temperature sensor, a Cotton-Region Shelter (CRS), while panels b)-e) illustrate the exposures viewed from the temperature sensor looking N, E, S, and W, respectively.

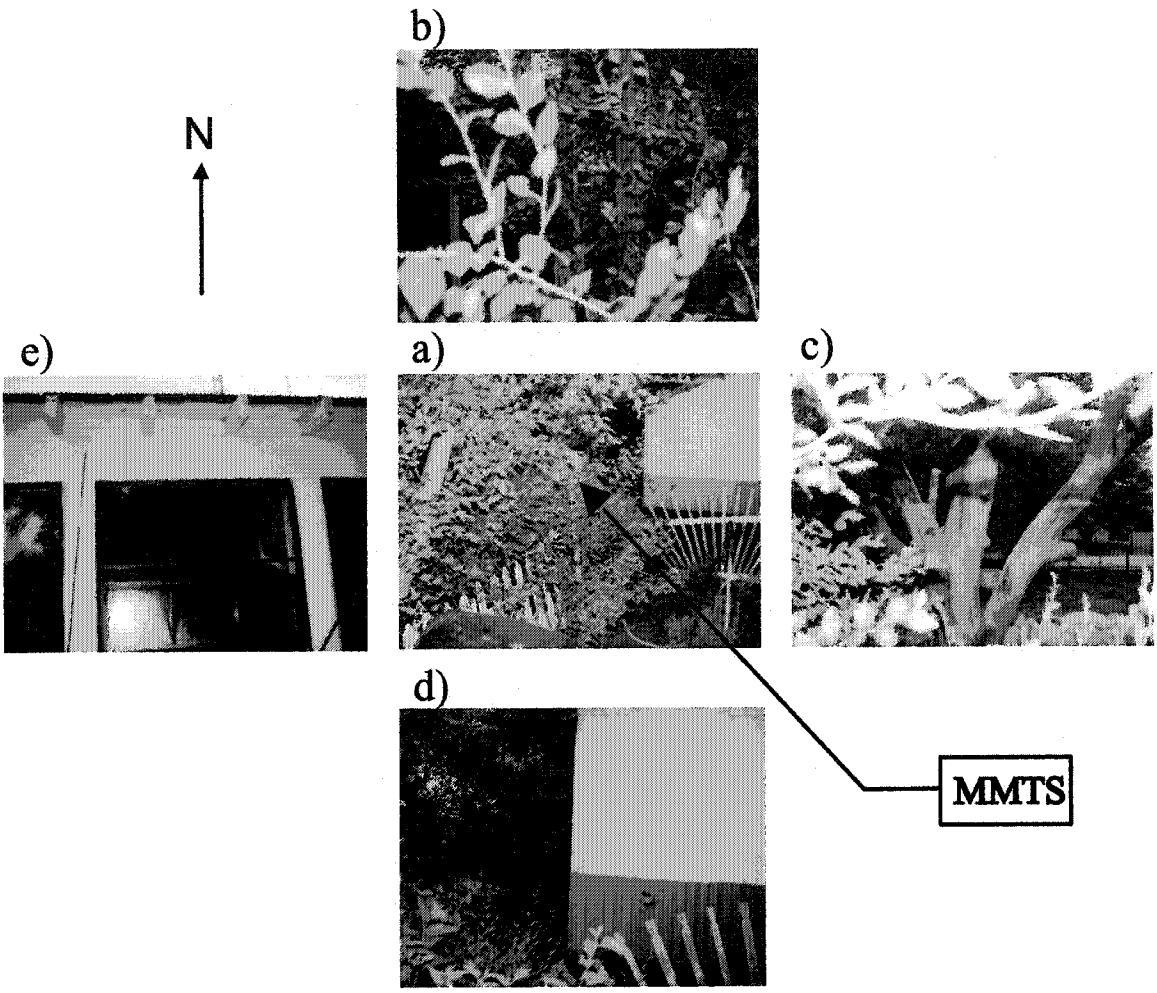

Figure 2.4. Same as Figure 2.3, except for the MMTS at Campo 7S, near Campo, Colorado.

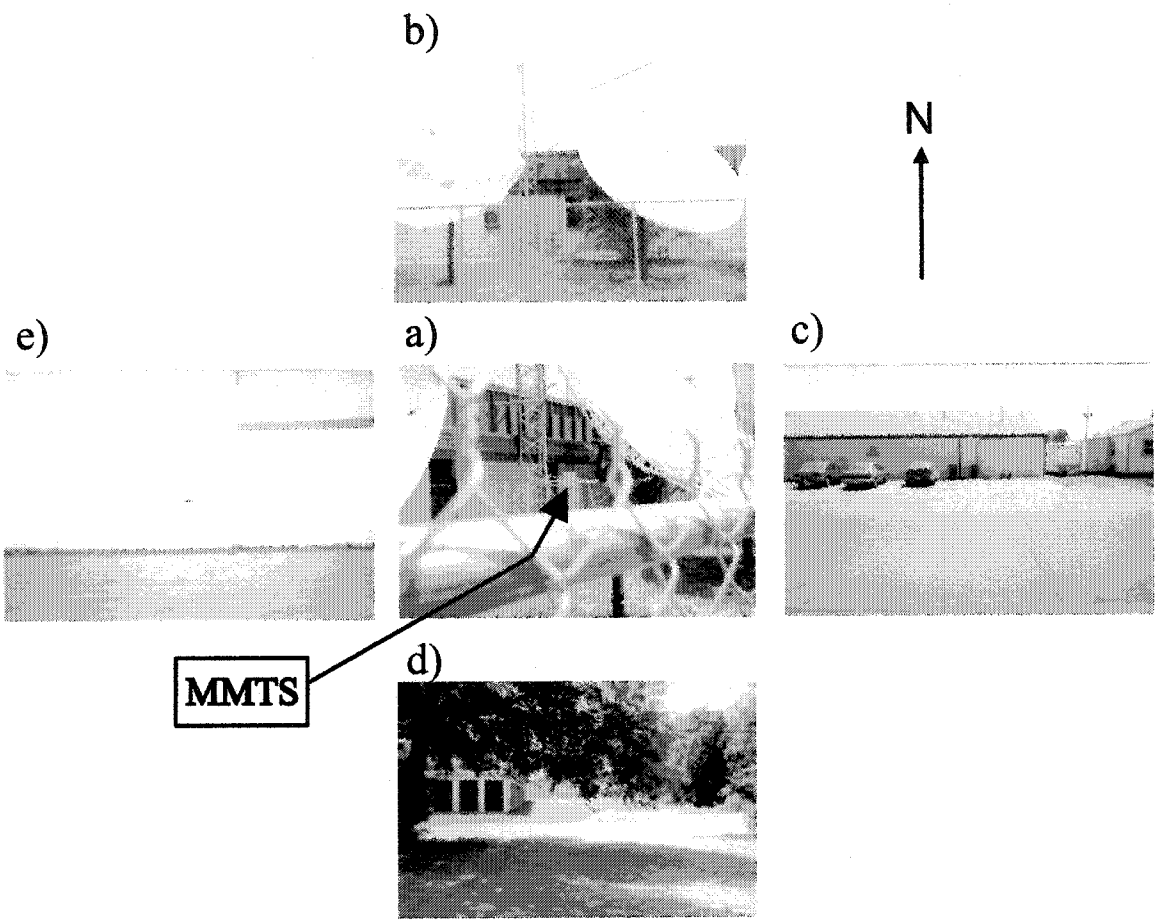

Figure 2.5. Same as Figure 2.4, except for Sterling, Colorado.

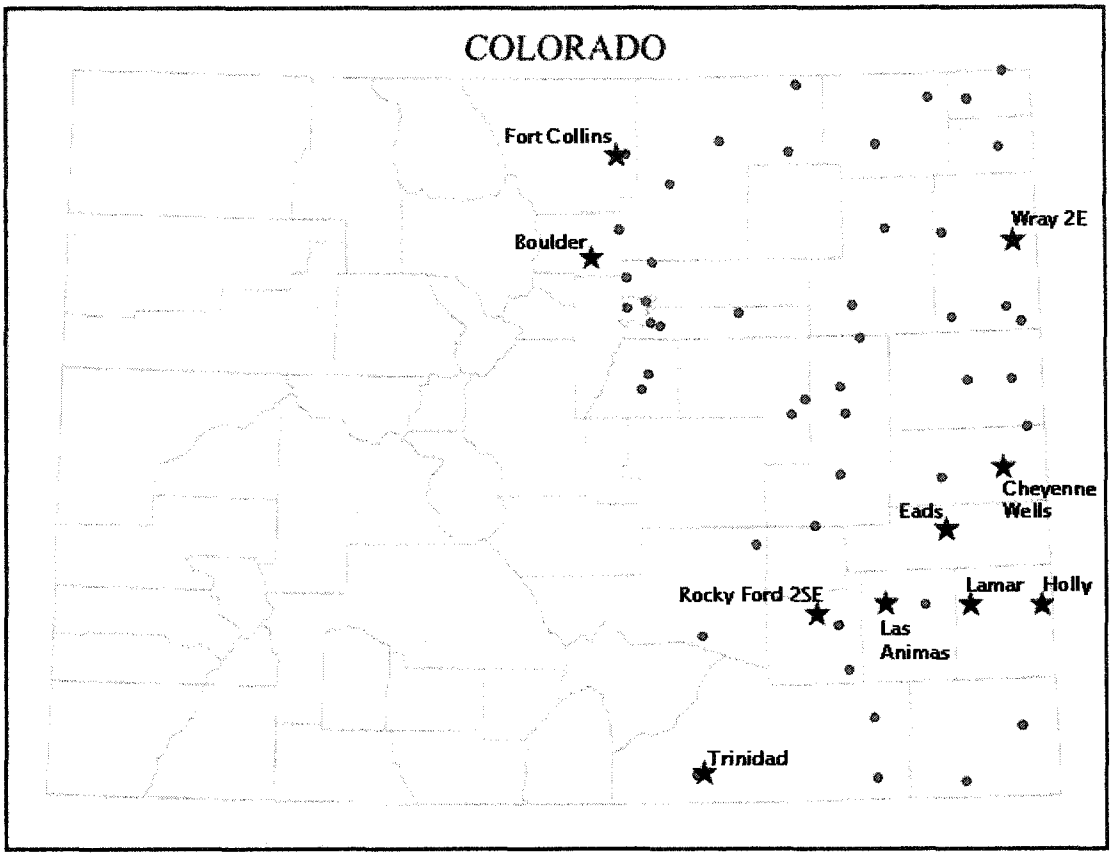

Figure 2.6. Map of study region, showing many of the surveyed COOP sites. The USHCN sites are indicated by stars.

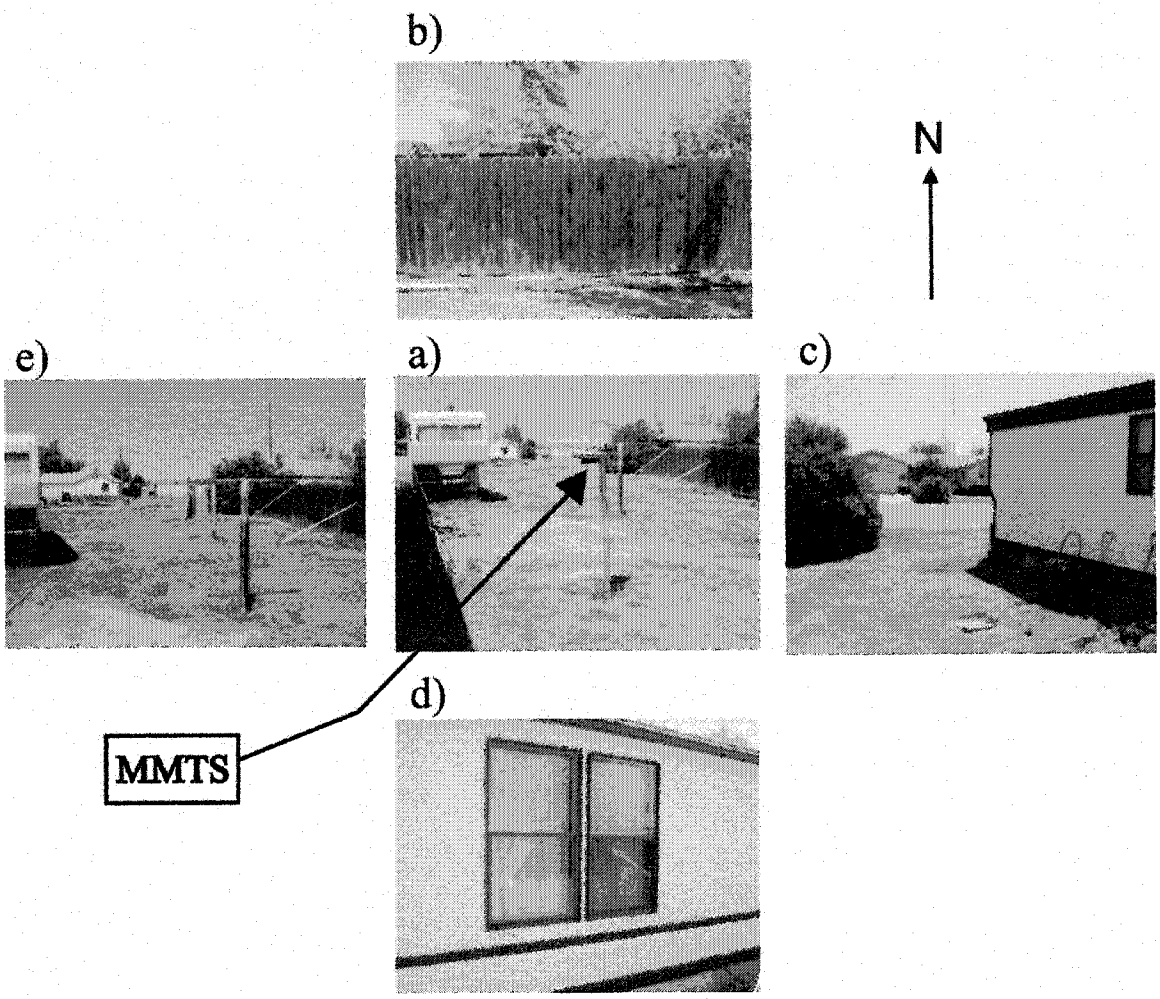

Figure 2.7. Same as Figure 2.4, except for Eads, Colorado.

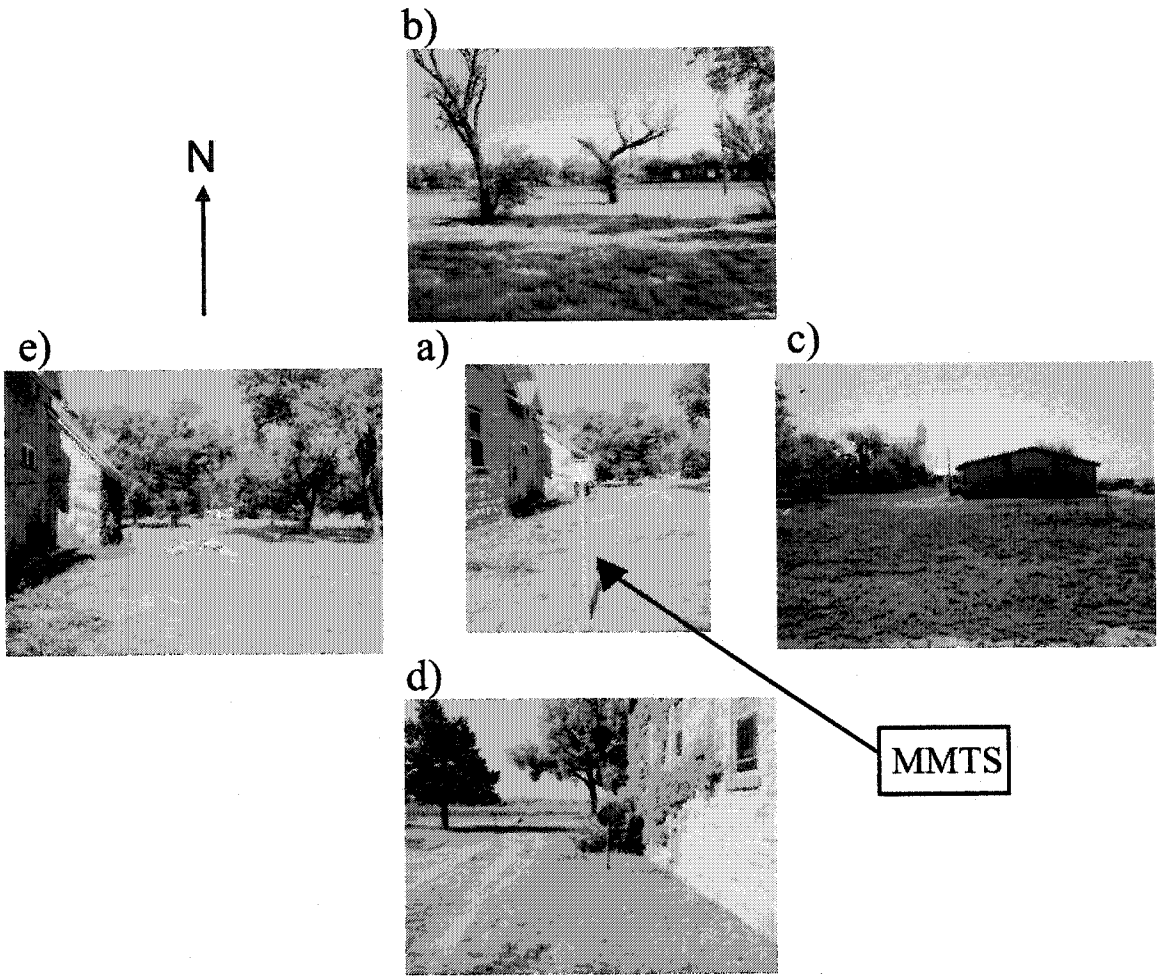

Figure 2.8. Same as Figure 2.4, except for Holly, Colorado.

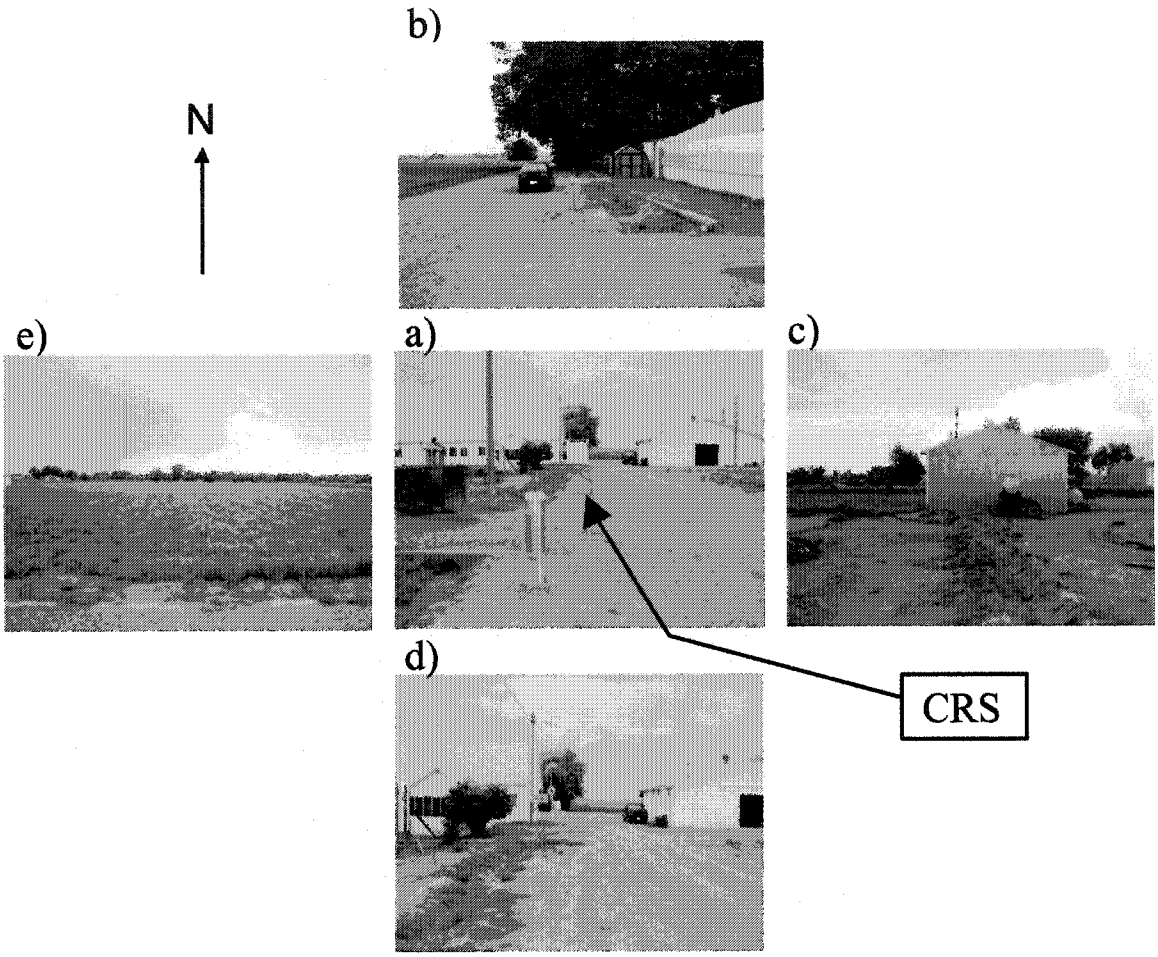

Figure 2.9. Same as Figure 2.4, except for Rocky Ford 2SE, near Rocky Ford, Colorado.

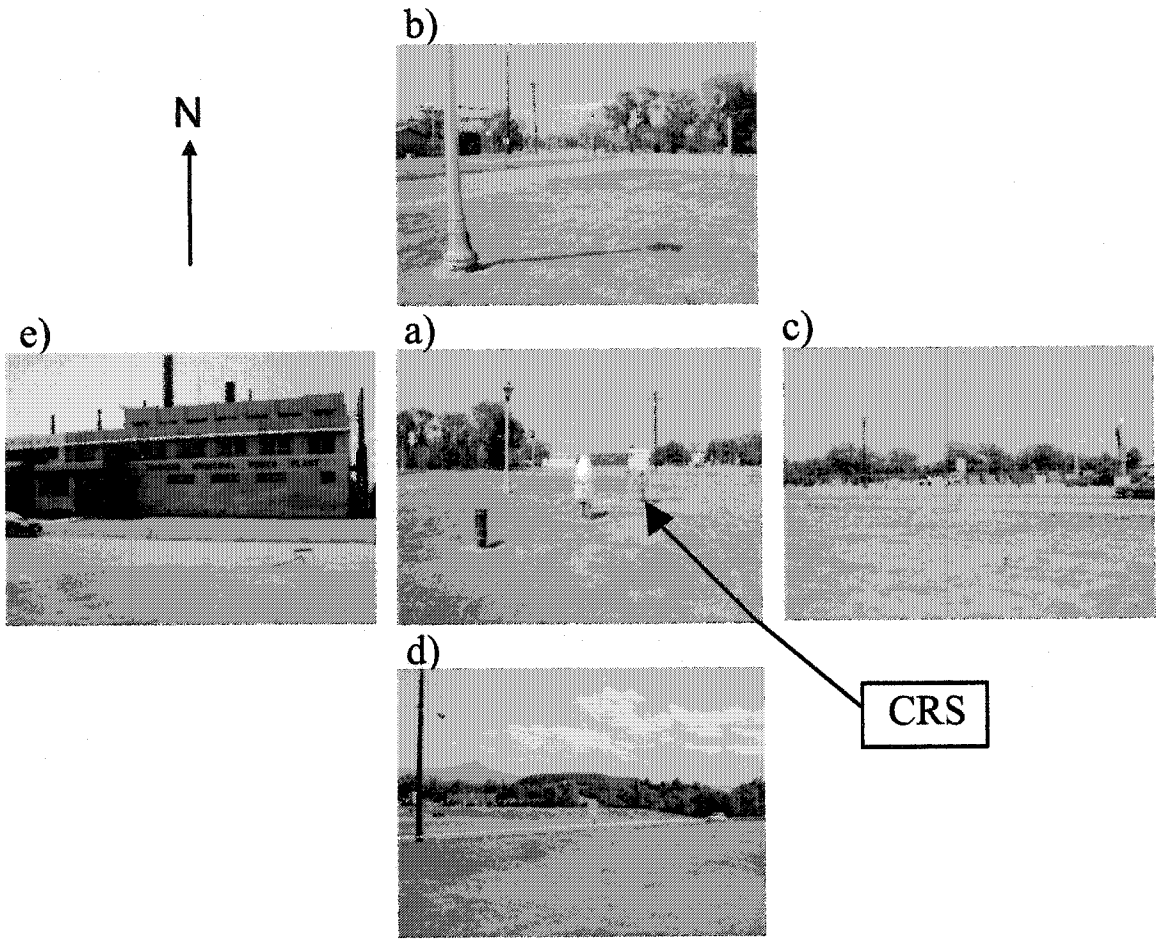

Figure 2.10. Same as Figure 2.4, except for Trinidad, Colorado.

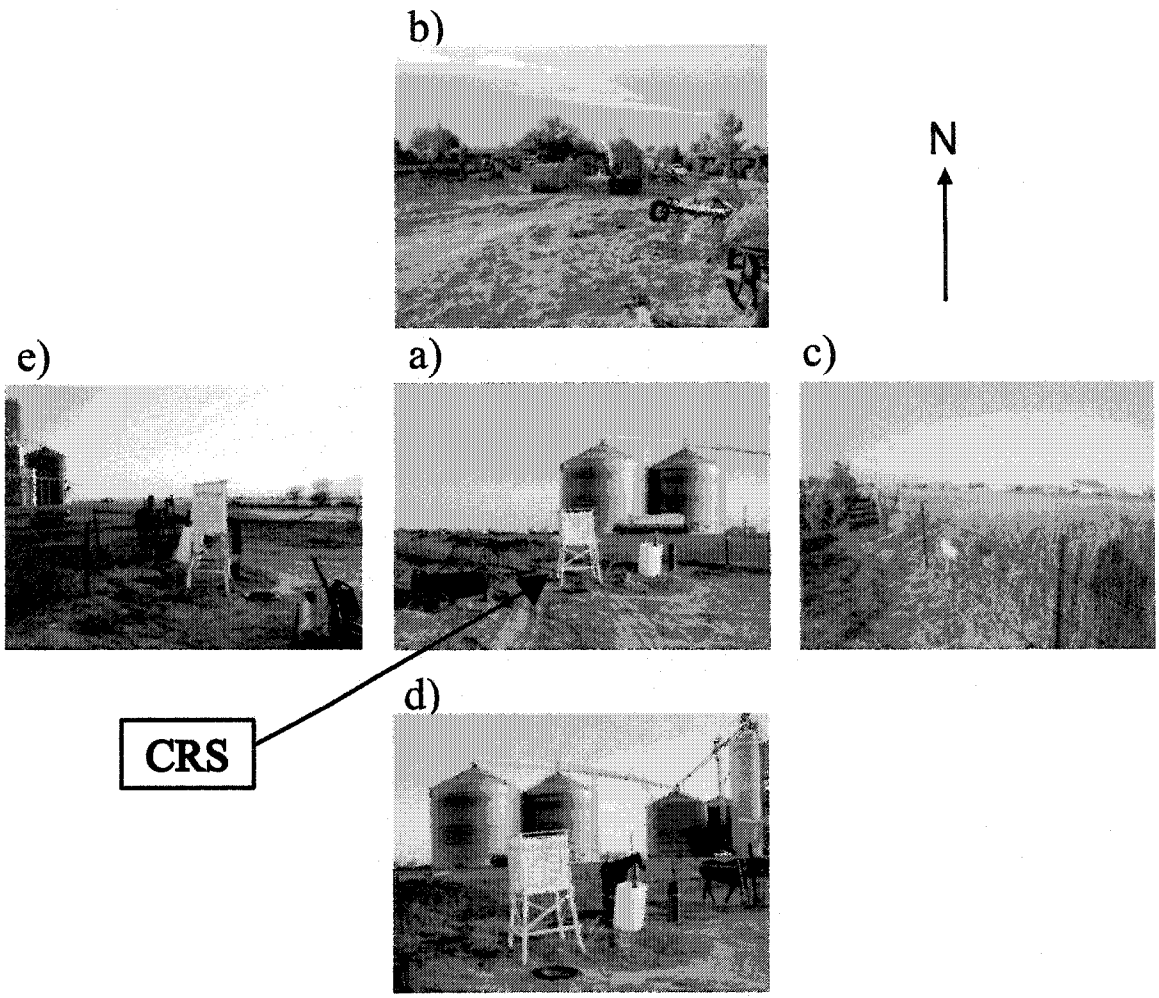

Figure 2.11. Same as Figure 2.4, except for Cheyenne Wells, Colorado.

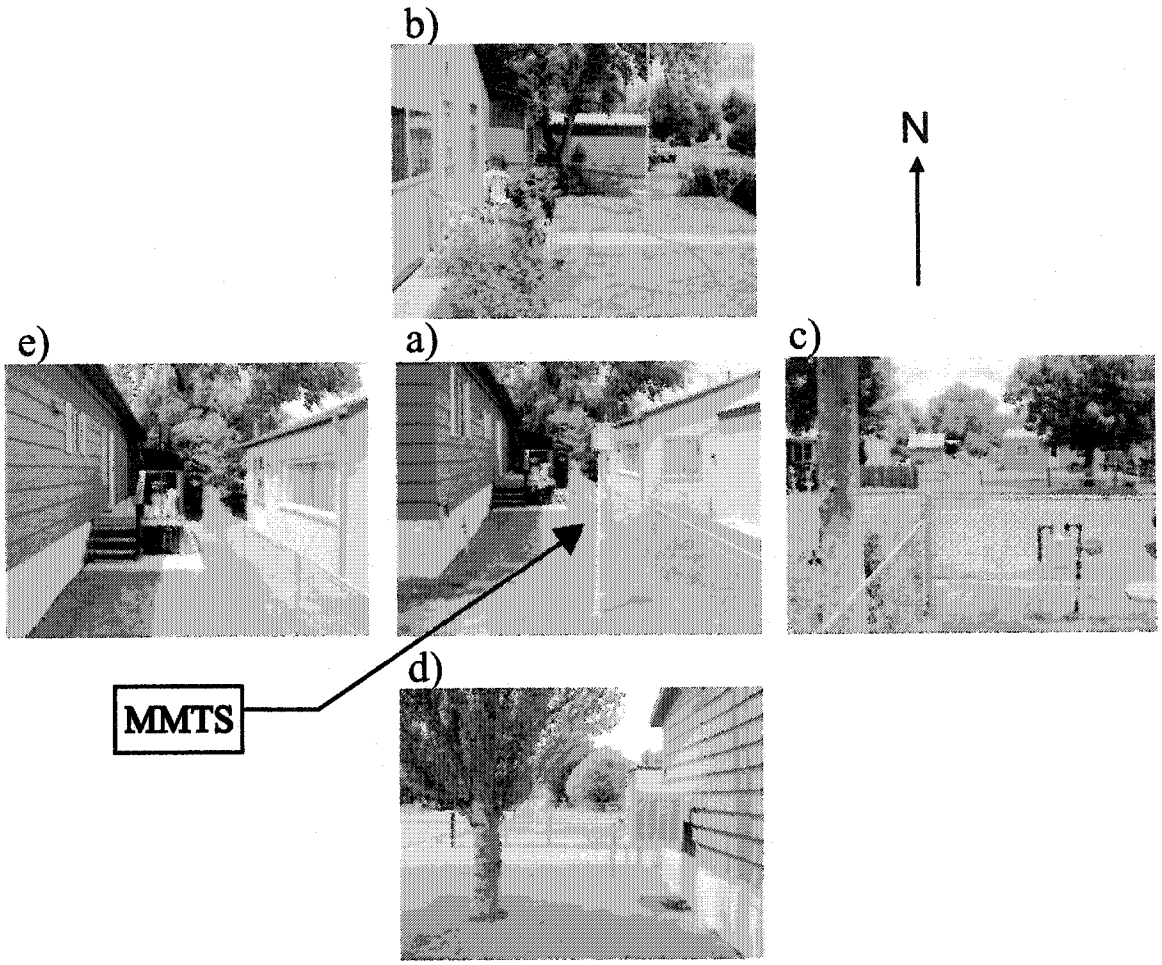

Figure 2.12. Same as Figure 2.4, except for Lamar, Colorado.

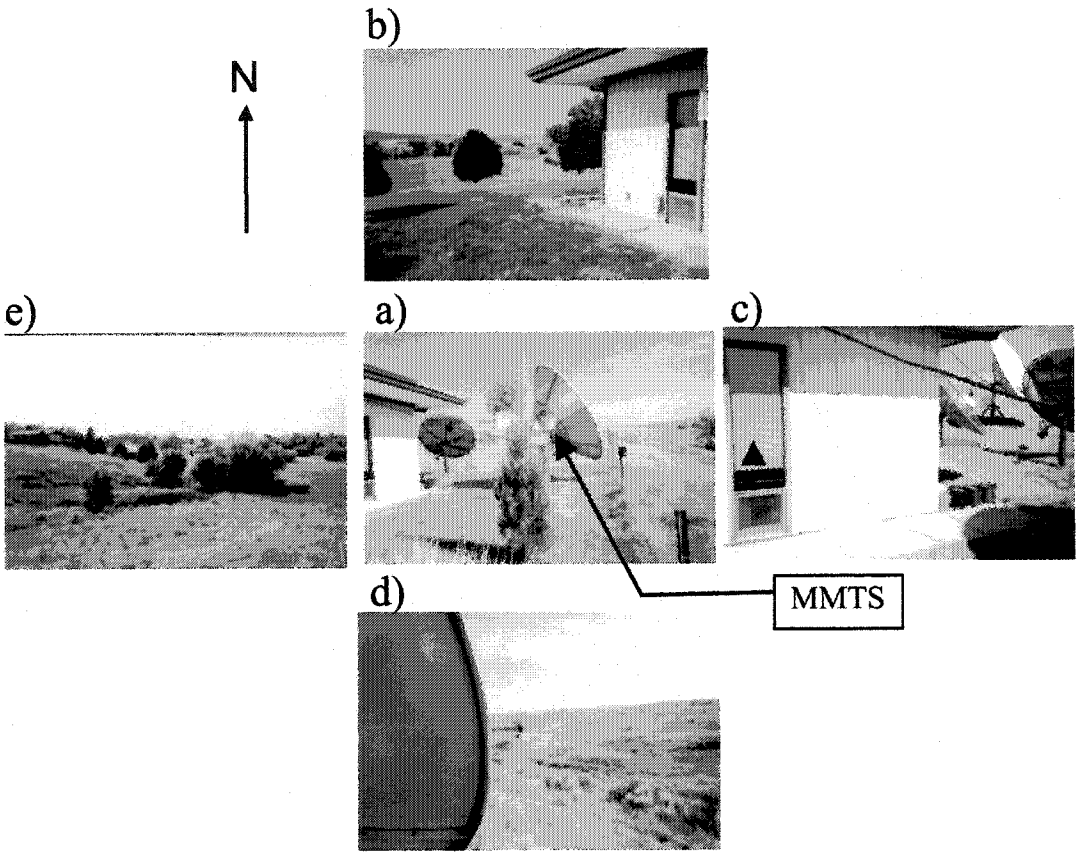

Figure 2.13. Same as Figure 2.4, except for Wray, Colorado.

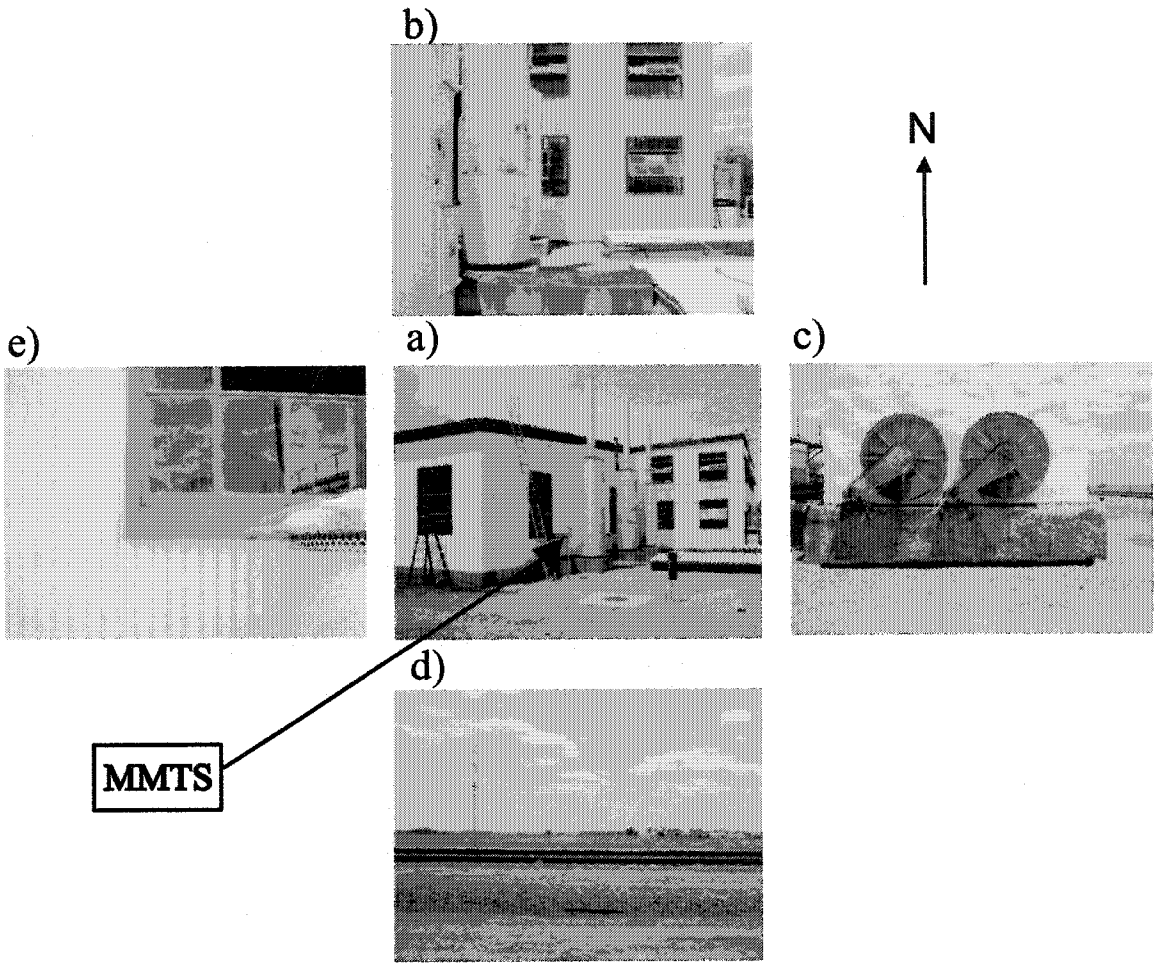

Figure 2.14. Same as Figure 2.4, except for Las Animas, Colorado.

CHAPTER 3

SURFACE HEAT CONTENT – AN INITIAL SURVEY

As discussed in Chapter 1, the term "global warming" has been used repeatedly to describe the observed increase in surface temperatures during the last century. Not surprisingly, therefore, surface temperature has been used as the primary metric to assess anthropogenically-forced climate change (e.g. Jones, 1995; Hurrell et al., 2000; Mann and Jones, 2003; Soon et al., 2004). In actuality, however, climate variability involves the entire climate system (Pielke, 1998; Pielke, 2003) and the concept of global warming must include assessments of units of heat (i.e. Joules) and not just air temperature. This chapter reports on initial work on this issue which was published in Pielke et al. (2004).

To help illustrate this point, recall that the heat content of air just above the surface (i.e. z just above ground level, so z=0 is assumed) can be expressed as

$$H = C_p T + Lq\,, \tag{3.1}$$

where C_p is the specific heat of air at constant pressure, T is the air temperature, L is the latent heat of vaporization, and q is the specific humidity. The quantity H is called the "moist enthalpy" and is often shown in units of Joules kg^{-1}. The surface dry enthalpy, which does not include moisture influences, is given by

$$S = C_p T\,. \tag{3.2}$$

Reported surface temperature trends have been monitoring S, in effect.

As (3.1) shows, however, T is not the only reservoir for heat. It is appropriate to also monitor H in any assessment of surface global warming. Surface heating gets partitioned in at least two ways. Some heating goes into changes in air temperature (C_pT), while some goes into evaporation/condensation of surface moisture (Lq). As such, H gives a truer representation of the actual effects of climatic heating trends on the near surface than does air temperature alone.

There may be cases, in fact, where H trends are at odds with indicated surface temperature trends. To give an example, in the case of desertification, surface temperatures may increase over time (thus labeled a "warming" by current standards), but specific humidity (q) values may decrease, so that H trends may decrease with time. As Pielke (2001a) has shown regarding heat content, at 1000 millibars, an increase of 1°C in the dewpoint temperature can produce the same change in heat content as a 2.5°C increase in air temperature. In the case of desertification, if temperature goes up by 1°C but dewpoint temperature goes down by 1°C, this could actually cause a *reduction* of the air's heat content in terms of Joules kg^{-1}! This would not constitute a "warming," therefore, as was first indicated by the temperature trends.

This point can be further stressed through a comparison of T and the equivalent temperature, T_E, which is given in Chapter 1 as

$$T_E = \frac{H}{C_p}. \tag{3.3}$$

The equivalent temperature accounts both for air temperature and any perceived contributions to the temperature from the heat content of atmospheric moisture. If the atmosphere is completely dry, T and T_E are equal. However, as atmospheric humidity

increases, T_E becomes larger than T, with the highest differences occurring at saturation (Figure 3.1). For the rest of this dissertation, we will refer almost solely to T_E, rather than H, to discuss trends in moist enthalpy/equivalent temperature.

To investigate the usefulness of monitoring variations of T_E in time, daily maximum and minimum values of both T_E and T have been calculated for an entire year (2002) in Fort Collins, Colorado, and at the Central Plains Experimental Range (CPER), administered by the United States Department of Agriculture – Agricultural Research Service (USDA-ARS), which is located 60 km northeast of Fort Collins. Both locations have high quality temperature and humidity observations. The Fort Collins site is a NWS COOP site (Station ID - 053005) located on the Colorado State University campus with nearby buildings, parking lots and irrigated grass, whereas the CPER site is a natural area, containing grasses and other steppe groundcovers native to the High Plains region of the Central United States.

Plots of T and T_E (with the corresponding values of H and S on the right axis) for 2002 (Figure 3.2) illustrate that T and T_E are nearly equal when the absolute humidity is low (e.g. cold winter days), as predicted by Figure 3.1. As absolute humidities increase, however, such as during the growing season, the differences between T and T_E also increase. The atmosphere, therefore, has less heat content on dry days for a given air temperature than it does on more humid days.

The average differences of the annually averaged maximum and minimum temperatures between the two sites (the value at Fort Collins minus the value at CPER) were found to be 0.25°C and 1.86°C, respectively. The differences in T_E were greater, however (2.69°C and 4.20°C, respectively). For the 2002 growing season, the

differences for T_E were 3.48°C (maximum) and 4.96°C (minimum), while the corresponding values for T were 0.91°C (maximum) and 1.82°C (minimum). Note that the differences between T_E and T are larger during the growing season, as opposed to the non-growing season. It appears, then, that the values of T_E are more sensitive to seasonal changes in surface vegetation characteristics and thus provide a more accurate monitor of surface heat variations, so that T_E would then be a more appropriate metric than T to assess global surface warming.

The difference between the temporal trends in surface and tropospheric temperatures (NRC, 2000), which has not yet been explained, may be due in part to the heating trend analyses of the surface and troposphere being for temperature alone and not including the more appropriate metric of equivalent temperature. Recent analyses of satellite data (e.g. Christy et al., 2003; Mears et al., 2003) have reduced but not entirely eliminated this difference.

The initial results from our station comparison between Fort Collins and CPER provide support for the findings by Kalnay and Cai (2003), in which temperature trends for both surface observations and the NCEP reanalysis product were investigated and it was concluded that land use variations are partially influencing the recently observed temperature changes in the eastern United States. This conclusion is reached because the NCEP reanalysis does not directly include local surface influences, whereas surface observations do include these influences. It is assumed by Kalnay and Cai (2003) that the difference in temperature trends between the surface observations and the NCEP reanalysis is primarily caused by this difference in accounting for land-use effects.

This conclusion is still in question, however. Trenberth (2004) claims that in addition to ignoring local surface influences, the NCEP reanalysis ignores changes in cloud coverage and surface moisture. Dominant land-use changes in the United States, such as conversion from forest to cropland, may be responsible for a *cooling* temperature trend over time, rather than a warming (Bonan, 2001). Equivalent temperature, unlike air temperature, is able to directly account for changes in surface moisture through latent heating. Air temperature *indirectly* responds to total heat content. Equivalent temperature could also be useful in the troposphere, where latent heating could be used to indirectly account for trends in cloud coverage. The portion of the recent surface temperature trends that is attributable to land-use changes as reported by Kalnay and Cai (2003) may in fact be too small (Vose et al., 2004) and should actually be treated as a lower limit for the actual magnitude of the influence of land-use changes (Cai and Kalnay, 2004). Finally, one must be aware that artificial trends introduced by station relocations and changes in the time of observation are also likely to influence the observed surface temperature trends and may, in some cases, overwhelm the possible effects from land-use changes alone (Vose et al., 2004).

In summary, the term "global warming" requires that we include surface heat as one of the metrics that are used to monitor this aspect of the climate system. The real changes in heat content of the Earth's climate are not fully described by temperature itself. Future assessments of climate trends and variability should be based not only on temperature but also on surface heat content.

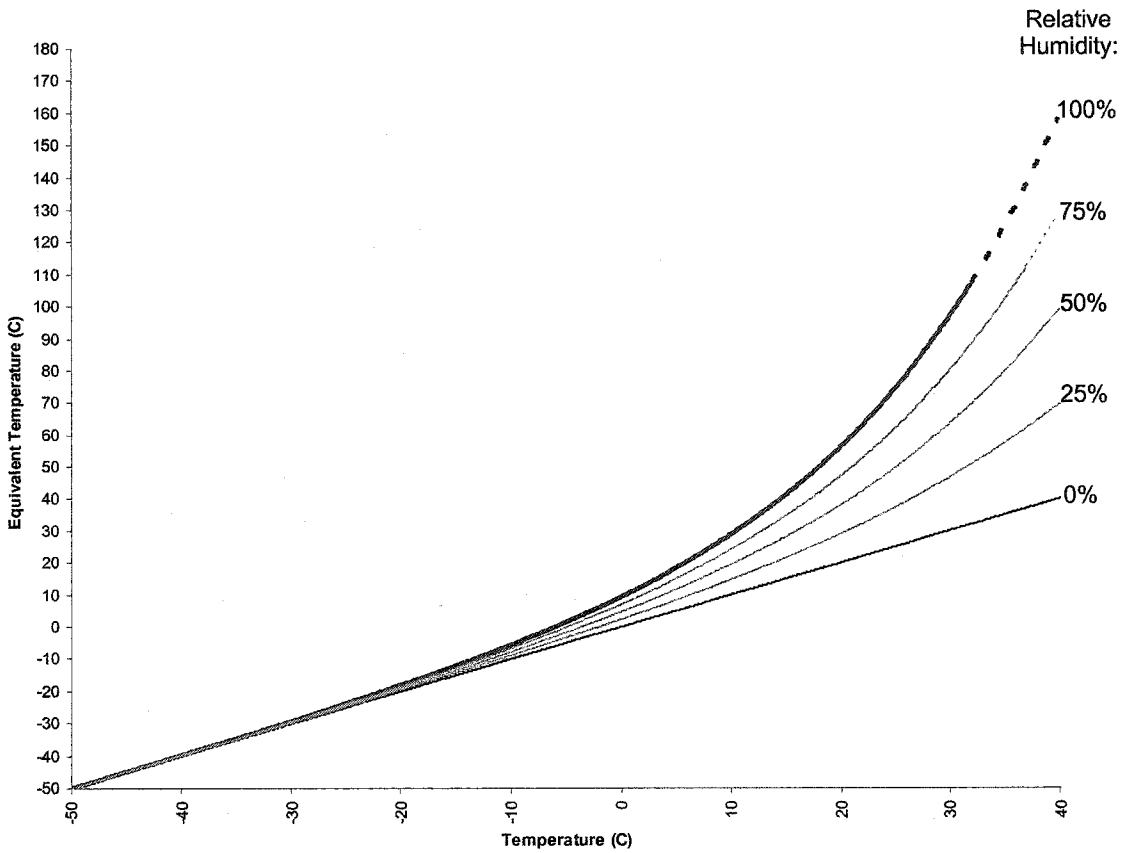

Figure 3.1. Effective temperature T_E (°C) as a function of air temperature T (°C), for selected relative humidity values.

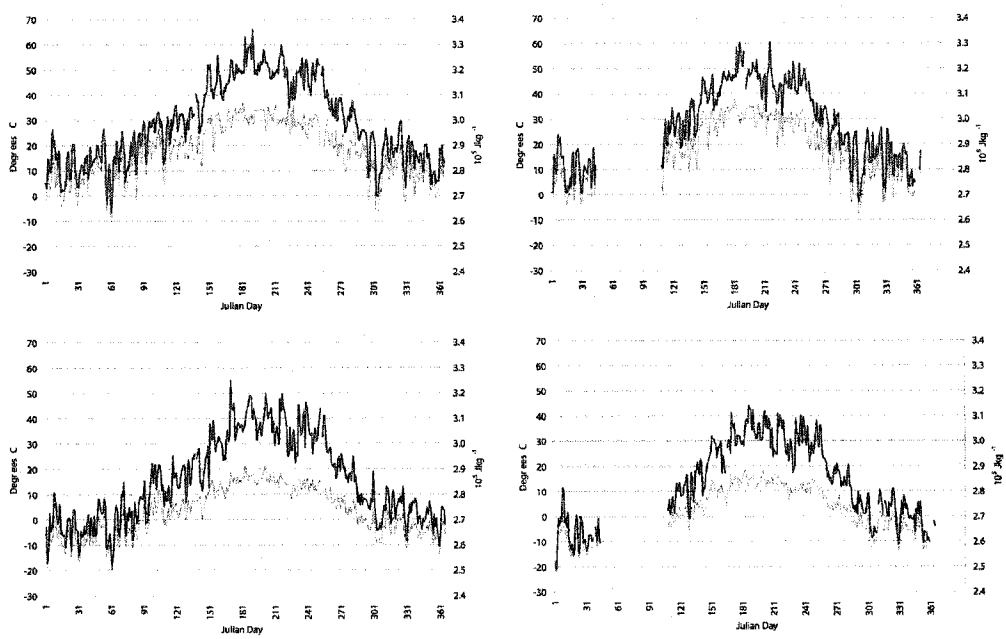

Figure 3.2. T_E and T, in °C (H and S, in 10^5 Jkg^{-1}), for both Fort Collins (left panels) and the CPER ungrazed site (right panels) during 2002. T (S) is represented by the grey lines, while T_E (H) is represented by the black lines. The top panels are for maximum daily temperature and the bottom panels are for minimum daily temperature.

CHAPTER 4

COMPARISONS OF TEMPERATURE AND EQUIVALENT TEMPERATURE TRENDS AT THE SURFACE

4.1 Data

Surface temporal trends in temperature and equivalent temperature were investigated for the years 1982-1997, for ISWO sites in the eastern half of the United States (Figure 4.1). For a complete listing of surface stations that were used, please see Appendix B. These data were obtained from the International Surface Weather Observations (ISWO) dataset, developed and maintained at the National Climatic Data Center in Asheville, North Carolina (NCDC, 1998). The data from the ISWO dataset has undergone extensive quality control to remove effects from station moves, instrument changes, and other data quality issues. The ISWO dataset consist of observations taken every three hours. In this investigation, primary emphases has been given to 1) differences between urban versus non-urban trends, and 2) the more general variations of temporal trends in temperature and equivalent temperature as a function of land cover type.

4.2 Methods

Daily means of temperature (T), dewpoint temperature (T_d), station elevation (z), and sea level pressure (p_o) were computed for each ISWO station listed in Appendix B. Monthly means were then computed from the daily data. From the monthly mean value for p_o, an approximation of the actual monthly mean pressure was calculated at each site, using the formula

$$p = p_0 e^{-z/h}, \tag{4.1}$$

where z represents the elevation of the surface observation station and h is the scale height (h = 8 km). Once p is known, (1.1) – (1.10) can be used to calculate the monthly mean specific humidity (q) and then the mean equivalent temperature (T_E).

The monthly values of T and T_E were then used to construct 1982-1997 time series of each variable. For each surface station, 24 time series were analyzed, 12 series for each variable (T, T_E). For each variable, one time series was constructed for each month of the year (e.g. the January time series consists of the values for January 1982, January 1983, … , January 1997).

For each time series the 1982-1997 trend was estimated using a basic linear regression model

$$y = \beta x + \varepsilon, \tag{4.2}$$

where β is the trend and ε is the error. If the heating trend is in fact exponential in nature, the trend estimate obtained from (4.2) will be a conservative estimate for the current trend. For an exponential time series, the heating trend will be focused into the latter years of the period of interest. A linear trend estimate for this time series will distribute the total observed change over the entire period, thus lowering the magnitude of the

estimated trend. Trend estimates were computed for only those time series having at least 10 available data points (years). These time series are usually serially correlated (i.e. autocorrelated), so that an autoregressive error model must be included in the error term ε. The autoregression procedure in the Statistical Analysis Software® (SAS) program was used to compute the T and T_E trend estimates. The Yule-Walker Method (Gallant and Goebel, 1976) was used as the autoregressive error model. The trend estimates accounted for autocorrelations covering up to four time intervals (i.e. lag-4), which means that any autocorrelations out to four years were corrected for in this analysis. This choice for the maximum lag interval was intended to remove most influences from interannual variability. Once a trend estimate (b) was obtained for a given time series, it was compared with the standard error (SE) of the time series to determine whether or not the trend was significantly different from zero. This was done by computing a Student's t value

$$t = b/SE \tag{4.3}$$

and comparing it to standard t values at specified significance levels ($t_{90\%}$, $t_{95\%}$, etc.). Appendix A provides a more complete discussion regarding the statistical methodology used to derive the trend estimates.

Once the T and T_E trend estimates were computed, summary statistics were computed for the entire surface dataset, for both T and T_E. These summary statistics were then compared with each other to determine whether or not there was a significant difference between the overall T and T_E trends. Comparisons were first done on an annual basis (i.e. including all observations throughout the year) and then on a seasonal basis (i.e. January-March, April-June, etc.). Once these annual and seasonal analyses

were conducted for the entire surface dataset, similar comparisons were done for the subsets of the T and T_E trends that were significant at the 90%, 95% and 99% significance levels. Significance testing was conducted using Z test statistics, which are also discussed in Appendix A.

Next, the variability of both T and T_E trends as a function of land use/land cover was examined. Each station's primary land cover was determined using the land-cover classes listed in Table 4.1. These land-cover classes were obtained from the National Land Cover Dataset (NLCD - Vogelmann et al., 2001) for the conterminous United States, at a resolution of 1 km. The predominant land-cover category for each station was determined for a 3-km X 3-km area (9 grid cells, or 9 km^2) grid of cells centered on the station of interest, by finding which land cover has the largest proportion of cells in that area. Once each station's primary land cover was determined, stations were grouped into common land-cover categories. Summary statistics for the T and T_E trends were then computed and compared for each land-cover category.

This land-cover classification technique was also used to classify each surface station as either rural or urban. Much attention has been given to the comparisons of urban vs. rural temperature trends (e.g. Gallo, 1996). Little significant difference has been found in maximum temperature trends but there are significant warming trends indicated in urban minimum temperatures, compared to rural minimum temperatures.

This study expands on these previous comparisons of air temperature to investigate similar trends in equivalent temperature. The comparisons of T and T_E trends were first done for all urban sites (183) and all non-urban sites (205) in the ISWO dataset.

Next, T and T_E trends were compared for five urban-rural pairs identified from this dataset (Figure 4.2, Table 4.2).

4.3 Temperature vs. Equivalent Temperature

4.3.1 Annual and Seasonal Patterns

Over all seasons, when the trend estimates of all stations are averaged together, the trends for T show cooling with time while the T_E trends are neutral (Table 4.3). The *difference* between the T and T_E trends is significant at >99%. When one only averages over those trends which are significantly different from zero at the 90% level, one notices the same patterns as when all stations are considered. The one exception is that T_E trends indicate warming instead of cooling, so that now the trends for T and T_E are of opposite sign. As one begins to look at the averages over those individual trends that are significant at the 95% and 99% levels, the T_E trends show an increasing amount of warming while the trends in T continue to indicate cooling.

It is useful to now compare these averaged trend estimates on a *seasonal* basis. In general, the annual cycle indicates a transition from slight warming in the winter and early spring, to slight cooling in the fall months (Figure 4.3, Table 4.4). The transition appears to be quicker for T trends than it does for T_E trends. During the winter months, both T and T_E trends show warming. As one progresses into the spring and summer months, the trends for T begin to indicate cooling, while those for T_E continue to show warming. Both T and T_E trends indicate cooling in the fall months. Average trend magnitudes are generally greatest in the fall (cooling) and winter (warming) and are smallest during the spring and summer. In all seasons, the averaged trends for T_E are

significantly greater in magnitude than those of T: T_E trends display more warming than T from the winter through the summer, while they display more cooling than T trends during the fall (Table 4.5).

The preceding results were for the case where all trends are considered. These same patterns are present when the analysis is narrowed to look only at those individual trends that are significantly different from zero at a specified significance level. As the trend significance increases, however, the difference between the averaged T and T_E trends becomes less significant during the winter and spring months (Table 4.5). Note, for instance, that at the 90% significance level, the spring difference between T and T_E trends is not as significant as it was when all trend estimates are considered. At the 95% and 99% significance levels, both winter and spring are noticeably less significant than they were when all trend estimates were considered. Even so, these differences between the T and T_E trends remain significant at over 99%.

4.3.2 Land Use/Land Cover Influences

The averaged T and T_E trends were then compared to see how they vary as a function of land cover, using the land-cover classes listed in Table 4.1. As Chapter 2 has illustrated, there are a wide variety of microclimates encountered at surface weather stations around the United States. The equivalent temperature at any given site is closely connected to the surface energy balance at that site, which in turn depends on the site's microclimate. The land cover of a surface observation site is a primary factor in describing that site's microclimate (Pielke et al., 2000; Pielke et al., 2002; Pielke, 2003).

On an annual basis, sites whose predominant land cover is forest tend to show cooling in both the averaged T and T_E trends, with the most significant cooling occurring for deciduous forests (Figure 4.4, Table 4.6). The difference between the T and T_E trends is not significant (Table 4.7). Grassland and shrubland sites tend to show warming in both the averaged T and T_E trends. These averaged trends are significant with the exception of the T trends for grassland sites. The difference between the T and T_E trend averages indicates that the T_E trends are significantly warmer than the T trends. This difference is significant at above 90% for shrubland sites and above 95% for grassland sites. Sites that are predominantly agricultural have the same tendencies as that of forest sites (i.e. both T and T_E trends indicate cooling), with the exception that the difference between the T and T_E trends is significant at above 90% (T_E cooling less than T) for small-grains sites. Both urban sites and sites close to major water bodies indicate warming with trends in T_E, but cooling with trends in T. For the urban sites, the difference between the T_E and T trends is significant at over 99%. The urban and water land covers are the only two classes for which it was observed that the T_E and T trends differ in sign on an *annual* basis. For the land-cover class labeled as "Other" (see Table 4.1), no significant average trend is noted for either T_E or T. Overall, the largest warmings are indicated for the predominantly grassland and shrubland sites (especially for T_E), while the greatest coolings are indicated at the predominantly forested and agricultural sites.

The corresponding annually-averaged trends in specific humidity for these land-cover classes (Figure 4.5, Table 4.8) indicate that specific humidity (q) has decreased over the 1982-1997 period for row crops and both deciduous and evergreen forests. All other classes show increasing trends for q. For those sites where q has decreased with

time, the T_E trends have more cooling/less warming than the T trends, since there is a decreasing amount of heat content due to atmospheric moisture over time. The opposite is true for those land-cover classes where q has increased over time, with T_E trends showing more warming/less cooling than the corresponding T trends.

A comparison of the percentages of individual heating trends that are significant at a specified significance level for each landscape type (Table 4.9) shows that in general, T_E exhibits higher percentages than T of individual trends that are significant. The exception to this is for those trends that are at least 99% significant In this case, the percentages of individual T_E trends and T trends meeting this significance level are comparable. For the heating trends at forested sites, a higher percentage of T_E trends are significant at specified significance levels than are T trends. For other land covers, the percentages are comparable. The highest percentages of significant trends for T generally occur for agricultural sites (e.g. row crops, small grains) while the highest percentages of significant trends for T_E occur for the mixed forests and for agricultural sites.

For any given trend value for a time series, one can roughly estimate the number of years required to be able to detect this trend at a specified significance, using the formula (Weatherhead et al., 2000):

$$n = \left[\frac{(2+z)}{|b|} \sigma \sqrt{\frac{1+\phi}{1-\phi}} \right]^{2/3} \tag{4.4}$$

where b is the estimated trend, σ is the variability of the trend estimate, z is the Z test statistic value for the specified significance level α, and φ is the autocorrelation ($0< \varphi <1$). The ratio $|b|/\sigma$ is known as the t-value for the trend in question. This calculation was done for the annually-averaged trends for each land-cover class in Figure 4.4 (see Table

4.10). An autocorrelation of 0.5 was assumed for this calculation. For T_E, the number of years needed to detect a trend at 90% significance ranged from 5 years for the shrubland sites up to about 57 years for the small-grains sites. If it is desired to detect these same trends at the 99% significance level, these values increase to about 7 years for shrubland sites and about 77 years for small-grains sites. For T, the number of years needed to detect a trend ranged from 5 years for the shrubland sites up to almost 60 years for the sites labeled as "Other". If it is desired to detect these same trends at the 99% significance level, the numbers of years increases to 7 years for the shrubland sites and about 80 years for the sites labeled as "Other".

Figure 4.6a shows that during the winter months, all land-cover classes but one (small grains) indicate warming for both T and T_E trends (also see Table 4.6). The small grains land-cover class indicates slight cooling for both T and T_E trends. The average T_E trends are of the same sign as the T trends in every land-cover class. The average T_E trends are also greater in magnitude than those of T. The most significant average trends were found for shrubland sites, which have more occurrences of significant individual trends in both T and T_E. The only land-cover classes showing differences between the T_E and T trends that are significant above 90% are the shrubland sites, the urban sites, and the water sites (Table 4.7). The sample sizes for the shrubland and water averages are small, however, so that the indicated significance of the differences between the T_E and T trends may not be totally trustworthy.

Moving into the spring months (Figure 4.6b, Table 4.6), there emerges a signature of average T and T_E trends that is very similar to that observed over the entire year (Figure 4.4). For grasslands and shrublands, there is more warming indicated for the T_E

trends than there is over the entire year. The average springtime T_E trend for these two land covers is indicated to be significantly different from zero (the sample size, however, is small). The urban and water land covers also show significant average warming trends for T_E. The differences between the averaged T_E and T trends (Table 4.7) are significant (T_E trends significantly more warming than T trends) for shrubland sites, sites with small-grain agriculture, and water sites; yet all of these averages suffer from small sample sizes.

The summer months (Figure 4.6c, Table 4.6) indicate that sites having a significant amount of human influence, such as agricultural sites (6-8) or urban sites (9), behave similarly to the annual case. On the other hand, natural environments like grasslands (4) and shrublands (5) indicate results that are largely different from the annual case, in that the average T and T_E trends are generally opposite in sign. The trends for T_E now show warming while T trends show cooling for the grassland sites and the shrubland sites.

Cooling trends are strongly indicated for both T and T_E during the fall season (Figure 4.6d, Table 4.6), with all forest sites showing average trends that are significantly different from zero for both T and T_E. The T_E trends are significantly cooler than the T trends (Table 4.7). Both the deciduous forest sites and the evergreen forest sites have large enough sample sizes to lend credibility to these findings; however, the mixed forest sites (3) do not. Significant cooling trends for both T and T_E are also observed for row crops, pastures, urban areas, water areas, and "Other" land classes (class #11). For most land-cover classes, the average T_E trends are significantly cooler than those of T. The only fall trends where warming is indicated are the T trends for grasslands, shrublands, and small-grains agriculture.

Returning to the annual case, if one only includes individual site trends that are significantly different from zero, as trend significance increases, the overall patterns for averaged heating trends (Figure 4.7, Tables 4.11-4.12) are very similar to when all trends are considered (Figure 4.4, Table 4.6). The magnitudes of the averaged trends increase as the individual trend significance increases. This is particularly true for T trends.

4.3.3 Overall Urban-Rural Differences

The land-cover classification scheme in Table 4.1 can be simplified to look only at urban stations (land-cover class #9) versus non-urban stations (all other classes). The rural and urban trend estimates for T_E indicate cooling and warming, respectively (Table 4.13). There is a significant difference (over 99% significance) between the urban and rural T_E trends. For T, both the urban and rural averaged trends indicate cooling. The difference between the urban and rural trends is significant, with urban sites indicating less cooling than the rural sites. This difference for T trends is not as significant as for the T_E trends, yet it is still significant, at over 99%.

Overall, Table 4.13 shows cooling for the T trends and mixed results for the T_E trends. The urban sites indicate less cooling/more warming than the rural sites for both T_E and T. Urban trends show warming for T_E while rural trends show cooling. For T, urban trends show a smaller cooling relative to the rural trends. The difference between the T_E and T trends at urban sites is significant, at over 99%. Rural sites do not have a significant difference between the average T_E and T trends. The averaged T_E and T trends for the rural sites both indicate cooling.

4.3.4 Urban-Rural Station Pairs

The bulk urban-rural comparison in the preceding section was then scaled down to look at individual pairs of urban and rural sites (Figure 4.2, Table 4.2). Each pair consisted of a rural site and an urban site located within 20 km of each other.

Averaging all the urban-rural site pairs together over all months (Table 4.14), at rural sites, the average T_E trends indicate warming, while the T trends indicate cooling. The difference between the rural T_E trends and the rural T trends is significant at over 95%. The same patterns are seen for the urban sites as for the rural sites, except that the difference between the average T_E and T trends is less significant (over 90%). Caution must be exercised in interpreting Table 4.14, because of the small number of sites considered; however, the results in Table 4.14 are similar to those in Table 4.13, showing that the T_E trends are generally warmer than the T trends. The only real notable difference between Tables 4.13 and 4.14 may be that for the subset of urban-rural station pairs T_E trends show warming (rather than cooling) in the rural areas. This potential difference may be due merely to the large difference in sample sizes between Tables 4.13 and 4.14.

Looking at the 1982-1997 trends for T and T_E that were computed for each individual month for the five urban-rural station pairs we considered (Figures 4.9, 4.11, 4.13, 4.15, 4.17), it is clear that in general, the annual cycle indicates that the greatest warming trends are in the winter and early spring months, while the greatest cooling occurs during the fall. It is notable that the signs of the trends are usually similar for both T and T_E, except for the spring and summer months. The trends for T_E are generally greater in magnitude than those of T, which means that either T_E shows more cooling

than T, or else it shows more warming than T. The results from the individual urban-rural station pairs are quite variable, indicating that local microclimates are very important in determining the characteristics of T and T_E trends at each site.

The results from each of these urban-rural pairings are now individually presented. The first site pair to be considered is in the greater metropolitan area of Washington, District of Columbia. The urban site, National Airport, is situated on the west bank of the Potomac River, just west of the Capitol district. The land-cover grid for this site (Figure 4.8a) shows that urban areas (land cover #9) are present on the east and west sides of the site, with a north-south strip of water running up the middle of the site (the Potomac River). The rural site is at Fort Belvoir in Virginia. Fort Belvoir is predominantly a deciduous-forest site (land cover #1), with deciduous forests indicated primarily on the southern and eastern portions of the site. Urban land cover is present on the site's northwestern quadrant (Figure 4.8b).

At both sites, the overall seasonal variations in trends are identical for both T (Figure 4.9a) and T_E (Figure 4.9b). Warming trends are indicated in the winter (especially in January), mixed signals are observed in the spring and summer, and cooling is indicated in the fall months. This is similar to the results for the entire surface dataset (Figure 4.3). There is no consistent difference in trend magnitudes for either T or T_E between National Airport and Fort Belvoir. In general, the spring and early summer months both show slight warming and the warming trend is usually greater for T_E than for T. In contrast, May has a cooling trend in both T and T_E for the urban and rural sites. Comparisons of T and T_E trends at National Airport and Fort Belvoir show that for most

months the magnitude of the T_E trend is greater than, and usually of the same sign as, the T trend, which is also similar to what was found for the surface dataset as a whole.

The next urban-rural site pair to consider is an urban site paired with a nearby grassland rural site. This site pair is located in Oklahoma City, Oklahoma. The urban site is at Tinker Air Force Base on the southeastern side of the city. Urban land covers dominate throughout the middle and western portions of the site, while grassland cover (land cover #4) is present at the site's south and east edges and pastures (land cover #8) dominate the northeast edges (Figure 4.10a). The rural site is at Will Rogers Airport on the city's southwest side. Urban land covers are present on the southwest edge of the Will Rogers Airport site, but grassland rings the site's north, east, and south edges (Figure 4.10b).

A comparison of the annual cycle of trends for Oklahoma City (Figure 4.11) and Washington (Figure 4.9) reveals some similar patterns in heating trends, especially for T (winter warming, mixed signals during the spring and summer, fall cooling). The sites at Oklahoma City, however, appear to commence winter warming sooner, starting in December instead of the following January. The T trends for the rural and urban sites (Figure 4.11a) are not consistently different. They both show warming in the late-fall and early-winter months, with neutral or slightly cooling trends during the rest of the year, especially in the summer. The T_E trends for the two sites (Figure 4.11b) are also not consistently different and the T_E trends - like the T trends - show warming in the late fall and early winter. During the late spring and summer months, however, T_E trends indicate much more warming than the T trends.

The trends for T and T_E tend to be similar in sign throughout the fall and winter months, with the T_E trends being slightly larger in magnitude than the T trends. During the spring and summer the T and T_E trends are often very close to neutral, and opposite in sign. The exception occurs in late spring and early summer, when the T_E trends indicate substantially more warming than the largely neutral T trends. This result may be directly tied to the rapid increase in atmospheric moisture and vegetation greenup (and its associated transpiration) which typically occurs in grassland regions during the late spring and early summer.

Minot, North Dakota, is also located in a grassland environment, large tracts of which have been converted to agricultural production of small grains such as wheat. The urban site, Minot Air Force Base, is almost exclusively urban (Figure 4.12a) as every cell in the site grid is so classified. The rural site is at Minot International Airport (Figure 4.12b). It has a small amount of urban land cover on its southwestern edge. Everything else, however, is covered with small-grains agriculture (land cover #7).

The seasonal patterns at this site are much different than the first two site pairs that have been considered and are, in fact, different than the overall patterns observed for the entire surface dataset (Figure 4.3). Cooling trends are indicated at Minot throughout the winter and early spring for both T (Figure 4.13a) and T_E (Figure 4.13b), whereas the T and T_E trends for the first two site pairs (Washington and Oklahoma City) indicated warming, especially in the winter. The heating trends at Minot are mixed for the remaining months. June, September, and December indicate warming trends for both T and T_E, while July and November indicate cooling. The other months are largely neutral.

Both the rural and the urban sites show that T_E trends are generally larger in magnitude than the T trends.

The next site pair to be considered is located on the southwestern edge of Miami, Florida. The urban site is the Miami/Kendall New Tamiami Airport near Kendall, Florida, and is characterized by urban land covers over all but its eastern sectors (Figure 4.14a). Water (land cover #10) is present in the southeast sector, with row crops (land cover #6) in the east sector and other miscellaneous land cover to the northeast (land cover #11). The rural site is at Homestead Air Force Base in Homestead, Florida. This site has extensive row crops everywhere except the northwest sector, which is urban (Figure 4.14b).

The site pair at Miami provides an example of how temperature trends may appear to be much warmer for urban areas as opposed to non-urban areas (Figure 4.15a), but if moisture effects are included, the trends between the rural and urban sites are more nearly equal (Figure 4.15b). The annual cycles of the T and T_E trends (Figures 4.15a and 4.15b, respectively) at both sites are similar to the overall pattern observed for the eastern United States (Figure 4.3), with warming earlier in the year progressing into cooling later in the year. December trends were not available for this analysis. Compared to the eastern United States as a whole, however, the peak of the early-year warming trends occurs later, towards the spring months. The fall cooling trends are not as prominent as they are for many of the other sites considered in this chapter. The greatest differences between the urban and rural trends are for temperature (Figure 4.15a). Temperature trends at the urban site predominantly indicate warming throughout the year. At the rural site, however, warming trends are limited to the winter and spring months, with slight cooling

(rather than warming) indicated during the fall. The trends for T_E (Figure 4.15b) are very similar between the two sites. Comparing the T and T_E trends at both sites, the T_E trends are consistently larger than the T trends. This difference is especially noticeable for the rural site.

The final rural-urban station pair considered in this study is located near Valparaiso, Florida. The urban site is Eglin Air Force Base, just north of Valparaiso (Figure 4.16a). This site is characterized by urban land covers in all sectors except the south sector, which has evergreen forest (land cover #2). The rural site is at Hurlburt Field in Valparaiso (Figure 4.16b). Urban land cover is present in the west and southeast sectors, and evergreen forest is present to the northeast. Every other sector consists of miscellaneous land covers such as wetlands.

The annual cycle of observed trends in T and T_E (Figures 4.17a and 4.17b, respectively) is similar to the general cycle observed throughout the eastern United States (Figure 4.3). For both T and T_E, there is a neutral to slight warming trend in all months except the fall, when more cooling is indicated. There is not a clear difference in the trends at the rural site versus the urban site. The trend magnitudes appear to be larger for T_E than they are for T, throughout the year. This is especially true for the urban site, Eglin Air Force Base. Missing data at Hurlburt Field makes it more difficult to compare the trends of T versus those of T_E, but where data are available (at least 10 years of data), the T_E trends are indeed larger in magnitude than those of T.

In summary, for the five urban-rural site pairs that have been considered, the annual cycles of T and T_E trends observed at these sites indicate warming trends during the first half of the year and cooling trends during the second half. The timings of the

largest warming and cooling trends and the transitions between these, however, are very site-dependent. The differences in trends between urban and rural sites are also very site-dependent. The T trends between urban and rural sites tend to differ significantly, while the corresponding T_E trends are usually more similar. For both urban and rural sites, both warming and cooling trends in T_E are generally greater in magnitude than the trends in T.

4.4 Discussion

To recall our initial hypothesis from Chapter 1, it was proposed that equivalent temperature T_E more accurately depicts near-surface heating trends than near-surface air temperature T and that this holds at both global and local scales. It was expected that this would be true, especially, at the local scales, as T_E should better reflect any spatial and temporal variations in land cover characteristics of the surface, including any characteristics associated with vegetation or the lack thereof. Trends in T_E should generally be of the same sign as the trends of T, but larger in magnitude, since moisture heating/cooling is being accounted for, in addition to dry air heating/cooling. For comparisons of T and T_E trends at individual sites, however, departures from the above relationship are to be expected, since unique microclimate characteristics present at each site can have an important influence on trend values.

The results for the entire surface dataset, averaged over all seasons (Table 4.3), indicate that the averaged T_E trends are neutral while the T trends are slightly cooling, which does not directly support our hypothesis that the T_E and T trends are of the *same sign*. The difference between the average T_E and T trends is significant but the magnitudes of the T_E trends are *less than* the corresponding magnitudes of the T trends, a

finding which also tends to reject the above hypothesis. For the most significant individual trends (i.e. trends that are significant at the 90% level, 95% level, etc.), the average T_E trends show a slight warming, while the trends in T show a slight cooling. When considered as a whole, these findings tend to contradict our initial hypothesis that T_E and T trends are generally of the same sign.

On a seasonal basis, the averaged T_E and T trends are generally of the same sign during the fall and winter months, with T_E trends being larger in magnitude and the difference between the T_E and T trends often being significant at the 90% level or higher (see Table 4.5 and Figure 4.3). This relationship holds even when considering only those trends that are significant at the 90% level and higher (Figures 4.3b – 4.3d), which offers general support for our initial hypothesis. During the summer, however, the signs of the T_E and T trends are usually opposite to each other, with T_E trends showing warming and T trends showing cooling. This pattern is also sometimes observed during the spring months. One likely reason why the T_E trends show a warming that is not indicated by the T trends is the increased atmospheric moisture during the spring and summer, which is at least partly influenced by vegetation transpiration during the growing season, along with increased evaporation caused by incoming solar energy during these months. The opposing signs of the average T_E and T trends in the spring and summer months do tend to contradict our hypothesis that T_E and T trends would have the same sign.

At this juncture, a valid concern could be raised, however, that if T and T_E values themselves are more similar during the non-growing season months, the trend magnitudes for T and T_E should also be more similar during these months. This is not what the results are showing. During the fall and winter, the trends in T_E are larger in magnitude than the

trends in T. The reason for this finding is not immediately clear. These results suggest that there may be some source of increasing moisture during the non-growing season that is not necessarily caused by seasonal variations in surface vegetation characteristics. If this is true, then this would suggest that surface moisture, and not land cover, is the driving influence behind surface heating trends (Trenberth, 2004).

The relatively higher number of significant trends in the winter (warming) and fall (cooling) as compared to the other seasons is interesting. In particular, it is unclear what exactly is causing the fall cooling. For cropland sites, fall cooling is plausibly caused by the higher surface albedos associated with post-harvest crop residues and bare soils that tend to reflect more solar radiation and thus suppress air temperatures (Bonan, 2001; Trenberth, 2004). The cooling observed for other land-cover classes, however, has yet to be explained. The same general seasonal pattern, including fall cooling, shows up in the plots of average T and T_E trends for almost all of the 11 land-cover classes covered in this study. It is unlikely, therefore, that the cropland phenomenon presented by Bonan (2001) and Trenberth (2004) provides the sole reason for the observed cooling. The winter months show warming for all land-cover classes except small-grains agriculture. During the spring and summer, results are not conclusively warm or cool.

The characteristics of the T and T_E trends for different land covers give mixed support (Figure 4.4, Table 4.7) for the initial surface hypothesis presented in Chapter 1. Forests and most agricultural areas show T and T_E trends that are of the same sign, showing general cooling, with the T_E trends being the larger of the two. This seems to be consistent with the negative trends in q (drying) observed for most of these land-cover classes (Figure 4.5), which would cause T_E trends to show relatively more cooling or less

warming compared to T trends. The results from grassland and shrubland sites also support our initial surface hypothesis, as the trends of T and T_E are again of the same sign with the T_E trends being larger than those of T. For these two land-cover classes, however, there are positive trends in q (moistening) over time, which will cause T_E trends to show relatively more warming or less cooling compared to T trends. Other land covers, however, have patterns that run contrary to our hypothesis. Urban and water sites generally show a warming in T_E but a cooling in T, with the only exceptions being during the fall and winter months. This investigation gives support to the ideas of Kalnay and Cai (2003) that land cover exerts a major influence on heating trends. In their study, shrubs with bare soil showed the largest warming trends and the trends for the broadleaf evergreen and deciduous forests had the least warming/most cooling. These results are similar to the findings in Figure 4.4, where land covers associated with drier regions like grasslands and shrublands had the warmest heating trends but forests generally had the coolest heating trends.

The results from the investigation of individual urban-rural pairs (Figures 4.8 – 4.17, Table 4.14) illustrate the possible influence of a site's land-cover characteristics on its T and T_E trends, both overall and as a function of season. Just as when all sites are considered, fall cooling and winter warming are observed to some degree for all of the urban-rural pairs analyzed in this study, with local exceptions. For example, one may consider the winter and spring cooling observed at Minot, North Dakota (Figure 4.13). Snow is common in Minot during the winter and early spring, so trends in the presence or absence of snow will presumably have a large influence on the cooling trends in both T and T_E that are observed during the winter and early spring. The sudden onset of

warming trends for June may be caused by the vegetation greenup during the late spring. In Miami, Florida (Figure 4.15), the tendency of warming trends to persist into the spring and summer months. This lingering warming stands out noticeably from the general patterns observed for the entire surface dataset which indicate winter warming and fall cooling, with mixed results for the spring and summer. The seasonal behavior of the heating trends in Miami may be somehow related to Miami's subtropical climate and the fact that the overall patterns that have been identified are largely influenced by the patterns observed at sites with more temperate climates, which are more common in the surface dataset used for this study.

In summary, the main findings from this chapter are as follows:

- Overall, T_E exhibits significantly more warming/less cooling than does T.
- Overall, the magnitude of the T_E trends is not greater than that of the T trends. Seasonally, however, particularly during the fall and winter months, T_E trends are greater in magnitude than the corresponding T trends. The trends for T_E are also generally greater than the T trends for each NLCD land-cover class.
- There is a clear seasonal transition for the surface heating trends through a given year, from the winter months, which show warming trends, into the fall months, which show cooling trends.
- During the fall and winter, the heating trends for T_E and T are of the same sign. For the spring and summer, however, they are of opposing sign.
- Comparing urban and rural stations, urban stations have significantly more warming and/or less cooling than the rural stations, for both T_E and T.
- Land cover and site microclimate have a large influence on local heating trends.

Table 4.1. Land cover classes from the National Land Cover Dataset (NLCD – Vogelmann et al., 2001).

Land Cover Class	Description
1	Deciduous Forest
2	Evergreen Forest
3	Mixed Forest
4	Grassland
5	Shrubland
6	Row Crops
7	Small Grains
8	Pasture/Hay
9	Urban
10	Water
11	Other - ice/snow, bare surfaces, wetlands, orchards

Table 4.2. Listing of stations in the urban-rural site pairings shown in Figure 4.2.

City	Urban Site	Rural Site
Oklahoma City, OK	Tinker Air Force Base	Will Rogers World Airport
Miami, FL	New Tamiami Airport	Homestead Air Force Base
Minot, ND	Minot Air Force Base	Minot International Airport
Valparaiso, FL	Eglin Air Force Base	Hurlburt Field
Washington, DC	National Airport	Fort Belvoir, Virginia

Table 4.3. Annually-averaged 1982-1997 equivalent temperature (T_E) and temperature (T) trends, with associated Z test statistic values testing whether or not the trends are significantly different from zero – see Appendix A for definition. Trend significance > 90% if $|Z| > 1.65$, significance > 95% if $|Z| > 1.96$, and significance > 99% if $|Z| > 2.58$). Also shown are the Z values for the difference between the T_E and T trends (same significance thresholds as above), for all individual trends and individual trends that are significant at or above the 90%, 95%, and 99% significance levels.

Significance Level	ΔT_E (°C/year)	$Z(\Delta T_E)$	ΔT (°C/year)	$Z(\Delta T)$	$Z(\Delta T_E - \Delta T)$
All Trends	0.00 ± 0.22	-0.03	-0.02 ± 0.11	-10.97	4.83
>90%	0.05 ± 0.37	3.34	-0.06 ± 0.17	-8.72	6.66
>95%	0.09 ± 0.39	3.52	-0.07 ± 0.19	-6.08	5.73
>99%	0.15 ± 0.43	2.84	-0.04 ± 0.22	-1.94	3.38

Table 4.4. Z test statistic values, calculated as in Table 4.3, for seasonally-averaged (winter, spring, summer, fall) equivalent temperature (T_E) and temperature (T) trends, 1982-1997, for all individual trends and individual trends that are significant at or above the 90%, 95%, and 99% significance levels. Significance criteria are as in Table 4.3. Missing Z values, indicated by "M", are for those averages where the sample size was less than 10.

T_E				
Season	**All Trends**	**>90%**	**>95%**	**>99%**
Winter (JFM)	12.99	11.89	9.45	M
Spring (AMJ)	5.01	3.97	3.56	1.21
Summer (JAS)	1.71	4.29	3.62	4.59
Fall (OND)	-19.88	-23.56	-26.71	M
T				
Season	**All Trends**	**>90%**	**>95%**	**>99%**
Winter (JFM)	9.90	7.60	5.15	M
Spring (AMJ)	-5.92	-0.39	0.67	0.55
Summer (JAS)	-14.92	-12.35	-9.99	-5.68
Fall (OND)	-14.82	-27.89	-14.91	M

Table 4.5. Z test statistic values for seasonally-averaged (winter, spring, summer, fall) differences between the equivalent temperature (T_E) and temperature (T) trends, 1982-1997, for all individual trends and individual trends that are significant at or above the 90%, 95%, and 99% significance levels. See Appendix A for calculation. Significance criteria are identical to those specified in Table 4.3.

Season	**All Trends**	**>90%**	**>95%**	**>99%**
Winter (JFM)	6.31	5.36	3.69	3.40
Spring (AMJ)	6.90	3.66	2.69	3.68
Summer (JAS)	7.39	8.05	6.49	32.89
Fall (OND)	-9.81	-10.27	-10.14	-33.85

Table 4.6. Z test statistic values for both annually-averaged and seasonally-averaged T_E and T trends (1982-1997) as a function of the land-cover classes in Table 4.1. The calculation of the Z values and the corresponding significance criteria are identical to those specified in Table 4.3. All trends are included in these calculations.

T_E					
Land Cover Class	**Annual**	**JFM**	**AMJ**	**JAS**	**OND**
Deciduous Forest	-5.24	1.27	-0.93	-2.91	-10.20
Evergreen Forest	-1.69	3.18	-0.25	0.70	-9.99
Mixed Forest	-0.24	0.51	-0.01	1.87	-5.65
Grassland	2.91	1.16	3.12	1.88	-0.08
Shrubland	3.13	4.65	4.10	0.70	-0.65
Row Crops	-4.24	3.03	-0.85	-4.40	-6.68
Small Grains	-0.11	-0.68	0.22	0.28	-0.05
Pasture/Hay	-3.05	3.18	0.57	-2.22	-8.81
Urban	3.31	11.34	5.62	3.82	-13.30
Water	3.24	4.37	2.69	3.13	-2.47
Other	0.62	3.19	1.62	0.89	-4.16
T					
Land Cover Class	**Annual**	**JFM**	**AMJ**	**JAS**	**OND**
Deciduous Forest	-7.35	0.47	-2.09	-6.34	-8.96
Evergreen Forest	-2.43	2.75	-1.31	-0.98	-9.84
Mixed Forest	-1.04	0.18	0.04	0.24	-5.17
Grassland	0.39	1.53	0.43	-3.08	1.53
Shrubland	2.97	4.20	0.71	-0.10	1.75
Row Crops	-6.08	2.97	-4.72	-8.52	-4.16
Small Grains	-3.04	-0.80	-2.12	-4.37	0.67
Pasture/Hay	-6.20	3.07	-3.60	-8.23	-6.30
Urban	-5.82	8.37	-2.18	-8.89	-10.63
Water	-0.84	2.77	-1.91	-0.48	-2.80
Other	0.12	3.00	0.12	0.45	-3.66

Table 4.7. Z test statistic values, calculated as in Table 4.5, for both annually-averaged and seasonally-averaged differences between T_E and T trends (1982-1997) as a function of the land-cover classes in Table 4.1. Significance criteria are identical to those specified in Table 4.3. All trends are included in these calculations.

Land Cover Class	Annual	JFM	AMJ	JAS	OND
Deciduous Forest	-1.04	0.79	0.06	0.32	-4.20
Evergreen Forest	-0.49	1.41	0.34	0.98	-5.10
Mixed Forest	0.32	1.20	-0.22	9.65	-23.46
Grassland	2.20	0.08	2.42	3.27	-0.90
Shrubland	1.72	16.84	19.70	4.84	-5.26
Row Crops	-0.95	1.21	1.01	-0.35	-3.59
Small Grains	1.73	-0.82	7.78	20.60	-2.62
Pasture/Hay	0.07	1.21	1.84	0.98	-4.03
Urban	5.48	5.83	6.03	6.75	-6.27
Water	3.33	15.49	18.66	16.50	-5.91
Other	0.51	1.39	1.40	0.69	-2.20

Table 4.8. Z test statistic values for annually-averaged q trends (1982-1997) as a function of the land-cover classes in Table 4.1. The calculation of the Z values and the corresponding significance criteria are identical to those specified in Table 4.3. All trends are included in these calculations.

Land Cover Class	All Trends
Deciduous Forest	-2.39
Evergreen Forest	-1.10
Mixed Forest	0.67
Grassland	3.99
Shrubland	2.55
Row Crops	-2.70
Small Grains	3.21
Pasture/Hay	0.72
Urban	9.40
Water	4.61
Other	0.87

Table 4.9. Percentages of individual trends of T and T_E that are significant at the significance levels of 90%, 95%, and 99%, for each land cover class in Table 4.1.

T			Land Cover Class	T_E		
>90%	>95%	>99%		>90%	>95%	>99%
4.8	2.4	0.7	Deciduous Forest	9.9	5.5	0.3
2.6	2.6	2.6	Evergreen Forest	7.1	2.6	0
9.4	5.7	1.9	Mixed Forest	16.7	9.3	1.9
5.9	3.3	1.3	Grassland	9.3	4.0	1.3
6.8	4.5	4.5	Shrubland	6.8	4.5	2.3
12.1	5.9	1.2	Row Crops	10.7	4.0	0.7
9.5	1.1	1.1	Small Grains	11.6	8.4	4.2
8.8	5.1	1.3	Pasture/Hay	8.6	3.5	0.8
8.5	4.1	0.8	Urban	8.9	4.6	1.0
4.2	4.2	1.1	Water	6.2	3.1	1.0
7.9	4.0	0.8	Other	4.8	3.2	0.8

Table 4.10. Number of years needed to detect the average trends of T and T_E presented in Figure 4.4, at the significance levels of 90%, 95%, and 99%, for each land cover class in Table 4.1.

T			Land Cover Class	T_E		
>90%	>95%	>99%		>90%	>95%	>99%
5	6	7	Deciduous Forest	6	7	9
9	9	12	Evergreen Forest	11	12	15
11	12	14	Mixed Forest	28	31	38
29	32	39	Grassland	8	8	10
5	5	7	Shrubland	5	5	7
7	7	9	Row Crops	8	9	11
6	7	9	Small Grains	57	62	77
6	7	8	Pasture/Hay	10	11	14
11	12	15	Urban	16	18	22
15	16	20	Water	6	7	8
59	65	80	Other	20	22	27

Table 4.11. Z test statistic values of annually-averaged T_E and T trends (1982-1997) as a function of the land-cover classes in Table 4.1, looking at all trends and only trends that are significant at specified significance levels (90%, 95%). The calculation of the Z values and the corresponding significance criteria are identical to those specified in Table 4.3. Missing Z values, indicated by "M", are for those averages where the sample size was less than 10.

T_E			
Land Cover Class	**All Trends**	**>90%**	**>95%**
Deciduous Forest	-5.24	-2.78	-1.31
Evergreen Forest	-1.69	0.04	0.80
Mixed Forest	-0.24	M	M
Grassland	2.91	1.82	0.63
Shrubland	3.13	1.92	M
Row Crops	-4.24	-1.87	-0.33
Small Grains	-0.11	M	M
Pasture/Hay	-3.05	-2.23	-1.59
Urban	3.31	5.24	4.11
Water	3.24	5.04	M
Other	0.62	2.47	M
T			
Land Cover Class	**All**	**>90%**	**>95%**
Deciduous Forest	-7.35	-4.30	-8.96
Evergreen Forest	-2.43	-1.37	-9.84
Mixed Forest	-1.04	M	-5.17
Grassland	0.39	-0.69	1.53
Shrubland	2.97	2.22	1.75
Row Crops	-6.08	-5.59	-4.16
Small Grains	-3.04	-3.88	0.67
Pasture/Hay	-6.20	-7.22	-6.30
Urban	-5.82	-4.95	-10.63
Water	-0.84	0.14	-2.80
Other	0.12	1.86	-3.66

Table 4.12. Z test statistic values, calculated as in Table 4.5, for annually-averaged differences between T_E and T trends (1982-1997) as a function of the land-cover classes in Table 4.1. Calculations are made for all trends and for those trends that are significant at or above the 90% and 95% significance levels. Significance criteria are identical to those specified in Table 4.3. Missing Z values, indicated by "M", are for those averages where the sample size was less than 10.

Land Cover Class	All Trends	>90%	>95%
Deciduous Forest	-1.04	-0.89	1.00
Evergreen Forest	-0.49	1.65	1.63
Mixed Forest	0.32	M	M
Grassland	2.20	7.81	3.28
Shrubland	1.72	3.40	M
Row Crops	-0.95	0.26	3.36
Small Grains	1.73	M	M
Pasture/Hay	0.07	0.32	0.19
Urban	5.48	6.86	5.27
Water	3.33	16.95	M
Other	0.51	5.23	M

Table 4.13. Average T_E and T trends (1982-1997) for surface sites in the eastern United States, their respective Z test statistic values (calculated as in Table 4.3), and the associated Z values for the urban-rural and T_E - T differences in average trends.

	ΔT_E (°C/year)	$Z(\Delta T_E)$	ΔT (°C/year)	$Z(\Delta T)$	Z value ($\Delta T_E - \Delta T$)
Urban sites	0.02 ± 0.22	3.31	-0.01 ± 0.10	-5.82	5.48
Rural sites	-0.02 ± 0.22	-3.43	-0.03 ± 0.12	-9.58	1.36
Z value (U – R)	4.77	-	3.47	-	-

Table 4.14. Same as Table 4.13, but only for the 5 urban-rural site pairs considered in this chapter. Missing Z values, indicated by "M", are for those averages where the sample size was less than 10.

	ΔT_E (°C/year)	$Z(\Delta T_E)$	ΔT (°C/year)	$Z(\Delta T)$	Z value ($\Delta T_E - \Delta T$)
Urban sites	0.06 ± 0.24	M	-0.01 ± 0.12	M	1.90
Rural sites	0.06 ± 0.23	M	-0.01 ± 0.12	M	2.00
Z value (U – R)	0.04	-	-0.08	-	-

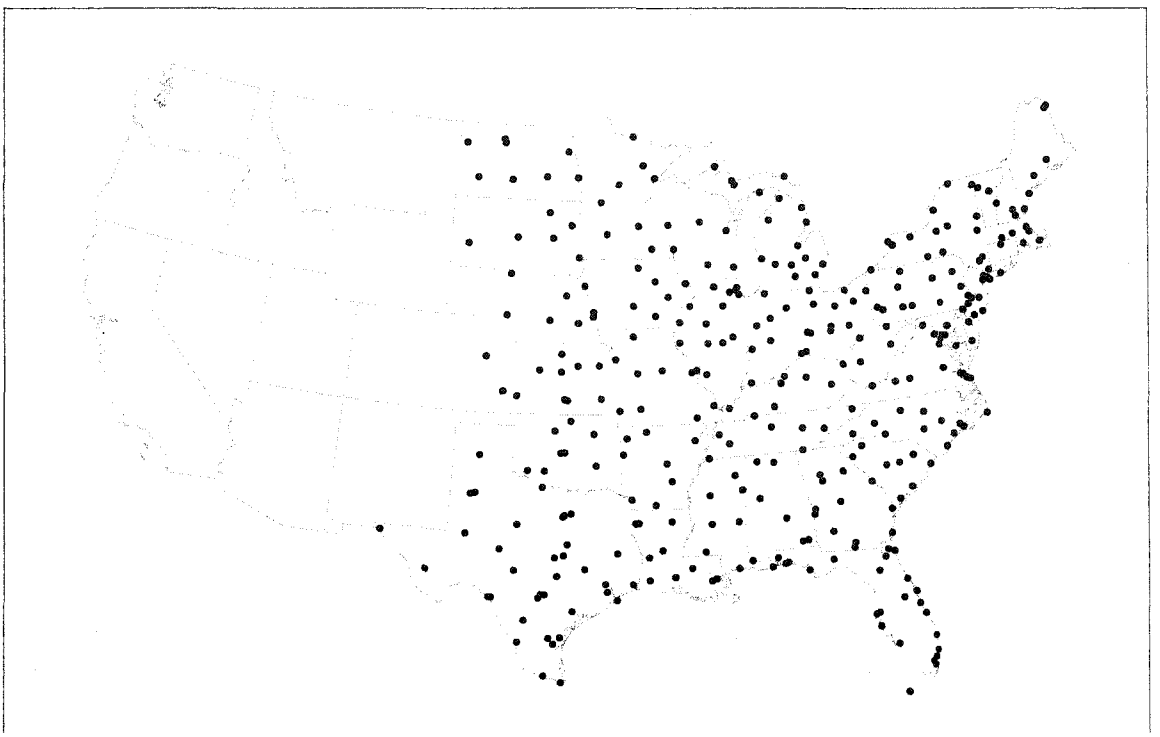

Figure 4.1. Locations of surface observation sites

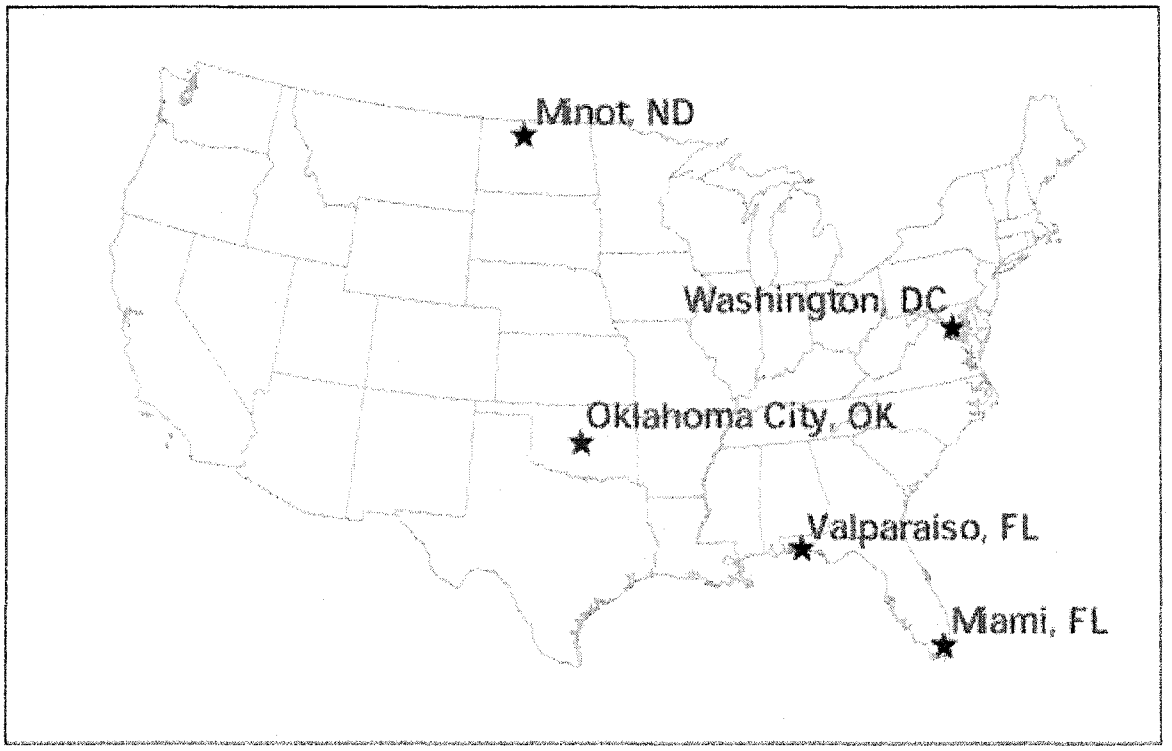

Figure 4.2. Locations of urban-rural site pairs

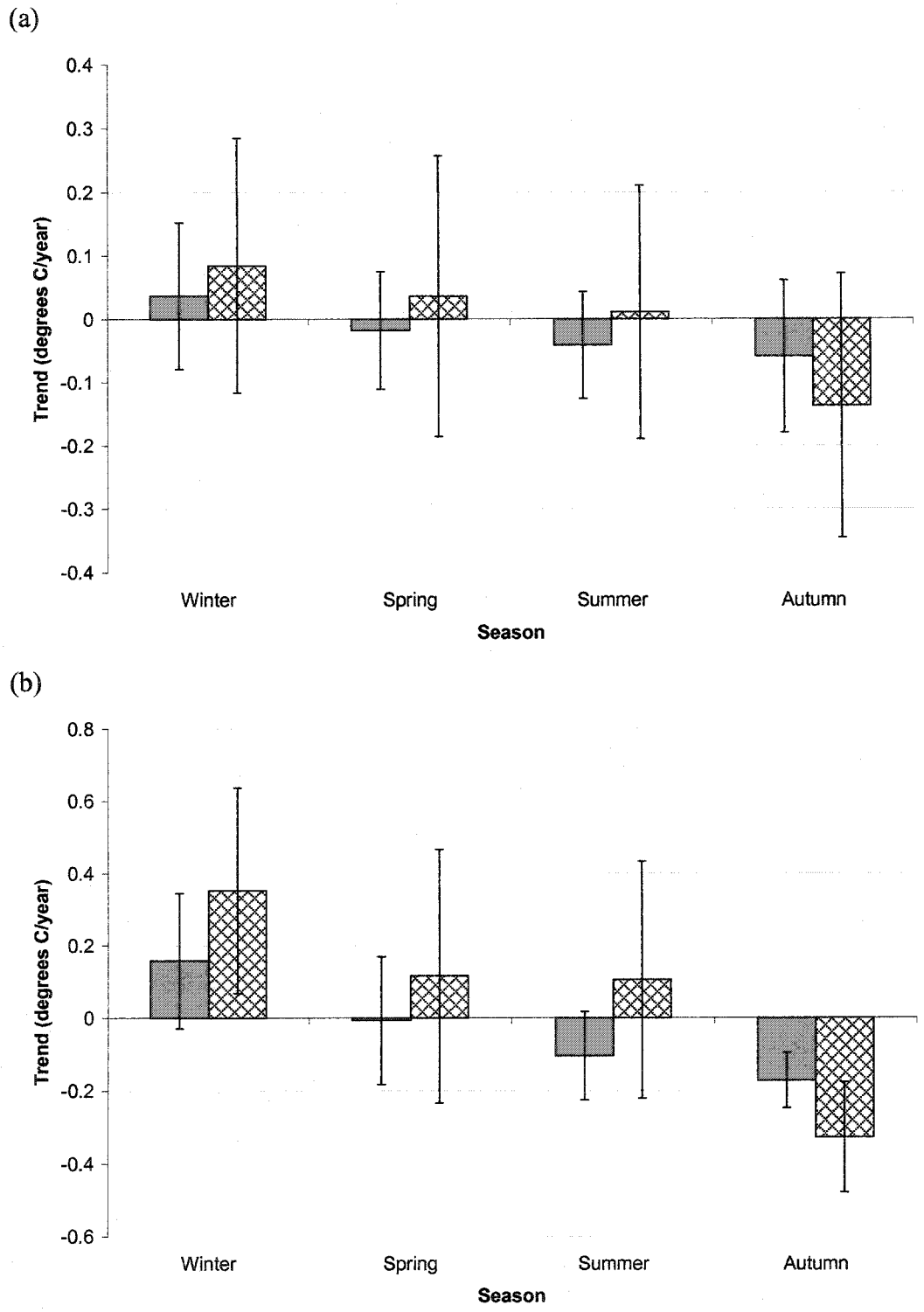

Figure 4.3. Seasonally-averaged 1982-1997 T trends (grey bars) and T_E trends (cross-hatched bars) for all individual trends (a), individual trends that are at least 90% significant (b), individual trends that are at least 95% significant (c), and individual trends that are at least 99% significant (d).

(c)

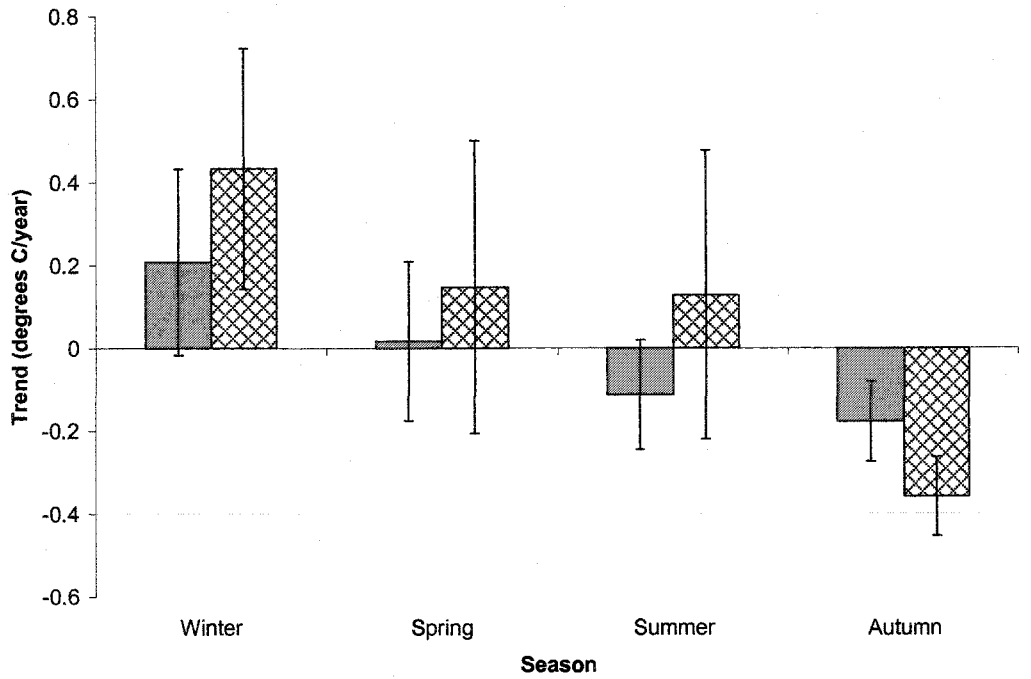

(d)

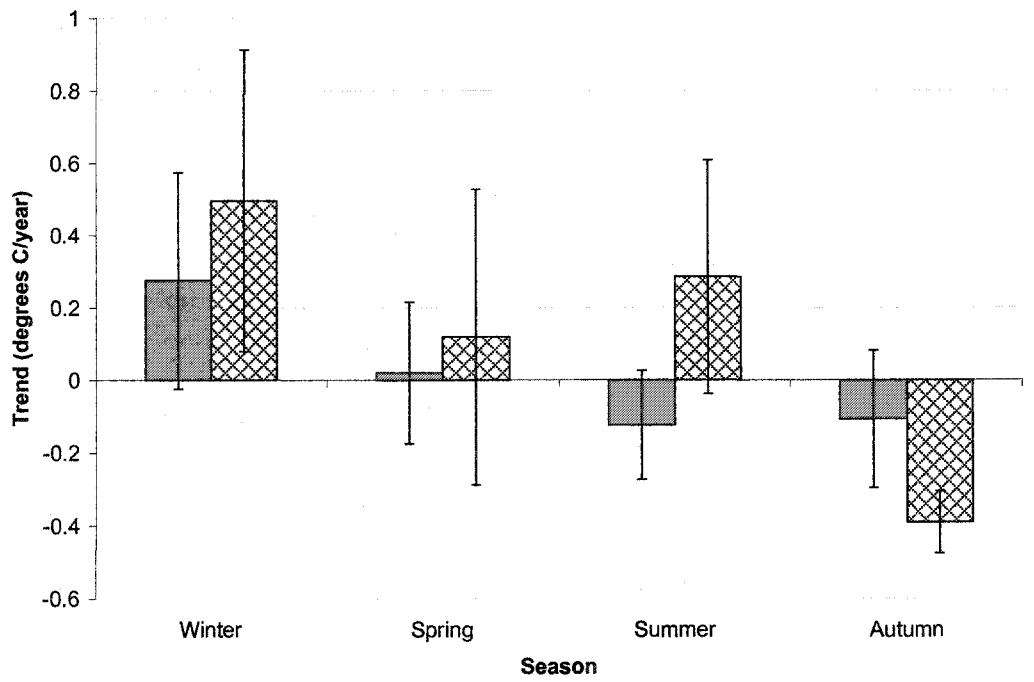

Figure 4.3. (continued)

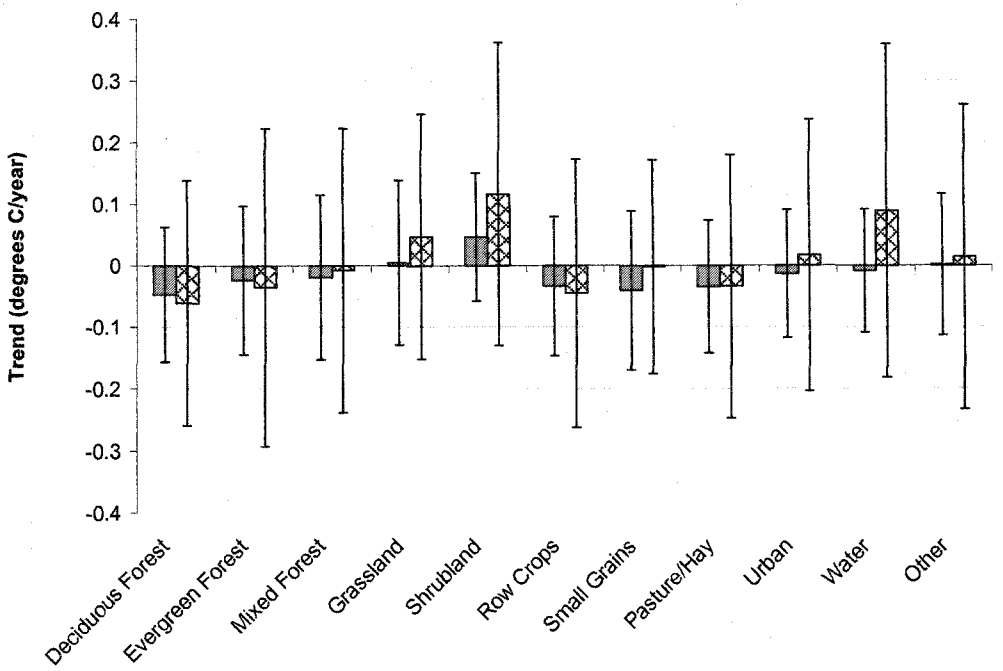

Figure 4.4. Annually-averaged T trends (grey bars) and T_E trends (cross-hatched bars) for 1982-1997, as a function of the land-cover classes listed in Table 4.1. All individual trends are considered.

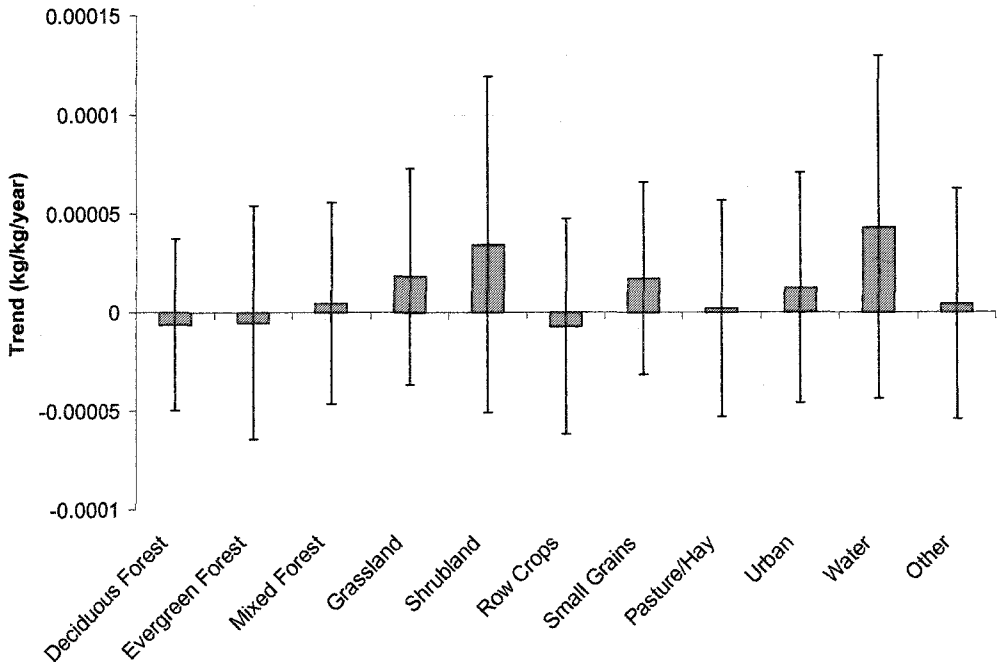

Figure 4.5. Annually-averaged q trends for 1982-1997, as a function of the land-cover classes listed in Table 4.1. All individual trends are considered.

(a)

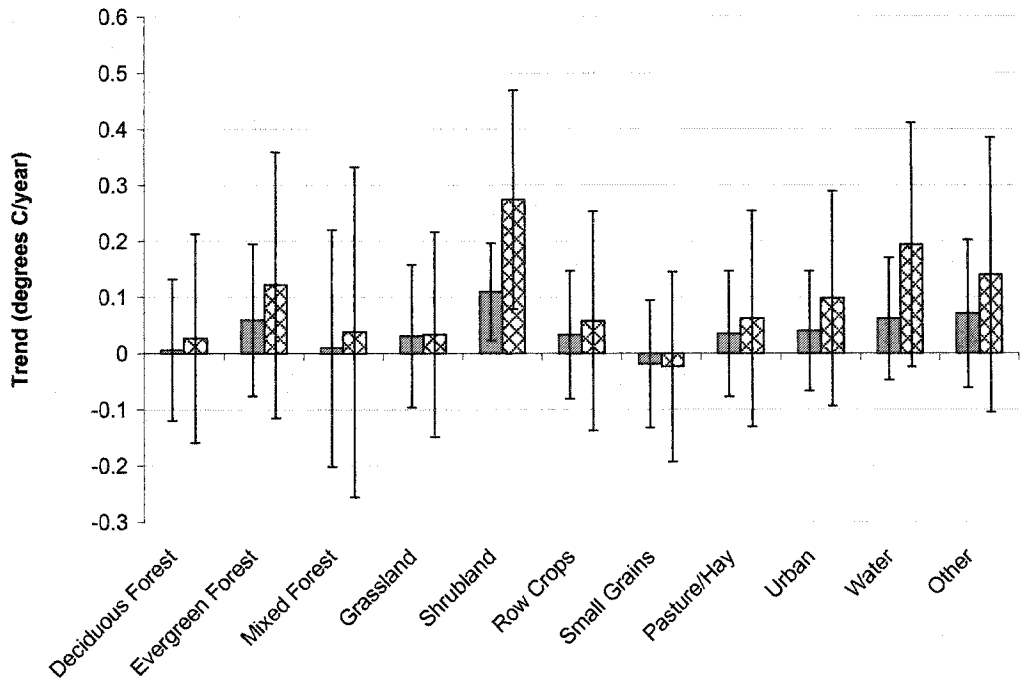

(b)

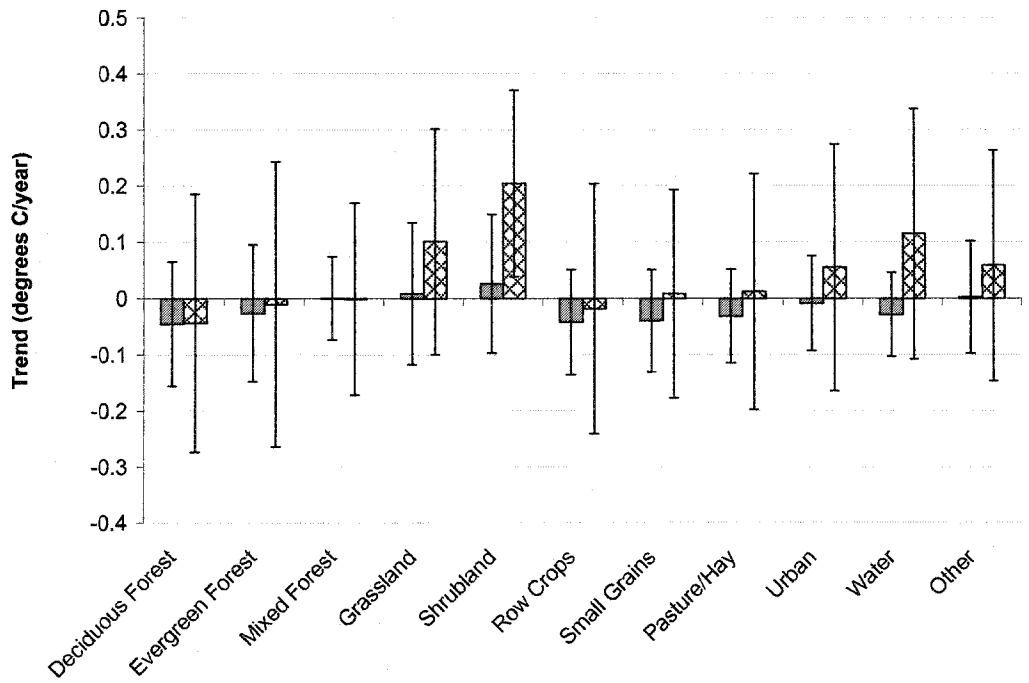

Figure 4.6. Seasonally-averaged T trends (grey bars) and T_E trends (cross-hatched bars) for 1982-1997, as a function of the land-cover classes listed in Table 4.1, for (a) winter, (b) spring, (c) summer, and (d) fall months.

(c)

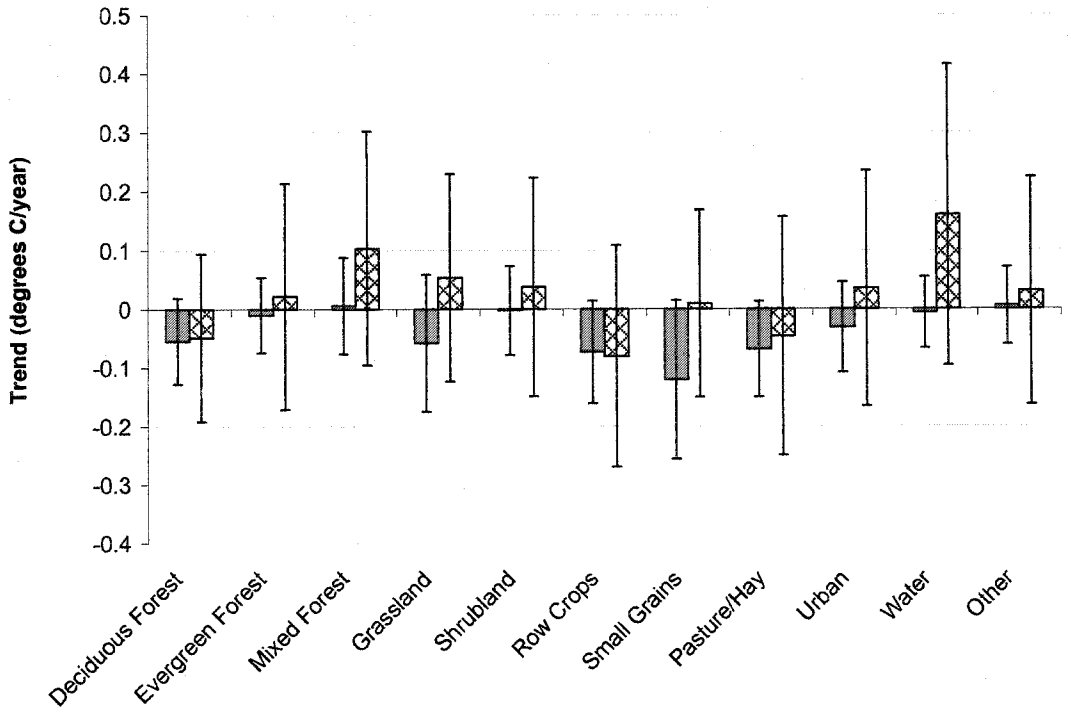

(d)

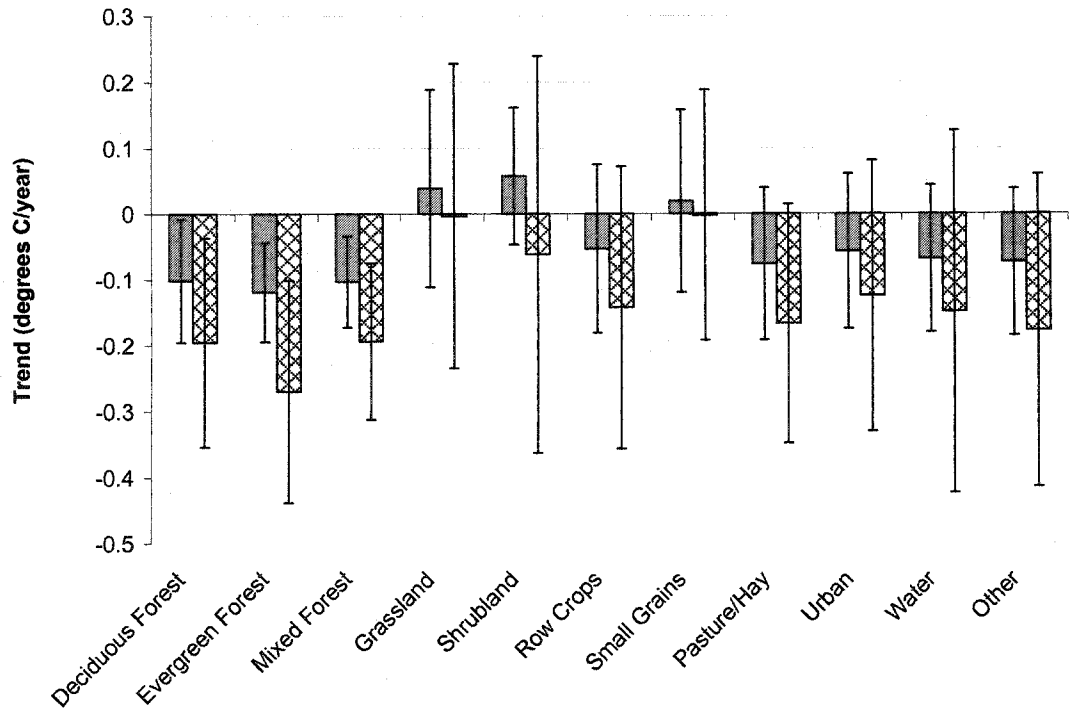

Figure 4.6. (continued)

(a)

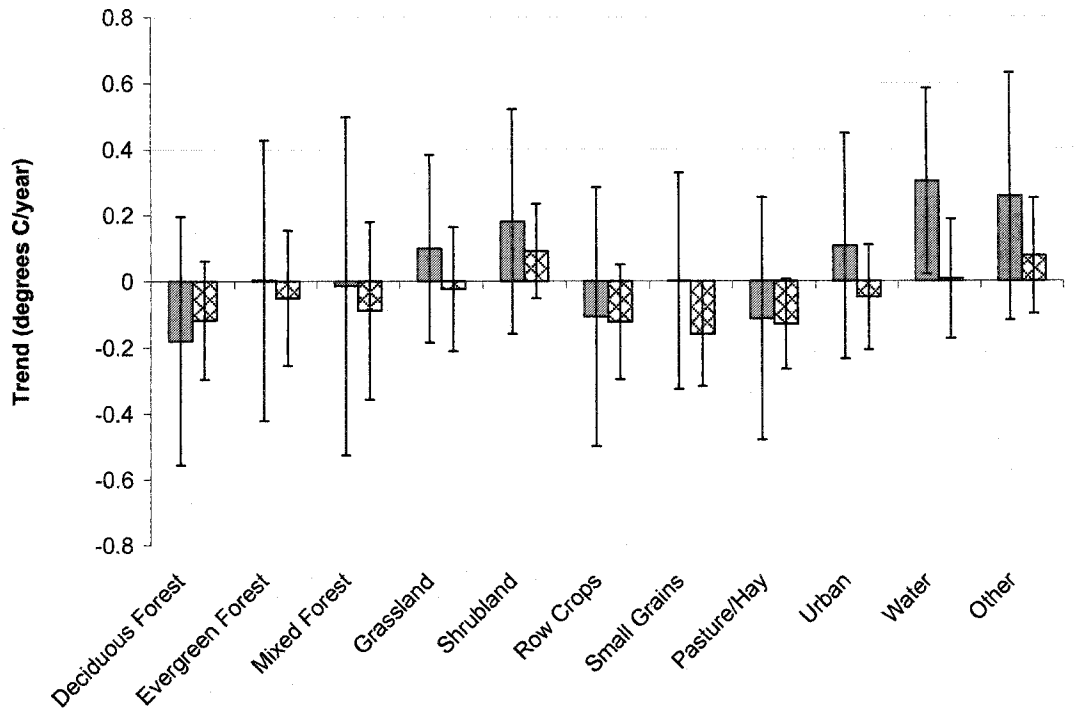

(b)

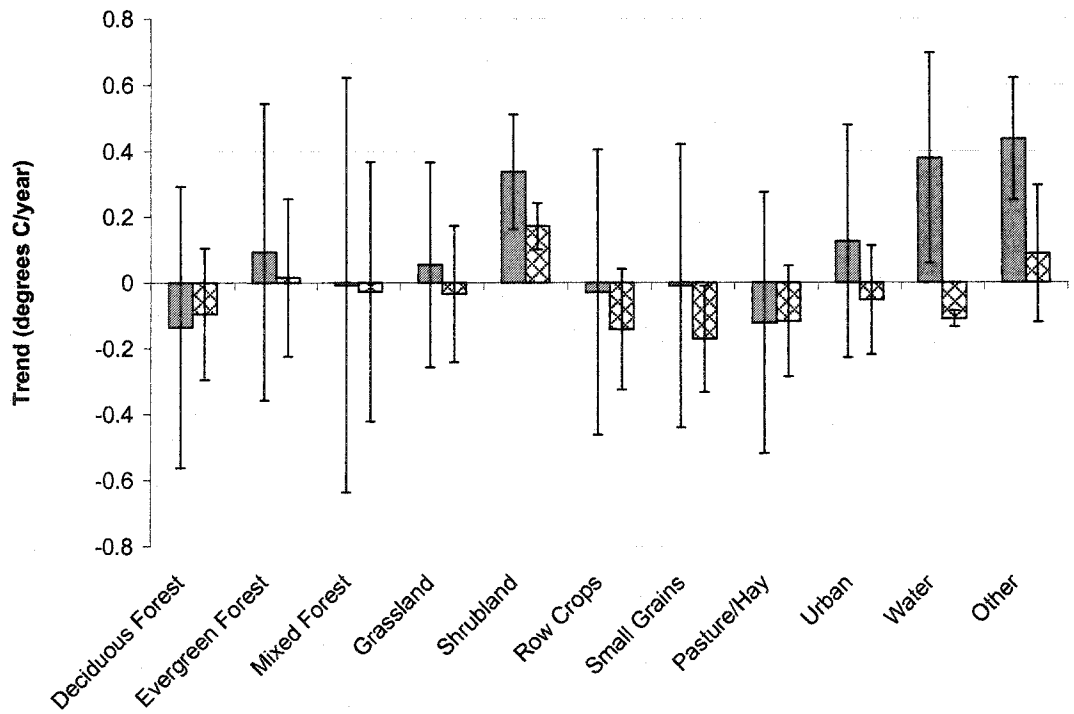

Figure 4.7. Annually-averaged T trends (grey bars) and T_E trends (cross-hatched bars) for 1982-1997, as a function of the land-cover classes listed in Table 4.1, for individual trends that are at least 90% significant (a) and individual trends that are at least 95% significant (b).

(a)

9	10	9
9	10	9
10	10	9

(b)

9	1	9
9	9	1
1	1	1

Figure 4.8. Land-cover characteristics for National Airport (a) and Fort Belvoir, Virginia (b), using the land-cover classifications in Table 4.1. Each cell has a resolution of 1 km.

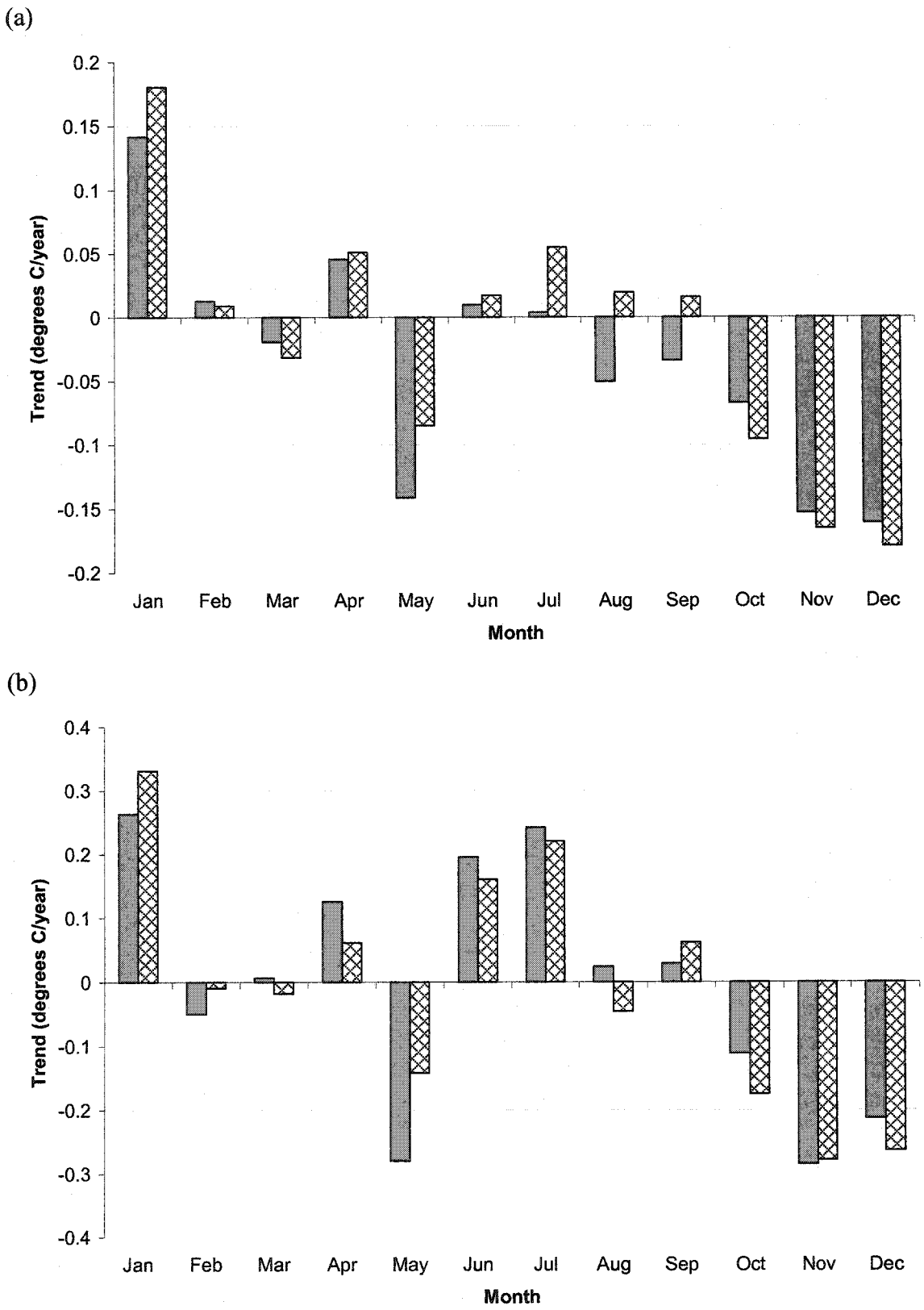

Figure 4.9. T trends (a) and T_E trends (b) during 1982-1997 for National Airport (grey bars) and Fort Belvoir, Virginia (cross-hatched bars).

(a)

9	9	8
9	9	8
9	4	4

(b)

4	4	4
9	9	4
9	4	4

Figure 4.10. Land-cover characteristics for Tinker Air Force Base (a) and Will Rogers World Airport (b), using the land-cover classifications in Table 4.1. Each cell has a resolution of 1 km.

(a)

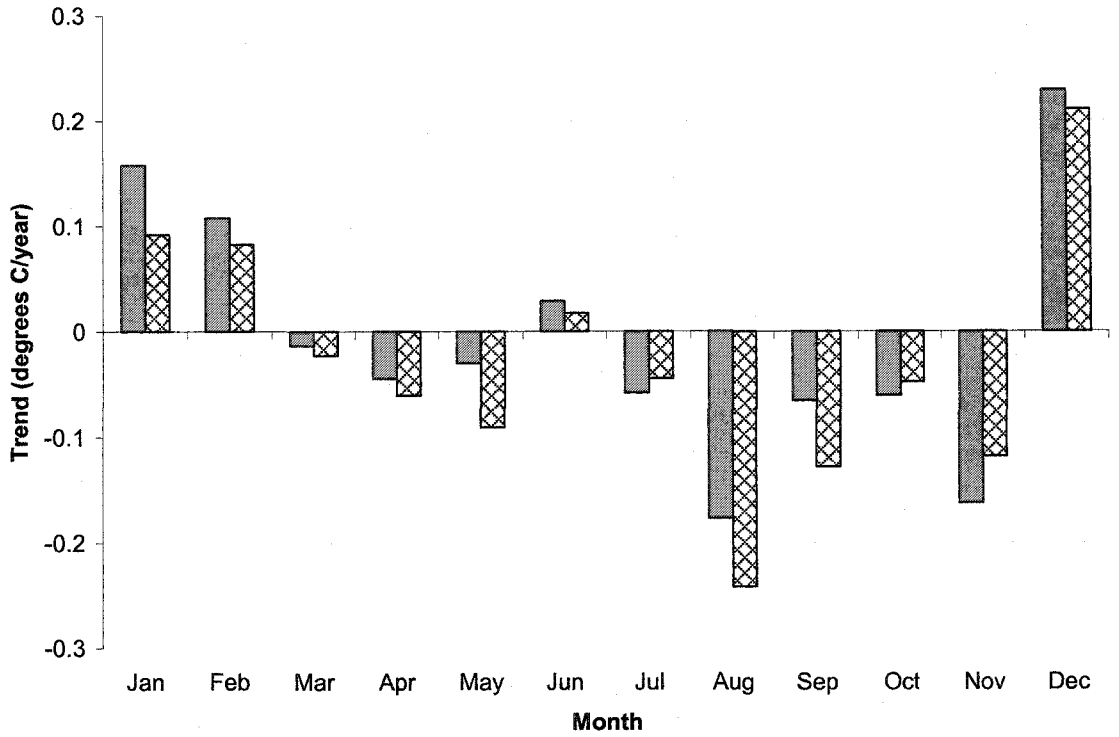

(b)

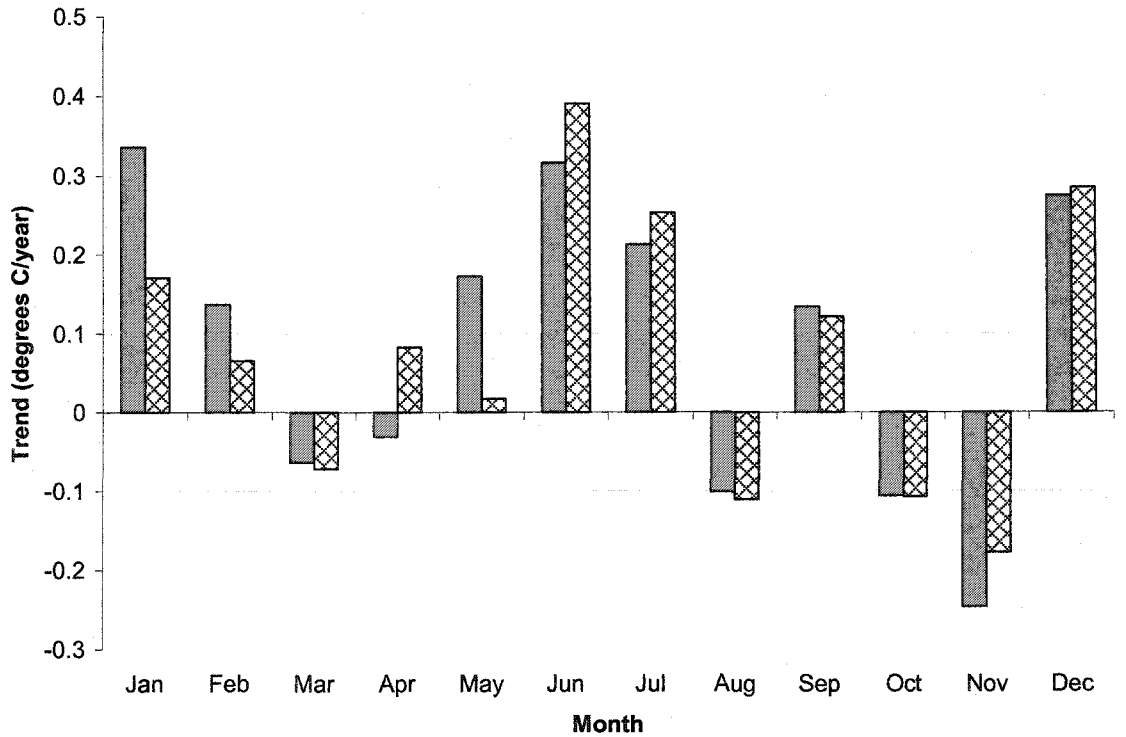

Figure 4.11. T trends (a) and T_E trends (b) during 1982-1997 for Tinker Air Force Base (grey bars) and Will Rogers World Airport (cross-hatched bars).

(a)

9	9	9
9	9	9
9	9	9

(b)

7	7	7
9	7	7
9	7	7

Figure 4.12. Land-cover characteristics for Minot Air Force Base (a) and Minot International Airport (b), using the land-cover classifications in Table 4.1. Each cell has a resolution of 1 km.

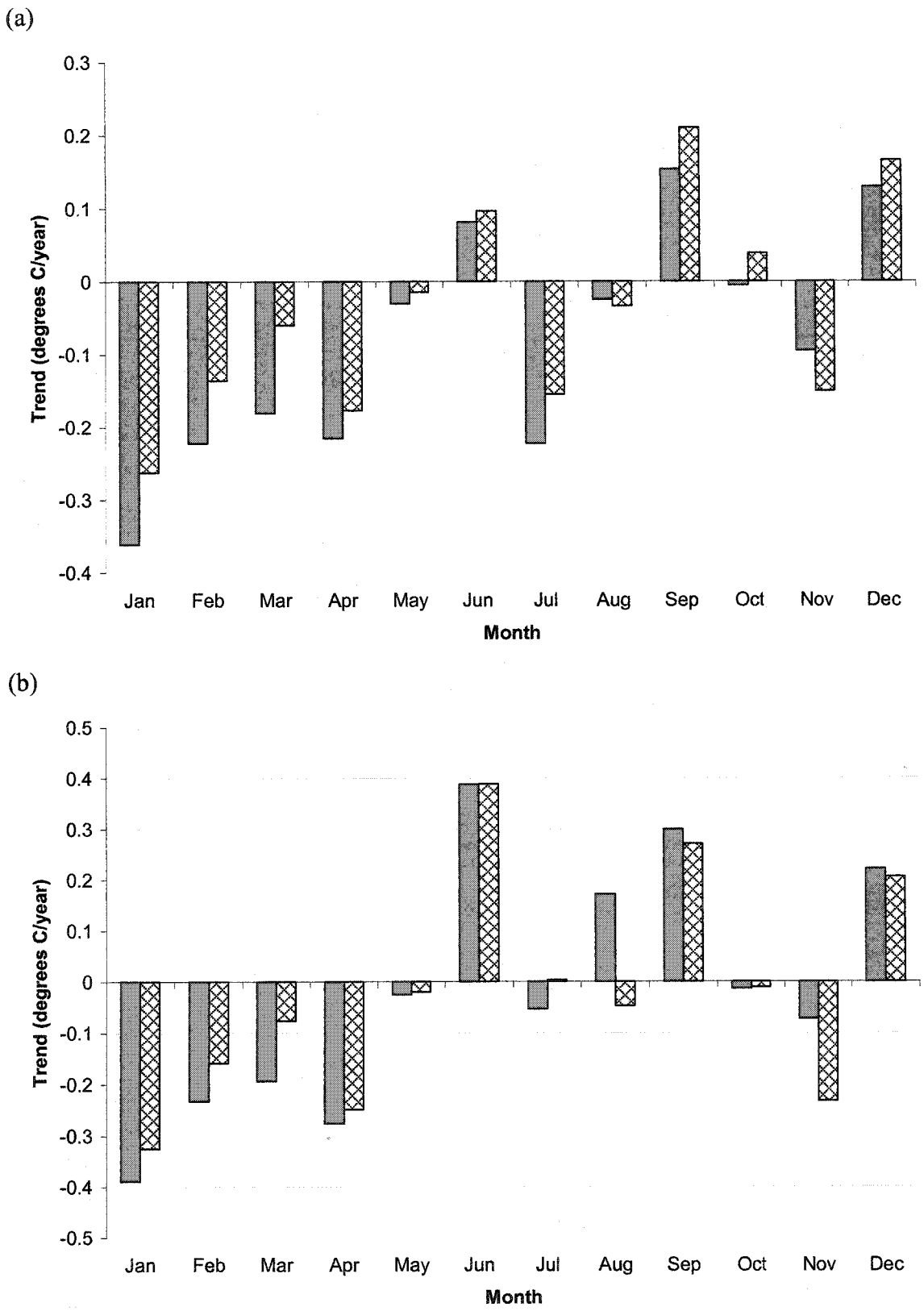

Figure 4.13. T trends (a) and T_E trends (b) during 1982-1997 for Minot Air Force Base (grey bars) and Minot International Airport (cross-hatched bars).

(a)

9	9	11
9	9	6
9	9	10

(b)

9	6	6
6	6	6
6	6	6

Figure 4.14. Land-cover characteristics for New Tamiami Airport (a) and Homestead Air Force Base (b), using the land-cover classifications in Table 4.1. Each cell has a resolution of 1 km.

(a)

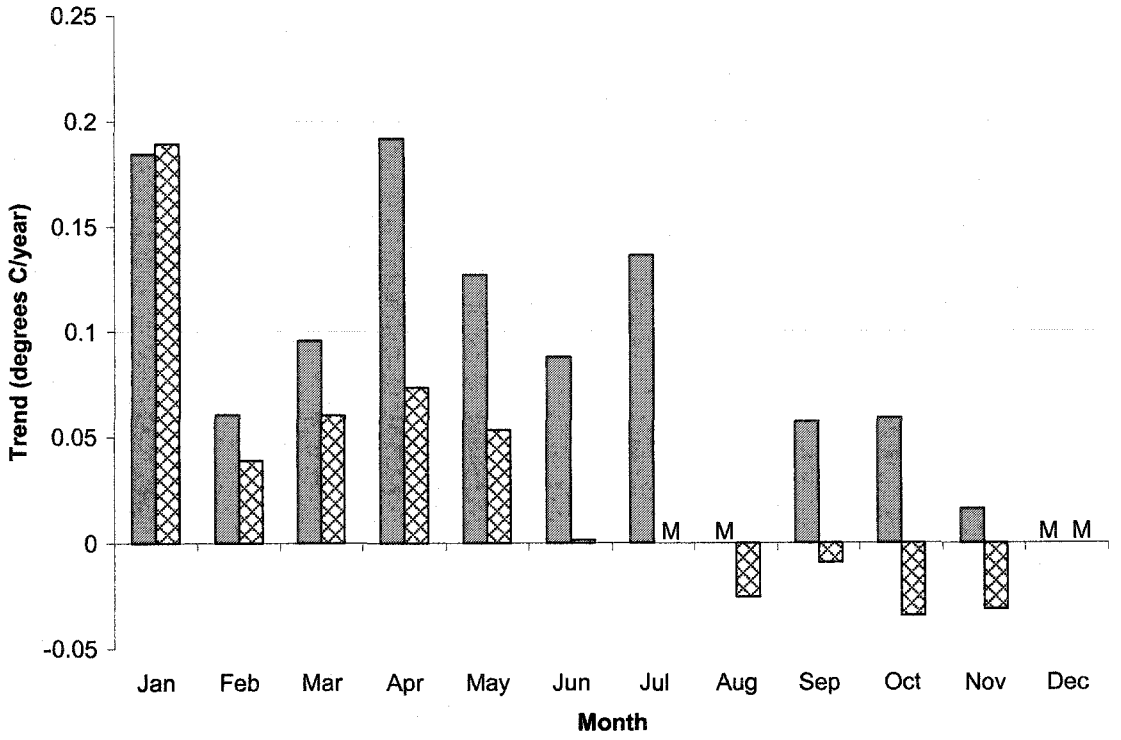

(b)

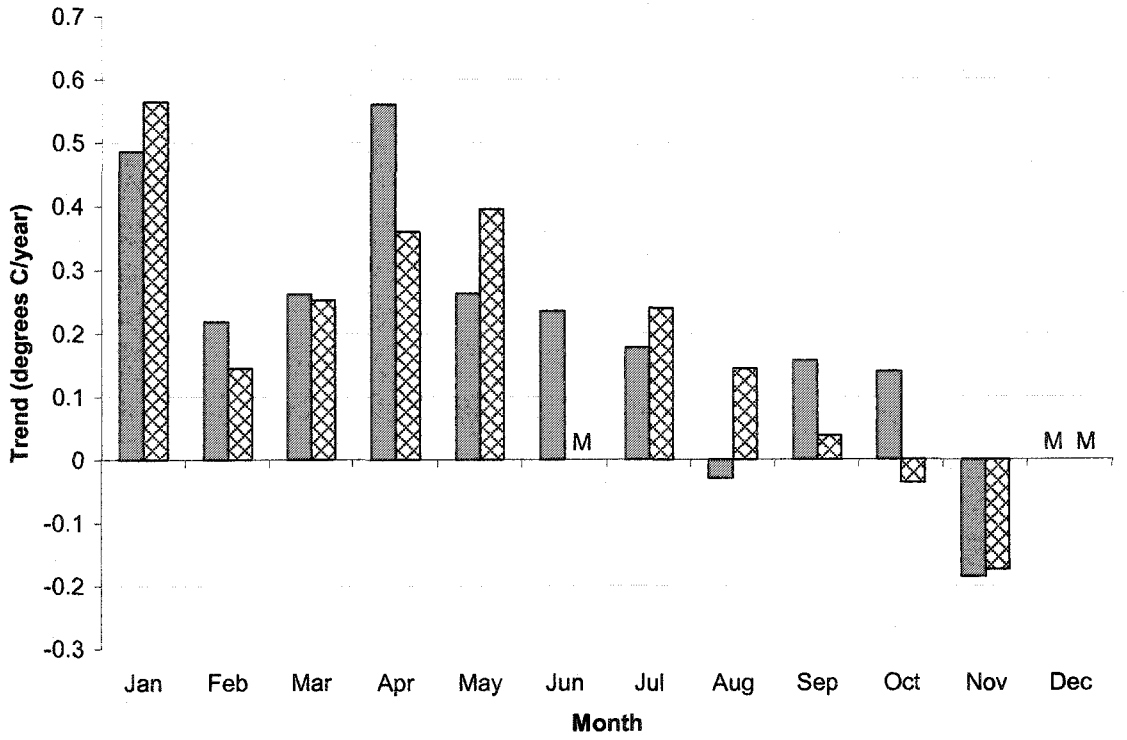

Figure 4.15. T trends (a) and T_E trends (b) during 1982-1997 for New Tamiami Airport (grey bars) and Homestead Air Force Base (cross-hatched bars).

(a)

9	9	9
9	9	9
9	2	9

(b)

11	11	2
9	11	11
11	11	9

Figure 4.16. Land-cover characteristics for Eglin Air Force Base (a) and Hurlburt Field (b), using the land-cover classifications in Table 4.1. Each cell has a resolution of 1 km.

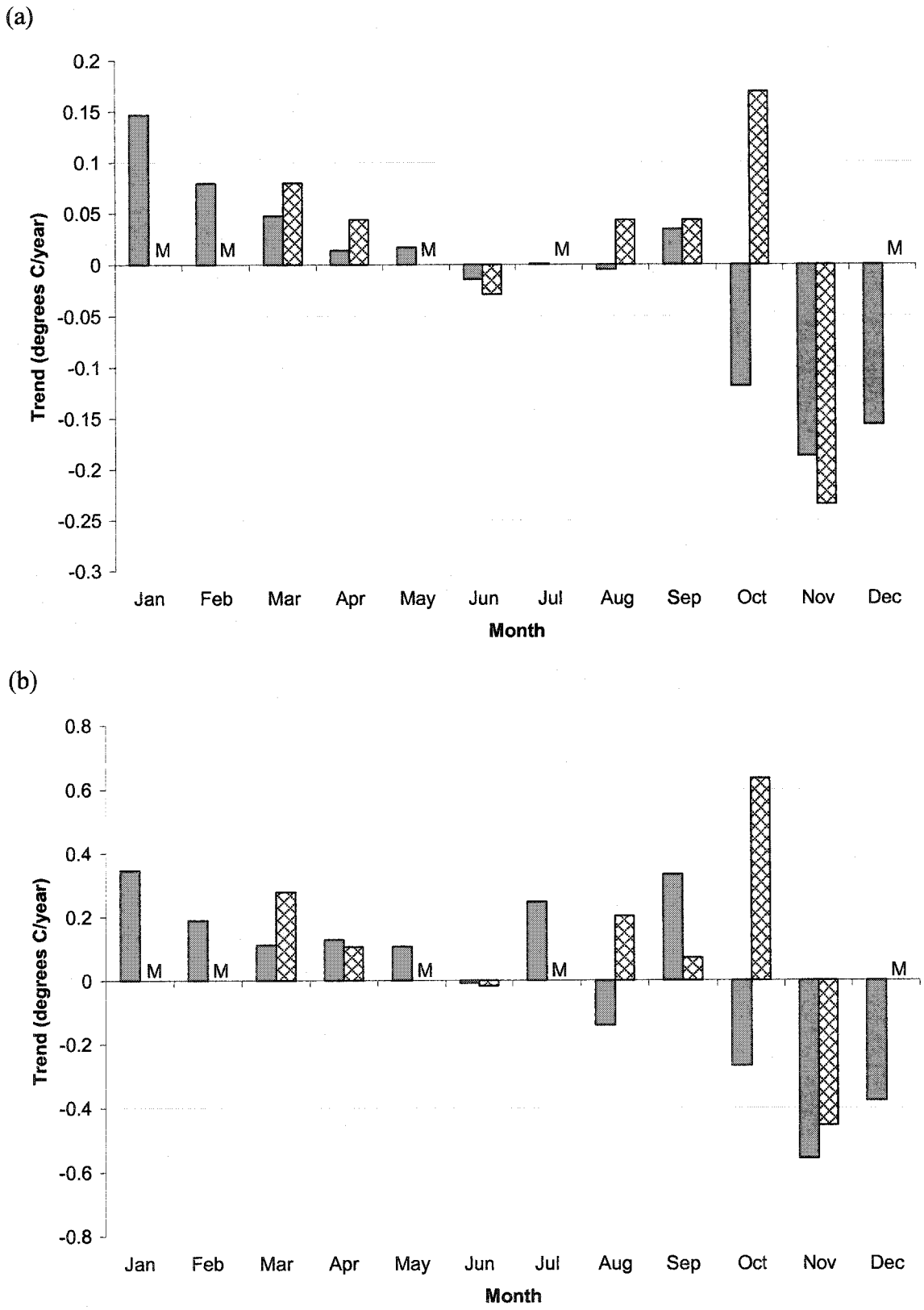

Figure 4.17. T trends (a) and T_E trends (b) during 1982-1997 for Eglin Air Force Base (grey bars) and Hurlburt Field (cross-hatched bars).

CHAPTER 5

TROPOSPHERIC TEMPERATURE AND THICKNESS TRENDS

Heating trends in the troposphere will now be considered, using temperature and thickness as metrics. As discussed in Chapter 1, debates continue regarding whether or not there is a discrepancy between the trends occurring at the surface versus those occurring in the troposphere. Hopefully, the following comparison of tropospheric heating trends in radiosonde and reanalysis datasets will help to shed some light on that issue.

5.1 Data

To investigate trends in temperature and thickness for the troposphere, radiosonde and operational forecast model reanalysis data were obtained for the years 1979-2001. As mentioned in Chapter 1, this study period has been selected because this is a period for which recent warming trends should emerge most clearly and also because this has been a period when global observations throughout the troposphere have become most reliable (Bengtssen et al., 1999). Monthly-averaged air temperatures and geopotential heights were computed from radiosonde and reanalyses datasets for selected sites around the world (Figure 5.1). The sites being considered here are all land-based, so this study does

not consider open-ocean areas. Appendix B includes a list of the stations for which these data were retrieved. The tropospheric levels of interest in this study are 1000, 850, 700, 500, 300, and 200 millibars.

The radiosonde data were obtained from the Comprehensive Aerological Reference Data Set (CARDS – Eskridge et al., 1995), which is maintained by the National Climatic Data Center in Asheville, North Carolina. The CARDS dataset used in this study was obtained from Dr. John Christy at the Earth System Science Center (ESSC) in Huntsville, Alabama, USA.

The two operational forecast model reanalysis datasets used in this study are the National Centers for Environmental Prediction (NCEP) Reanalysis product (Kalnay et al., 1996) and the European Centre for Medium-Range Weather Forecasts (ECMWF) 40-year reanalysis product (ERA40 – Simmons and Gibson, 2000). The NCEP reanalysis data was provided by Dr. Thomas Chase at the Cooperative Institute for Research in Environmental Sciences in Boulder, Colorado, USA. The ERA40 dataset was obtained directly from the ECMWF Hadley Centre's on-line dataserver. Both reanalysis datasets are available at a grid resolution of 2.5°.

5.2 Methods

5.2.1 Data Extraction

5.2.1a CARDS

The Climatological Averaging of Temperature Soundings (CATS) program, designed and maintained by ESSC (Norris, 2002), was used to extract data from the CARDS radiosonde dataset. The CATS program is written in Fortran 90 and is intended

for use on UNIX system platforms. It is originally designed to extract radiosonde temperature data at specific pressure levels and then compute either monthly or pentadic (5-day) averages of these daily temperatures. The user is prompted to specify a list of sounding sites, the processing period, the minimum number of daily observations to make a monthly or pentadic average (usually 28 and 5, respectively), the release time (00GMT, 12GMT, or both), and a list of pressure levels to retrieve data from. By default, the program computes these averages for a set of mandatory pressure levels (Table 5.1), but it has the option of computing the averages for a user-specified set of pressure levels. This study utilizes the mandatory pressure level set provided in the CATS software package. The user is asked to specify if the data to be processed are to be represented as actual values or as anomalies (compared to the average value for the user-specified processing period).

For this study, the CATS program was run on the CARDS dataset to retrieve daily radiosonde temperature (T) data and then use these data to compute monthly averages for the period of 1979-2001. These data were obtained for each of the mandatory pressure levels (Table 5.1) but only the pressure levels at 1000, 850, 700, 500, 300, and 200 millibars were analyzed. After temperatures were retrieved, CATS was modified and then used again on the above two radiosonde datasets to obtain monthly-averaged geopotential heights from 1979-2001, at the levels just mentioned. Thicknesses were then computed from the geopotential heights for the 1000-200mb layer, the 1000-500mb layer, and the 700-500mb layer.

Thickness values provide an excellent way to track layer-averaged temporal warming/cooling trends. This is because for a given atmospheric layer, its thickness

values are proportional to the mean temperature of that layer. To show that this is true, it is useful to note that the ideal gas law, $p = \rho RT$, and the hydrostatic equation, $dp/dz = -\rho g$, can be combined to give the relation

$$dz = \frac{RT}{g}\frac{dp}{p}, \tag{5.1}$$

which can be integrated between pressure levels p_1 and p_2 to give

$$D = \frac{R}{g}\int_{p_2}^{p_1} T\frac{dp}{p} = \frac{R\overline{T}_v}{g}\ln\left(\frac{p_1}{p_2}\right), \tag{5.2}$$

where D is the thickness of the atmospheric layer between pressure levels p_1 and p_2.

5.2.1b Reanalysis Data

In an effort to compare the radiosonde data, hereafter referred to as CARDS, with the corresponding NCEP and ERA40 data, monthly-averaged reanalysis data were extracted for 1979-2001 from grid cells that were collocated with the stations in the CARDS dataset (see station list in Appendix B). Since the reanalysis datasets were in the GRIB data format, the values of temperature (T) and geopotential height were extracted using the Grid Analysis and Display System (GRADS) program, which has built-in functions designed to read GRIB-formatted data.

5.2.2 Trend Analysis

Time trends in T and D were examined for the CARDS, NCEP, and ERA40 datasets over the period of 1979-2001. First, raw time series of the monthly averages of both T and D were inspected for each site (Appendix C). This provided an initial indicator of actual warming/cooling trends that may be expected in this analysis. After

this, in a manner similar to Chapter 4, individual 1979-2001 time series were constructed for each month of the year and linear regression analyses were performed on each time series using the Statistical Analysis Software® (SAS) program, in order to estimate warming/cooling trends at each site as indicated by the CARDS and reanalyses datasets. Trends were estimated only for those time series having at least 15 data points (years) available. As was done for the surface site analysis, autocorrelations of up to lag-4 (i.e. 4 years) were accounted for, in an attempt to remove effects from interannual variability.

5.3 Tropospheric Heating Trends

5.3.1 Time Series

The raw time series of T and D trends for the CARDS, ERA40, and NCEP datasets, upon initial inspection, do not indicate any obvious heating trends over time (Appendix C). To the naked eye, the overall time series at each site look fairly neutral for both T and D. The primary variations are caused by the annual T and D cycles, with greater cycle amplitudes observed for higher-latitude sites.

The T time series of the CARDS and reanalysis datasets usually agree well with each other. In a relatively small number of cases, however, the values of the CARDS and reanalysis datasets are displaced from each other by some value. There is no consistent pattern in these displacements between dataset values. For some of these sites, it is either the ERA40 or the NCEP reanalysis that is displaced from the other datasets (e.g. 912170 - Guam/Taguac). Also, a few sites show that the CARDS T values are displaced from the reanalysis values (e.g. 637410 - Nairobi/Dagoretti, 723650 - Albuquerque). This latter problem was only observed in the lowest layers of the troposphere (1000 mb). The D

time series of the CARDS and reanalysis datasets are in agreement for all sites except the South Pole (890090), where the ERA40 time series tends to have a warm bias.

5.3.2 Annually-Averaged Trends

To begin the tropospheric trend analysis, for each site, all observed trends for each month were averaged together, to obtain an annually-averaged trend estimate at each pressure level of interest (Figure 5.2a, Table 5.2). Overall, the estimated T trends from the CARDS and NCEP datasets indicate cooling at the 200-mb level while the T trends from the ERA40 dataset indicate slight but insignificant warming. At all other levels, significant warming trends are generally indicated, especially for the ERA40 dataset. The Z test statistics for the difference between the ERA40 and the CARDS T trends (Table 5.3) indicate that the T trends from the ERA40 dataset are significantly warmer than their respective CARDS trends (at the 90% significance level or greater) at 200, 300, and 850 mb, with insignificant differences elsewhere (ERA40 trends warmer at 500 mb and 700 mb, but cooler at 1000 mb). For the differences between the NCEP and CARDS T trends (Table 5.4), NCEP trends show significantly less warming (at least 90% significance) at the upper levels, i.e., more cooling at 200 mb and less warming at 300 mb. NCEP also has significantly more cooling than the CARDS data at 1000 mb. Significant warming relative to the CARDS trends is observed at 700 mb for the NCEP dataset, with insignificant trend differences at the adjacent pressure levels (500 mb, 850 mb).

All of the D trends indicate warming (Tables 5.5-5.6), with the greatest warming for the ERA40 dataset and the least warming for the CARDS dataset. The ERA40 D

trends are significantly more positive than the CARDS D trends throughout the entire troposphere, with at least 95% significance. The corresponding differences between the NCEP and CARDS D trends are not as significant. NCEP trends are more positive than the CARDS trends, with a difference of at least 90% significance for lower-tropospheric trends (both 700-500 mb and 1000-500 mb). For the troposphere as a whole, however (1000-200 mb), there is virtually no difference between the NCEP and CARDS D trends.

When considering only those individual trends that are significant at the 90% level or greater (Figure 5.2b, Table 5.2), the same overall pattern is observed as for when all trends are included. The differences between the average ERA40 and CARDS T trends are similar to those in the case of all trends (Table 5.3). The difference at 500 mb is the notable exception, however, as ERA40 now indicates less warming than does the CARDS dataset. These differences are significant (at 90% significance or greater) at both the 200-mb and 300-mb pressure levels, with ERA40 indicating more warming than the radiosonde dataset. The differences are insignificant at all other levels, with ERA40 trends being insignificantly warmer than the CARDS trends at the 700mb and 850mb levels and insignificantly cooler than the CARDS trends at 500 mb and 1000 mb. With regards to the corresponding differences between the T trends of the NCEP and CARDS datasets (Table 5.4), as for the case when all trends were considered, the NCEP trends are significantly cooler than the CARDS trends at both the 200-mb and 300-mb levels. The differences at 700 mb and 1000 mb are no longer significant, although NCEP still indicates more warming relative to the CARDS dataset at 700 mb and more cooling at 1000 mb. Unlike the case when all trends were considered, the difference between the

NCEP and CARDS T trends at both 500 mb and 850 mb now show that NCEP trends are cooler relative to the corresponding CARDS trends.

The D trends that are significant at the 90% level or greater (Tables 5.5-5.6) give average positive trends for all of the datasets. The ERA40 D trends are more positive than the corresponding CARDS trends, but this difference is not significant anywhere in the troposphere. For the differences between the NCEP and CARDS datasets, the averaged trends for NCEP are still significantly more positive than the CARDS trends for 700-500 mb (as was the case when all trends were considered). These differences are not significant for 1000-200 mb or 1000-500 mb. In fact, for 1000-200 mb, NCEP shows less positive D trends than the CARDS data.

If one only considers those T trends that are significant at 95% or greater (Table 5.2, Figures 5.2c-d), the overall results are very similar to those observed for all trends. The ERA40 warming trend at 300 mb is still the most significant warming trend among all the datasets at this level. Cooling is still indicated at 200 mb for both the NCEP and CARDS datasets (ERA40 is neutral), while warming is indicated by all datasets at lower levels in the troposphere.

Differences between those ERA40 and CARDS T trends that are 95% significant or greater (Table 5.3) show that the near-neutral trend indicated by ERA40 at 200 mb differs significantly from the cooling indicated by the CARDS data. Elsewhere, however, these differences are insignificant. ERA40 indicates more warming than CARDS at 300, 700, and 850 mb, but these differences are mixed at both 500 mb and 1000 mb.

The corresponding differences between the NCEP and CARDS T trends (Table 5.4) show that at 300 mb, the difference between the NCEP cooling trends and the

CARDS warming trends is significant at 95%. NCEP trends are no longer significantly cooler than the CARDS trends at 200 mb. At 1000 mb, where NCEP has shown more cooling relative to CARDS in all the other cases that have been considered, the difference between NCEP and CARDS is again significant at over 95% for the case when only individual trends having at least 95% significance are considered. When this criteria is further narrowed to include only those individual trends that are at least 99% significant, the difference between the averaged NCEP and CARDS trends is no longer significant, although the NCEP trend still shows less warming than the CARDS trend.

For those individual D trends that are significant at 95% or greater (Tables 5.5-5.6), most of the average trends are positive, indicating warming. The exception to this is the NCEP average D trend for the whole troposphere (1000-200 mb) when only trends that are at least 99% significant are considered (-0.39 ± 2.87 meters/year).

The differences between the ERA40 and CARDS D trends indicate that ERA40 trends are relatively less positive than CARDS for the troposphere as a whole (1000-200 mb) but are relatively more positive than the CARDS data for the lower troposphere (700-500 mb, 1000-500 mb). These differences, however, are not significant. The corresponding differences for the NCEP and CARDS datasets are significant at over 95% for the troposphere as a whole (1000-200 mb). The CARDS data shows positive trends for 1000-200 mb while the NCEP trends are mixed, showing negative values when individual trends of 95% significance or greater are considered and showing positive values when individual trends of 99% significance or greater are considered. For the lower troposphere, NCEP D trends are more positive than the CARDS trends, but none of these differences are significant.

5.3.3 Seasonal Patterns

5.3.3a Winter

When compared to the annually-averaged cases discussed in Section 5.3.2, for which the ERA40 reanalysis indicated neutral or slightly warming trends (see Figure 5.2a, Table 5.2), the winter (January-March) patterns for all T trends (Figure 5.3a, Table 5.7) now indicate cooling for the ERA40 average trend at 200 mb. Everything else is largely unchanged, however, with NCEP still showing the largest cooling trend at 200 mb and ERA40 still generally showing the largest warming trends throughout the troposphere.

When all trends are considered, the only significant difference between the average T trend of the CARDS dataset and a reanalysis dataset (either NCEP or ERA40) occurs for the difference between the ERA40 and CARDS T trends at 300 mb. The ERA40 warming trend at 300 mb is greater than the corresponding CARDS warming trend, at 90% significance (Table 5.8). At other pressure levels, the ERA40 trends show more warming than CARDS at 700 mb and 850 mb, less warming at 500 mb and 1000 mb, and less cooling at 200 mb. The differences between the NCEP and CARDS T trends (most of which are insignificant - see Table 5.9) show that NCEP has more cooling than the CARDS data at 200 mb, less warming at 300, 500, and 1000 mb, and slightly more warming at 700 and 850 mb.

Average wintertime D trends all indicate a small increase over time (Tables 5.10-11). The difference between the average ERA40 and CARDS wintertime D trends is not significant for 700-500 mb but is significant at greater than 90% for the troposphere as a

whole (1000-200 mb) and significant at greater than 99% for 1000-500 mb. For the NCEP – CARDS average D trend differences, NCEP trends are slightly more positive (warmer) than the corresponding CARDS trends, but none of the differences are significant.

If this investigation is narrowed to include only those individual trends that are at least 90% significant, the average ERA40 T trends, compared to the corresponding CARDS trends, show significantly more warming (90% significance) at 300 mb (Figure 5.3b, Table 5.8). The ERA40 trends are insignificantly warmer than the CARDS trends at 200 mb and insignificantly cooler between 700-1000 mb. The ERA40 warming trends are significantly less than the CARDS warming trends (over 99% significance) at 500 mb. The 500-mb layer also shows that the NCEP warming trend is significantly less than the CARDS warming trend (Table 5.9), but at only 90% significance, as compared to 99% significance for the ERA40 – CARDS trend difference at this level. Elsewhere, NCEP T trends show more cooling than CARDS at 200 mb and less warming than CARDS at 300, 700, 850, and 1000 mb. None of these trend differences are significant.

The averages of the individual D trends that are at least 90% significant indicate increases in D (warming) for all of the datasets (Tables 5.10-11). The difference between the average ERA40 and CARDS D trends is significant for both 1000-200 mb and 1000-500 mb, with ERA40 showing greater increases. There are no significant differences, however, between the NCEP and CARDS datasets, although NCEP generally indicates slightly more positive trends.

An analysis of only those individual trends that are significant at the 95% level or higher proved to be increasingly difficult, since sample sizes become very small at

seasonal time scales. Overall, however (Figures 5.3c-5.3d, Tables 5.7-5.11), there are continued cooling trends in T at the 200-mb level. Warming trends in T are the rule at all other pressure levels. The ERA40 and CARDS average warming trends become more and more significant throughout the middle levels of the troposphere (between 300-700 mb). For those individual trends that are significant at 99% or greater, warming is indicated at the 1000-mb level for all of the datasets in this analysis. There are too few individual trends at this significance level, however, to confidently determine whether or not this is a significant finding.

5.3.3b Spring

Proceeding into the spring months (April-June), the plots of the averaged T trends for all trend observations (Figure 5.4a, see also Table 5.12) indicate that there is no longer any cooling at 200 mb for the ERA40 T trends. The NCEP dataset is the only dataset that shows cooling at this level. At all other levels, either near-neutral or warming trends are indicated. The ERA40 warming trend indicated at 300 mb is larger in magnitude compared to the winter months.

The differences between the ERA40 and CARDS T trends for the spring months (Table 5.13) show that when all trend estimates are considered, ERA40 indicates a significantly larger warming trend than does the CARDS data at both 200 mb and 300 mb (significance is above 99% in both cases). ERA40 shows significantly less warming than the CARDS data, however, at the 1000-mb level (90% significance). At all other levels, the differences between the estimated T trends are insignificant. At 500 mb, ERA40

shows slightly less warming than the CARDS data. At both 700 and 850 mb, the ERA40 data show slightly more warming than the CARDS data.

For the differences between the NCEP and CARDS T trends for the spring months (Table 5.14), when all trend estimates are considered, at 200 mb, the cooling indicated by NCEP is significantly different from the slight warming indicated by the CARDS data, with a significance of well over 99%. The differences between NCEP and CARDS are also significant at over 99% for the 300-mb level, where NCEP has a smaller warming compared to the CARDS dataset. At 1000 mb, the difference between NCEP and CARDS is similar to the ERA40 - CARDS difference at this level, in that the CARDS data indicates significantly more warming than the NCEP dataset (over 95% significance). In fact, NCEP shows neutral conditions or a slight cooling at the 1000-mb level.

The average springtime D trends almost exclusively show a positive trend with time (Tables 5.15-16). The lone exception to this is the average NCEP negative (cooling) trend indicated for the troposphere as a whole (1000-200 mb). The ERA40 D trends are more positive than the CARDS trends and in fact are significantly more positive for both 1000-200 mb and 1000-500 mb. The NCEP data exhibit similar or slightly more positive D trends than the CARDS data for the lower troposphere (700-500 mb and 1000-500 mb). This difference is significant at over 99% for 1000-500 mb. For the troposphere as a whole, however, the average NCEP trends show decreasing D values compared to the increasing values of D observed in the corresponding average CARDS trends, but this difference is insignificant.

Looking at only those individual trends that are significant at 90% or greater (Figure 5.4b, Table 5.12), the difference between the ERA40 and CARDS average T trends at upper levels (200 mb and 300 mb) is significant (Table 5.13). At 200 mb, ERA40 exhibits warming while the CARDS dataset shows cooling, and the difference is significant at over 95%. At 300 mb, ERA40 shows significantly more warming than the CARDS data (significance level greater than 90%). The ERA40 - CARDS differences at all other pressure levels are similar to the differences when all individual trend estimates are considered, with the difference at 1000 mb (ERA40 having less warming than CARDS) no longer being significant.

The differences between the upper-level NCEP and CARDS average T trends (Table 5.14) indicate that NCEP has significantly more cooling than does the CARDS data at 200 mb (over 90% significance). At 300 mb, NCEP shows cooling while CARDS shows warming and this difference is significant at over 95%. The differences of the NCEP and CARDS T trends between 500-850 mb were insignificant, with NCEP warming more than the CARDS data at 500 and 700 mb and NCEP warming less than CARDS at 850 mb. At 1000 mb, the NCEP dataset has an average cooling trend while the CARDS average trend is warming. Data were insufficient, however, to determine whether or not this difference was significant.

Only lower-tropospheric (1000-500 mb, 700-500 mb) D trends were investigated for the case in which only trends that were at least 90% significant were considered (Tables 5.15-16). Data were insufficient to investigate D trends for the entire troposphere (1000-200 mb). At the lower-levels, there are no significant differences between the CARDS and reanalysis datasets. The positive trends indicated by the ERA40 and

CARDS D data for 700-500 mb are very similar. The averaged NCEP D trends show slightly more positive values than the trends for the CARDS data, for both 1000-500 mb and 700-500 mb.

When only those individual trends that are at least 95% significant are considered, sample sizes become small, which makes it much more difficult to compare trends between the CARDS and reanalysis datasets. Figures 5.4c and 5.4d illustrate that the same overall patterns are observed as in the case of including individual trends that are at least 90% significant (Figure 5.4b). The only significant differences between the CARDS and reanalysis datasets are at 200 mb, in the case where only those individual trends being at least 95% significant are considered (Tables 5.13, 5.14). At 200 mb, the average NCEP T trends show significantly more cooling than CARDS, at over 95%. The average ERA40 trends, on the other hand, are significantly warmer relative to CARDS, at over 95% significance.

For the individual trends that were at least 95% significant, only the average D trends for 700-500 mb were able to be considered. The other layers did not have sufficient data to complete the intended analyses (see Tables 5.15-16). The average D trends for 700-500 mb were positive for all of the datasets. Both reanalysis datasets have average D trends that were more positive than the CARDS dataset, but these differences are not significant.

5.3.3c Summer

The summer months of July through September continue many of the same general patterns that emerge during the spring months (Figure 5.5, Table 5.17). When all

individual trends are considered, the average NCEP T trend at 200 mb still indicates a cooling and the other datasets indicate a warming trend (Figure 5.5a). All other levels indicate a warming trend, with the ERA40 warming trends being the most significant (Table 5.17).

For all individual trends, the average T trends for ERA40 are significantly warmer than the average CARDS trends in the upper troposphere (200 and 300 mb; Table 5.18). The differences are significant at over 99%. The ERA40 average T trends are also significantly warmer at both 700 and 850 mb (95% significance and 90% significance, respectively). At 500 mb, ERA40 shows a larger warming trend than does the CARDS data and at 1000 mb, ERA40 shows a lesser warming trend than does the CARDS data; however, these differences are insignificant.

For all individual trends, NCEP T trends in the upper troposphere show significantly less warming, or even cooling, compared to the corresponding CARDS trends (Table 5.19). This pattern was also observed in the spring months. At 200 mb, NCEP is cooling while CARDS is warming and the difference is significant at over 99%. At 300 mb, the difference is significant at over 95%, with NCEP showing less warming than CARDS. In the middle levels, NCEP average T trends are also warmer than the CARDS trends, with the difference being significant at over 95% for the 700-mb layer. At 850 mb, this pattern begins to change and at 1000 mb, NCEP shows significantly *less* warming than the CARDS data, with a difference exceeding 95% in significance.

The average D trends in the case where all individual trends are included (Tables 5.20-5.21) show that in general, the trends from the reanalysis datasets are more positive

than the CARDS data. With the exception of the average D trend from the CARDS data for 700-500 mb, positive trends are indicated.

For those individual trends that are at least 90% significant, the same general patterns are seen in T trends (Figure 5.5b) as when all trends were considered (Figure 5.5a). Warming trends are generally observed for the lower-middle troposphere. These same results persist for the cases when individual trends that are at least 95% significant are analyzed (Figures 5.5c, 5.5d).

In the case where only individual trends having over 90% significance are considered, the differences between the ERA40 and CARDS T trends are significant only at 850 mb (Table 5.18). At this level, ERA40 shows significantly less warming than the CARDS data (over 95% significance). At all other layers, the differences are insignificant, and mixed in sign. The ERA40 average T trends are slightly warmer than the CARDS trends at 200, 500, 700, and 1000 mb. The ERA40 average T trends are slightly cooler than the CARDS trends at 300 mb. Interestingly, the difference between the ERA40 and CARDS datasets at 300 mb in this case (individual trends of 90% significance or higher) is of opposite sign to the same difference for the case where all individual trends were considered. This type of sign reversal was not observed in either the spring or winter seasons (Tables 5.8, 5.13) and it was not observed on an annual basis (Table 5.3).

The differences between the NCEP and CARDS average T trends, for the case of individual trends having over 90% significance (Table 5.19), indicate that NCEP continues to have significantly less warming than the CARDS data in the upper-troposphere, similar to the case when all individual trends were considered. No other

levels show significant differences between these two datasets. NCEP average T trends are slightly warmer than the CARDS trends at 500 and 700 mb and are slightly cooler at both 850 and 1000 mb.

For those individual trends that are at least 95% significant, sample sizes decreased to the point where it was not feasible to perform a comparison of the CARDS and reanalysis average T trends for some of the pressure levels. Differences between the ERA40 and reanalysis average T trends were examined only for 200, 300, and 850 mb (Table 5.18). The ERA40 trends show less warming than the CARDS data at both 300 and 850 mb, but these differences are insignificant. ERA40 does, however, indicate more warming than CARDS at 200 mb and this difference is significant at over 90%. The NCEP - CARDS average T trend differences (Table 5.19) were only examined at 500 mb and the difference at this level is almost zero.

For the case where only those individual D trends of 90% significance or higher are considered, trend comparisons between the CARDS and reanalysis datasets (Table 5.20) were conducted only for 700-500 mb for the NCEP reanalysis and only for 1000-200 mb and 700-500 mb for the ERA40 reanalysis. The NCEP – CARDS difference was significant at over 90% for 700-500 mb, with NCEP indicating positive D trends compared to the negative D trends for the CARDS data. The ERA40 – CARDS D trend differences for 1000-200 mb and 700-500 mb are insignificant, with ERA40 showing more positive trends relative to the CARDS data. Data were insufficient to examine those cases where only trends of 95% significance or greater are included.

5.3.3d Fall

The T trends averaged together from all individual trend estimates show that for the fall months (October – December), all the datasets indicate cooling trends at 200 mb (Figure 5.6a, Table 5.22). At every other pressure level, with the exception of the warming trend indicated by ERA40 at 300 mb, most of the averaged T trends show slight warming. The CARDS average T trends show a slight cooling at 700 and 850 mb that is not indicated in any other season.

The average T trends for the ERA40 data are warmer than the CARDS trends at all pressure levels but are significantly warmer at only two levels: 300 mb and 850 mb (Table 5.23). At 300 mb, the difference between the ERA40 and CARDS warming trends is significant at over 99%. At 850 mb, the difference between the ERA40 and CARDS warming trends is significant at over 95%. On the other hand, for the comparisons between the NCEP and CARDS average T trends (Table 5.24), there are no significant differences at any pressure level. NCEP shows more cooling/less warming than the CARDS data in the upper troposphere (200-300 mb) and at 1000 mb, while for the middle levels (500-850 mb), NCEP shows more warming/less cooling.

The average D trends (Tables 5.25-5.26) show that for the troposphere as a whole, ERA40 indicates a positive trend while both the NCEP and CARDS datasets have negative trends. This is also the case for 700-500 mb. For the lower troposphere, at 700-500 mb and 1000-500 mb, the CARDS data consistently indicate a negative trend, while the reanalysis trends are either neutral or positive with time.

Considering only those individual trends that have a significance of 90% or greater (Figure 5.6b, Table 5.22), the same general patterns are seen as when all

individual trends are considered. From Table 5.23, the differences between the ERA40 and CARDS average T trends follow the same general patterns as for the case when all individual trends were considered, with significant differences at both 300 mb and 850 mb. Data were insufficient at 700 mb to compare the T trends for this particular layer. The differences between the NCEP and CARDS average T trends (Table 5.24) still show that NCEP trends are relatively cooler for the upper troposphere. In fact, at 300 mb, the NCEP cooling, compared to the CARDS warming, is significant at over 99%. NCEP still shows slightly less warming than CARDS at 1000 mb and now NCEP has less warming than CARDS at 500 mb. At all other levels, NCEP indicates more warming than CARDS, but not significantly so.

For the case where only individual trends at 90% significance or greater are considered, average D trend comparisons were conducted only for 700-500 mb (Tables 5.25-5.26). For this layer, both the ERA40 and NCEP datasets have slight positive D trends compared to negative D trends for CARDS. The differences between the CARDS and reanalysis trends are not significant. For the cases where only individual trends at 95% significance and greater are considered, sample sizes became too small to confidently compare the CARDS and reanalysis D trends.

This issue of small sample sizes also became an issue for comparing CARDS and reanalysis average T trends in the cases considering only those individual trends that are significant at 95% or greater (Figures 5.6c, 5.6d, Table 5.22). ERA40 - CARDS comparisons were able to be conducted only for the levels at 200, 300, 500, and 850 mb (Table 5.23). ERA40 T trends are significantly warmer than the CARDS trends at both 300 mb (90%) and at 850 mb (95%), in a manner similar to our previous cases. Both the

200-mb and 500-mb differences are insignificant. The NCEP - CARDS differences of averaged T trends were only analyzed at 200 mb and at 850 mb (Table 5.24). In both cases NCEP trends indicate less cooling than the CARDS trends, but these differences are insignificant.

5.3.4 Eastern United States Tropospheric Temperature Trends

Tropospheric temperature trends were analyzed for the years 1982-1997 for CARDS sites in the eastern United States (Table 5.27), with particular attention given to the trends in the lower troposphere. Recall that the overall surface T trends for the eastern half of the United States (see Chapter 4) indicate a cooling trend for the period 1982-1997. Seasonally, there appears to be a progression from winter warming trends to fall cooling trends at the surface.

The annually-averaged tropospheric T trends (Figure 5.7) show neutral or slight warming T trends for the lower and middle troposphere. The only significant warmings are indicated for the CARDS dataset at both 500 and 1000 mb. The upper troposphere (200 and 300 mb) shows significant warming for both the CARDS and ERA40 datasets, while the T trends for the NCEP dataset show more cooling, with a significant cooling indicated at 200 mb.

The tropospheric T trends for the winter months (Figure 5.8a) generally show warming at all levels except 200 mb, where cooling is indicated by all of the datasets. Several of these warming trends are significant (Table 5.28). The NCEP cooling trend at 200 mb is significant. This prevalence of winter warming trends is consistent with what was found for the wintertime surface trends.

Proceeding into the spring and summer months (Figures 5.8b-c), the estimated average T trends become more neutral, particularly for the lower and middle troposphere. The only significant trends (Table 5.28) are the NCEP cooling at 200 mb and the CARDS warming at 1000 mb, along with some of the upper-level ERA40 warming trends. This pattern also agrees with the findings for the surface, in which heating trends became more neutral during the spring and summer months.

The tropospheric T trends for the fall months (Figure 5.8d, Table 5.28) do not show a conclusive cooling like the surface trends in Chapter 4. The middle troposphere does show a slight but insignificant cooling that is not indicated in the other seasons. The 1000-mb layer shows a slight but insignificant warming, which contrasts with the surface cooling indicated in Chapter 4.

The T trends for the eastern United States generally do not differ significantly between the CARDS and ERA40 datasets (Table 5.29). The NCEP dataset shows significantly cooler T trends than the CARDS dataset both at upper levels and near the surface (Table 5.30) but the two datasets are in relative agreement at the other pressure levels.

5.4 Discussion

The results for the T trends indicate that slight cooling may be present in the uppermost troposphere, while for the lower and middle troposphere, neutral or warming trends are present. For T, the ERA40 reanalysis tends to have the largest warming trends, while the NCEP data has the smallest warming trends (and has the largest cooling trends at certain pressure levels, e.g., 200 mb). As these comparisons are narrowed to only look

at more significant trends or to look at individual seasons, significant trends do emerge, such as the NCEP cooling at 200 mb and the ERA40 warming at 300 mb.

For T trends, the CARDS-indicated heating trends are generally in between those of the ERA40 and NCEP reanalyses. This would indicate, then, that in general, the CARDS data do agree with available reanalysis datasets, and that previous findings about reanalysis-indicated heating trends (e.g. Chase et al., 2000) are confirmed in the CARDS data trends.

For averaged D trends, all datasets generally show slight warming annually, as evidenced by the slightly positive trend values. Seasonally, these same positive trends are observed except during the fall months when more negative (cooling) trends are observed, especially, with the CARDS and NCEP data. This fall cooling matches up with the findings for the surface heating trends discussed in Chapter 4. With few exceptions, the ERA40 and NCEP reanalyses both indicate more positive D trends than the CARDS data, with ERA40 showing more positive trends than NCEP.

Unlike for T, where NCEP trends showed the least warming/most cooling, for the D data it is the CARDS data that show the least warming. In fact, when all trends are considered, it is fairly common to find the ERA40 average trend results being significantly more positive than the trends from the CARDS dataset, both on an annual basis and on a seasonal basis. When all individual trends are considered, the differences between the NCEP and CARDS D trends are really not that remarkable, except at lower levels (e.g. 1000-500 mb) when all seasonal trends are averaged together. In this case, the NCEP trends are also significantly warmer than the CARDS trends. These differences become insignificant for both the ERA40 and NCEP reanalyses when only higher-

significance trends are considered; thus, any existing disagreements between the CARDS and reanalysis data, although real, are probably not major.

Still, both the ERA40 and NCEP D data tend to show more positive trends (warming) at the lower levels than the CARDS D data, especially on an annual basis. This is a discrepancy that deserves at least some attention. The discrepancy in trends may be a sign of geopotential heights at lower levels not being properly quantified by either the CARDS or the renalysis datasets, or both.

For NCEP, the T trends generally indicate upper-tropospheric cooling, along with mixed results for the average D trends over the entire troposphere. These results, therefore, do not support previous claims about NCEP data indicating that the troposphere as a whole is warming over time (Santer et al., 2003a, Santer et al., 2003b).

Recalling the initial hypothesis for tropospheric heating trends, it was anticipated that in all datasets, the upper troposphere would show a significant cooling trend but the lower troposphere would show no significant warming or cooling. When all 200-mb trend estimates are averaged together over all months (Figure 5.2a), NCEP and CARDS data both show significant cooling trends (Table 5.2). The average trends at the lower levels do not support the initial hypothesis, however, as they generally show warming with time.

At seasonal time scales, the lower-tropospheric heating trends become even more significant. The fall months, in particular, show a consistent cooling, primarily in the D trend data, which does not tend to support the initial hypothesis that lower-tropospheric heating trends will be insignificant.

Looking at only those individual trends that are significant at 90% or greater (Figures 5.2b), the NCEP cooling trend at 200 mb supports the initial hypothesis, while the ERA40 warming trend at 300 mb does not support the initial hypothesis. The slight warming in the lower and middle troposphere also does not support the initial hypothesis.

When all CARDS sites are considered, the seasonal variations of both the T and D trends indicate that the lower-middle troposphere warming trends peak in magnitude during the summer months. Conversely, the 200-mb cooling trends are smallest during the summer months. Recalling the results from Chapter 4 for surface heating trends in the eastern United States, the greatest surface warming is found to occur during the winter months. Therefore, the seasonal cycles of the surface and troposphere could possibly be completely out of phase. If that is indeed the case, this finding would provide a further verification of previous claims that the surface and tropospheric heating trends may be at odds (e.g. Pielke, 1998; Bengtssen et al., 1999).

It is important to note, however, that these tropospheric data include sites from around the globe, whereas the surface data in Chapter 4 are only for the eastern United States. In addition to this, the tropospheric data are available for the period 1979-2001 while the surface data are only available from 1982-1997. When only 1982-1997 tropospheric temperature data for the eastern United States are considered, the seasonal patterns of the tropospheric and surface data tend to agree more with each other, showing the greatest warming trends for the winter and the most cooling (least warming) during the fall months. There were relatively few tropospheric sites included in this comparison, however, so this agreement in seasonal patterns between the tropospheric and surface T trends is a preliminary finding.

The average D trend results for all the tropospheric sites show an increased tendency towards negative, or cooling, trends in the lower troposphere during the fall months, especially in the CARDS data. Even though this result is valid for selected sites around the globe and not just the eastern United States, it could possibly be tied to results from the surface analysis in Chapter 4, which indicate that for the eastern United States, most surface cooling trends also occur during the fall months. This is a plausible connection, considering that the lower levels of the troposphere have the most interactions with the surface and near-surface boundary layer. Any heating patterns observed at the surface could reasonably be expected to be mirrored, to a lesser degree, in the lowest layers of the troposphere.

In summary, the main findings from this chapter are as follows:

- For the upper troposphere, cooling T trends are indicated (which supports the initial hypothesis). Slight warming trends are indicated for the lower and middle troposphere, especially with the D trends (which does not support the initial hypothesis).
- For both T and D, ERA40 has the greatest number of significant tropospheric warming trends, while NCEP has the greatest number of significant tropospheric cooling trends (especially at upper levels). The trend values for CARDS are usually in between the corresponding ERA40 and NCEP trend values and thus compare favorably to the ERA40 and NCEP datasets.
- Seasonal patterns of tropospheric T trends in the eastern United States are in agreement with surface trends.

Table 5.1. List of mandatory pressure levels for the tropospheric analysis.

Pressure Level (millibars)	Included in Analysis?
1000	√
850	√
700	√
500	√
400	
300	√
200	√
150	
100	
70	
50	
30	
20	
10	

Table 5.2. Z test statistic values of annually-averaged 1979-2001 temperature trends of CARDS, ERA40, and NCEP datasets. See Appendix A for definition of Z value. Trend significance > 90% if |Z| > 1.65, significance > 95% if |Z| > 1.96, and significance > 99% if |Z| > 2.58. Missing Z values, indicated by "M", are for those averages where the sample size was less than 10.

Pressure Level (mb)	All Trends	>90%	>95%	>99%
CARDS				
200	-2.67	-2.38	-3.04	-2.00
300	5.82	5.39	3.52	2.86
500	4.37	4.79	3.37	1.20
700	3.17	3.00	2.00	0.52
850	2.82	3.19	2.32	M
1000	-3.64	2.34	3.09	2.41
ERA40				
200	0.75	-0.22	0.00	-8.31
300	17.37	23.81	19.79	-0.62
500	6.37	3.95	4.60	4.09
700	6.41	6.03	6.47	3.23
850	8.19	8.17	6.74	1.24
1000	2.89	1.57	1.78	-0.16
NCEP				
200	-11.61	-9.85	-8.31	-5.59
300	2.25	-0.07	-0.62	-0.74
500	5.61	4.66	4.09	2.73
700	6.35	3.98	3.23	2.05
850	4.31	1.51	1.24	0.31
1000	0.75	0.45	-0.16	0.69

Table 5.3. Z test statistic values of differences between annually-averaged 1979-2001 temperature trends of CARDS and ERA40 datasets (ERA40 – CARDS). See Appendix A for definition of Z value. Significance criteria are as in Table 5.2.

Pressure Level (mb)	All Trends	>90%	>95%	>99%
200	2.36	1.83	2.69	2.28
300	5.44	2.23	1.62	0.99
500	0.66	-1.52	-0.40	0.35
700	1.49	1.09	1.36	1.43
850	2.99	0.92	1.26	0.37
1000	-1.08	-0.30	-0.62	0.16

Table 5.4. Z test statistic values of differences between annually-averaged 1979-2001 temperature trends of CARDS and NCEP datasets (NCEP – CARDS). See Appendix A for definition of Z value. Significance criteria are as in Table 5.2.

Pressure Level (mb)	All Trends	>90%	>95%	>99%
200	-4.78	-1.92	-0.01	0.02
300	-3.26	-3.73	-2.91	-2.47
500	0.09	-0.88	-0.58	0.02
700	1.72	0.03	0.07	0.66
850	0.87	-1.17	-0.69	-0.69
1000	-2.34	-1.48	-2.36	-1.08

Table 5.5. Annually-averaged thickness trends and Z test statistic values (see definition in Appendix A; significance criteria in Table 5.2) of 1979-2001 trend differences between the ERA40 and CARDS datasets, and between the NCEP and CARDS datasets.

ERA40 – CARDS D trends				
Sig. Level	**Layer**	**ERA40 (m/year)**	**CARDS (m/year)**	**Z value**
All	1000-200mb	0.72±1.23	0.15±1.82	4.40
>90%	1000-200mb	2.24±1.49	2.08±2.91	0.30
>95%	1000-200mb	2.57±1.39	2.72±2.84	-0.23
>99%	1000-200mb	2.20±0.42	3.61±2.45	-0.98
All	1000-500mb	0.21±0.68	0.05±0.95	2.45
>90%	1000-500mb	0.94±1.11	0.45±1.66	1.37
>95%	1000-500mb	0.86±1.14	0.22±1.77	1.30
>99%	1000-500mb	1.22±1.19	0.23±1.54	1.17
All	700-500mb	0.11±0.38	0.01±0.50	3.41
>90%	700-500mb	0.36±0.66	0.23±1.04	0.86
>95%	700-500mb	0.43±0.69	0.37±0.99	0.34
>99%	700-500mb	0.47±0.80	0.28±1.24	0.54
NCEP – CARDS D trends				
Sig. Level	**Layer**	**NCEP (m/year)**	**CARDS (m/year)**	**Z value**
All	1000-200mb	0.16±1.79	0.15±1.82	0.05
>90%	1000-200mb	1.50±3.21	2.08±2.91	-0.76
>95%	1000-200mb	0.49±2.33	2.72±2.84	-2.69
>99%	1000-200mb	-0.39±2.87	3.61±2.45	-2.12
All	1000-500mb	0.17±0.94	0.05±0.95	1.65
>90%	1000-500mb	0.90±1.59	0.45±1.66	1.15
>95%	1000-500mb	0.55±1.32	0.22±1.77	0.73
>99%	1000-500mb	0.37±1.94	0.23±1.54	0.15
All	700-500mb	0.06±0.54	0.01±0.50	1.69
>90%	700-500mb	0.59±0.86	0.23±1.04	2.09
>95%	700-500mb	0.49±0.82	0.37±0.99	0.57
>99%	700-500mb	0.39±0.95	0.28±1.24	0.29

Table 5.6. Z test statistic values for the annually-averaged 1979-2001 thickness trends for the ERA40, CARDS, and NCEP datasets. See Appendix A for definition of Z value. Significance criteria are as in Table 5.2. Missing Z values, indicated by "M", are for those averages where the sample size was less than 10.

Sig. Level	Layer	CARDS	ERA40	NCEP
All	1000-200mb	1.46	10.00	1.55
>90%	1000-200mb	4.04	9.39	2.81
>95%	1000-200mb	4.39	9.46	0.90
>99%	1000-200mb	M	M	M
All	1000-500mb	0.82	5.36	3.19
>90%	1000-500mb	1.71	5.34	3.18
>95%	1000-500mb	0.65	3.97	1.82
>99%	1000-500mb	0.54	3.68	M
All	700-500mb	0.35	6.13	2.64
>90%	700-500mb	1.70	4.64	5.40
>95%	700-500mb	2.20	4.20	3.60
>99%	700-500mb	0.86	2.50	1.55

Table 5.7. Same as Table 5.2, but for the winter months (JFM). Missing Z values, indicated by "M", are for those averages where the sample size was less than 10.

Pressure Level (mb)	All Trends	>90%	>95%	>99%
CARDS				
200	-2.39	-3.85	-4.48	M
300	2.40	1.98	1.03	M
500	3.48	11.52	8.02	M
700	2.70	3.82	6.94	M
850	2.72	2.74	1.91	M
1000	1.63	1.47	M	M
ERA40				
200	-1.13	-2.21	-1.91	-0.74
300	6.64	9.42	7.56	M
500	3.07	2.94	4.33	M
700	3.61	3.84	4.97	M
850	4.97	4.17	3.09	M
1000	1.79	1.21	M	M
NCEP				
200	-5.32	-6.74	-4.81	M
300	1.31	0.62	0.23	M
500	2.52	3.47	2.41	M
700	3.30	1.74	1.48	M
850	2.73	1.31	1.09	-0.19
1000	0.81	0.80	M	M

Table 5.8. Same as Table 5.3, but for the winter months (JFM). Missing Z values, indicated by "M", are for those averages where the sample size was less than 10.

Pressure Level (mb)	All Trends	>90%	>95%	>99%
200	0.84	1.59	2.16	M
300	1.90	1.72	1.20	M
500	-0.55	-2.98	-1.34	M
700	0.21	-0.56	-1.34	M
850	1.25	-0.21	-0.05	M
1000	-0.22	0.01	M	M

Table 5.9. Same as Table 5.4, but for the winter months (JFM). Missing Z values, indicated by "M", are for those averages where the sample size was less than 10.

Pressure Level (mb)	All Trends	>90%	>95%	>99%
200	-1.60	0.43	0.87	M
300	-0.97	-0.92	-0.63	M
500	-0.69	-1.93	-1.65	M
700	0.34	-1.53	-2.16	M
850	0.10	-1.16	-0.87	M
1000	-0.83	-0.52	M	M

Table 5.10. Same as Table 5.5, but for the winter months (JFM). Missing Z values, indicated by "M", are for those averages where the sample size was less than 10.

ERA40 – CARDS D trends				
Sig. Level	**Layer**	**ERA40 (m/year)**	**CARDS (m/year)**	**Z value**
All	1000-200mb	0.70±1.49	0.20±2.11	1.72
>90%	1000-200mb	2.80±1.27	3.40±2.38	-0.75
>95%	1000-200mb	2.95±1.12	4.35±1.86	M
>99%	1000-200mb	2.65± 0	4.56±1.91	M
All	1000-500mb	0.26±0.90	0.09±1.17	2.86
>90%	1000-500mb	0.96±1.38	0.48±2.13	0.64
>95%	1000-500mb	1.26±1.56	0.32±2.50	M
>99%	1000-500mb	2.17±0.45	0.37±1.90	M
All	700-500mb	0.14±0.46	0.08±0.56	0.90
>90%	700-500mb	0.52±0.65	0.53±0.95	-0.05
>95%	700-500mb	0.57±0.63	0.97±0.43	-1.63
>99%	700-500mb	0.91±0.40	0.69±0.36	M
NCEP – CARDS D trends				
Sig. Level	**Layer**	**NCEP (m/year)**	**CARDS (m/year)**	**Z value**
All	1000-200mb	0.21±1.46	0.20±2.11	0.04
>90%	1000-200mb	1.94±2.40	3.40±2.38	M
>95%	1000-200mb	2.49±2.60	4.35±1.86	M
>99%	1000-200mb	M	4.56±1.91	M
All	1000-500mb	0.17±0.86	0.09±1.17	0.52
>90%	1000-500mb	1.05±1.65	0.48±2.13	0.70
>95%	1000-500mb	0.70±1.79	0.32±2.50	M
>99%	1000-500mb	0.62±2.06	0.37±1.90	M
All	700-500mb	0.12±0.44	0.08±0.56	0.72
>90%	700-500mb	0.70±0.71	0.53±0.95	0.51
>95%	700-500mb	0.69±0.84	0.97±0.43	M
>99%	700-500mb	0.39±1.23	0.69±0.36	M

Table 5.11. Same as Table 5.6, but for the winter months (JFM). Missing Z values, indicated by "M", are for those averages where the sample size was less than 10.

Sig. Level	Layer	CARDS	ERA40	NCEP
All	1000-200mb	0.84	4.18	1.29
>90%	1000-200mb	M	7.63	2.55
>95%	1000-200mb	M	8.33	M
>99%	1000-200mb	M	M	M
All	1000-500mb	0.69	2.62	1.81
>90%	1000-500mb	0.75	2.41	2.12
>95%	1000-500mb	M	M	M
>99%	1000-500mb	M	M	M
All	700-500mb	1.51	3.27	3.11
>90%	700-500mb	2.37	3.81	4.09
>95%	700-500mb	M	3.16	M
>99%	700-500mb	M	M	M

Table 5.12. Same as Table 5.2, but for the spring months (AMJ). Missing Z values, indicated by "M", are for those averages where the sample size was less than 10.

Pressure Level (mb)	All Trends	>90%	>95%	>99%
CARDS				
200	0.22	M	M	M
300	3.81	2.79	M	M
500	2.82	2.70	M	M
700	2.19	2.23	1.24	M
850	1.57	1.36	1.36	M
1000	2.87	2.40	M	M
ERA40				
200	4.53	3.70	5.82	8.43
300	9.46	13.71	10.49	15.93
500	2.41	1.58	2.31	M
700	2.69	4.10	4.08	M
850	3.70	3.46	3.27	M
1000	0.82	M	M	M
NCEP				
200	-6.64	-6.35	-12.50	M
300	0.38	-0.11	-0.04	M
500	2.77	2.91	3.46	M
700	3.12	3.94	3.75	M
850	2.50	0.71	0.43	M
1000	-0.11	-1.16	M	M

Table 5.13. Same as Table 5.3, but for the spring months (AMJ). Missing Z values, indicated by "M", are for those averages where the sample size was less than 10.

Pressure Level (mb)	All Trends	>90%	>95%	>99%
200	2.76	2.19	2.41	M
300	2.98	1.67	1.33	M
500	-0.49	-0.96	-0.11	M
700	0.08	0.75	1.02	M
850	1.10	0.43	0.53	M
1000	-1.80	-1.07	M	M

Table 5.14. Same as Table 5.4, but for the spring months (AMJ). Missing Z values, indicated by "M", are for those averages where the sample size was less than 10.

Pressure Level (mb)	All Trends	>90%	>95%	>99%
200	-4.12	-1.90	-1.96	M
300	-2.74	-2.36	-1.49	M
500	-0.33	0.10	0.38	M
700	0.41	0.71	0.86	M
850	0.40	-0.75	-0.77	M
1000	-2.22	M	M	M

Table 5.15. Same as Table 5.5, but for the spring months (AMJ). Missing Z values, indicated by "M", are for those averages where the sample size was less than 10.

ERA40 – CARDS D trends				
Sig. Level	**Layer**	**ERA40 (m/year)**	**CARDS (m/year)**	**Z value**
All	1000-200mb	0.58±1.10	0.17±1.35	1.98
>90%	1000-200mb	2.99±1.27	1.70±2.04	M
>95%	1000-200mb	3.07±1.40	3.17±0.87	M
>99%	1000-200mb	1.83± 0	2.56± 0	M
All	1000-500mb	0.17±0.61	0.12±0.84	3.79
>90%	1000-500mb	1.34±1.13	0.79±1.17	M
>95%	1000-500mb	1.34±1.13	0.60±1.20	M
>99%	1000-500mb	1.25± 0	1.74± 0	M
All	700-500mb	0.09±0.37	0.04±0.45	0.90
>90%	700-500mb	0.43±0.68	0.44±0.70	-0.04
>95%	700-500mb	0.67±0.67	0.34±0.65	1.25
>99%	700-500mb	0.59±0.79	0.14±1.00	M
NCEP – CARDS D trends				
Sig. Level	**Layer**	**NCEP (m/year)**	**CARDS (m/year)**	**Z value**
All	1000-200mb	-0.14±1.11	0.17±1.35	-1.49
>90%	1000-200mb	0.01±1.83	1.70±2.04	M
>95%	1000-200mb	-0.22±1.75	3.17±0.87	M
>99%	1000-200mb	M	2.56± 0	M
All	1000-500mb	0.14±0.51	0.12±0.84	3.38
>90%	1000-500mb	1.01±0.28	0.79±1.17	0.52
>95%	1000-500mb	1.09±0.24	0.60±1.20	M
>99%	1000-500mb	M	1.74± 0	M
All	700-500mb	0.11±0.36	0.04±0.45	1.35
>90%	700-500mb	0.54±0.58	0.44±0.70	0.47
>95%	700-500mb	0.60±0.58	0.34±0.65	1.08
>99%	700-500mb	1.04±0.53	0.14±1.00	M

Table 5.16. Same as Table 5.6, but for the spring months (AMJ). Missing Z values, indicated by "M", are for those averages where the sample size was less than 10.

Sig. Level	Layer	CARDS	ERA40	NCEP
All	1000-200mb	1.02	4.40	-1.11
>90%	1000-200mb	M	M	0.03
>95%	1000-200mb	M	M	M
>99%	1000-200mb	M	M	M
All	1000-500mb	1.22	2.36	2.27
>90%	1000-500mb	2.35	M	M
>95%	1000-500mb	M	M	M
>99%	1000-500mb	M	M	M
All	700-500mb	0.94	2.53	3.32
>90%	700-500mb	2.52	2.84	3.88
>95%	700-500mb	1.82	3.62	4.03
>99%	700-500mb	M	M	M

Table 5.17. Same as Table 5.2, but for the summer months (JAS). Missing Z values, indicated by "M", are for those averages where the sample size was less than 10.

Pressure Level (mb)	All Trends	>90%	>95%	>99%
CARDS				
200	2.56	2.27	M	M
300	4.66	7.10	6.27	M
500	1.67	0.58	0.56	M
700	1.32	0.43	M	M
850	3.48	6.18	4.55	M
1000	3.22	0.97	M	M
ERA40				
200	2.63	19.49	17.43	M
300	12.47	16.90	14.50	M
500	5.34	1.95	M	M
700	6.02	M	M	M
850	8.37	10.31	9.48	M
1000	1.82	M	M	M
NCEP				
200	-4.48	-5.33	-3.88	M
300	3.34	1.26	M	M
500	5.29	2.24	1.50	M
700	6.16	M	M	M
850	4.64	M	M	M
1000	0.47	0.97	0.63	M

Table 5.18. Same as Table 5.3, but for the summer months (JAS). Missing Z values, indicated by "M", are for those averages where the sample size was less than 10.

Pressure Level (mb)	All Trends	>90%	>95%	>99%
200	2.63	0.82	1.94	M
300	3.19	-0.75	-1.12	M
500	1.37	0.26	M	M
700	2.06	1.09	M	M
850	1.80	-2.09	-1.02	M
1000	-1.27	0.05	M	M

Table 5.19. Same as Table 5.4, but for the summer months (JAS). Missing Z values, indicated by "M", are for those averages where the sample size was less than 10.

Pressure Level (mb)	All Trends	>90%	>95%	>99%
200	-4.38	-3.78	M	M
300	-2.21	-3.25	M	M
500	1.10	0.28	0.00	M
700	2.11	1.10	M	M
850	0.07	-0.68	M	M
1000	-1.99	-0.01	M	M

Table 5.20. Same as Table 5.5, but for the summer months (JAS). Missing Z values, indicated by "M", are for those averages where the sample size was less than 10.

ERA40 – CARDS D trends				
Sig. Level	**Layer**	**ERA40 (m/year)**	**CARDS (m/year)**	**Z value**
All	1000-200mb	1.06±1.00	0.53±1.60	2.33
>90%	1000-200mb	2.35±0.78	2.12±2.80	0.30
>95%	1000-200mb	2.41±0.90	2.54±2.93	M
>99%	1000-200mb	M	5.27±0.87	M
All	1000-500mb	0.35±0.47	0.16±0.80	2.39
>90%	1000-500mb	0.90±0.41	0.97±1.78	M
>95%	1000-500mb	0.98±0.31	0.54±1.51	M
>99%	1000-500mb	0.64± 0	0.25±1.80	M
All	700-500mb	0.15±0.29	-0.01±0.50	3.04
>90%	700-500mb	0.30±0.55	-0.18±1.48	1.09
>95%	700-500mb	0.35±0.62	0.10±1.77	M
>99%	700-500mb	-0.43±0.06	-0.26±2.17	M
NCEP – CARDS D trends				
Sig. Level	**Layer**	**NCEP (m/year)**	**CARDS (m/year)**	**Z value**
All	1000-200mb	0.73±2.77	0.53±1.60	0.53
>90%	1000-200mb	4.86±4.43	2.12±2.80	M
>95%	1000-200mb	-1.55± 0	2.54±2.93	M
>99%	1000-200mb	-1.55± 0	5.27±0.87	M
All	1000-500mb	0.34±1.35	0.16±0.80	3.47
>90%	1000-500mb	1.17±2.35	0.97±1.78	M
>95%	1000-500mb	-0.23±1.09	0.54±1.51	M
>99%	1000-500mb	M	0.25±1.80	M
All	700-500mb	0.05±0.80	-0.01±0.50	0.66
>90%	700-500mb	0.75±1.14	-0.18±1.48	1.86
>95%	700-500mb	0.61±1.13	0.10±1.77	M
>99%	700-500mb	-0.27± 0	-0.26±2.17	M

Table 5.21. Same as Table 5.6, but for the summer months (JAS). Missing Z values, indicated by "M", are for those averages where the sample size was less than 10.

Sig. Level	Layer	CARDS	ERA40	NCEP
All	1000-200mb	2.74	8.79	2.20
>90%	1000-200mb	2.63	11.26	M
>95%	1000-200mb	M	M	M
>99%	1000-200mb	M	M	M
All	1000-500mb	1.65	6.29	2.12
>90%	1000-500mb	M	M	M
>95%	1000-500mb	M	M	M
>99%	1000-500mb	M	M	M
All	700-500mb	-0.23	5.73	0.64
>90%	700-500mb	-0.40	2.01	2.70
>95%	700-500mb	M	M	M
>99%	700-500mb	M	M	M

Table 5.22. Same as Table 5.2, but for the fall months (OND). Missing Z values, indicated by "M", are for those averages where the sample size was less than 10.

Pressure Level (mb)	All Trends	>90%	>95%	>99%
CARDS				
200	-3.69	-1.90	M	M
300	1.50	2.94	1.81	M
500	0.78	1.20	M	M
700	-0.06	-0.44	M	M
850	2.11	-0.68	-0.78	M
1000	0.78	0.15	M	M
ERA40				
200	-2.44	-1.68	-1.51	-0.50
300	7.67	11.91	13.86	M
500	2.49	1.46	1.01	M
700	1.30	M	M	M
850	0.79	3.56	M	M
1000	1.42	0.41	M	M
NCEP				
200	-7.77	-4.98	-4.18	M
300	0.06	-2.00	-1.73	M
500	1.53	0.32	M	M
700	1.28	0.00	M	M
850	-0.41	-0.38	-0.02	M
1000	0.20	0.01	M	M

Table 5.23. Same as Table 5.3, but for the fall months (OND). Missing Z values, indicated by "M", are for those averages where the sample size was less than 10.

Pressure Level (mb)	All Trends	>90%	>95%	>99%
200	0.44	0.58	0.84	M
300	3.18	1.72	1.82	M
500	1.07	-0.07	-0.05	M
700	0.87	M	M	M
850	2.25	2.32	2.11	M
1000	0.30	0.19	M	M

Table 5.24. Same as Table 5.4, but for the fall months (OND). Missing Z values, indicated by "M", are for those averages where the sample size was less than 10.

Pressure Level (mb)	All Trends	>90%	>95%	>99%
200	-1.52	-0.34	0.01	M
300	-1.16	-3.46	M	M
500	0.28	0.76	M	M
700	0.87	0.37	M	M
850	1.29	0.16	0.51	M
1000	-0.44	-0.10	M	M

Table 5.25. Same as Table 5.5, but for the fall months (OND). Missing Z values, indicated by "M", are for those averages where the sample size was less than 10.

ERA40 – CARDS D trends				
Sig. Level	**Layer**	**ERA40 (m/year)**	**CARDS (m/year)**	**Z value**
All	1000-200mb	0.55±1.21	-0.23±1.99	2.97
>90%	1000-200mb	0.23±1.92	0.31±3.96	M
>95%	1000-200mb	-0.61±1.82	1.23±3.64	M
>99%	1000-200mb	2.10± 0	2.21±3.40	M
All	1000-500mb	0.07±0.63	-0.17±0.91	1.85
>90%	1000-500mb	-0.42±0.65	-0.35±1.43	M
>95%	1000-500mb	-0.73±0.03	-0.41±1.59	M
>99%	1000-500mb	M	-0.18±1.44	M
All	700-500mb	0.05±0.37	-0.07±0.48	2.21
>90%	700-500mb	0.10±0.72	-0.08±0.95	0.60
>95%	700-500mb	0.09±0.75	-0.07±0.94	M
>99%	700-500mb	0.38±0.98	0.63±0.80	M
NCEP – CARDS D trends				
Sig. Level	**Layer**	**NCEP (m/year)**	**CARDS (m/year)**	**Z value**
All	1000-200mb	-0.12±1.36	-0.23±1.99	0.40
>90%	1000-200mb	0.09±2.45	0.31±3.96	M
>95%	1000-200mb	0.44±2.56	1.23±3.64	M
>99%	1000-200mb	0.19±3.81	2.21±3.40	M
All	1000-500mb	0.05±0.85	-0.17±0.91	0.14
>90%	1000-500mb	-0.08±1.27	-0.35±1.43	M
>95%	1000-500mb	-0.43±0.76	-0.41±1.59	M
>99%	1000-500mb	-0.88± 0	-0.18±1.44	M
All	700-500mb	-0.02±0.42	-0.07±0.48	0.87
>90%	700-500mb	0.18±0.97	-0.08±0.95	0.64
>95%	700-500mb	-0.08±0.95	-0.07±0.94	M
>99%	700-500mb	-0.12±0.96	0.63±0.80	M

Table 5.26. Same as Table 5.6, but for the fall months (OND). Missing Z values, indicated by "M", are for those averages where the sample size was less than 10.

Sig. Level	Layer	CARDS	ERA40	NCEP
All	1000-200mb	-1.02	4.05	-0.76
>90%	1000-200mb	M	M	M
>95%	1000-200mb	M	M	M
>99%	1000-200mb	M	M	M
All	1000-500mb	-1.64	0.94	0.53
>90%	1000-500mb	-0.79	M	M
>95%	1000-500mb	M	M	M
>99%	1000-500mb	M	M	M
All	700-500mb	-1.64	1.49	-0.55
>90%	700-500mb	-0.31	0.57	M
>95%	700-500mb	M	0.42	M
>99%	700-500mb	M	M	M

Table 5.27. List of CARDS stations used for surface-troposphere trend comparisons in the eastern United States.

CARDS#	Station Name	Latitude (dd)	Longitude (dd)	Elevation (m)
722010	KEY WEST INT AP	24.55	-81.75	1
722350	JACKSON/THOMPSON FLD	32.317	-90.067	91
722500	BROWNSVILLE	25.9	-97.433	7
722510	CORPUS CHRISTI	27.767	-97.5	14
722610	DEL RIO	29.367	-100.91	313
723270	NASHVILLE	36.25	-86.567	180
724510	DODGE CITY	37.767	-99.967	791
725200	PITTSBURGH/MOON TOWNSH	40.533	-80.233	360
726450	GREEN BAY	44.483	-88.133	210
727120	CARIBOU	46.867	-68.017	191
727640	BISMARCK	46.767	-100.75	503

Table 5.28. Z test statistic values of annually-averaged and seasonally-averaged 1982-1997 temperature trends of CARDS, ERA40, and NCEP datasets for the stations in Table 5.27. See Appendix A for definition of Z value. Significance criteria are as in Table 5.2.

Pressure Level (mb)	Annual	Winter (JFM)	Spring (AMJ)	Summer (JAS)	Fall (OND)
CARDS					
200	1.73	1.34	1.89	4.05	0.69
300	-0.15	1.12	-1.12	-0.59	-0.19
500	0.21	1.22	-0.26	-0.02	-0.58
700	1.94	2.65	0.68	1.04	-0.42
850	5.41	4.74	0.92	1.56	3.07
1000	3.19	-0.26	0.38	2.72	2.00
ERA40					
200	0.65	1.14	-0.62	0.05	0.47
300	1.47	1.88	-0.02	0.79	0.39
500	0.80	1.16	-0.01	1.54	-0.56
700	1.60	2.35	0.61	1.38	-0.85
850	8.56	5.59	1.78	3.68	4.28
1000	4.42	-0.24	1.34	5.66	2.78
NCEP					
200	-0.65	-0.21	-2.05	-0.30	0.64
300	0.47	1.61	-0.99	0.03	-0.06
500	0.50	1.69	-0.47	0.22	-0.45
700	0.33	2.26	-0.23	-0.51	-0.86
850	1.81	3.34	-0.78	-0.48	1.99
1000	-4.71	-2.33	-2.73	-3.99	-0.92

Table 5.29. Z test statistic values of differences between annually-averaged and seasonally-averaged 1982-1997 temperature trends of CARDS and ERA40 datasets (ERA40 – CARDS) for the eastern United States. See Appendix A for definition of Z value. Significance criteria are as in Table 5.2.

Pressure Level (mb)	Annual	Winter (JFM)	Spring (AMJ)	Summer (JAS)	Fall (OND)
200	0.82	0.10	0.67	0.76	0.05
300	1.77	0.38	0.70	1.30	0.63
500	-0.37	-0.38	-0.10	0.06	-0.24
700	0.38	-0.17	0.20	0.98	0.05
850	1.10	0.40	0.81	0.96	0.40
1000	-1.09	-0.16	-1.20	-1.34	-0.20

Table 5.30. Z test statistic values of differences between annually-averaged and seasonally-averaged 1982-1997 temperature trends of CARDS and NCEP datasets (NCEP – CARDS) for the eastern United States. See Appendix A for definition of Z value. Significance criteria are as in Table 5.2.

Pressure Level (mb)	Annual	Winter (JFM)	Spring (AMJ)	Summer (JAS)	Fall (OND)
200	-5.54	-1.27	-2.45	-6.18	-2.60
300	2.67	-1.09	-1.21	-1.49	-1.06
500	-1.22	-0.51	-0.67	-1.11	-0.26
700	0.18	0.17	-0.06	0.16	0.12
850	0.43	0.22	0.19	0.48	0.10
1000	-1.79	-0.89	-1.92	-1.59	-0.08

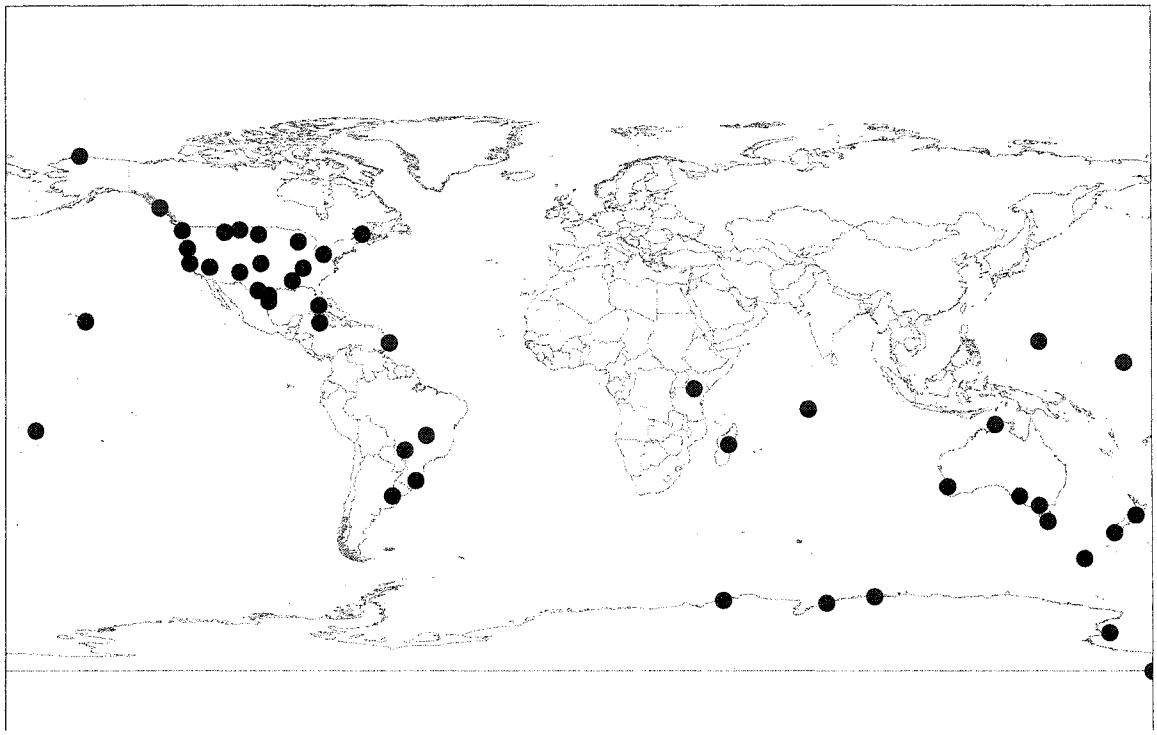

Figure 5.1. Map of sites used in the comparisons of the CARDS and reanalysis datasets.

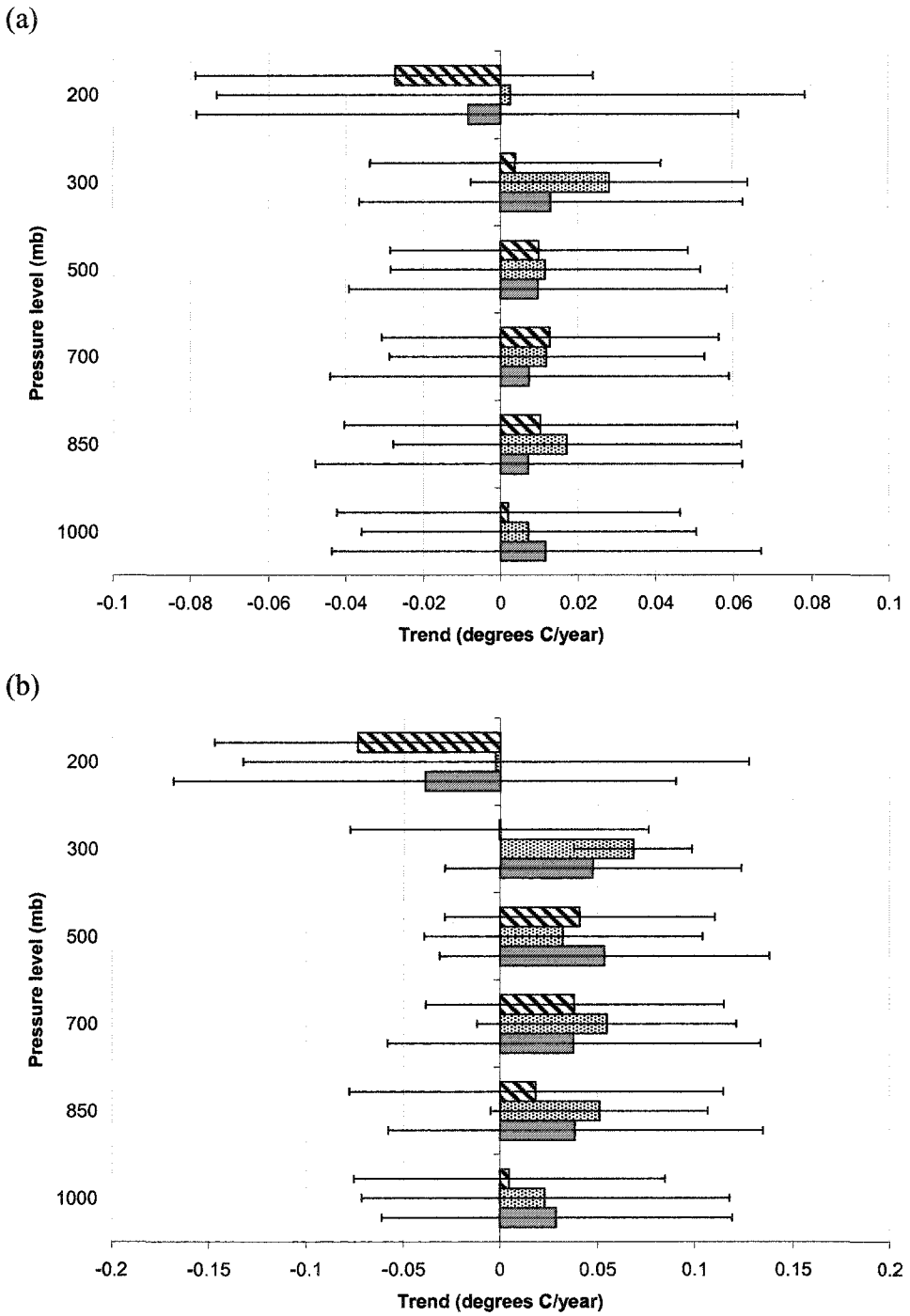

Figure 5.2. Annually-averaged T trends (error bars indicate standard deviations) at selected pressure levels, for the sites shown in Figure 5.1 and listed in Appendix B. Results are shown for all trends (a) and those individual trends whose significance exceeds 90% (b), 95% (c), and 99% (d). NCEP trends are shown by the striped bars, ERA40 trends are shown by the light stippled bars, and the CARDS trends are shown by the dark grey bars.

(c)

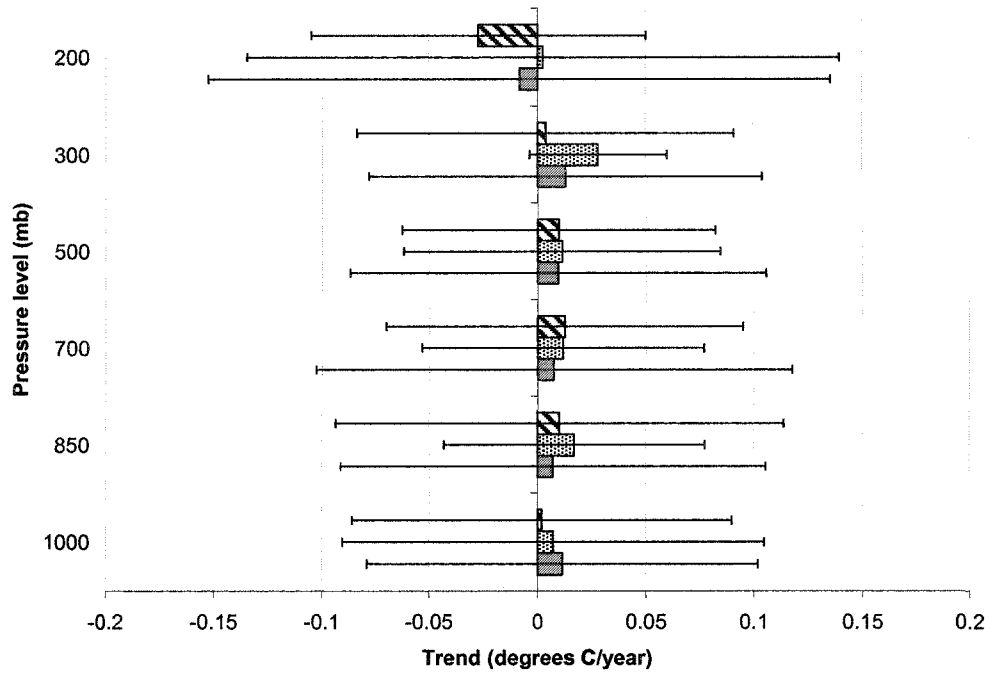

(d)

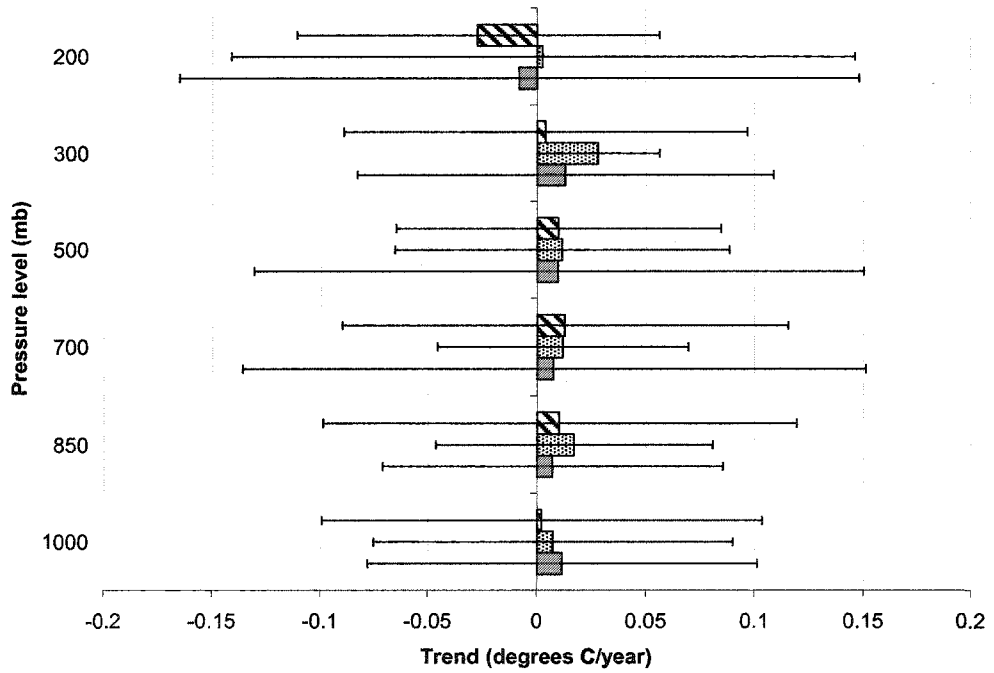

Figure 5.2. (continued)

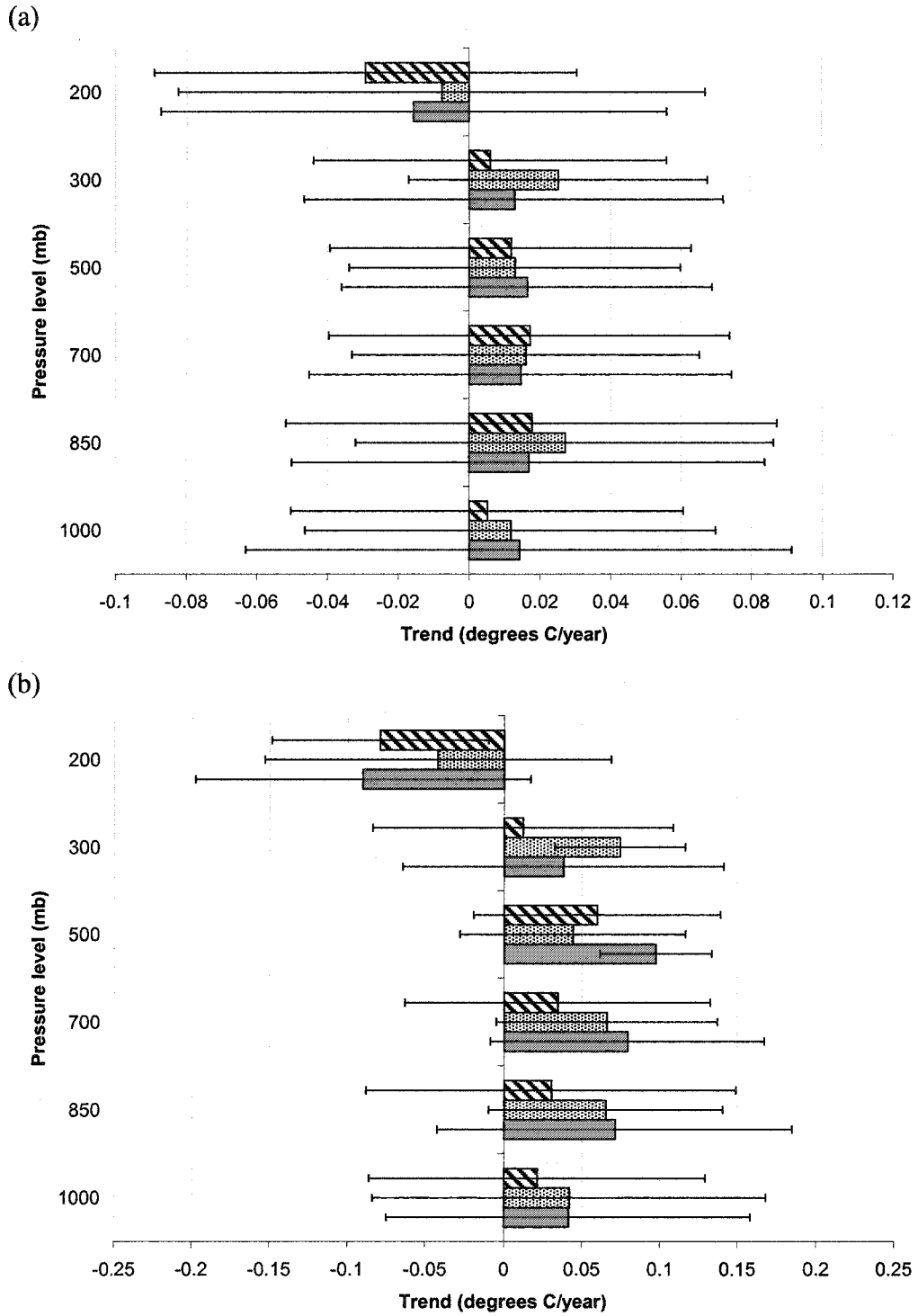

Figure 5.3. Same as Figure 5.2, but for the winter months (JFM).

(c)

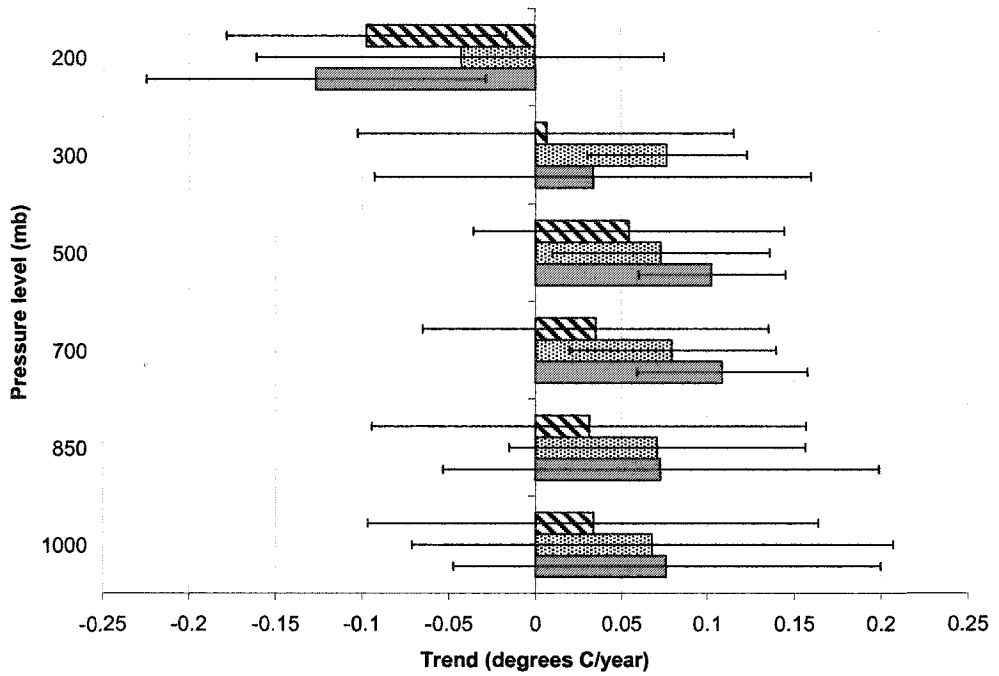

(d)

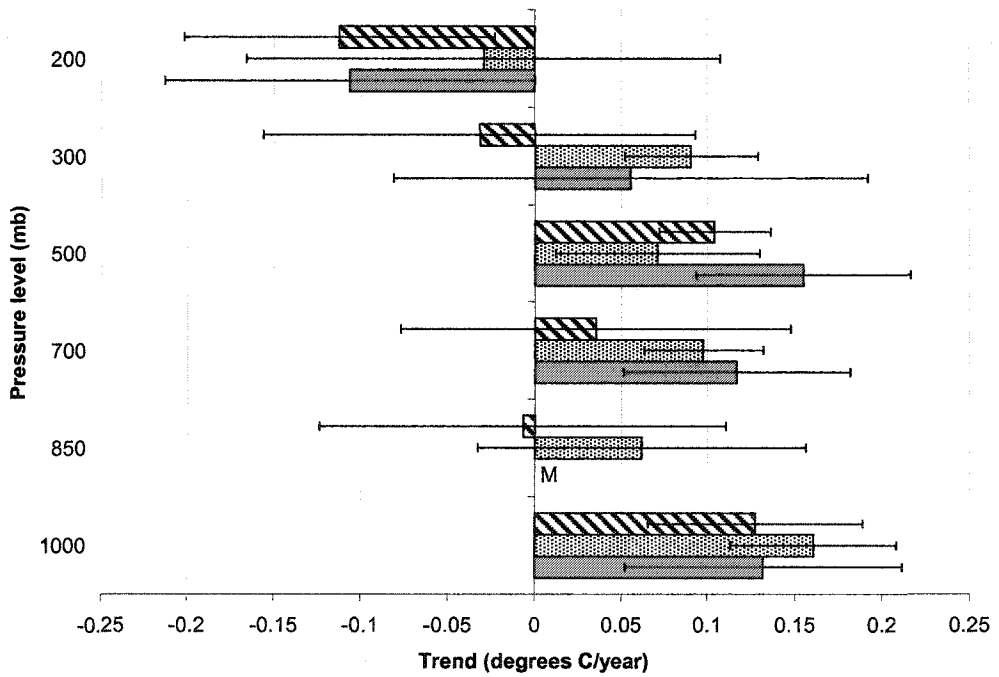

Figure 5.3. (continued)

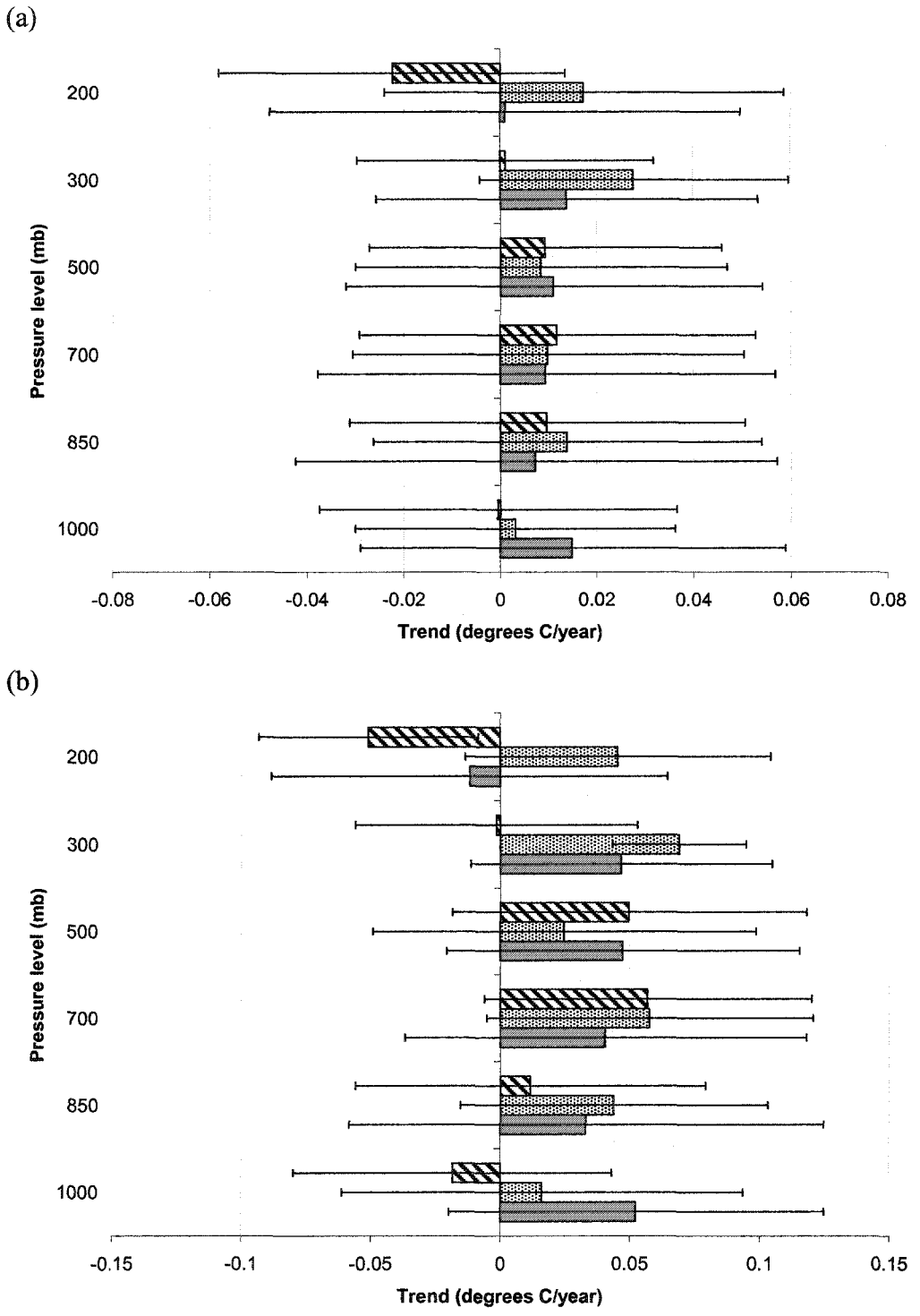

Figure 5.4. Same as Figure 5.2, but for the spring months (AMJ).

(c)

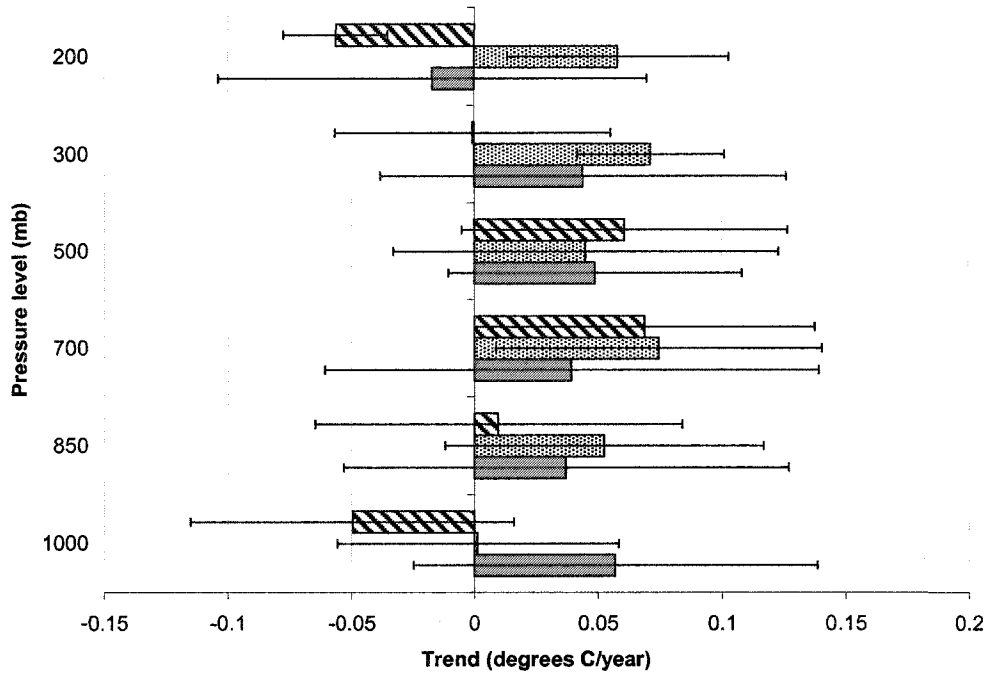

(d)

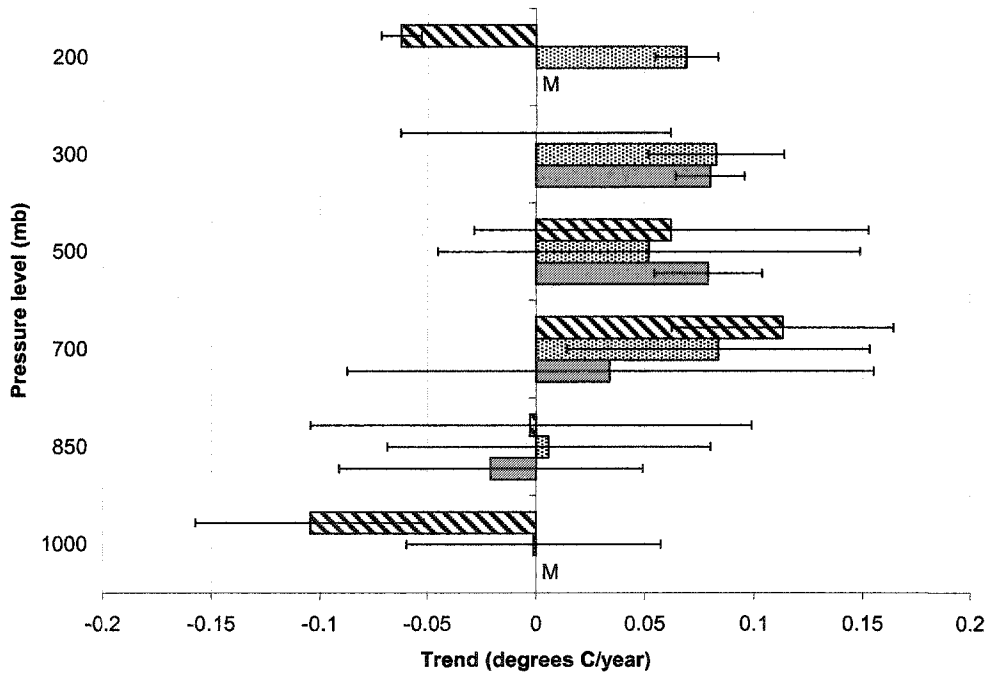

Figure 5.4. (continued)

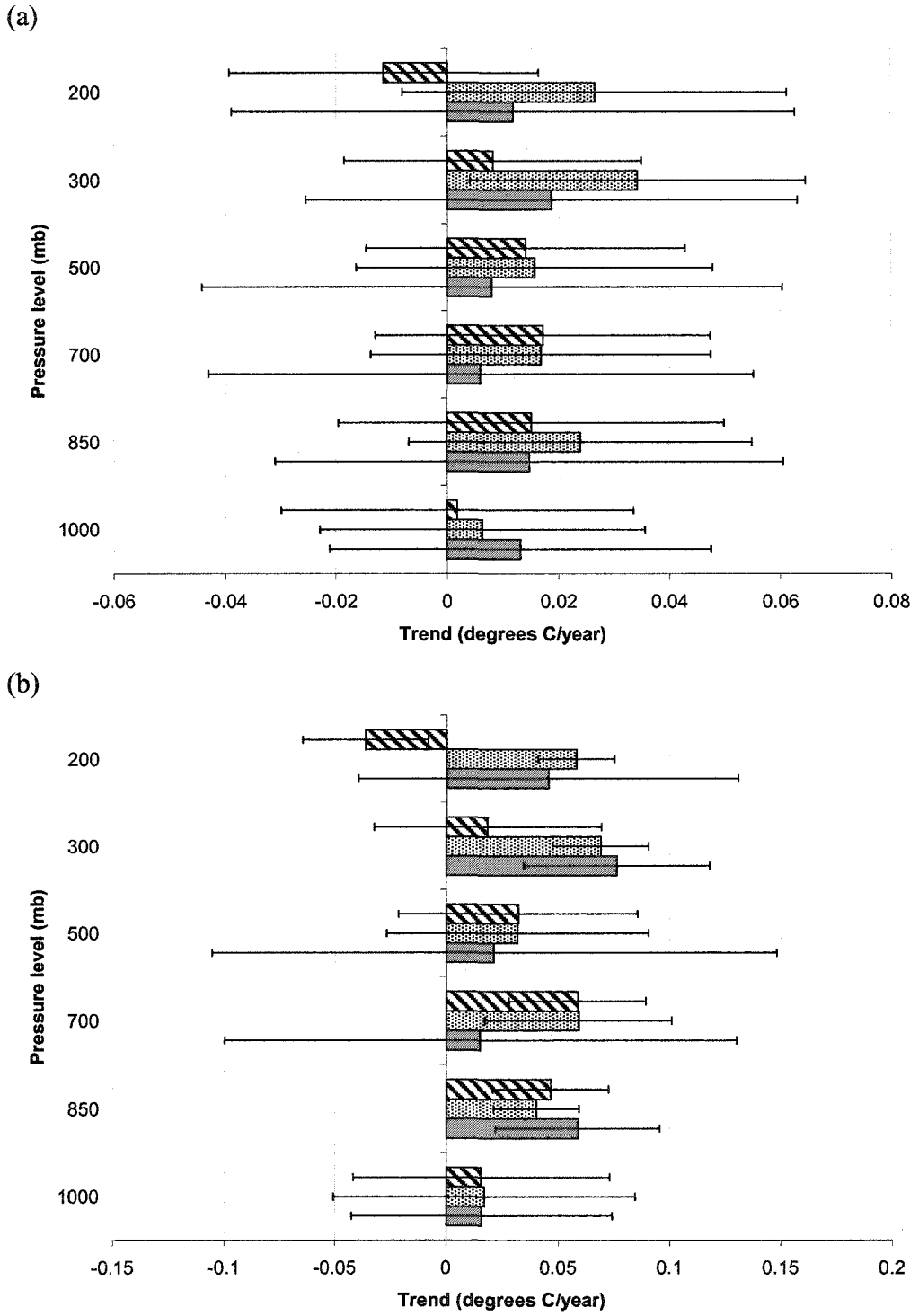

Figure 5.5. Same as Figure 5.2, but for the summer months (JAS).

(c)

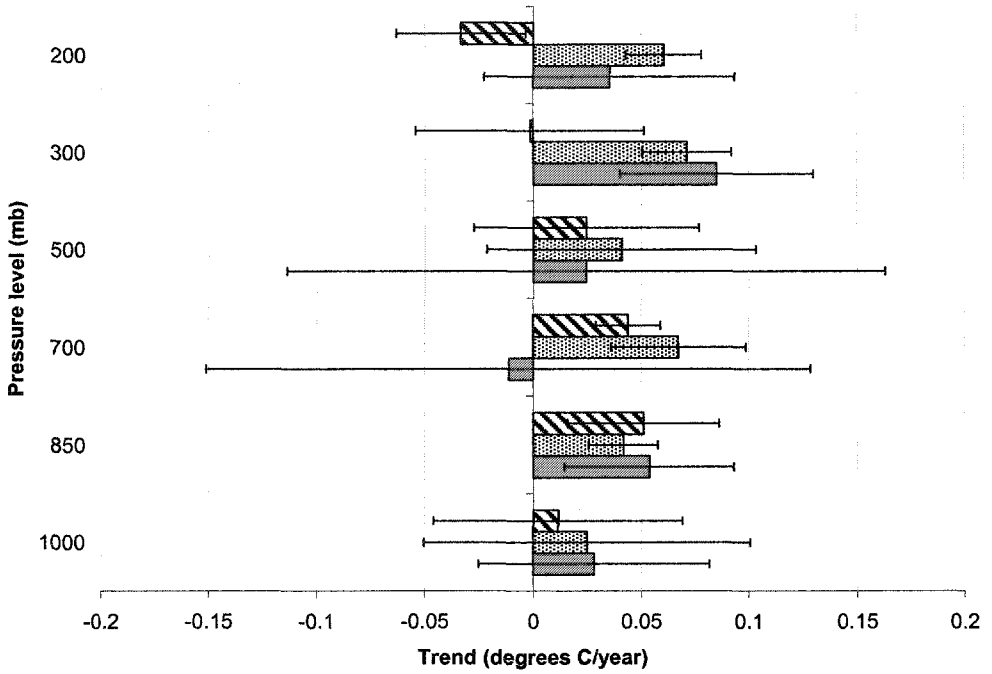

(d)

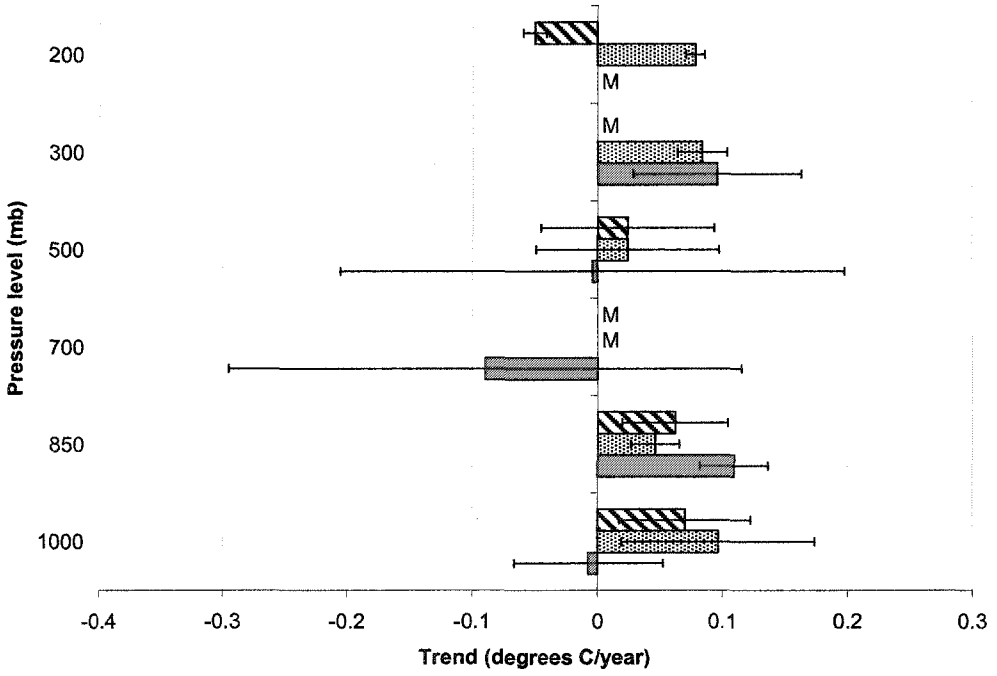

Figure 5.5. (continued)

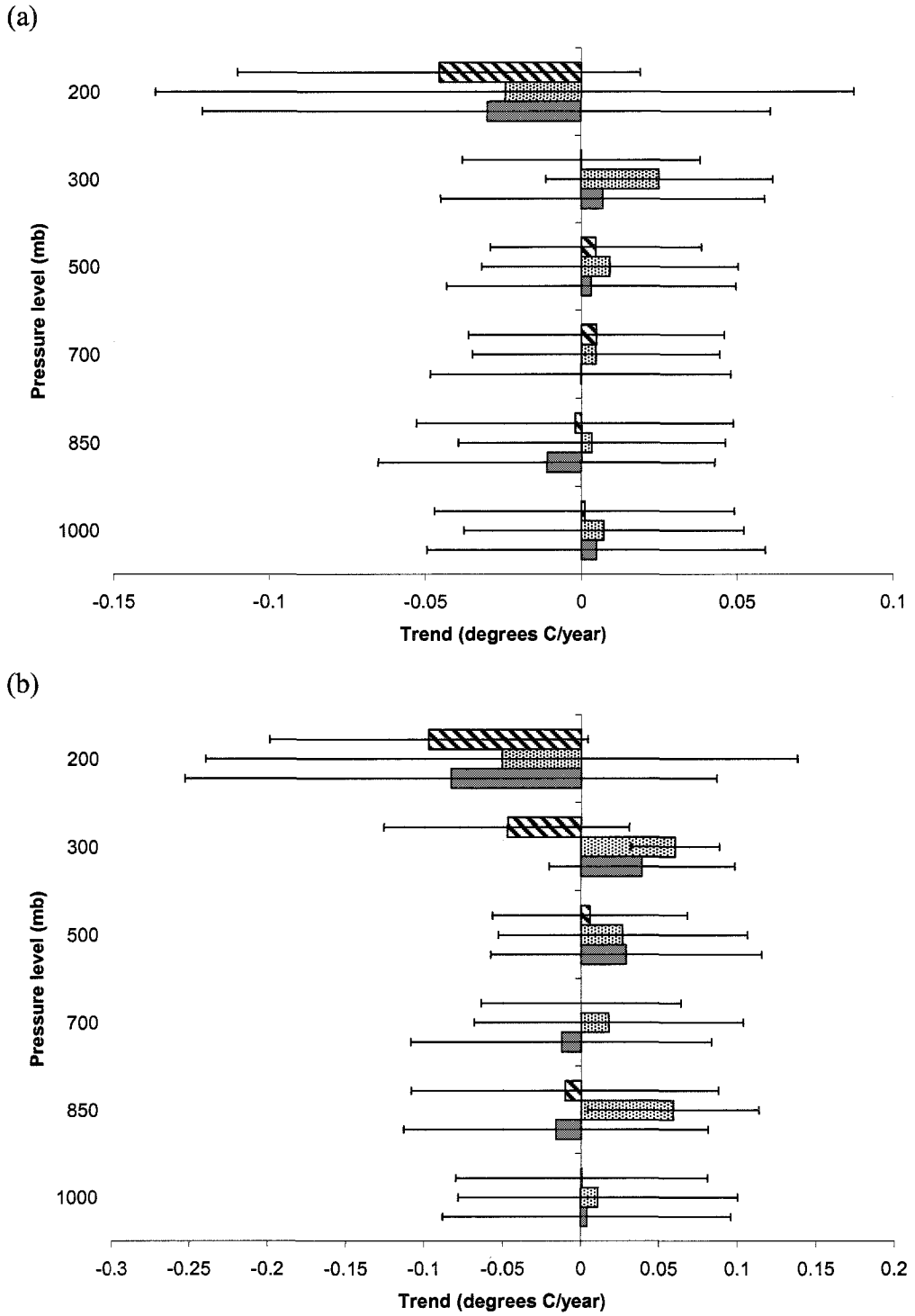

Figure 5.6. Same as Figure 5.2, but for the fall months (OND).

(c)

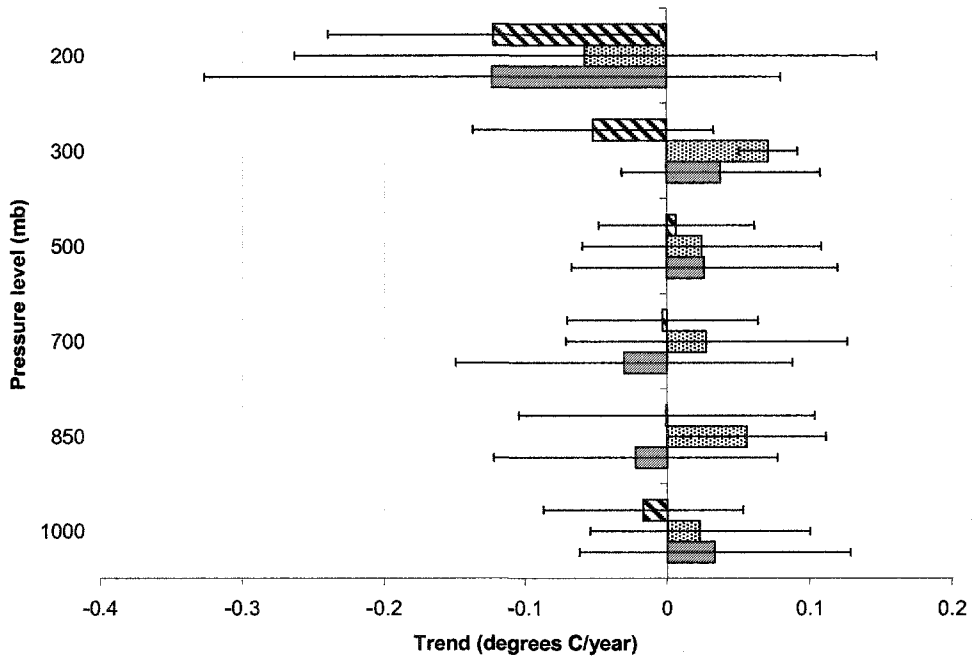

(d)

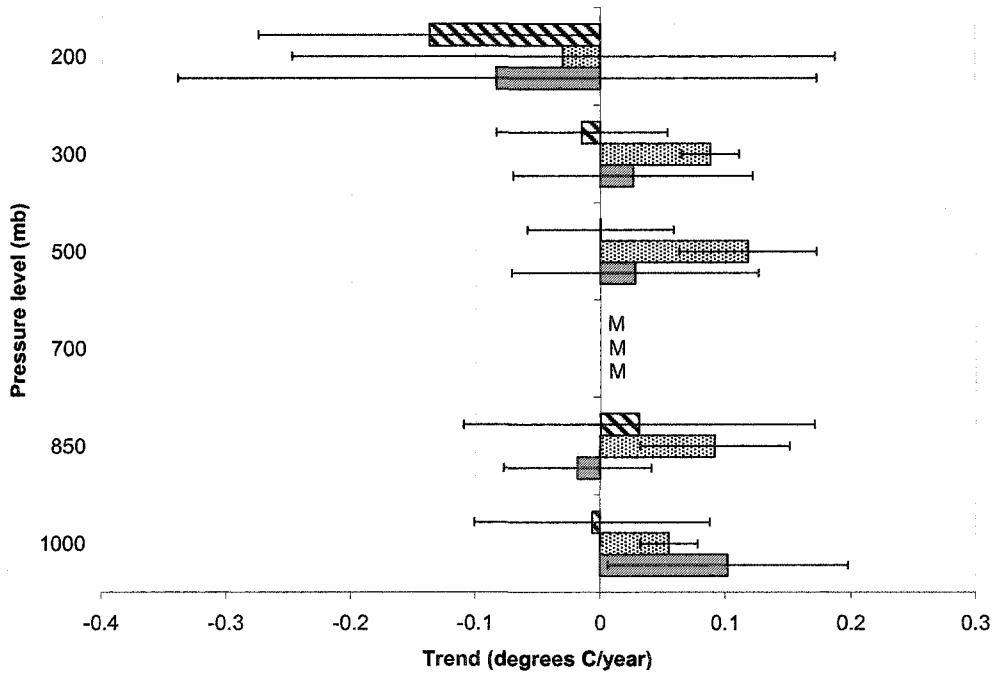

Figure 5.6. (continued)

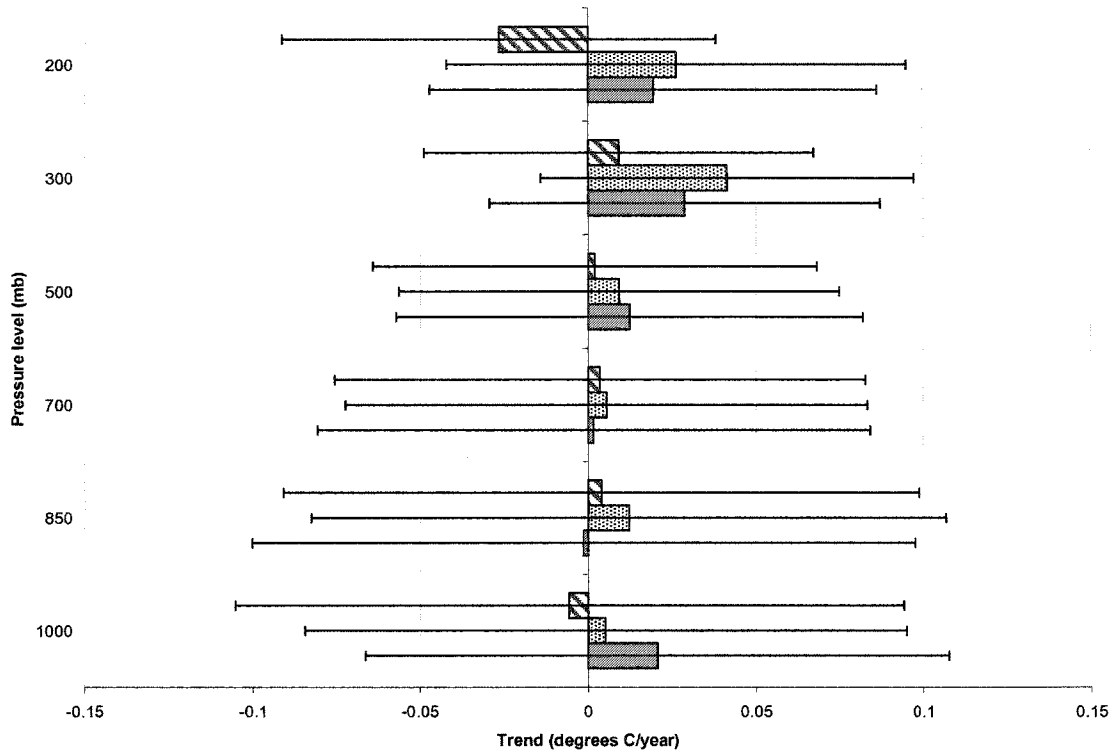

Figure 5.7. Annually-averaged T trends (error bars indicate standard deviations) at selected pressure levels, for all individual trends, eastern United States. NCEP trends are shown by the striped bars, ERA40 trends are shown by the light stippled bars, and the CARDS trends are shown by the dark grey bars.

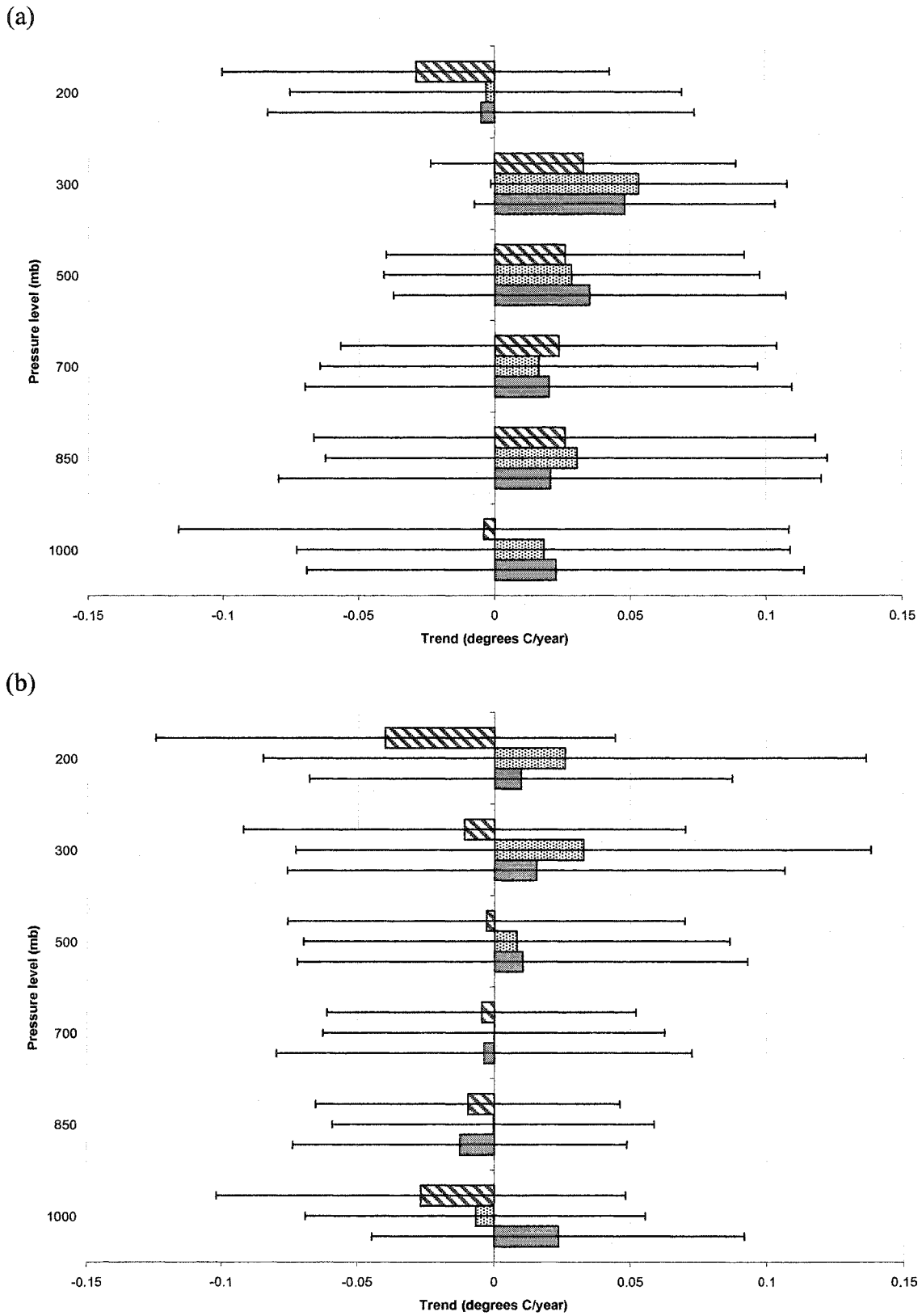

Figure 5.8. Same as Figure 5.7, but for the winter months (a), the spring months (b), the summer months (c), and the fall months (d).

(c)

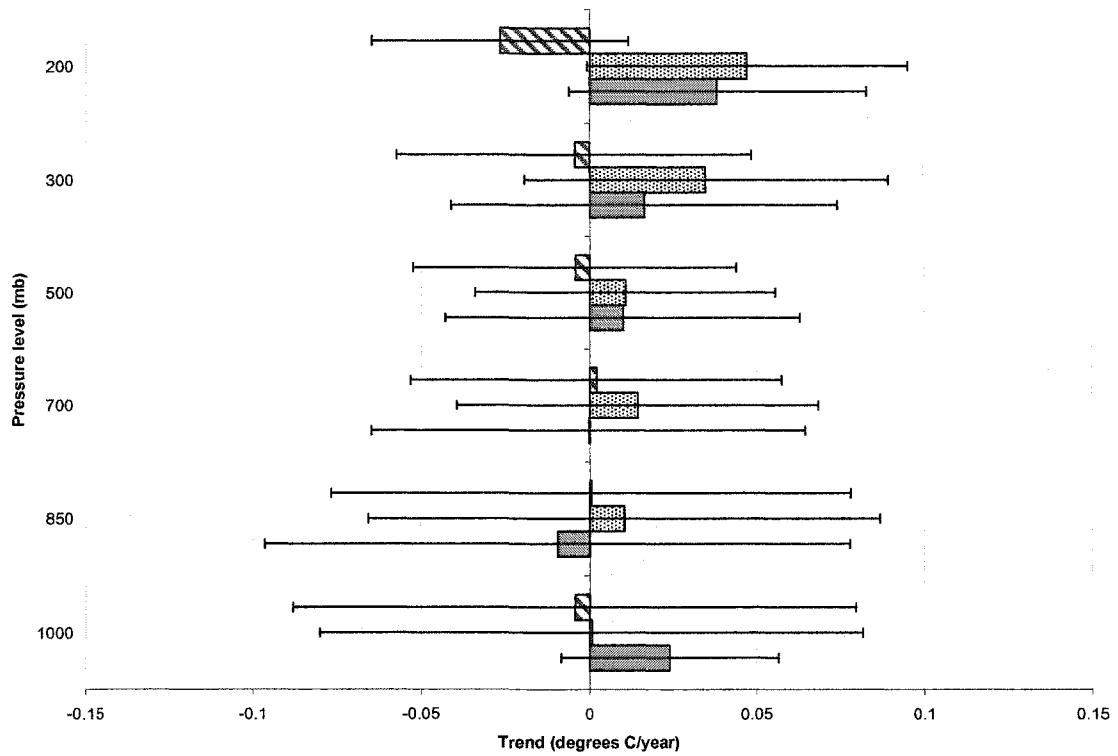

(d)

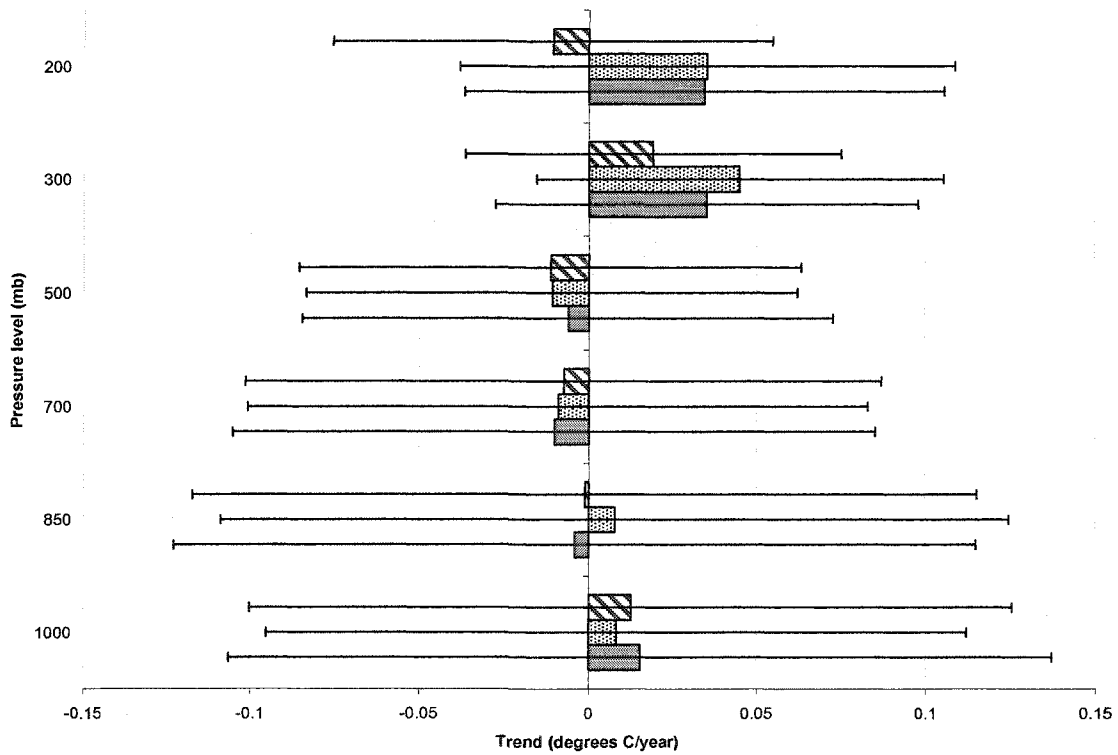

Figure 5.8. (continued)

CHAPTER 6

DISCUSSION AND CONCLUSIONS

It is clear that in order to completely understand surface warming/cooling trends, we must better understand the surface energy budget and its role in determining surface heating trends. The land cover characteristics of a given site will have a large influence on surface heating patterns and, as Chapter 2 has illustrated, these influences are likely to be quite complicated. As an initial attempt to better incorporate these land cover influences, we have attempted to show in this dissertation that, for the monitoring of surface trends, moist enthalpy, or equivalent temperature, is a more appropriate metric than air temperature. Generally, equivalent temperature should better depict contributions to surface heating caused by vegetation and other land cover characteristics, as it is expected to be more sensitive to land cover variations than air temperature alone. Although localized discrepancies will be encountered because of site-specific surface characteristics, overall, equivalent temperature heating trends will be of the same sign as temperature trends but will be larger in magnitude than the temperature trends. This is because equivalent temperature is directly accounting not only for dry air temperature (sensible heating) trends but also trends in heating driven by surface and atmospheric moisture (latent heating).

The overall results from this study indicate that the equivalent temperature trends are neutral while the temperature trends indicate cooling. The overall magnitudes of the equivalent temperature trends are not significantly larger than the temperature trends. They are, in fact, significantly smaller than the temperature trends, indicating less cooling than temperature, a condition which tends to contradict our initial hypothesis. If only higher-significance trends are considered, equivalent temperature trends show warming while temperature trends still indicate cooling. This finding contradicts our initial claim that the signs of the temperature and equivalent temperature trends would be the same.

We have helped to demonstrate that, outside of the growing season, equivalent temperature and temperature values are very similar to each other. It is during the growing season that the differences between the two quantities become most apparent (see Chapter 3). Equivalent temperature does, in fact, appear to be more sensitive than air temperature alone to annual variations in vegetation and other land surface characteristics. This finding also is generally borne out in the seasonal variations in temperature and equivalent temperature heating trends. The seasonal trend variations are larger in amplitude than are the temperature trend variations. As we have previously noted, it could be expected that if temperature and equivalent temperature values are more similar during the non-growing season months, the trend magnitudes should also be more similar. The fact that the non-growing season equivalent temperature trends are still larger in magnitude than the temperature trends leads us to suspect that it is not only annual cycles of vegetation greenup and senescence, but also general atmospheric moisture variations, that drive the differences between equivalent temperature and temperature. There are other vegetative factors that could be influencing this finding, but

are not investigated here, including reforestation, and the accompanying changes of tree species composition and basal areas, which has been reported over large areas in the eastern United States study area (Birdsey and Heath, 1995). All of these will help to increase or retain near-surface atmospheric moisture and will thus influence the relationship between the temperature and equivalent temperature trends.

The seasonal patterns in the surface temperature and equivalent temperature trends indicate a warming during the winter months, which then transitions, through the spring and summer, to cooling during the fall months. The amplitude of this pattern is larger for equivalent temperature trends than for temperature trends. These results were quite puzzling at certain times of the year. The cooling trends indicated during the fall months are of particular interest. It is not at all clear why both the average temperature and equivalent temperature surface heating trends should indicate cooling in the fall, then immediately switch sign to indicate the largest warming of the year during the winter months. This result should be looked into more closely.

During the fall through early spring, surface temperature and equivalent temperature trends are of the same sign. The summer months, however, give much more mixed results. Although average trends are largely neutral, the equivalent temperature trends often show warming with time, while temperature trends show slight cooling with time. This finding contradicts our initial expectations that the temperature and equivalent temperature trends would be of the same sign. However, this may not be entirely unexpected. After all, it is during these summer months that vegetation transpiration is at a maximum. For summer, even if surface temperature trends happen to show cooling in a particular circumstance, the increased vegetation transpiration is likely to provide a

heating source because of increased near-surface atmospheric moisture. This seems to be borne out further when these seasonal trend comparisons are analyzed for different land cover types, and also in the urban-rural pair comparisons we conducted (Chapter 4). Forest sites, irrigated agriculture sites, and urban sites show this summertime discrepancy between temperature and equivalent temperature trends, whereas the discrepancy is not nearly as obvious for drier sites such as grasslands.

What is evident from these comparisons - especially those from the urban-rural pairs - is that local site characteristics do have a large influence on the differences between surface equivalent temperature and temperature trends, and that we must better understand these site microclimates in order to better explain the differences between the equivalent temperature and temperature trends indicated in our analysis.

The possible connections between surface heating trends and tropospheric heating trends remain a mystery. On an annual basis (averaging over all seasons) slight cooling appears to be occurring in the upper troposphere, whereas at other pressure levels both the temperature and thickness data considered in this study indicate slight warming trends. NCEP indicates cooling at 200 mb, confirming our initial expectations, yet ERA40 shows warming at 300 mb, a finding that completely contradicts what we expected. The overall results, however, agree with our initial expectations that the upper troposphere would show a cooling trend, while the lower troposphere is remaining neutral or warming slightly.

Turning our attention to seasonal patterns in heating trends, to lend more credence to the idea that there may be a discrepancy between the surface and troposphere regarding heating trends, we found that the seasonal patterns of tropospheric heating trends (both

temperature and thickness) for selected sites around the globe are almost completely out of phase with those heating trends occurring at the surface for the eastern United States. In the troposphere, our results indicated maximum warming trends during the summer, with more neutral trends during the winter. Compare this with the surface, which shows maximum warming trends in the winter, with more neutral trends in the summer.

In the midst of all the aforementioned evidence of a surface-troposphere trend discrepancy, however, one particular result that the troposphere and surface do have in common is the fall cooling trends. For the troposphere, this cooling shows up primarily with the thickness trends. In fact, in the troposphere, this cooling shows up at lower levels, which could be expected to have more contact with the surface boundary layer. This may provide at least one much sought-after connection between the heating trends in the troposphere and at the earth's surface. In addition, when temperature trends were compared between the troposphere and the surface for the eastern United States, the seasonal patterns of surface and tropospheric trends were generally in agreement with each other. For this comparison, the greatest warming trends in both the troposphere and at the surface occurred during the winter months, while the least warming (most cooling) was found during the fall months. These findings are restricted, however, by the relatively small number of tropospheric sites that were available to conduct this surface-troposphere comparison. It would be useful to repeat such a comparison in a region where there are a greater number of tropospheric sites available to compare with surface sites, to see how robust this agreement in seasonal trends really is.

Another goal of this dissertation was to perform, for the troposphere, a much-needed comparison of heating trends between radiosonde and reanalysis datasets. The

temperature trend values estimated from the radiosonde data were generally between those trends estimated by both reanalyses considered in this study (NCEP, ERA40). The radiosonde thickness trends, however, showed less warming/more cooling than both reanalysis datasets, especially on an annual basis. It is not certain what may be causing this difference, so it definitely deserves more attention.

One of the initial goals of this study was to analyze equivalent temperature trends not only at the surface but also for the troposphere. This further analysis was expected to be very instrumental in determining whether or not using equivalent temperature as a primary metric to monitor heating trends would help to explain existing discrepancies between the surface and troposphere. Unfortunately, we were unable to obtain consistent radiosonde relative humidity for the troposphere, so this much-needed comparison was not performed. A tropospheric analysis of equivalent temperature should therefore be undertaken as a logical next step to the analyses performed in this dissertation. A comparison of radiosonde and reanalysis trends of upper-tropospheric zonal winds, as mentioned previously, would also be instructive in determining tropospheric heating trends. Such a comparison was initially planned for this dissertation, but not completed, as radiosonde wind data at 200 mb were not readily available for this study.

The study periods chosen for this study to estimate heating trends (troposphere: 1979-2001, surface: 1982-1997) were dictated primarily by the available datasets. The ISWO data were only for the years 1982-1997, while for the troposphere, the CARDS radiosonde data were only available after 1979. It would be preferable, of course, to conduct these trend analyses over a much longer time period, to help reduce the error in the estimated trends.

We assumed a constant latent heating term, L, in the computations of equivalent temperature. In reality, although L varies slightly with air temperature, it was concluded that this slight variation with T would only negligibly impact the calculations of equivalent temperature.

We were only able to look at five urban-rural station pairs for the surface heating trend analyses in Chapter 5. This made it virtually impossible to do a thorough examination of urban versus rural surface heating trends. The urban-rural comparison performed in this dissertation would greatly benefit by expanding the comparison to analyze as many urban-rural station pairs as is possible.

Equivalent temperature is a more accurate measure of heating trends than air temperature by itself. Moist heating effects are implicitly included in air temperature, but air temperature, by itself, is not total heat content. Using equivalent temperature to measure both surface and tropospheric heating trends would help interpret both the heating trends themselves and the causes behind these observed heating trends. Equivalent temperature trends also add much useful information about seasonal cycles in heating trends, particularly regarding growing season versus non-growing season heating trends. Equivalent temperatures are useful for diagnosing spatial variations in heating trends as a function of land cover and would also help to further explain any connections between tropospheric and surface heating trends. Ideally, controlled experiments would be needed that change surface moisture and land cover conditions over time, with accompanying metadata, and investigate how both temperature and equivalent temperature respond to these changes. Further work should also consider performing a surface energy flux analysis at selected surface sites that measure air temperatures, in an

attempt to better understand site microclimates and their possible influences on near-surface temperature and total heat content. Principal components analysis would be useful to identify the different ways, categorized by geographical region and by land-cover type, in which land use and land cover can influence near-surface heating trends. A higher-resolution land cover dataset would be useful in this exercise. Any specific sites that show up as outliers within these identified categories could then be targeted for further studies investigating their local microclimates, to better understand how temperature and equivalent temperature are related under these local conditions.

In summary, then, there are several key points that this dissertation has helped to illustrate. They are as follows:

- If we continue to use surface data on a widespread basis, we must make a concerted effort to greatly improve our metadata on surface observation sites, focusing particularly on photographic documentation of site exposures.
- Based on existing problems with documentation of surface station microclimates and the complex land-atmosphere interactions that occur at these sites, temperature by itself is not sufficient for monitoring heating trends. Moist enthalpy (equivalent temperature) is a more appropriate metric to monitor these heating trends, since it *is* atmospheric heat content. We have shown that moist enthalpy is more sensitive than air temperature to annual variations in surface vegetation cover.
- Overall, our estimated surface and tropospheric heating trends show slight warming for the surface and lower troposphere, with cooling indicated for the upper troposphere. This finding contradicts our expectations for insignificant

trends in the surface and lower troposphere but it does support our expectation that significant cooling trends would be indicated for the upper troposphere.

- Moist enthalpy trends generally indicate more warming/less cooling than temperature trends. Overall, moist enthalpy trends are not greater in magnitude than temperature trends, thus contradicting our initial expectations. On a seasonal basis, however, particularly during the non-growing season, moist enthalpy trends are greater in magnitude than temperature trends.
- The CARDS radiosonde dataset compares favorably to both the ERA40 and NCEP reanalyses. The ERA40 reanalysis is generally warmer than the CARDS dataset, while the NCEP reanalysis is generally cooler.
- Cooling trends are indicated at the surface during the fall months, thus supporting similar findings from previous studies (e.g. Bonan, 2001).
- While connections between the surface and troposphere regarding heating trends remain unclear, one common feature we found in this study is the fall cooling trends indicated for the lower troposphere as well as for the surface.

If the science community will continue to explore other ways of measuring heating trends and strive to further understand land-atmosphere interactions, particularly with respect to the surface energy budget, we can expect breakthroughs regarding our understanding of surface heating trends and hopefully resolve existing issues about how the surface and tropospheric heating trends are connected to each other.

REFERENCES

Angell, J.K., 1988: Variations and Trends in Tropospheric and Stratospheric Global Temperatures, 1958-87. *J. Climate*, **1**, 1296-1313.

Angell, J.K., 2000: Difference in radiosonde temperature trend for the period 1979-1998 of MSU data and the period 1959-1998 twice as long. *Geophys. Res. Lett.*, **27**(15), 2177-2180.

Bengtsson, L., E. Roeckner, and M. Stendel, 1999: Why is the global warming proceeding much slower than expected? *J. Geophys. Res.*, **104**, 3865-3876.

Birdsey, R.A., and L.S. Heath, 1995: Carbon changes in U.S. forests. In: Joyce LA (Ed) Productivity of America's forests and climate change. Gen. Tech. Rep. RM-271. USDA Forest Service, Rocky Mountain Forest and Range Experiment Station, Fort Collins, Colorado, U.S.A. pp 56–70.

Bonan, G.B., 2001: Observational Evidence for Reduction of Daily Maximum Temperatures by Croplands in the Midwest United States. *J. Climate*, **14**, 2430-2442.

Cai, M., and E. Kalnay, 2004: Reply to: Impact of land-use change on climate. *Nature*, **427**, 214.

Chase, T.N., R.A. Pielke, Sr., J.A. Knaff, T.G.F. Kittel, and J. Eastman, 2000: A comparison of regional trends in 1979-1997 depth-averaged tropospheric temperatures. *Intl. J. Clim.*, **20**, 503-518.

Christy, J.R., and R.W. Spencer, 1995: Assessment of Precision in Temperatures from the Microwave Sounding Units. *Climatic Change*, **20**, 613-629.

Christy, J.R., R.W. Spencer, and W.D. Braswell, 2000: MSU tropospheric temperatures: Dataset construction and radiosonde comparisons. *J. Atmos. Oceanic. Tech.*, **17**, 1153-1170.

Christy, J.R. R.W. Spencer, W.B. Norris., W.D. Braswell, and D.E. Parker, 2003: Error estimates of Version 5.0 of MSU/AMSU bulk atmospheric temperatures. *J. Atmos. Oceanic Tech.*, **20**, 613-629.

Christy, J.R., and W.B. Norris, 2004: What may we conclude about global tropospheric temperature trends? *Geophys. Res. Lett.*, **31**, L02611, doi:10.1029/2003GL019361.

Davey, C.A., and R.A. Pielke, Sr., 2005: Microclimate exposures of surface-based weather stations - implications for the assessment of long-term temperature trends. *Bull. Amer. Meteor. Soc.*, in press.

Devore, J.L., 1995: *Probability and Statistics for Engineering and the Sciences (4th ed.)*. Duxbury Press, 743 pp.

Eskridge, R., A. Alduchov, I. Chernykh, Z. Panmao, A. Polansky, and S. Doty, 1995: A Comprehensive Aerological Research Data Set (CARDS): Rough and Systematic Errors. *Bull. Amer. Meteor. Soc.*, **76**, 1759-1775.

Free, M., I. Durre, E. Aguilar, D. Seidel, T.C. Peterson, R.E. Eskridge, J.K. Luers, D. Parker, M. Gordon, J. Lanzante, S. Klein, J. Christy, S. Schroeder, B. Soden, L.M. McMillin, and E. Weatherhead, 2002: Creating Climate Reference Datasets – CARDS Workshop on Adjusting Radiosonde Temperature Data for Climate Monitoring. *Bull. Amer. Meteor. Soc.*, **83**, 891-899.

Gaffen, D.J., 1994: Temporal Inhomogeneities in Radiosonde Temperature Records. *J. Geophys. Res.*, **99**(D2), 3667-3676.

Gaffen, D.J., M.A. Sargent, R.E. Habermann, and J.R. Lanzante, 2000b: Sensitivity of tropospheric and stratospheric temperature trends to radiosonde data quality. *J. Climate*, **13**, 1776-1796.

Gallant, A.R., and J.J. Goebel, 1976: Nonlinear Regression With Autocorrelated Errors. *J. Amer. Stat. Assoc.*, **71**(356), 961-967.

Gallo, K.P., 1996: The Influence of Land Use/Land Cover on Climatological Values of the Diurnal Temperature Range. *J. Climate*, **9**, 2941-2944.

Hansen, J., and S. Lebedeff, 1987: Global Trends of Measured Surface Air Temperature. *J. Geophys. Res.*, **92**, 13345-13372.

Hansen, J., H. Wilson, M. Sato, R. Ruedy, K. Shah, and E. Hansen, 1995: Satellite and Surface Temperature Data at Odds? *Climatic Change*, **30**, 103-117.

Hurrell, J.W., and K.E. Trenberth, 1996: Satellite versus surface estimates of air temperature since 1979. *J. Climate*, **9**, 2222-2232.

Hurrell, J.W., and K.E. Trenberth, 1997: Spurious trends in satellite MSU temperatures from merging different satellite records. *Nature*, **386**, 164-167.

Hurrell, J.W., and K.E. Trenberth, 1998: Difficulties in Obtaining Reliable Temperature Trends: Reconciling the Surface and Satellite Microwave Sounding Unit Records. *J. Climate*, **11**, 945-967.

Hurrell, J.W., S.J. Brown, K.E. Trenberth, and J.R. Christy, 2000: Comparison of Tropospheric Temperatures from Radiosondes and Satellites: 1979-1998. *Bull. Amer. Meteor. Soc.*, **81**(9), 2165-2177.

Intergovernmental Panel on Climate Change (IPCC), 1990: *Climate Change, The IPCC Scientific Assessment*. Cambridge University Press, 365 pp.

IPCC, 1996: *Climate Change 1995, The Science of Climate Change*. Cambridge University Press, 570 pp.

IPCC, 2001: *Climate Change 2001, The Scientific Basis*. Cambridge University Press, 881 pp.

Jones, P.D., 1988: Hemispheric surface air temperature variations: Recent trends and an update to 1987. *J. Climate*, **1**, 654-660.

Jones, P.D., 1994b: Hemispheric surface air temperature variations: A reanalysis and an update to 1993. *J. Climate*, **7**, 1794-1802.

Jones, P.D., 1995: Land Surface Temperatures – Is the Network Good Enough? *Climatic Change*, **31**, 545-558.

Kalnay, E., et al., 1996: The NCEP/NCAR 40-year reanalysis project. *Bull. Amer. Meteor. Soc.*, **77**, 437-471.

Kalnay, E., and M. Cai, 2003: Impact of urbanization and land-use change on climate. *Nature*, **423**, 528-531.

Karl, T.R., C.N. Williams, Jr., F.T. Quinlan, and T.A. Boden, 1990: United States Historical Climatology Network (HCN) Serial Temperature and Precipitation Data, Environmental Science Division, Publication No. 3404, Carbon Dioxide Information and Analysis Center, Oak Ridge National Laboratory, Oak Ridge, TN, 389 pp.

Karl, T.R., V.E. Derr, D.R. Easterling, C.K. Folland, D.J. Hoffman, S. Levitus, N. Nicholls, D.E. Parker, and G.W. Withee, 1995: Critical issues for long-term climate monitoring. *Climatic Change*, **31**, 185-221.

Lanzante, J.R., S.A. Klein, and D.J. Seidel, 2003a: Temporal homogenization of monthly radiosonde temperature data. Part I: Methodology. *J. Climate*, **16**, 224-241.

Lanzante, J.R., S.A. Klein, and D.J. Seidel, 2003b: Temporal homogenization of monthly radiosonde temperature data. Part II: Trends, sensitivities and MSU comparison. *J. Climate*, **16**, 242-262.

Luers, J.K., and R.E. Eskridge, 1998: Use of radiosonde data in climate studies. *J. Climate*, **11**, 1002-1019.

Mann, M.E., and P.D. Jones, 2003: Global surface temperatures over the past two millennia. *Geophys. Res. Lett.*, **30**(15), 1820, doi:10.1029/2003GRL017814.

Mears, C.A., M.C. Schabel, and F.J. Wentz, 2003: A reanalysis of the MSU channel 2 tropospheric temperature record. *J. Climate*, **16**, 3650-3664.

National Research Council, 1999: Adequacy of Climate Observing Systems. NRC Panel on Climate Observing Systems Status, National Academy Press, Washington, D.C., 51 pp.

National Research Council, 2000: Reconciling observations of global temperature change. Panel on Reconciling Observations, Climate Research Committee, Board on Atmospheric Sciences and Climate, National Academy Press, Washington, D.C., 85 pp.

Norris, W.B., 2002: Climatological Averaging of Temperature Soundings (CATS) Users Manual. Available from Earth System Science Center, Huntsville, Alabama, USA, 389 pp.

NCDC, 1998: The International Surface Weather Observations (ISWO) CD-ROM set. Data jointly provided by the U.S. Dept. of Commerce/NOAA and the U.S. Air Force Combat Climatology Center. National Climatic Data Center, Asheville, North Carolina, U.S.A.

Oort, A.H., and H. Liu, 1993: Upper-Air Temperature Trends over the Globe, 1958-89. *J. Climate*, **6**, 292-307.

Parker, D.E., M. Gordon, D.P.N. Cullum, D.M.H. Sexton, C.K. Folland, and N. Raymer, 1997: A new global gridded radiosonde temperature data base and recent temperature trends. *Geophys. Res. Lett.*, **24**, 1499-1502.

Pielke Sr., R.A., 1998: Climate prediction as an initial value problem. *Bull. Amer. Meteor. Soc.*, **79**, 2743-2746.

Pielke Sr., R.A., T. Stohlgren, W. Parton, J. Moeny, N. Doesken, L. Schell, and K. Redmond, 2000: Spatial representativeness of temperature measurements from a single site. *Bull. Amer. Meteor. Soc.*, **81**, 826-830.

Pielke Sr., R.A., 2001a: Influence of the spatial distribution of vegetation and soils on the prediction of cumulus convective rainfall. *Rev. Geophys.*, **39**, 151-177.

Pielke, Sr., R.A., T.N. Chase, T.G.F. Kittel, J.A. Knaff, and J. Eastman, 2001b: Analysis of 200 mbar zonal wind for the period 1958-1997. *J. Geophys. Res.*, **106**(D21), 27287-27290.

Pielke, Sr., R.A., T.N. Chase, L. Schell, W. Parton, N. Doesken, K. Redmond, J. Moeny, T. McKee, and T.G.F. Kittel, 2002: Problems in evaluating regional and local trends in temperature: An example from eastern Colorado, USA. *Int. J. Climatol.*, **22**, 421-434.

Pielke Sr., R.A., 2003: Heat storage within the Earth system. *Bull. Amer. Meteor. Soc.*, **84**, 331-335.

Pielke Sr., R.A., and T.N. Chase, 2004: Technical Comment: Contributions of Anthropogenic and Natural Forcing to Recent Tropopause Height Changes. *Science*, **303**, 1771b.

Pielke Sr., R.A., C. Davey, and J. Morgan, 2004: Assessing "global warming" with surface heat content. *Eos*, **85**(21), 210-211.

Rogers, R.R., and M.K. Yau, 1989: *A Short Course in Cloud Physics (3rd Edition).* Pergamon Press, New York, **293** pp.

Santer, B.D., R. Sausen, T.M.L. Wigley, J.S. Boyle, K. Achutarao, C. Doutriaux, J.E. Hansen, G.A. Meehl, E. Roeckner, R. Ruedy, G. Schmidt, and K.E. Taylor, 2003a: Behavior of tropopause height and atmospheric temperature in models, reanalyses, and observations: Decadal changes. *J. Geophys. Res.*, **108**(D1), doi:10.1029/2002JD002258.

Santer, B.D., M.F. Wehner, T.M.L. Wigley, R. Sausen, G.A. Meehl, K.E. Taylor, C. Ammann, J. Arblaster, W.M. Washington, J.S. Boyle, and W. Bruggemann,

2003b: Contributions of Anthropogenic and Natural Forcing to Recent Tropopause Height Changes. *Science*, **301**, 479-483.

Simmons, A.J., and J.K. Gibson, 2000: *ERA-40 Project Report Series No. 1. The ERA-40 Project Plan.* European Centre for Medium-Range Weather Forecasts, 62 pp.

Soon, Willie W.-H, D.R. Legates, and S. Baliunas, 2004: Estimation and representation of long-term (>40 year) trends of Northern-Hemisphere-gridded surface temperatue: A note of caution. *Geophys. Res. Lett.*, **31**, L03209, doi10:1029/2003GRL019141.

Spencer, R.W., and J.R. Christy, 1990: Precise Monitoring of Global Temperature Trends from Satellites. *Science*, **247**, 1558-1562.

Stohlgren, T.J., personal communication, January, 2005.

Trenberth, K.E., 2004: Rural land-use change and climate. *Nature*, **427**, 213.

Vinnikov, K.Y., P. Groisman, and K. Lugina, 1990: The empirical data on modern global climate changes (temperature and precipitation). *J. Climate*, **3**, 662-677.

Vinnikov, K.Y., and N.C. Grody, 2003: Global warming trend of mean tropospheric temperature observed by satellites. *Science*, **302**, 269-272.

Vogelmann, J.E., S.M. Howard, L. Yang, C.R. Larson, B.K. Wylie, and N. Van Driel, 2001: Completion of the 1990s National Land Cover Data Set for the Conterminous United States from Landsat Thematic Mapper Data and Ancillary Data Sources. *Photogrammetric Engineering and Remote Sensing*, **67**, 650-662.

Vose, R.S., T.R. Karl, D.R. Easterling, C.N. Williams, and M.J. Menne, 2004: Impact of land-use change on climate. *Nature*, **427**, 213-214.

Weatherhead, E.C., et al., 2000: Detecting the recovery of total column ozone. *J Geophys. Res.*, **105**(D17), 22,201-22,210.

World Meteorological Organization, 1996: *Guide to Meteorological Instruments and Methods of Observation.* WMO Report No. 8, 6th ed., 433 pp.

APPENDIX A

STATISTICAL METHODOLOGY

A.1 Statistical Hypothesis Testing

Devore (1995) defines a statistical hypothesis as a claim regarding either the value of a single population characteristic or the values of multiple population characteristics. These characteristics can be estimated from sample data. The primary objective of a statistical hypothesis test is to determine which of two contradictory claims (statistical hypotheses) about the estimated population characteristic is correct. Generally, one of these claims is initially favored and is termed the "null" hypothesis, or H_0, while an alternative hypothesis, H_a, is considered in case the evidence indicates that H_0 should be rejected. These tests can be conducted at various significance levels, or α values. The α value is the probability of rejecting the null hypothesis H_0 when it is actually true. Typical values of α are .10 (for 90% significance), .05 (for 95% significance), and .01 (for 99% significance).

A test statistic, which is a function of the sample data, is used to conduct the hypothesis test. The form of this test statistic varies depending on the test being run. The trend significance tests described below are one such type of hypothesis testing procedure. Another type of hypothesis test concerns the difference between two population means, μ_1 and μ_2, and whether or not this difference is significantly different from some given value, Δ_0. In this case, the null hypothesis, H_0, is that $\mu_1 - \mu_2 = \Delta_0$, while the alternative hypothesis, H_a, is that $\mu_1 - \mu_2 \neq \Delta_0$. For large enough sample sizes ($m \geq 30$ and $n \geq 30$), the test statistic is given by

$$Z = \frac{x - y - \Delta_0}{\sqrt{\left(\frac{s_1^2}{m} + \frac{s_2^2}{n}\right)}}$$

where x and y are the sample means (with standard deviations s_1 and s_2) corresponding to μ_1 and μ_2, respectively. For a two-tailed level α test such as this, H_0 will be rejected if either $Z \geq Z_{\alpha/2}$ or $Z \leq -Z_{\alpha/2}$. For the standard α values of .10, .05, and .01, the critical test statistic values are $Z_{\alpha/2} = 1.65$, 1.96, and 2.58, respectively. Finally, for large enough sample size n, one can test whether or not a population mean is significantly different from zero by using the test statistic

$$Z = \frac{x}{s/\sqrt{n}},$$

where x and s are the sample mean and standard deviation, and performing the same steps outlined above.

A.2 Trend Analysis

For temporal trend analysis, it is common to use a linear model expressed as

$$y = \beta t + \varepsilon$$

where β represents the trend to be estimated and ε represents the error. The traditional assumptions are that the observational data used to estimate the trend are obtained in an experimentally controlled environment. It is also assumed that the errors ε are normally distributed around zero and that errors are uncorrelated across observations, so that the observations themselves are independent of each other. In these conditions, the ordinary least squares (OLS) estimates provide the best estimates of the actual trend β. In these conditions, the ratio of the trend estimate, b, to the standard error of the trend estimate, SE(b), given by

$$\tau = b/\ SE(b),$$

is distributed as Student's t and is used to determine whether or not an estimated trend b is significantly different from zero (using the same criteria as for the aforementioned Z test statistics). This is done by comparing τ to a specified significance level α, discussed in the previous section of this appendix. The ratio τ will have associated with it a certain significance probability, the probability of obtaining a larger value of τ than was actually calculated in the observation sample. If this probability is less than the specified significance level α, it is then likely that the actual trend β is significantly different from zero.

The above scenario assumes a well-controlled environment where each measurement (observation) is independent from all the other measurements. This is not typically the case with temperature measurements, where errors are frequently correlated across observations. This is what is referred to as autocorrelation. In this case, if it is assumed that the observation errors are independent of each other and normally distributed around zero, this will tend to exaggerate the overall error. Autocorrelation between observations must be properly accounted for in the error term. To do this, the error term for each observation, ε_t, must be replaced with the term

$$v_t = \varepsilon_t - \sum_{i=1}^{m} \varphi_i v_{t-i}$$

which accounts for all autocorrelations up to lag m. The vector $\varphi = (\varphi_1,\ldots,\varphi_m)$ is the vector of autoregressive parameters while $v = (v_1,\ldots,v_m)$ is the error vector.

The Yule-Walker (YW) method (Gallant and Goebel, 1976) is a commonly used estimation method used for the autoregressive error model and has been used in the trend analyses covered in this dissertation. Basically, this method alternates between estimating the actual trend value, β, using generalized least squares (GLS), and estimating the

autoregressive parameters φ using the YW equations applied to the sample autocorrelation function. The YW equations are given as

$$R\varphi_{est} = -r$$

where φ_{est} is the current estimation of the autoregressive parameters, $r = (r_1,\ldots,r_m)$ is the vector of sample autocorrelations covering lags 1 through m, and R is the Toeplitz matrix, the i,jth element of which is $r_{|i-j|}$.

To obtain a best estimate for the actual trend β, first, an OLS estimate of β is found. Next, the autoregressive parameter vector φ is estimated using the YW equations, which also provide an initial estimate of the variance σ^2. Using σ^2, and calculating V using φ, the variance matrix $\Sigma = \sigma^2 V$ can then be calculated. The variance matrix Σ is then used, through GLS, to derive a new estimate, b, for the actual trend β. This cycle then repeats itself as necessary until a best estimate of β is obtained. Once this best estimate is obtained, a t-ratio (b/SE) is then computed for the trend estimate to determine whether or not this estimate is significantly different from zero.

APPENDIX B

STATION LISTS

Table B.1. List of CARDS stations used for tropospheric trend analysis. Latitude (longitude) values are negative for the southern (western) hemispheres.

CARDS#	Station Name	Latitude (dd)	Longitude (dd)	Elevation (m)
526810	MINQIN	38.633	103.083	1367
619010	ST HELENA ISLAND	-15.96	-5.7	630
619020	ASCENSION IS./WIDE AWA	-7.967	-14.4	83
619670	DIEGO GARCIA NAS	-7.7	72.4	2
619760	SERGE-FROLOW/TROME.	-15.88	54.517	7
619880	RODRIGUES/PLAINE	-19.68	63.417	58
619950	VACOAS	-20.3	57.5	425
619960	MARTIN DE VIVIES	-37.8	77.533	27
619980	PORT-AUX-FRANCAIS	-49.35	70.25	20
637410	NAIROBI/DAGORETTI	-1.3	36.75	1798
638940	DAR ES SALAAM ARPT	-6.867	39.2	55
639850	SEYCHELLES INTL	-4.667	55.517	3
670270	MAJUNGA/MAHAJANGA	-14.88	50.25	88
670830	ANTANANARIVO/IVATO	-18.8	47.483	1279
671970	FT DAUPHIN	-25.03	46.95	8
673410	MAPUTO/MAVALANE	-25.91	32.567	39
677740	HARARE/BELVEDERE	-17.83	31.017	1471
679640	BULAWAYO/GOETZ	-20.15	28.617	1343
681100	WINDHOEK	-22.56	17.1	1700
681740	PIETERSBURG	-23.86	29.45	1242
682630	PRETORIA/IRENE	-25.91	28.217	1525
684240	UPINGTON/PIERRE VAN	-28.4	21.267	850
684420	BLOEMFONTEIN/HERTZO	-29.1	26.3	1359
685880	DURBAN/LOUIS BOTHA	-29.96	30.95	8
700260	POINT BARROW	71.3	-156.78	12
703080	ST PAUL ISLAND	57.15	-170.21	10
703980	ANNETTE ISLAND	55.033	-131.56	37
722010	KEY WEST INT AP	24.55	-81.75	1
722350	JACKSON/THOMPSON FLD	32.317	-90.067	91
722500	BROWNSVILLE	25.9	-97.433	7
722510	CORPUS CHRISTI	27.767	-97.5	14
722610	DEL RIO	29.367	-100.91	313
722930	MIRAMAR NAS	32.867	-117.15	147
723270	NASHVILLE	36.25	-86.567	180
723650	ALBUQUERQUE	35.05	-106.61	1619

CARDS#	Station Name	Latitude (dd)	Longitude (dd)	Elevation (m)
723870	DESERT ROCK/MERCURY	36.617	-116.01	1007
724510	DODGE CITY	37.767	-99.967	791
724930	OAKLAND INT AP	37.75	-122.21	6
725200	PITTSBURGH/MOON TOWNSH	40.533	-80.233	360
725970	MEDFORD	42.367	-122.86	397
726450	GREEN BAY	44.483	-88.133	210
727120	CARIBOU	46.867	-68.017	191
727640	BISMARCK	46.767	-100.75	503
727680	GLASGOW	48.217	-106.61	696
727750	GREAT FALLS	47.483	-111.35	1118
727850	SPOKANE	47.633	-117.53	720
727970	QUILLAYUTE	47.95	-124.55	56
783840	GRAND CAYMAN	19.3	-81.367	3
785260	SAN JUAN/ISLA VERDE	18.433	-66	3
785830	BELIZE	17.533	-88.3	5
789540	GRANTLEY ADAMS INTL	13.067	-59.5	47
821930	BELEM/VAL DE CAES	-1.383	-48.483	16
823320	MANAUS/PONTA PELADA	-3.15	-59.983	84
824000	FERNANDO DE NORONHA	-3.85	-32.417	45
825990	NATAL/AUGUSTO SEVER	-5.917	-35.25	49
829000	RECIFE/CURADO	-8.05	-34.916	11
832080	VILHENA ARPT	-12.73	-60.133	652
833780	BRASILIA ARPT.	-15.86	-47.933	1061
836120	CAMPO GRANDE INTL	-20.46	-54.667	567
837460	RIO DE JANEIRO/GALE	-22.81	-43.25	42
837800	SAO PAULO	-23.61	-46.65	802
838400	CURITIBA/AFONSO PEN	-25.51	-49.167	908
839710	PORTO ALEGRE ARPT.	-30	-51.183	3
846280	LIMA/CALLO	-12	-77.117	11
854420	ANTOFAGASTA	-23.41	-70.467	137
854690	ISLA DE PASCUA/EASTER	-27.15	-109.48	47
855430	QUINTERO	-32.78	-71.517	3
857990	PUERTO MONTT	-41.43	-73.117	84
859340	PUNTA ARENAS	-53.03	-70.85	38
870470	SALTA AIRPORT	-24.85	-65.483	1221
871550	RESISTENCIA AIRPORT	-27.45	-59.05	52
873440	CORDOBA AERO	-31.31	-64.217	474
874180	MENDOZA AIRPORT	-32.83	-68.783	704
875760	BUENOS AIRES/EZEIZA ARPT	-34.81	-58.533	20
876230	SANTA ROSA AIRPORT	-36.56	-64.267	189
877150	NEUQUEN AIRPORT	-38.95	-68.133	271
878270	ALMIRANTE ZAR	-43.23	-65.3	42
878600	COMODORO RIVADAVIA	-45.78	-67.45	46
890090	AMUNDSEN/SCOTT	-90	180	2835

CARDS#	Station Name	Latitude (dd)	Longitude (dd)	Elevation (m)
890220	HALLEY BAY	-75.51	-26.6	30
890500	BELLINGSHAUSEN	-62.2	-58.933	16
895120	NOVOLAZAREVSKAYA	-70.76	11.833	140
895320	SYOWA	-69	39.583	18
895420	MOLODEZHNAYA	-67.66	45.85	40
895710	DAVIS	-68.58	77.983	12
895920	MIRNYY	-66.55	93.017	59
896110	WILKES/CASEY	-66.26	110.567	12
896640	MCMURDO	-77.85	166.667	24
912170	GUAM/TAGUAC	13.55	144.833	111
912850	HILO	19.716	-155.06	11
913760	MAJURO	7.0833	171.383	3
915170	HONIARA	-9.433	160.05	56
915920	NOUMEA	-22.26	166.45	69
916430	FUNAFUTI	-8.517	179.217	2
916800	NANDI	-17.75	177.45	19
917650	FATUNA IS./PAGO PAGO I	-14.33	-170.71	2
918010	PENRHYN	-9	-158.05	1
918430	RAROTONGA	-21.2	-159.81	7
919250	ATUONA	-9.817	-139.01	52
919300	BORA-BORA	-14.8	-138.81	3
919380	PAPEETE/TAHITI	-17.55	-149.61	2
919430	TAKAROA	-14.48	-145.03	3
919480	RIKITEA	-23.13	-134.96	89
919540	TUBUAI	-23.35	-149.48	3
919580	RAPA	-27.61	-144.33	2
931120	WHENUAPAI	-36.8	174.6	31
932910	GISBORNE	-38.66	177.983	8
933080	NEW PLYMOUTH AERO	-39.03	174.183	48
934170	PARAPARAUMU	-40.9	174.983	7
936140	HOKITIKA (SOUTH)	-42.71	170.983	44
938440	INVERCARGILL ARPT	-46.41	168.333	1
939860	CHATHAM ISLAND	-43.95	-176.56	48
939970	RAOUL IS/KERMADEC	-29.25	-177.91	36
940350	PORT MORESBY	-9.433	147.217	28
941200	DARWIN AIRPORT	-12.43	130.867	32
942030	BROOME M.O.	-17.95	122.217	9
942120	HALLS CREEK	-18.23	127.667	407
942380	TENNANT CREEK	-19.63	134.183	374
942870	CAIRNS M.O.	-16.58	145.733	2
942940	TOWNSVILLE	-19.25	146.767	5
942990	WILLIS ISLAND	-16.3	149.983	6
943000	CARNARVON	-24.88	113.65	4
943020	LEARMONTH	-22.23	114.083	6

CARDS#	Station Name	Latitude (dd)	Longitude (dd)	Elevation (m)
943120	PORT HEDLAND	-20.38	118.617	11
943260	ALICE SPRINGS	-23.8	133.883	546
943320	MT ISA ARPT	-20.66	139.483	344
943460	LONGREACH M O	-23.43	144.25	193
943670	MACKAY M.O.	-21.11	149.167	31
943740	ROCKHAMPTON/AIRPORT	-23.38	150.467	14
944030	GERALDTON	-28.8	114.7	34
944300	MEEKATHARRA	-26.6	118.483	511
944610	GILES	-25.03	128.3	600
945100	CHARLEVILLE	-26.41	146.267	305
945780	BRISBANE AIRPORT	-27.43	153.083	5
946100	PERTH INTL ARPT	-31.93	115.967	21
946370	KALGOORLIE	-30.78	121.467	360
946380	ESPERANCE M.O.	-33.81	121.883	25
946530	CEDUNA	-32.13	133.7	19
946590	WOOMERA	-31.15	136.8	169
946720	ADELAIDE ARPT	-34.95	138.533	6
946930	MILDURA	-34.23	142.083	50
947110	COBAR M.O.	-31.48	145.833	244
947500	NOWRA	-34.95	150.55	119
947670	SYDNEY ARPT	-33.95	151.183	3
947760	WILLIAMTOWN AERODROME	-32.78	151.816	8
947910	COFFS HARBOUR ARPT	-30.31	153.117	5
948020	ALBANY AIRPORT	-34.93	117.8	69
948210	MT GAMBIER/ARPT M.O.	-37.73	140.783	69
948650	LAVERTON AERODROME	-37.85	144.733	21
949070	EAST SALE AERODROME	-38.1	147.133	8
949100	WAGGA ARPT	-35.15	147.45	213
949260	CANBERRA AIRPORT	-35.3	149.183	577
949680	LAUNCESTON AIRPORT	-41.53	147.2	178
949750	HOBART AIRPORT	-42.83	147.483	27
949950	LORD HOWE ISLAND	-31.53	159.067	48
949960	NORFOLK ISLAND ARPT	-29.03	167.933	109
949980	MACQUARIE ISLAND	-54.48	158.933	6
961630	PADANG/TABING	-0.883	100.35	3
962370	PANGKALPINANG/PANG.	-2.167	106.133	33
969960	COCOS ISLAND ARPT	-12.18	96.817	3
971800	UJUNG PANDANG/HASAN	-5.067	119.55	14
973720	KUPANG/PENFUI	-10.16	123.667	108
975600	BIAK/MOKMER	-1.183	136.117	11

Table B.2. List of ISWO stations used for surface temperature and moist enthalpy trend analyses.

Station ID	Station Name	State Abbr.
722010	KEY WEST	FL
722020	MIAMI, INT'L AIRPORT	FL
722025	FORT LAUDERDALE/HOLLYWOOD	FL
722026	HOMESTEAD, AFB	FL
722029	MIAMI/KENDALL, NEW TAMIAMI AIRPORT	FL
722030	WEST PALM BEACH	FL
722040	MELBOURNE	FL
722045	VERO BEACH	FL
722050	ORLANDO	FL
722056	DAYTONA BEACH	FL
722060	JACKSONVILLE, INT'L AIRPORT	FL
722066	JACKSONVILLE, MAYPORT NAVAL STATION	FL
722067	JACKSONVILLE, CECIL FIELD NAS	FL
722070	SAVANNAH	GA
722080	CHARLESTON	SC
722085	BEAUFORT, MCAS	SC
722106	FORT MYERS	FL
722110	TAMPA, INT'L AIRPORT	FL
722115	SARASOTA/BRADENTON	FL
722116	SAINT PETERSBURG	FL
722120	CROSS CITY	FL
722130	WAYCROSS	GA
722137	BRUNSWICK	GA
722140	TALLAHASSEE	FL
722146	GAINESVILLE	FL
722160	ALBANY	GA
722166	VALDOSTA, REGIONAL AIRPORT	GA
722170	MACON	GA
722180	AUGUSTA	GA
722190	ATLANTA	GA
722200	APALACHICOLA	FL
722210	VALPARAISO, EGLIN AFB	FL
722215	CRESTVIEW	FL
722225	PENSACOLA, FOREST SHERMAN AFB	FL
722226	MILTON, WHITING FIELD NAS	FL
722230	MOBILE	AL

Station ID	Station Name	State Abbr.
722250	COLUMBUS, FORT BENNING	GA
722255	COLUMBUS, METRO AIRPORT	GA
722260	MONTGOMERY	AL
722268	DOTHAN	AL
722269	OZARK, FORT RUCKER	AL
722270	MARIETTA, DOBBINS AFB	GA
722280	BIRMINGHAM	AL
722286	TUSCALOOSA	AL
722287	ANNISTON	AL
722310	NEW ORLEANS, INT'L AIRPORT	LA
722315	NEW ORLEANS, LAKEFRONT AIRPORT	LA
722317	BATON ROUGE	LA
722340	MERIDIAN	MS
722350	JACKSON	MS
722358	MCCOMB	MS
722359	GREENWOOD	MS
722390	LEESVILLE, FORT POLK	LA
722400	LAKE CHARLES	LA
722405	LAFAYETTE	LA
722410	BEAUMONT/PORT ARTHUR	TX
722420	GALVESTON (722422, 722423)	TX
722430	HOUSTON, INTERCONTINENTAL AIRPORT	TX
722435	HOUSTON, HOBBY AIRPORT	TX
722445	COLLEGE STATION/BRYAN	TX
722446	LUFKIN	TX
722448	TYLER	TX
722470	LONGVIEW (722447)	TX
722480	SHREVEPORT	LA
722485	BOSSIER CITY, BARKSDALE AFB	LA
722486	MONROE	LA
722500	BROWNSVILLE	TX
722506	MCALLEN	TX
722510	CORPUS CHRISTI	TX
722516	KINGSVILLE, NAS	TX
722517	ALICE	TX
722520	LAREDO	TX
722526	COTULLA	TX
722530	SAN ANTONIO, INT'L AIRPORT	TX

Station ID	Station Name	State Abbr.
722535	SAN ANTONIO, KELLY AFB	TX
722536	SAN ANTONIO, RANDOLPH AFB	TX
722540	AUSTIN	TX
722550	VICTORIA	TX
722556	BEEVILLE, CHASE FIELD NAS	TX
722560	WACO	TX
722576	KILLEEN, FORT HOOD	TX
722577	TEMPLE	TX
722590	DALLAS/FORT WORTH, INT'L AIRPORT	TX
722595	FORT WORTH, CARSWELL AFB	TX
722596	FORT WORTH, MEACHAM FIELD	TX
722610	DEL RIO, INT'L AIRPORT	TX
722615	DEL RIO, LAUGHLIN AFB	TX
722620	GUADALUPE PASS	TX
722630	SAN ANGELO	TX
722640	MARFA	TX
722650	MIDLAND/ODESSA	TX
722660	ABILENE	TX
722670	LUBBOCK, INT'L ARPT	TX
722675	LUBBOCK, REESE AFB	TX
722700	EL PASO	TX
723013	WILMINGTON (723011)	NC
723040	CAPE HATTERAS	NC
723060	RALEIGH/DURHAM	NC
723066	GOLDSBORO, SEYMOUR JOHNSON AFB	NC
723075	OCEANA, NAS	VA
723080	NORFOLK	VA
723086	NEWPORT NEWS	VA
723090	CHERRY POINT, MCAS	NC
723095	NEW BERN	NC
723096	JACKSONVILLE, NEW RIVER MCAF	NC
723100	COLUMBIA	SC
723106	FLORENCE	SC
723110	ATHENS	GA
723120	GREER/GREENVILLE	SC
723125	ANDERSON	SC
723140	CHARLOTTE	NC
723145	HICKORY	NC

Station ID	Station Name	State Abbr.
723150	ASHEVILLE	NC
723170	GREENSBORO	NC
723183	BRISTOL (723181)	TN
723193	WINSTON-SALEM (723190, 723191)	NC
723200	ROME	GA
723230	HUNTSVILLE	AL
723235	MUSCLE SHOALS/FLORENCE	AL
723240	CHATTANOOGA	TN
723260	KNOXVILLE	TN
723265	CROSSVILLE	TN
723270	NASHVILLE	TN
723300	POPLAR BLUFF	MO
723306	COLUMBUS, AFB	MS
723320	TUPELO (723301, 723303)	MS
723340	MEMPHIS	TN
723346	JACKSON	TN
723347	DYERSBURG	TN
723405	LITTLE ROCK, AFB	AR
723407	JONESBORO	AR
723408	BLYTHEVILLE, EAKER AFB	AR
723415	HOT SPRINGS	AR
723417	PINE BLUFF	AR
723418	TEXARKANA	AR
723419	EL DORADO	AR
723440	FORT SMITH	AR
723445	FAYETTEVILLE	AR
723446	HARRISON	AR
723489	CAPE GIRARDEAU	MO
723495	JOPLIN	MO
723510	WICHITA FALLS, SHEPPARD AFB	TX
723520	ALTUS, AFB	OK
723530	OKLAHOMA CITY, WILL ROGERS AIRPORT	OK
723535	ENID, VANCE AFB	OK
723540	OKLAHOMA CITY, TINKER AFB	OK
723546	PONCA CITY	OK
723550	LAWTON, FORT SILL/POST FIELD AF	OK
723560	TULSA	OK
723566	MCALESTER	OK

Station ID	Station Name	State Abbr.
723630	AMARILLO	TX
724010	RICHMOND	VA
724016	CHARLOTTESVILLE	VA
724030	STERLING	VA
724035	QUANTICO, MCAS	VA
724037	FORT BELVOIR	VA
724040	LEXINGTON PARK, PATUXENT RIVER NAS	MD
724045	SALISBURY	MD
724050	WASHINGTON, NATIONAL AIRPORT	VA
724060	GLEN BURNIE/BALTIMORE, BWI AIRPORT	MD
724070	ATLANTIC CITY	NJ
724075	MILLVILLE	NJ
724080	PHILADELPHIA, INT'L AIRPORT	PA
724085	PHILADELPHIA, NORTHEAST AIRPORT	PA
724086	PHILADELPHIA, WILLOW GROVE NAS	PA
724088	DOVER, AFB	DE
724089	WILMINGTON	DE
724096	TRENTON/WRIGHTSTOWN, MCGUIRE AFB	NJ
724100	LYNCHBURG	VA
724110	ROANOKE	VA
724125	BLUEFIELD	WV
724140	CHARLESTON	WV
724170	ELKINS	WV
724175	CLARKSBURG	WV
724176	MORGANTOWN	WV
724177	MARTINSBURG	WV
724210	COVINGTON/CINCINNATI OH, INT'L AIRPORT	KY
724220	LEXINGTON	KY
724230	LOUISVILLE	KY
724236	JACKSON	KY
724240	FORT KNOX, GODMAN AAF	KY
724243	LONDON/CORBIN (723290, 723291, 723293)	KY
724250	HUNTINGTON	WV
724273	PARKERSBURG (724270, 724271)	WV
724280	COLUMBUS, INT'L AIRPORT	OH
724285	COLUMBUS, RICKENBACKER AFB	OH
724286	ZANESVILLE	OH
724290	DAYTON, INT'L AIRPORT	OH

Station ID	Station Name	State Abbr.
724297	CINCINNATI, LUNKEN FIELD	OH
724320	EVANSVILLE	IN
724338	BELLEVILLE, SCOTT AFB	IL
724340	ST. LOUIS, INT'L AIRPORT	MO
724345	CHESTERFIELD, SPIRIT OF ST. LOUIS AIRPORT	MO
724350	PADUCAH (746715)	KY
724373	TERRE HAUTE (724370, 724371)	IN
724380	INDIANAPOLIS	IN
724386	LAFAYETTE, PURDUE UNIV.	IN
724390	SPRINGFIELD	IL
724396	QUINCY	IL
724400	SPRINGFIELD	MO
724450	COLUMBIA	MO
724455	KIRKSVILLE	MO
724456	VICHY/ROLLA	MO
724460	KANSAS CITY	MO
724467	WARRENSBURG/SEDALIA, WHITEMAN AFB	MO
724500	WICHITA, AIRPORT	KS
724505	WICHITA, MCCONNELL AFB	KS
724506	HUTCHINSON	KS
724507	CHANUTE	KS
724510	DODGE CITY	KS
724515	GARDEN CITY	KS
724550	FT RILEY, MARSHALL AAF	KS
724555	MANHATTAN	KS
724556	EMPORIA	KS
724560	TOPEKA	KS
724580	CONCORDIA	KS
724585	RUSSELL	KS
724586	SALINA	KS
724650	GOODLAND	KS
725020	NEWARK	NJ
725025	TETERBORO	NJ
725030	NEW YORK, LA GUARDIA AIRPORT	NY
725035	CENTRAL ISLIP	NY
725036	POUGHKEEPSIE	NY
725037	WHITE PLAINS	NY
725038	NEWBURGH	NY

Station ID	Station Name	State Abbr.
725040	BRIDGEPORT	CT
725060	EAST FALMOUTH, OTIS ANGB	MA
725070	PROVIDENCE	RI
725080	WINDSOR LOCKS, BRADLEY FIELD	CT
725087	HARTFORD, BRAINARD FIELD	CT
725090	BOSTON	MA
725095	WORCESTER	MA
725097	WEYMOUTH, SOUTH WEYMOUTH NAS	MA
725115	HARRISBURG	PA
725116	LANCASTER	PA
725125	DU BOIS	PA
725126	ALTOONA	PA
725127	JOHNSTOWN	PA
725130	WILKES-BARRE/SCRANTON	PA
725140	WILLIAMSPORT	PA
725150	BINGHAMTON	NY
725156	ELMIRA/CORNING	NY
725170	ALLENTOWN	PA
725180	ALBANY	NY
725185	GLENS FALLS	NY
725190	SYRACUSE	NY
725196	ROME, GRIFFISS AFB	NY
725200	PITTSBURGH, PITTSBURGH INT'L AIRPORT	PA
725205	PITTSBURGH, ALLEGHENY CO. AIRPORT	PA
725210	AKRON/CANTON	OH
725240	CLEVELAND	OH
725246	MANSFIELD	OH
725250	YOUNGSTOWN	OH
725260	ERIE	PA
725266	BRADFORD	PA
725280	BUFFALO	NY
725287	NIAGARA FALLS	NY
725290	ROCHESTER	NY
725300	CHICAGO, O'HARE INT'L AIRPORT	IL
725305	WEST CHICAGO	IL
725306	GLENVIEW, NAS	IL
725315	CHAMPAIGN/URBANA	IL
725316	DECATUR	IL

Station ID	Station Name	State Abbr.
725320	PEORIA	IL
725330	FORT WAYNE	IN
725335	PERU, GRISSOM AFB	IN
725340	CHICAGO, MEIGS FIELD	IL
725350	SOUTH BEND	IN
725360	TOLEDO	OH
725366	FINDLAY	OH
725370	DETROIT, METRO	MI
725376	DETROIT, WILLOW RUN	MI
725377	MOUNT CLEMENS, SELFRIDGE ANGB	MI
725386	HARBOR BEACH	MI
725387	COPPER HARBOR	MI
725390	LANSING	MI
725395	JACKSON	MI
725400	SPICKARD/TRENTON	MO
725430	ROCKFORD	IL
725440	MOLINE/DAVENPORT IA	IL
725450	CEDAR RAPIDS	IA
725455	BURLINGTON	IA
725460	DES MOINES	IA
725465	OTTUMWA	IA
725466	LAMONI	IA
725470	DUBUQUE	IA
725480	WATERLOO	IA
725485	MASON CITY	IA
725490	FORT DODGE	IA
725500	OMAHA, EPPLEY AIRFIELD	NE
725510	LINCOLN	NE
725520	GRAND ISLAND	NE
725530	OMAHA, WSO	NE
725540	BELLEVUE, OFFUTT AFB	NE
725560	NORFOLK	NE
725570	SIOUX CITY	IA
725610	SIDNEY	NE
725620	NORTH PLATTE	NE
725660	SCOTTSBLUFF	NE
725670	VALENTINE	NE
726050	CONCORD	NH

Station ID	Station Name	State Abbr.
726055	PORTSMOUTH, PEASE AFB	NH
726060	PORTLAND	ME
726088	BANGOR (726071)	ME
726116	LEBANON	NH
726130	MOUNT WASHINGTON	NH
726145	MONTPELIER/BARRE	VT
726170	BURLINGTON	VT
726185	AUGUSTA	ME
726223	MASSENA (726221)	NY
726225	PLATTSBURGH, AFB	NY
726227	WATERTOWN	NY
726350	GRAND RAPIDS	MI
726357	KALAMAZOO	MI
726360	MUSKEGON	MI
726370	FLINT	MI
726375	PONTIAC/OAKLAND	MI
726379	SAGINAW	MI
726387	TRAVERSE CITY	MI
726390	ALPENA	MI
726395	OSCODA, WURTSMITH AFB	MI
726399	SEUL CHOIX POINT	MI
726400	MILWAUKEE	WI
726410	MADISON	WI
726430	LA CROSSE	WI
726435	EAU CLAIRE	WI
726440	ROCHESTER	MN
726450	GREEN BAY	WI
726456	OSHKOSH	WI
726463	WAUSAU (726460, 726461)	WI
726500	SPENCER	IA
726510	SIOUX FALLS	SD
726530	CHAMBERLAIN	SD
726540	HURON	SD
726546	WATERTOWN	SD
726550	SAINT CLOUD	MN
726556	REDWOOD FALLS	MN
726557	ALEXANDRIA	MN
726580	MINNEAPOLIS-ST. PAUL	MN

Station ID	Station Name	State Abbr.
726590	ABERDEEN	SD
726620	RAPID CITY	SD
726686	PIERRE	SD
727120	CARIBOU	ME
727125	LIMESTONE, LORING AFB	ME
727340	SAULT STE. MARIE	MI
727347	PELLSTON	MI
727430	MARQUETTE/ISHPEMING, AIRPORT	MI
727435	MARQUETTE/GWINN, K. I. SAWYER AFB	MI
727440	HANCOCK	MI
727450	DULUTH	MN
727455	HIBBING	MN
727470	INTERNATIONAL FALLS	MN
727500	BRAINERD, PEQUOT LAKES	MN
727530	FARGO	ND
727535	JAMESTOWN	ND
727554	TOFTE	MN
727575	GRAND FORKS, AFB	ND
727580	DEVILS LAKE	ND
727640	BISMARCK	ND
727645	DICKINSON	ND
727650	ROSEGLEN	ND
727670	WILLISTON	ND
727675	MINOT, AFB	ND
727676	MINOT, INT'L AIRPORT	ND
743920	BRUNSWICK, NAS	ME
743945	MANCHESTER	NH
744600	MARSEILLES	IL
744860	NEW YORK, JOHN F KENNEDY AIRPORT	NY
744865	WESTHAMPTON BEACH	NY
744900	BEDFORD, HANSCOM AFB	MA
744910	SPRINGFIELD/CHICOPEE, WESTOVER AFB	MA
745700	DAYTON, WRIGHT-PATERSON AFB	OH
745940	CAMP SPRINGS, ANDREWS AFB	MD
745980	HAMPTON, LANGLEY AFB	VA
746710	FORT CAMPBELL, AAF	KY
746716	BOWLING GREEN	KY
746930	FAYETTEVILLE, FORT BRAGG	NC

Station ID	Station Name	State Abbr.
747300	SANDERSON	TX
747400	JUNCTION	TX
747540	ALEXANDRIA, ENGLAND AFB	LA
747686	BILOXI, KEESLER AFB	MS
747750	PANAMA CITY, TYNDALL AFB	FL
747770	VALPARAISO, HURLBURT FIELD	FL
747810	VALDOSTA, MOODY AFB (722167)	GA
747900	SUMTER, SHAW AFB	SC
747910	MYRTLE BEACH, AFB	SC
747946	CAPE CANAVERAL,NASA (747945)	FL

APPENDIX C

TROPOSPHERIC TEMPERATURE AND THICKNESS TIME SERIES

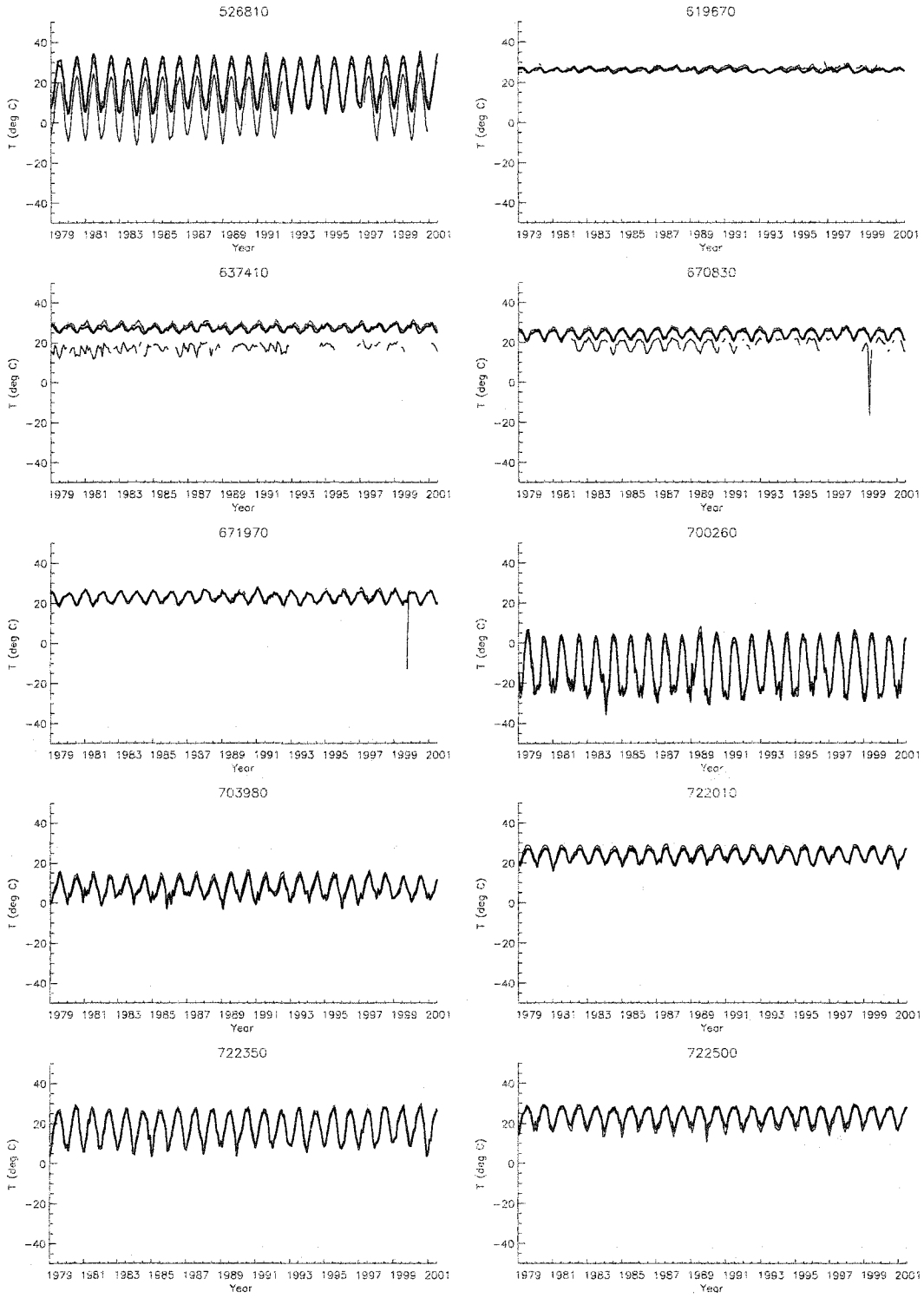

Figure C.1. 1979-2001 temperature time series at 1000 mb, for CARDS stations listed in Appendix B. ERA40 time series are shown in grey, NCEP time series are shown in thick black, and radiosonde time series are shown in thin black.

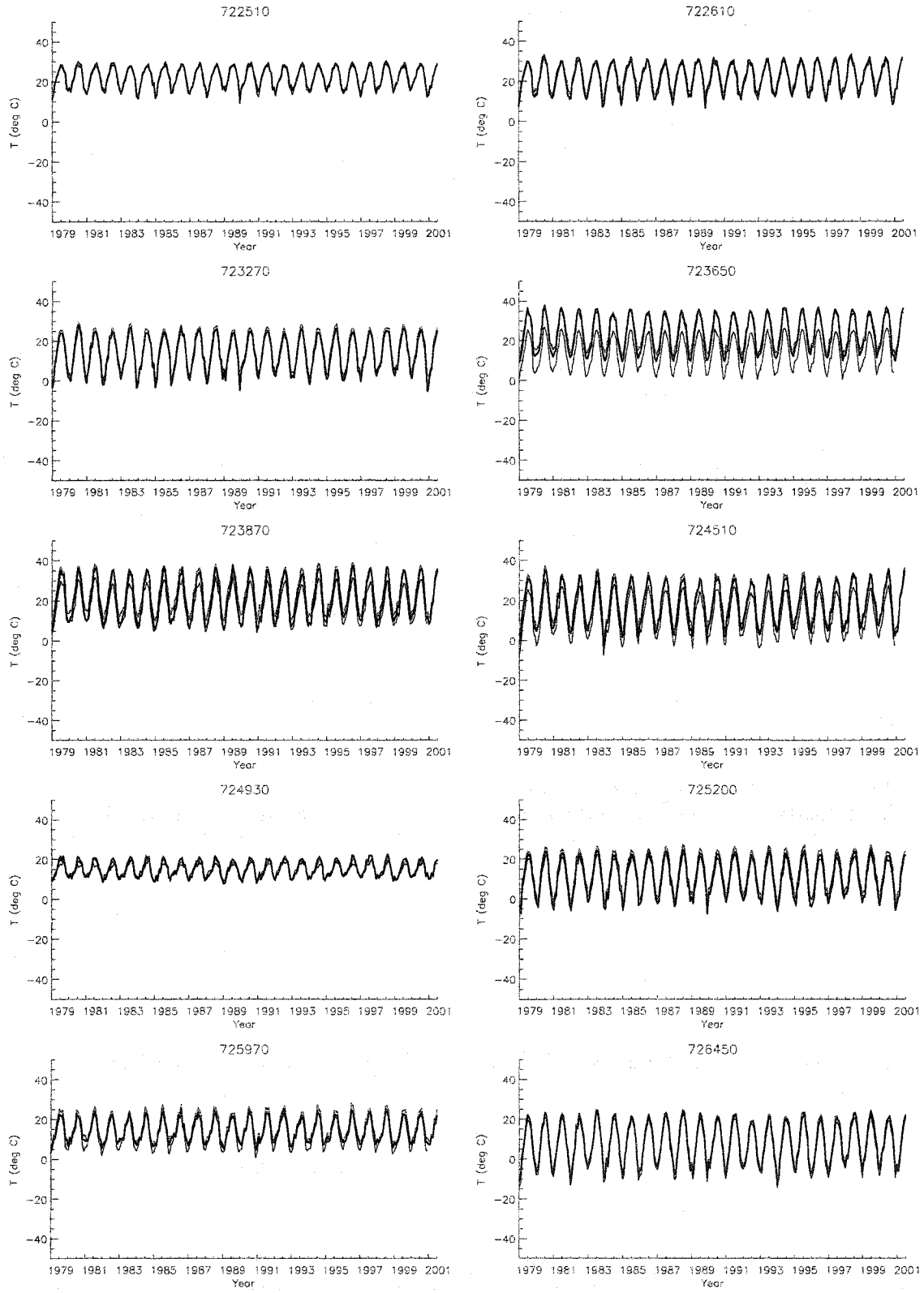

Figure C.1. (continued)

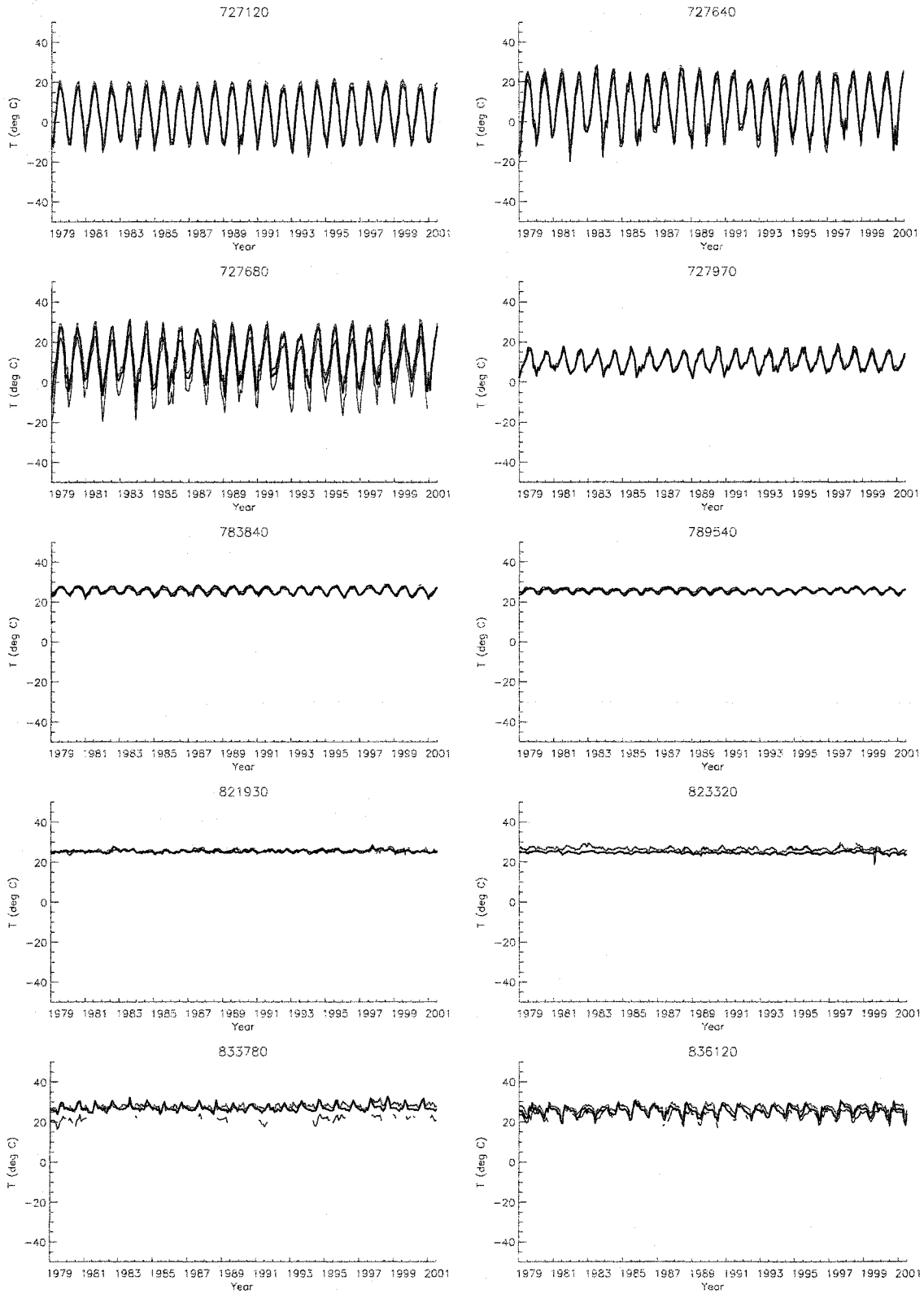

Figure C.1. (continued)

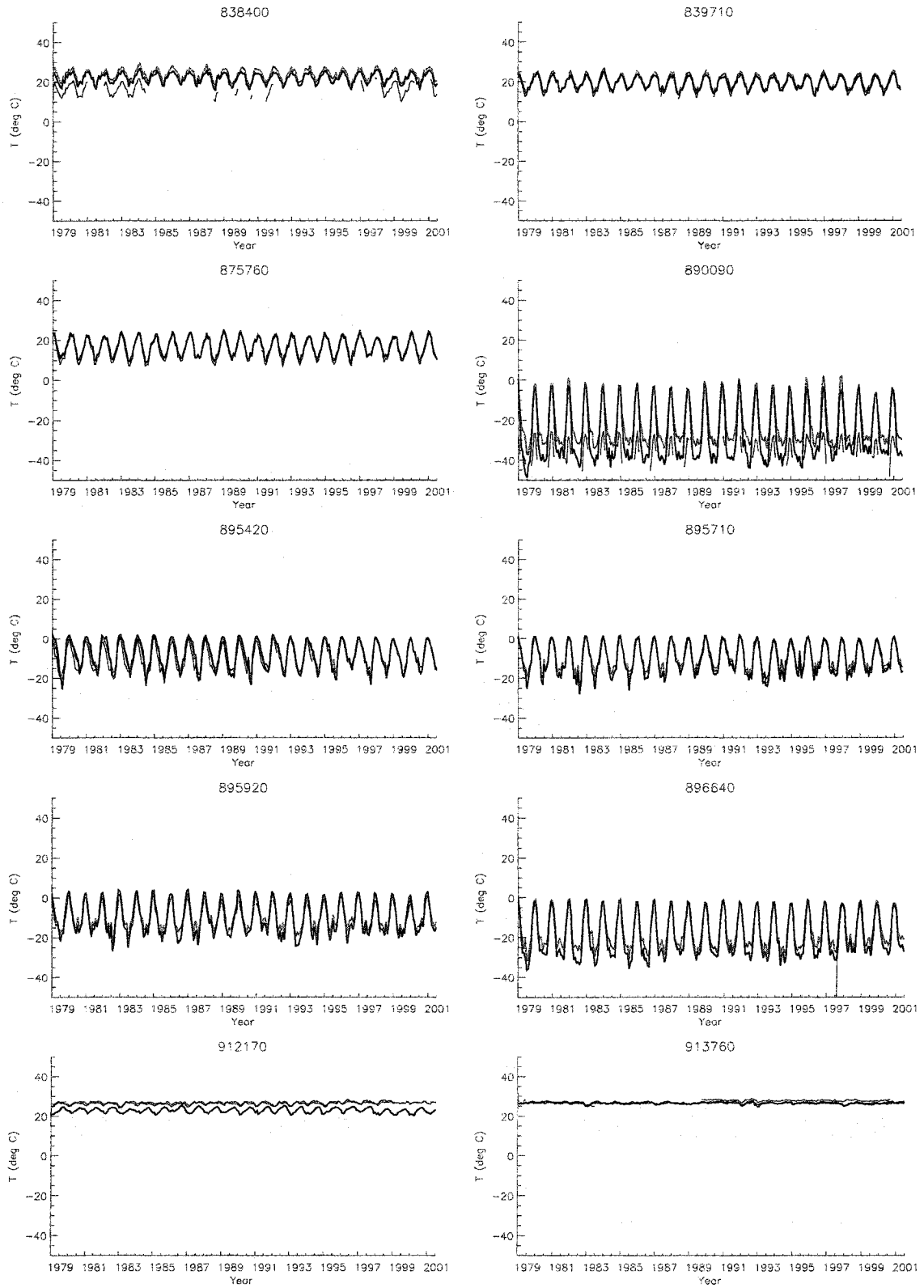

Figure C.1. (continued)

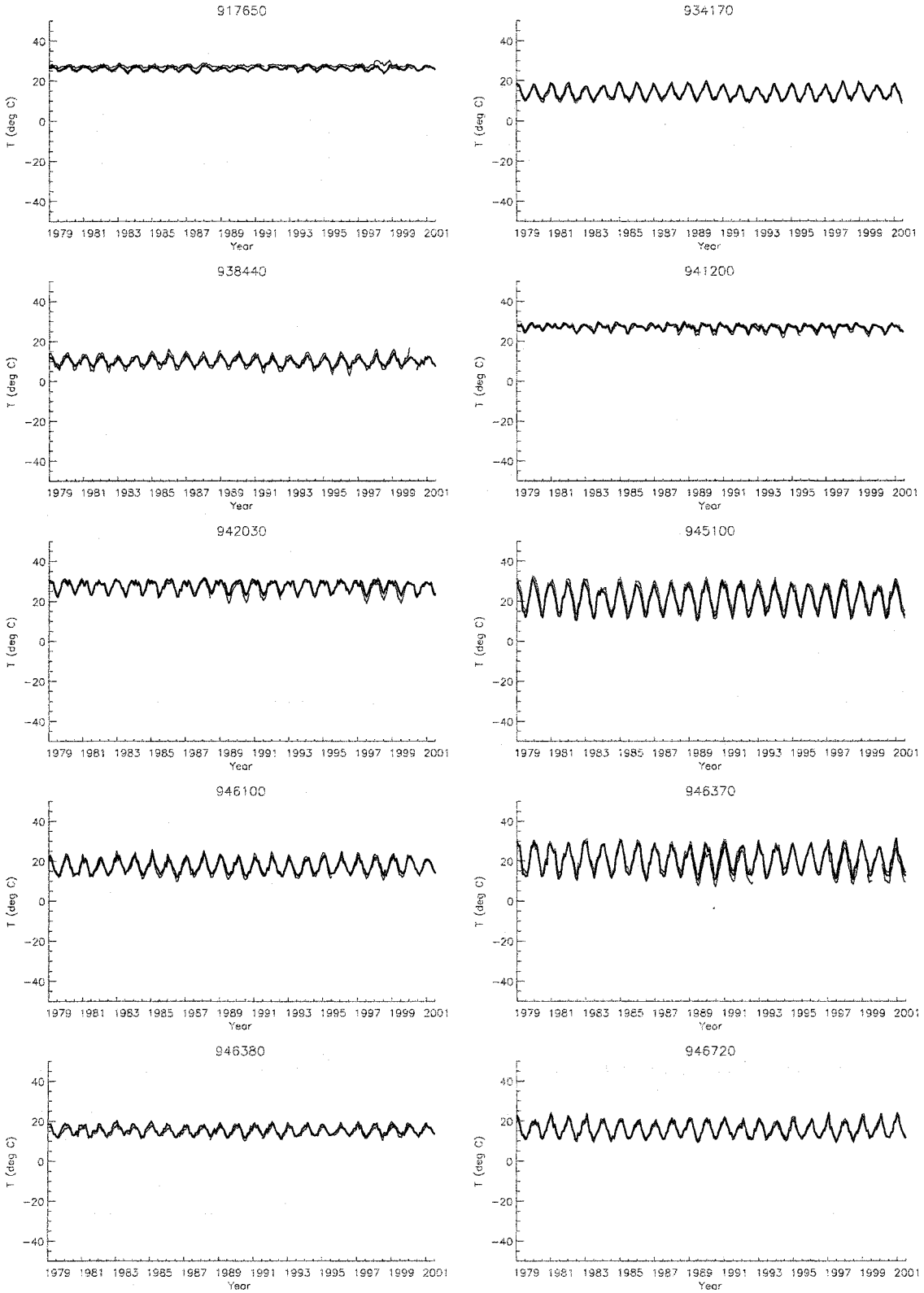

Figure C.1. (continued)

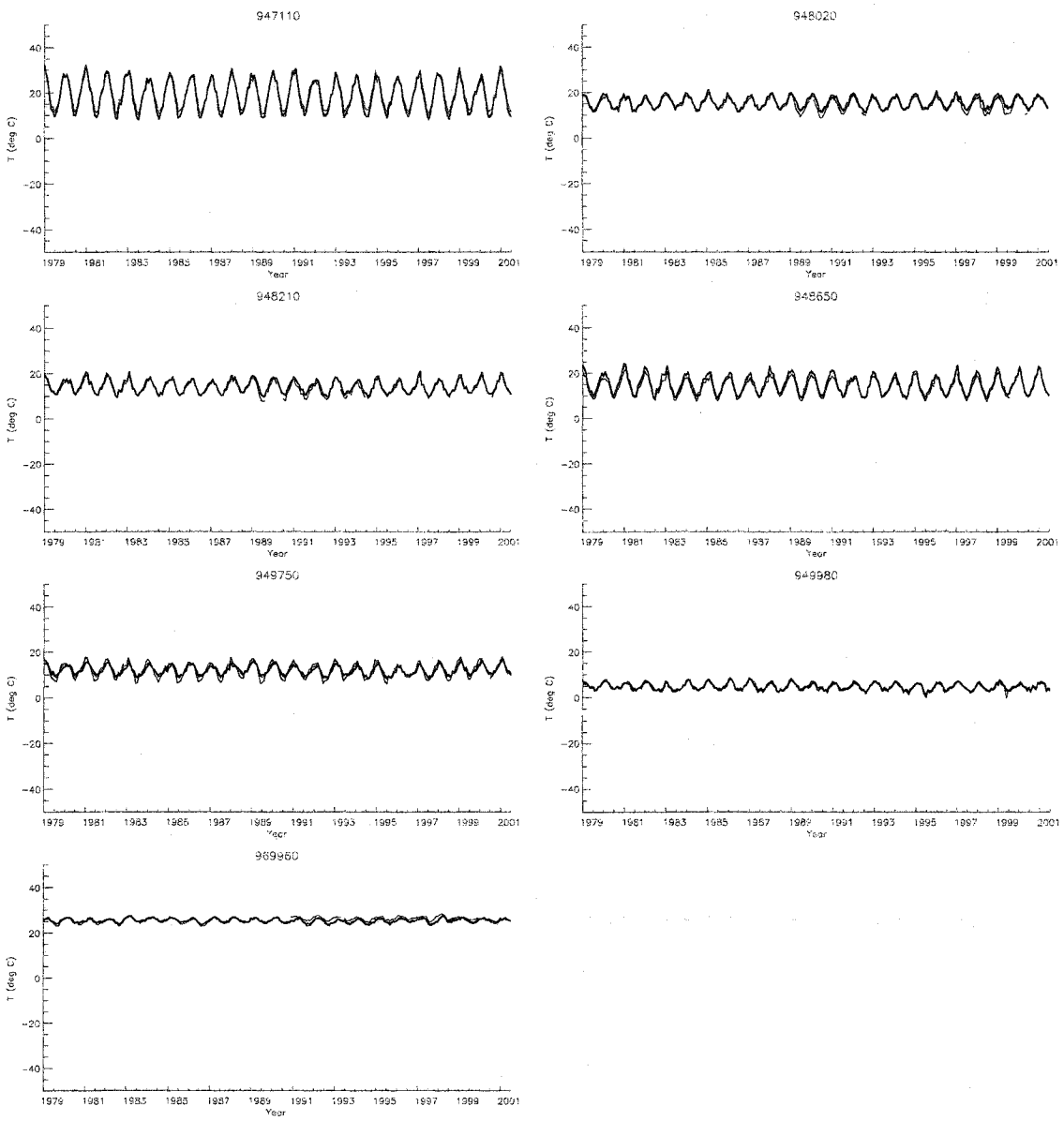

Figure C.1. (continued)

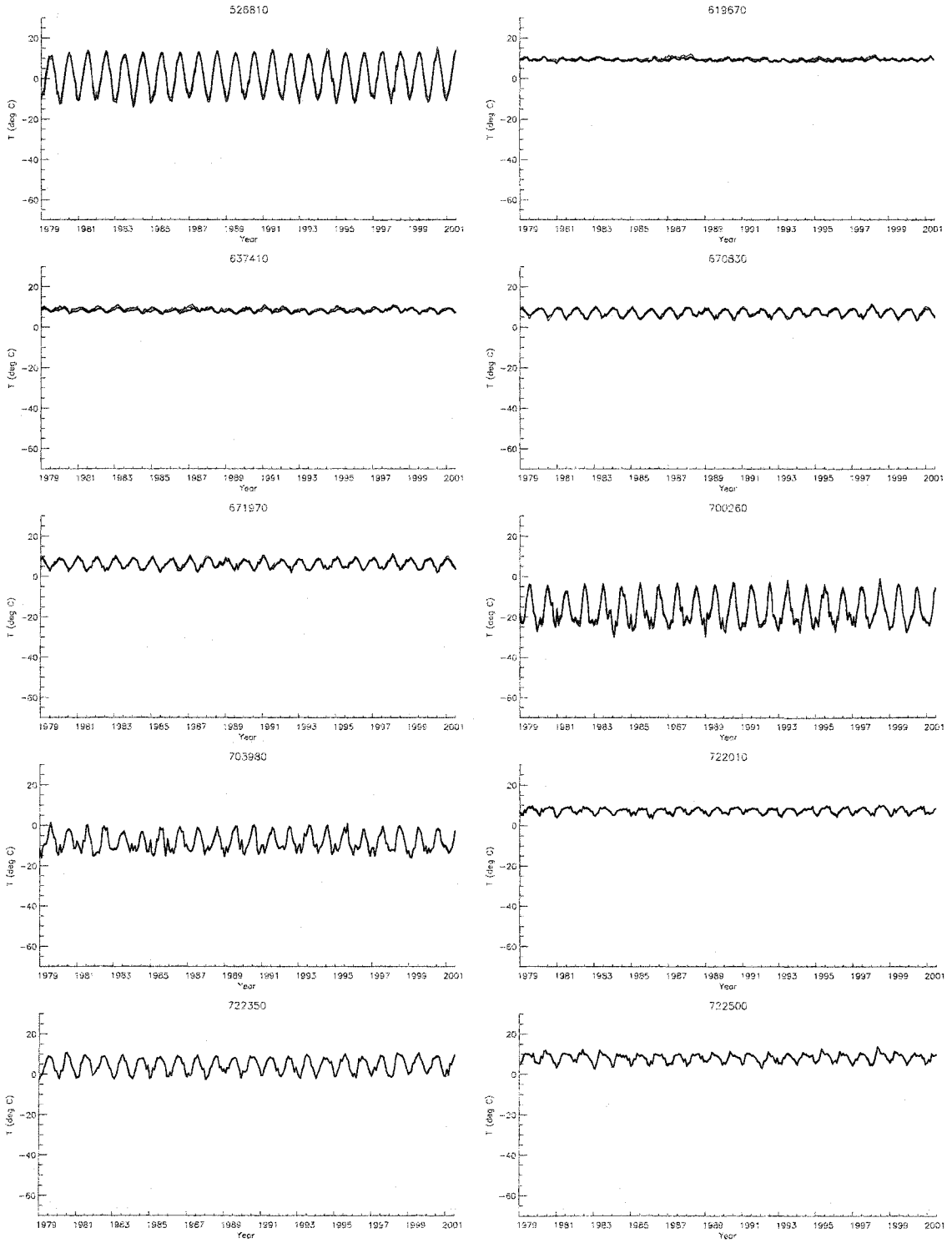

Figure C.2. Same as Figure C.1, but for 700 mb.

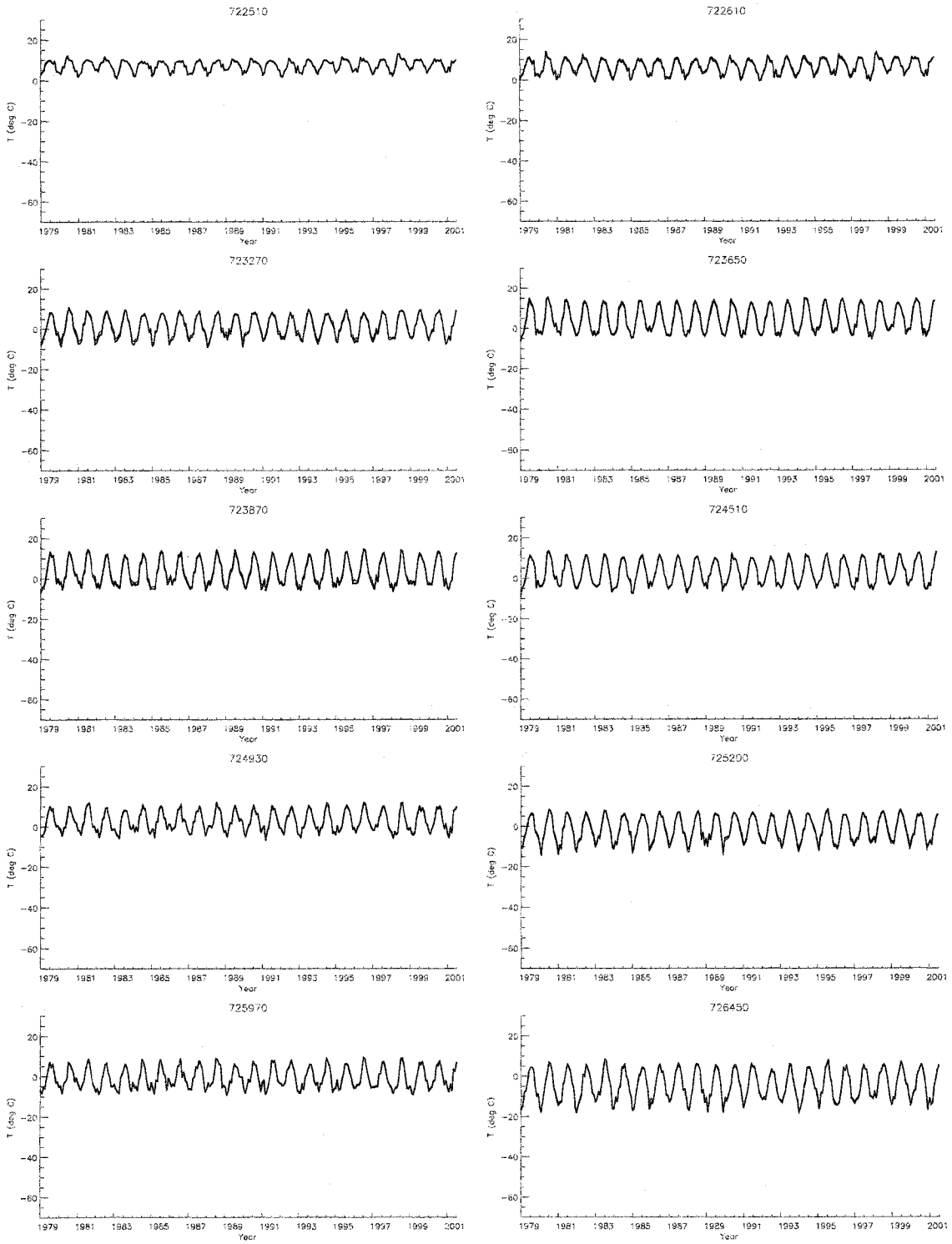

Figure C.2. (continued)

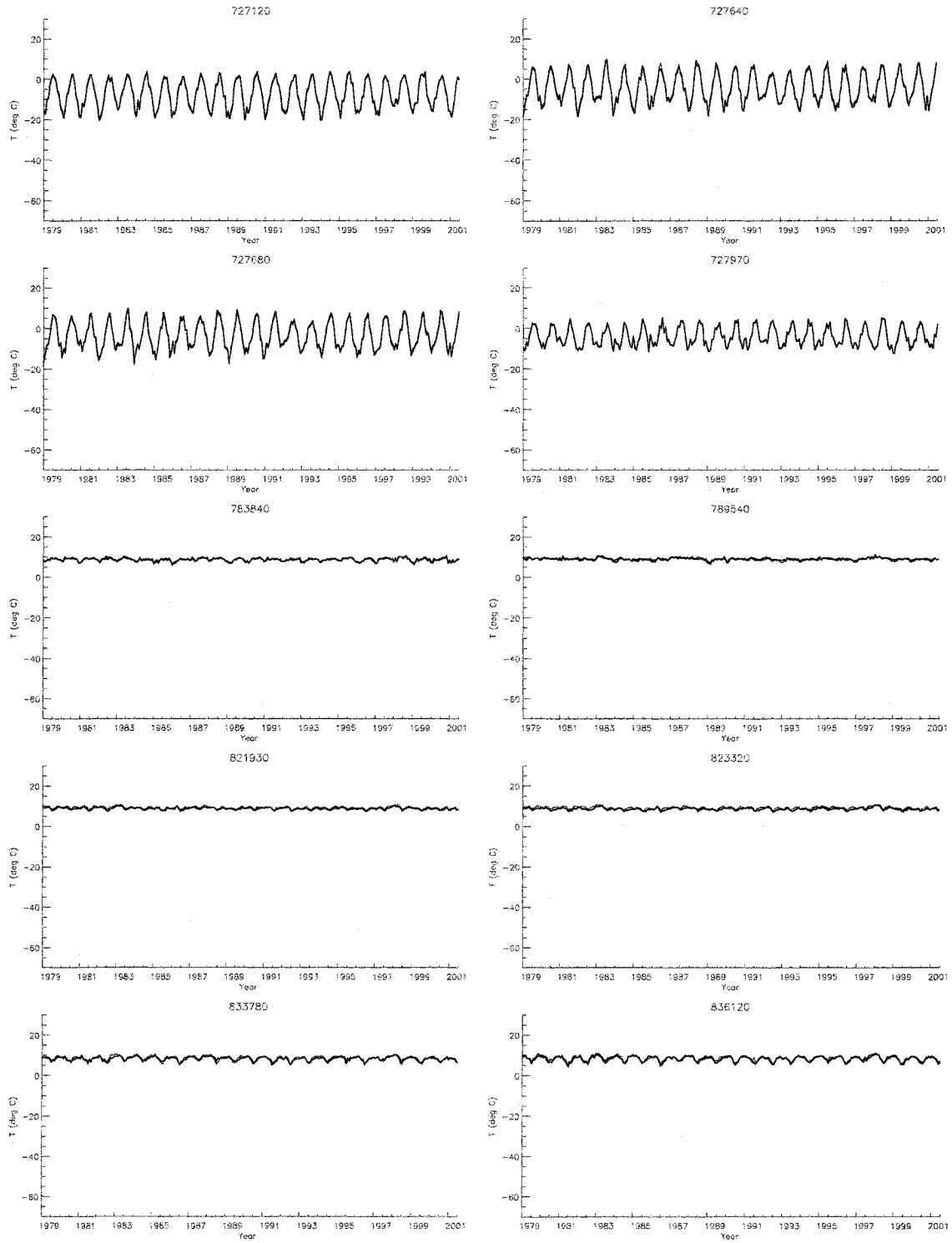

Figure C.2. (continued)

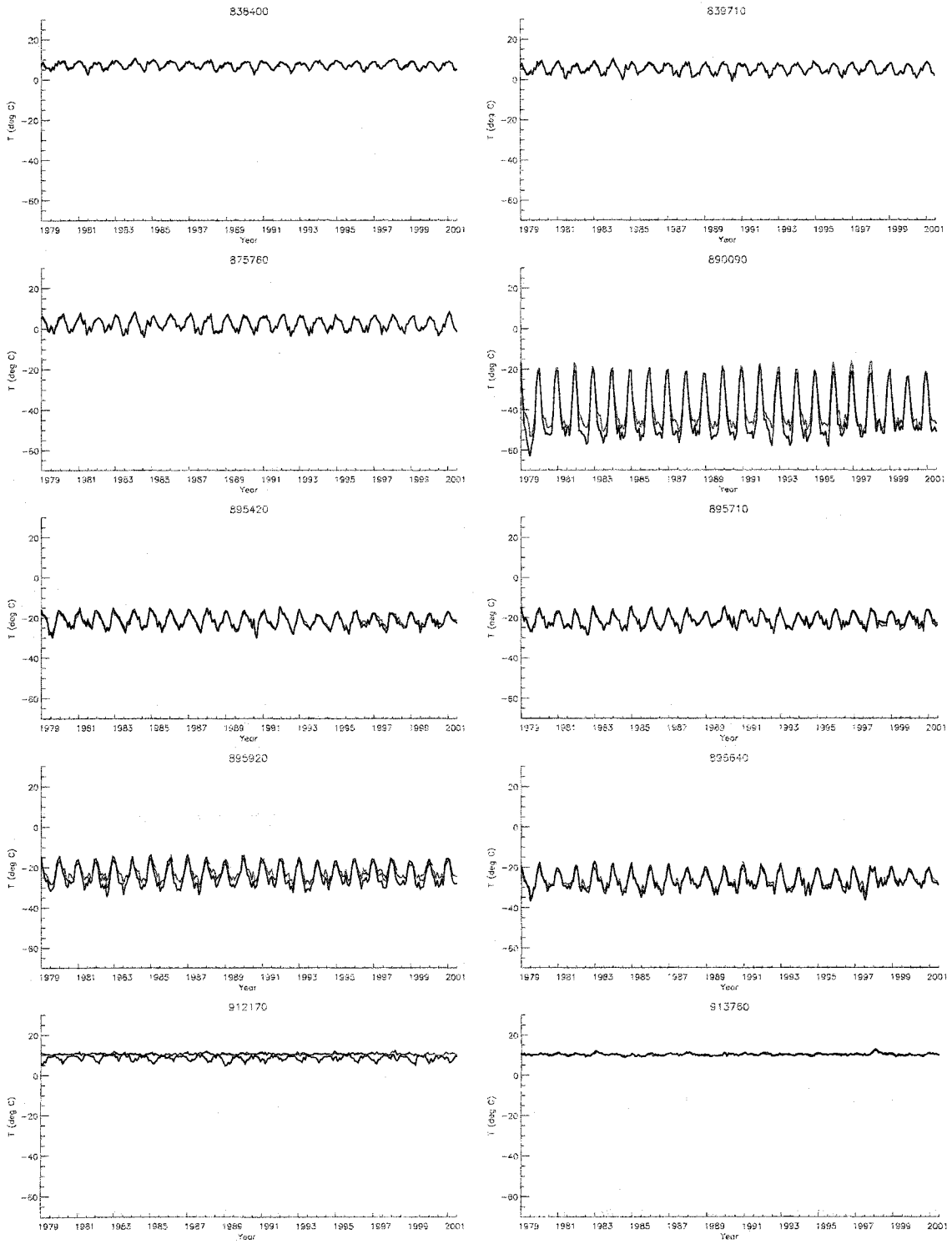

Figure C.2. (continued)

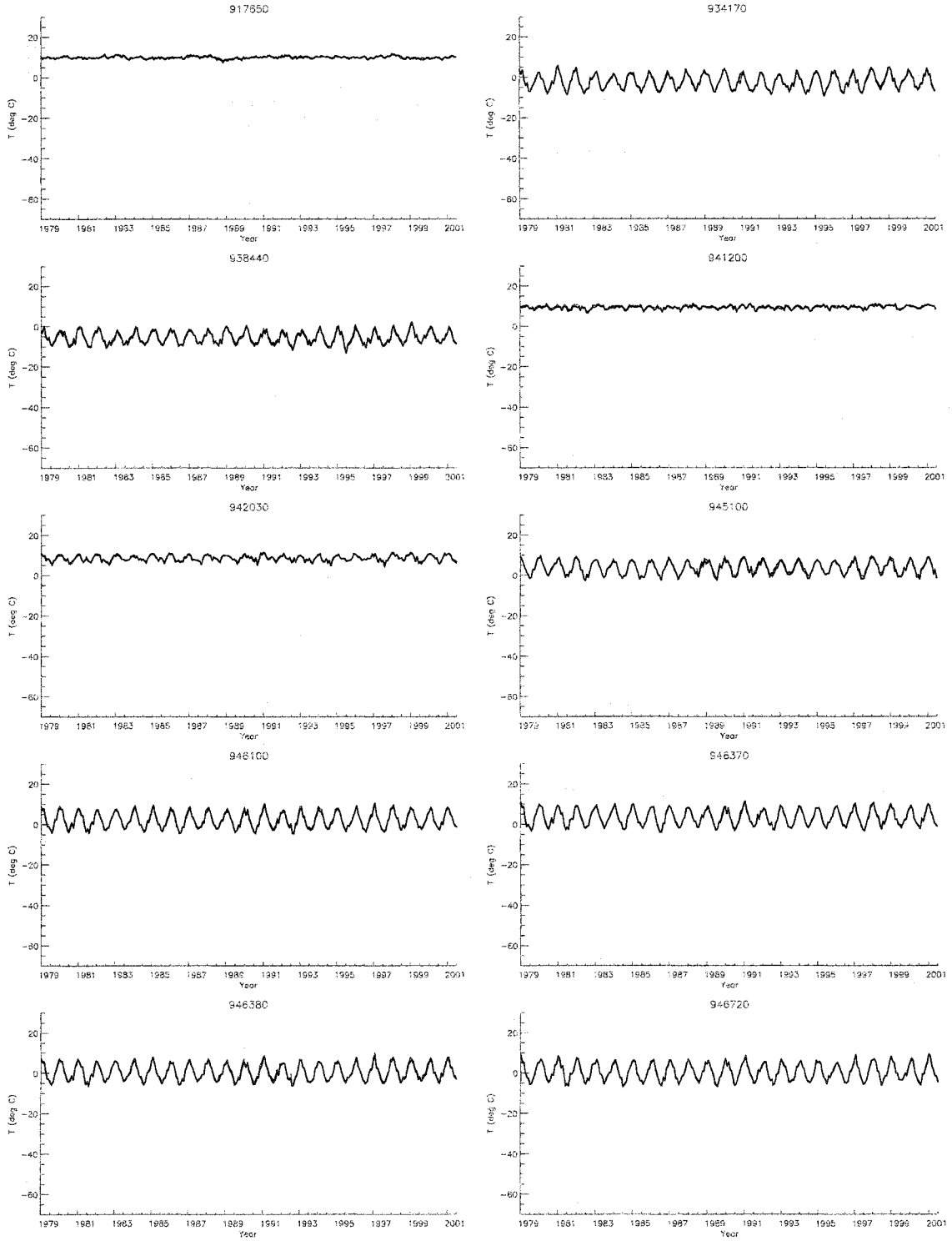

Figure C.2. (continued)

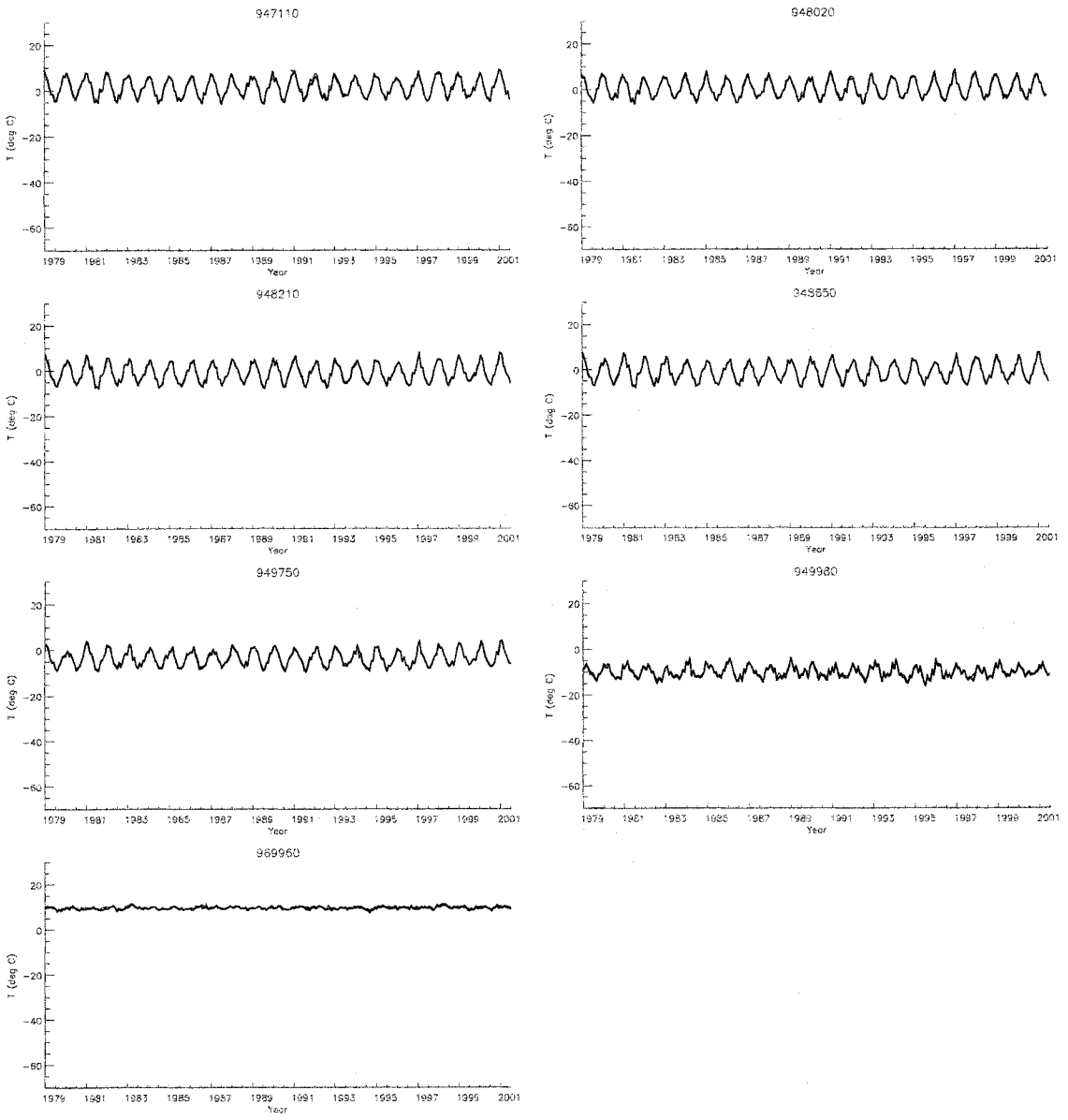

Figure C.2. (continued)

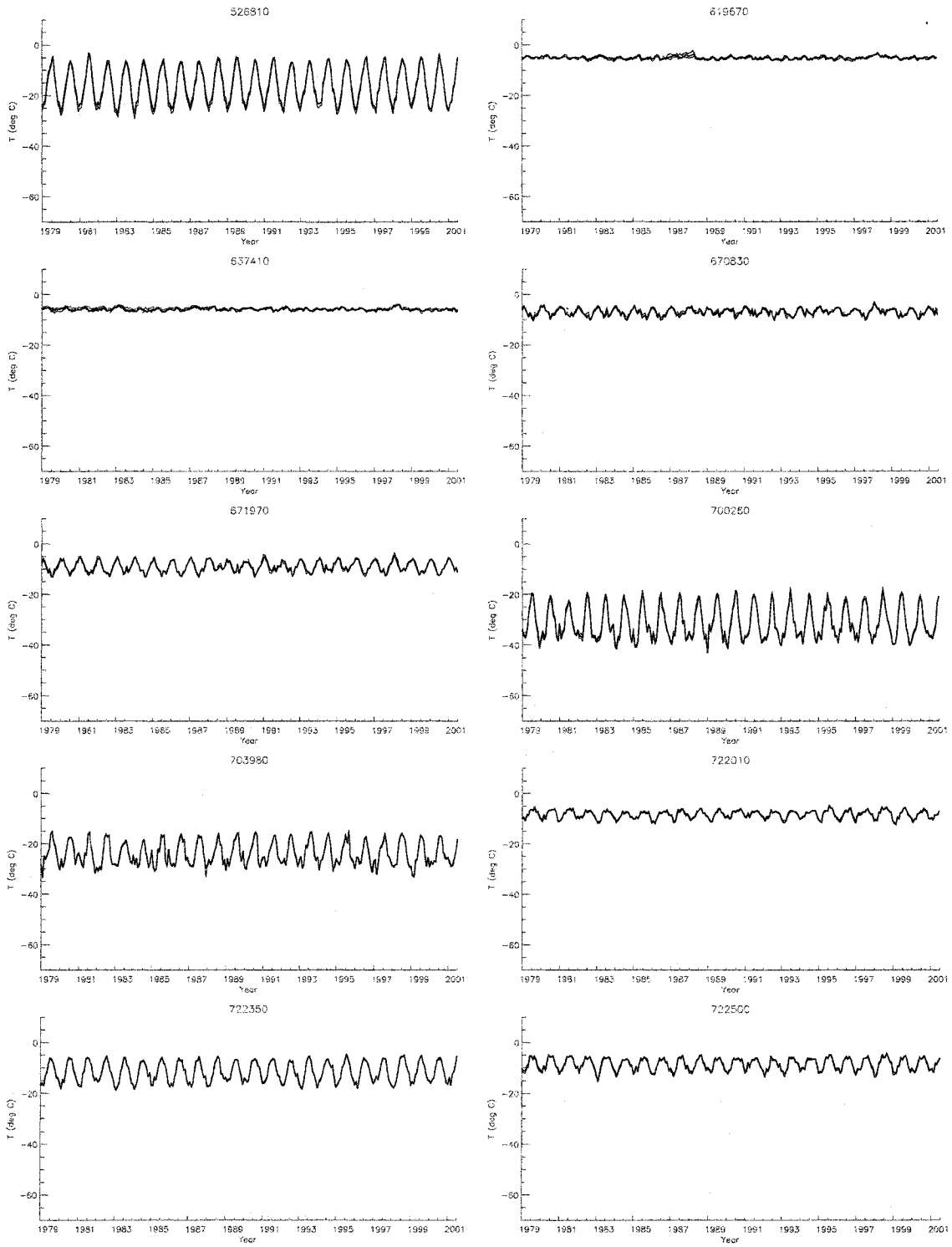

Figure C.3. Same as Figure C.1, but for 500 mb.

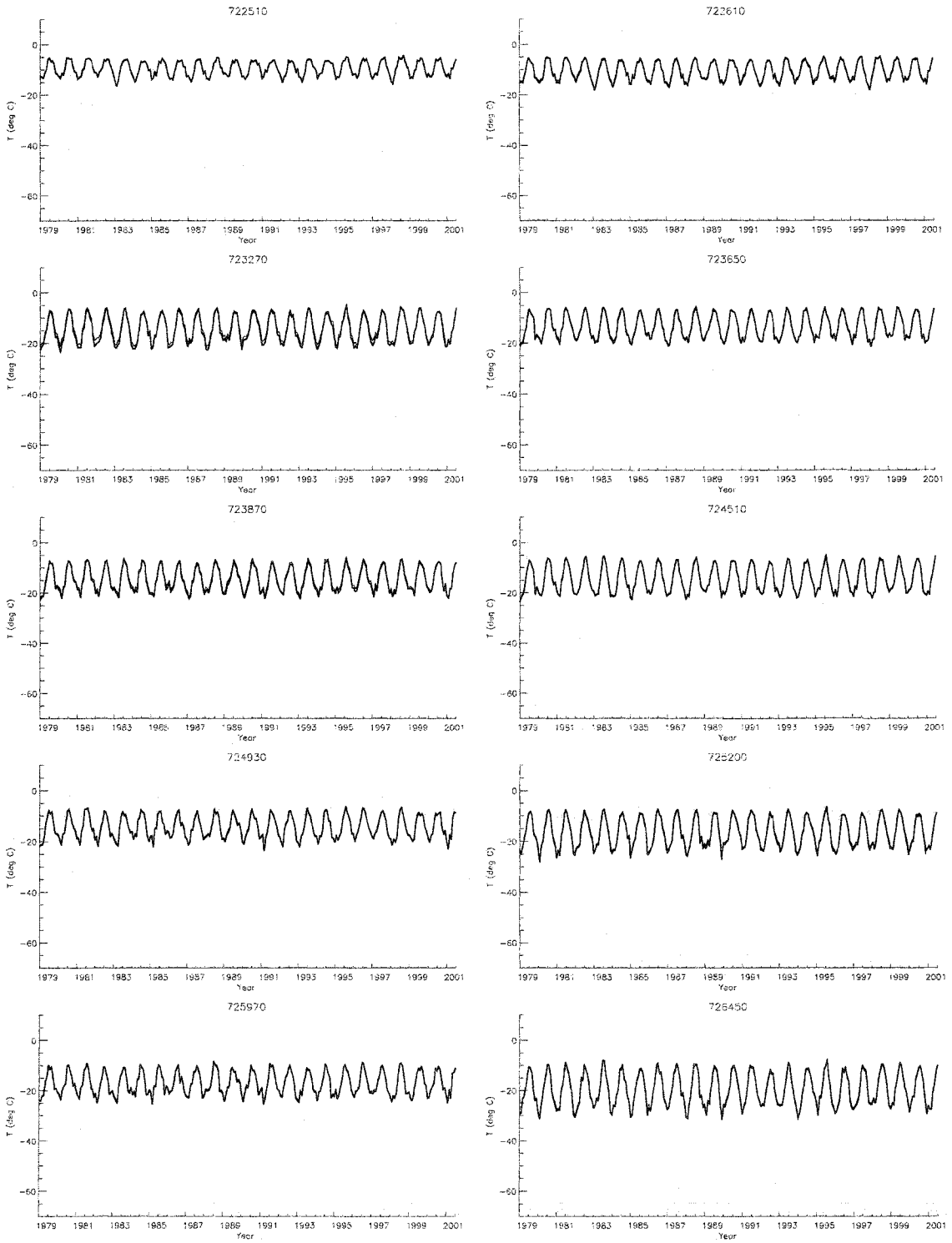

Figure C.3. (continued)

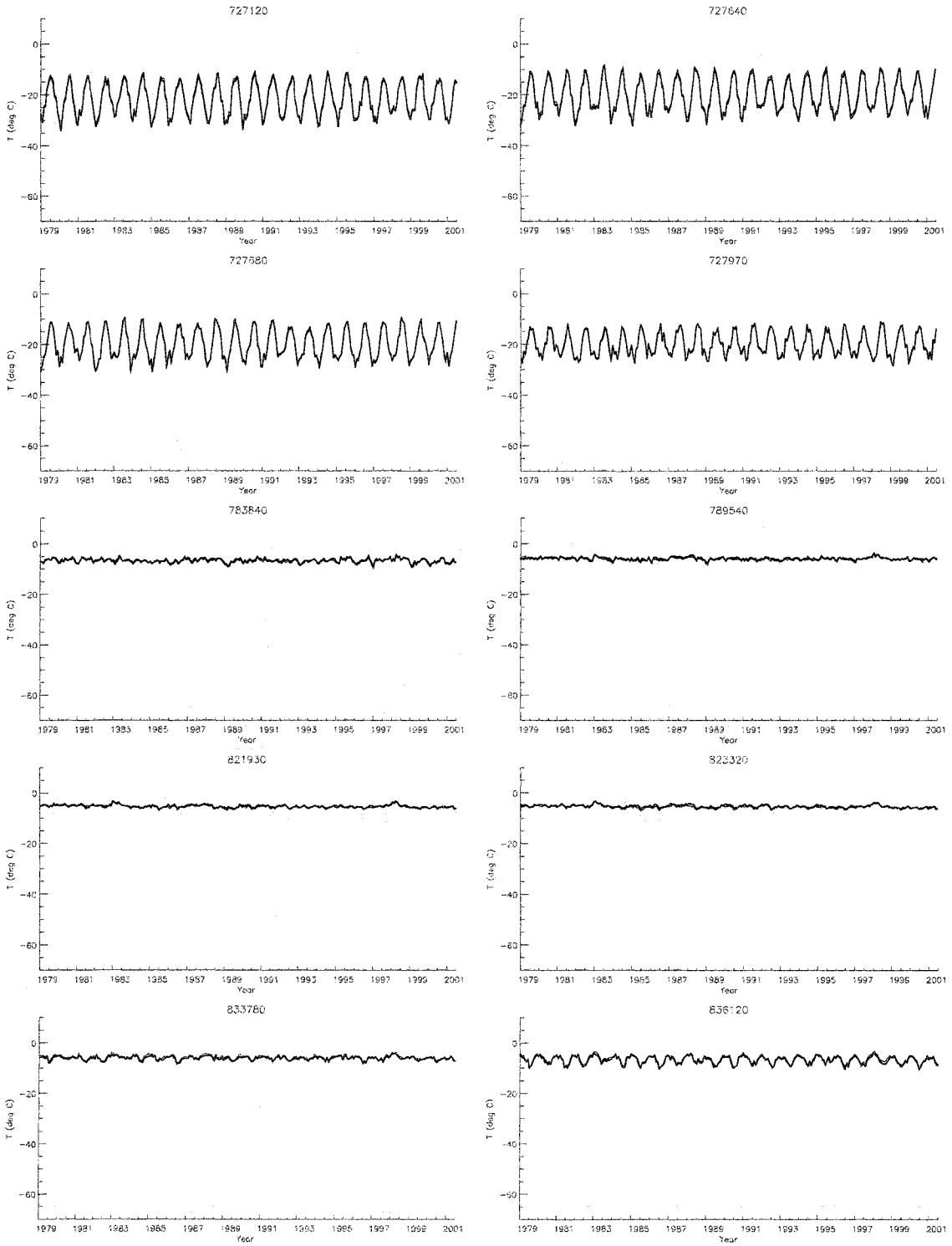

Figure C.3. (continued)

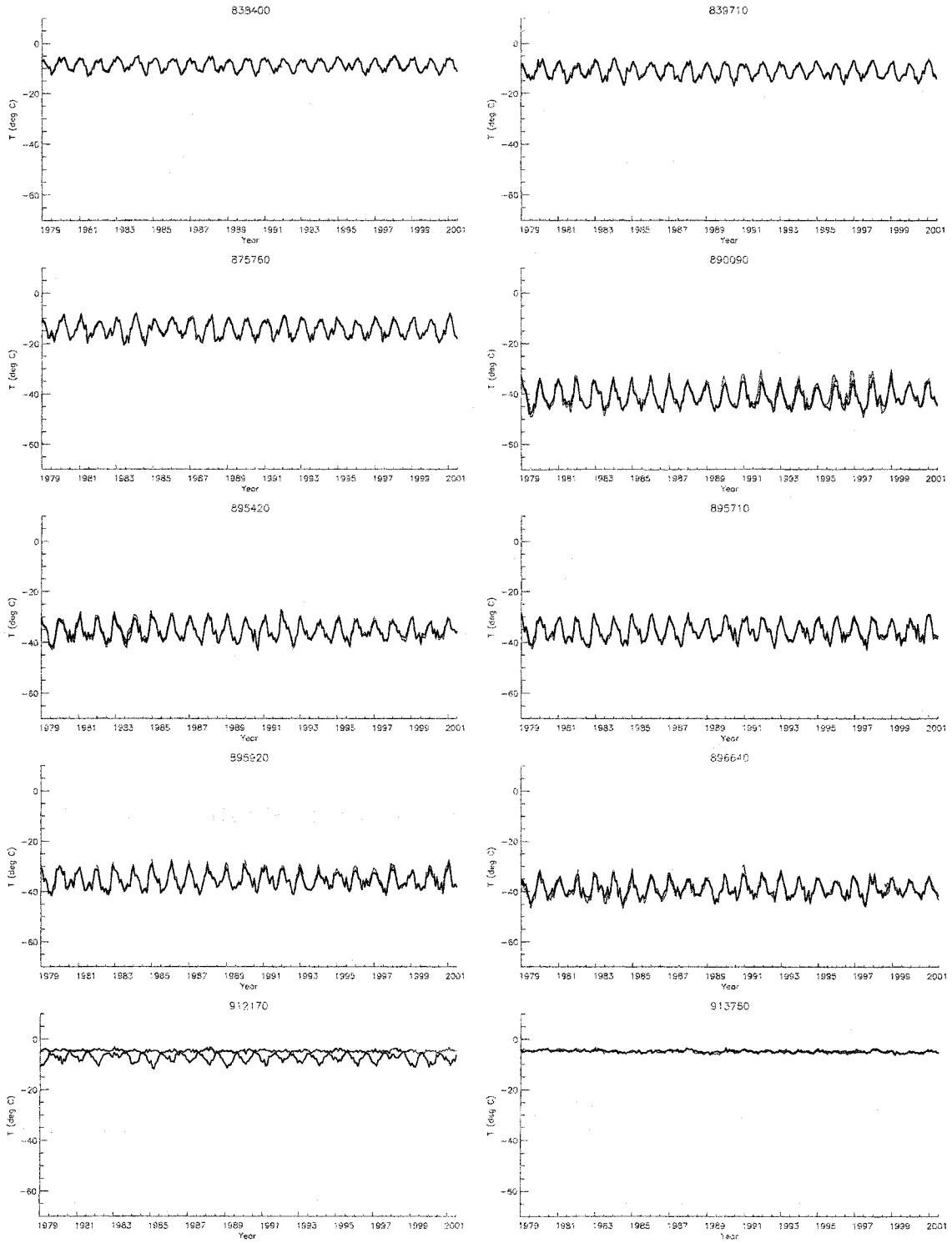

Figure C.3. (continued)

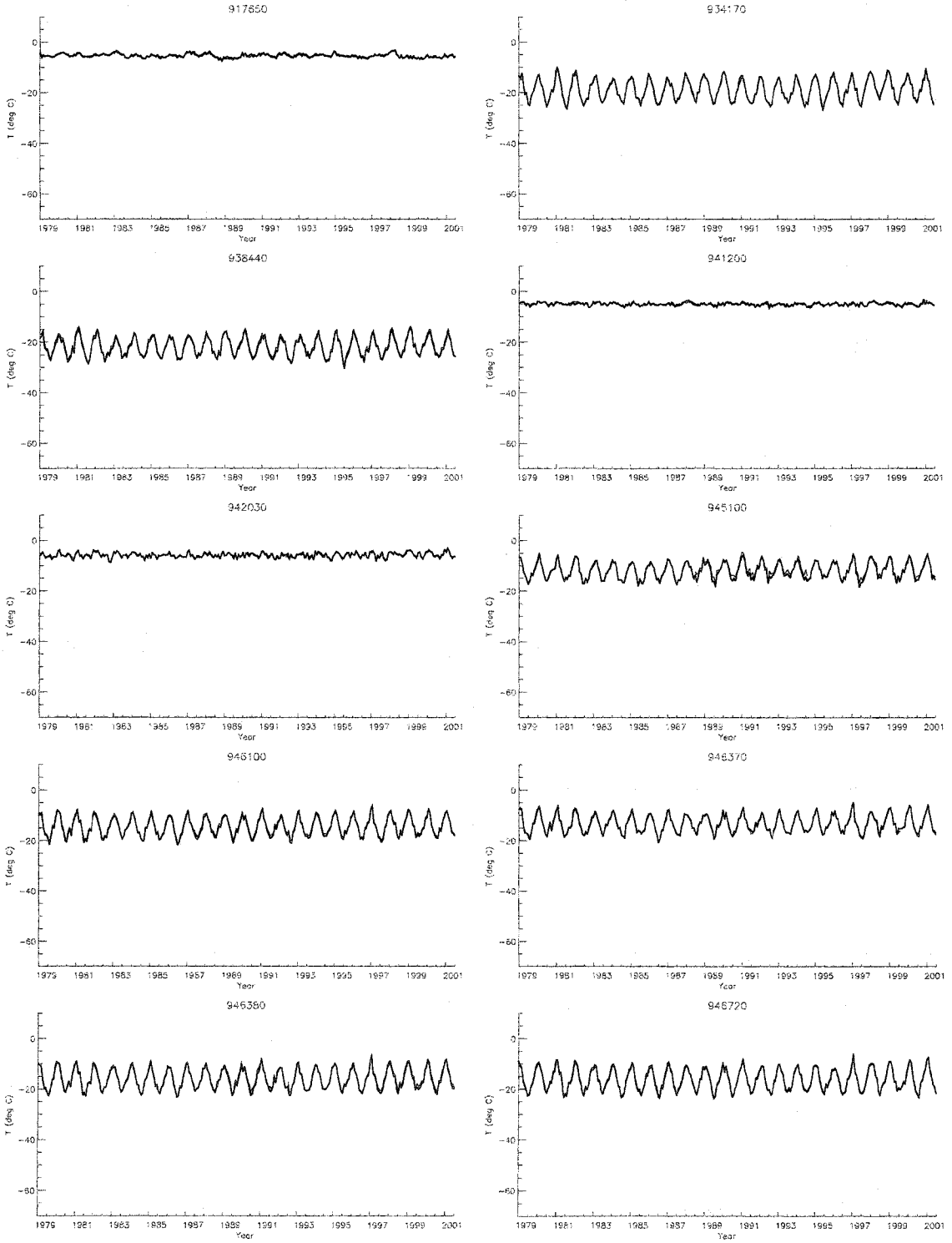

Figure C.3. (continued)

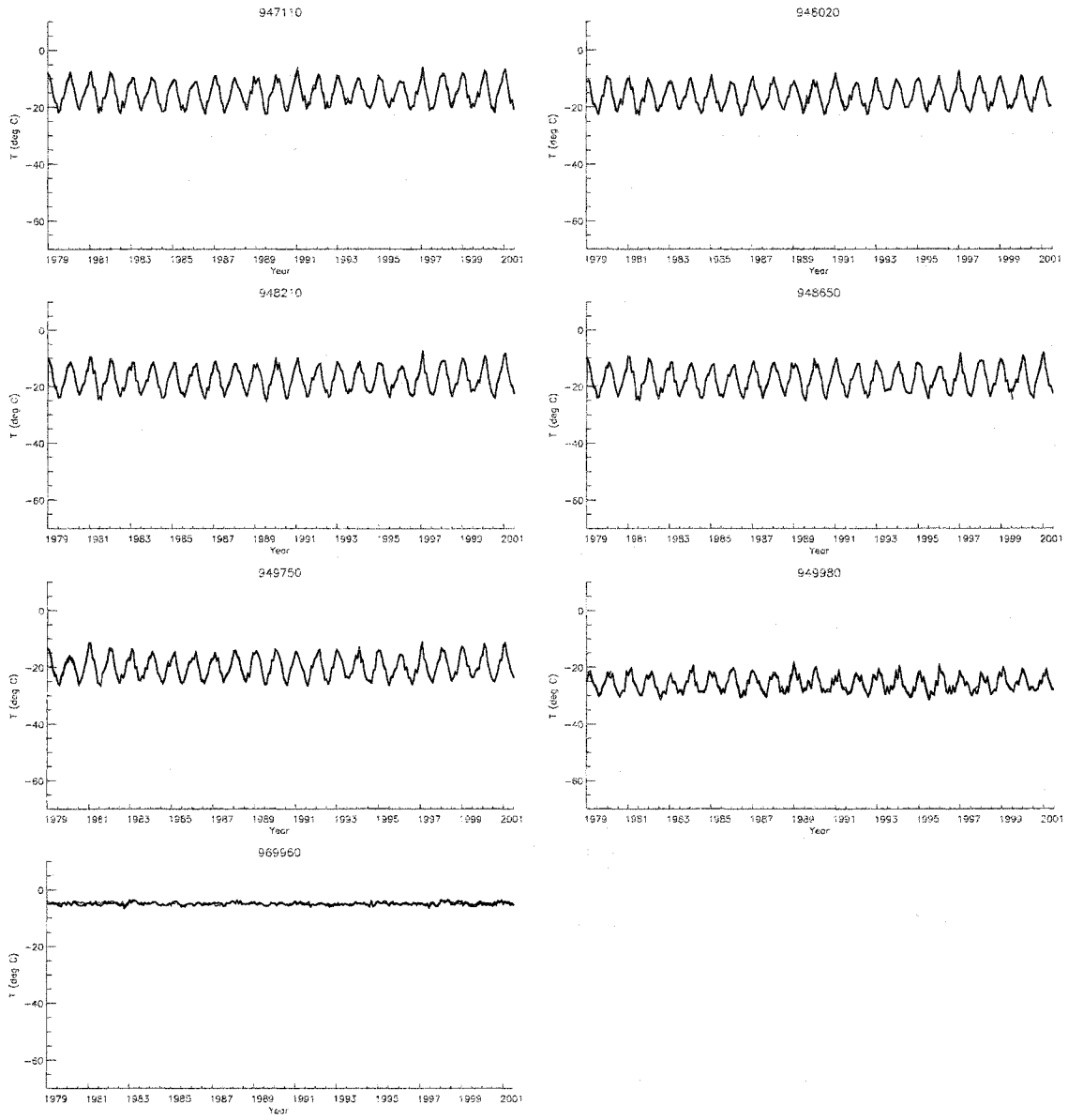

Figure C.3. (continued)

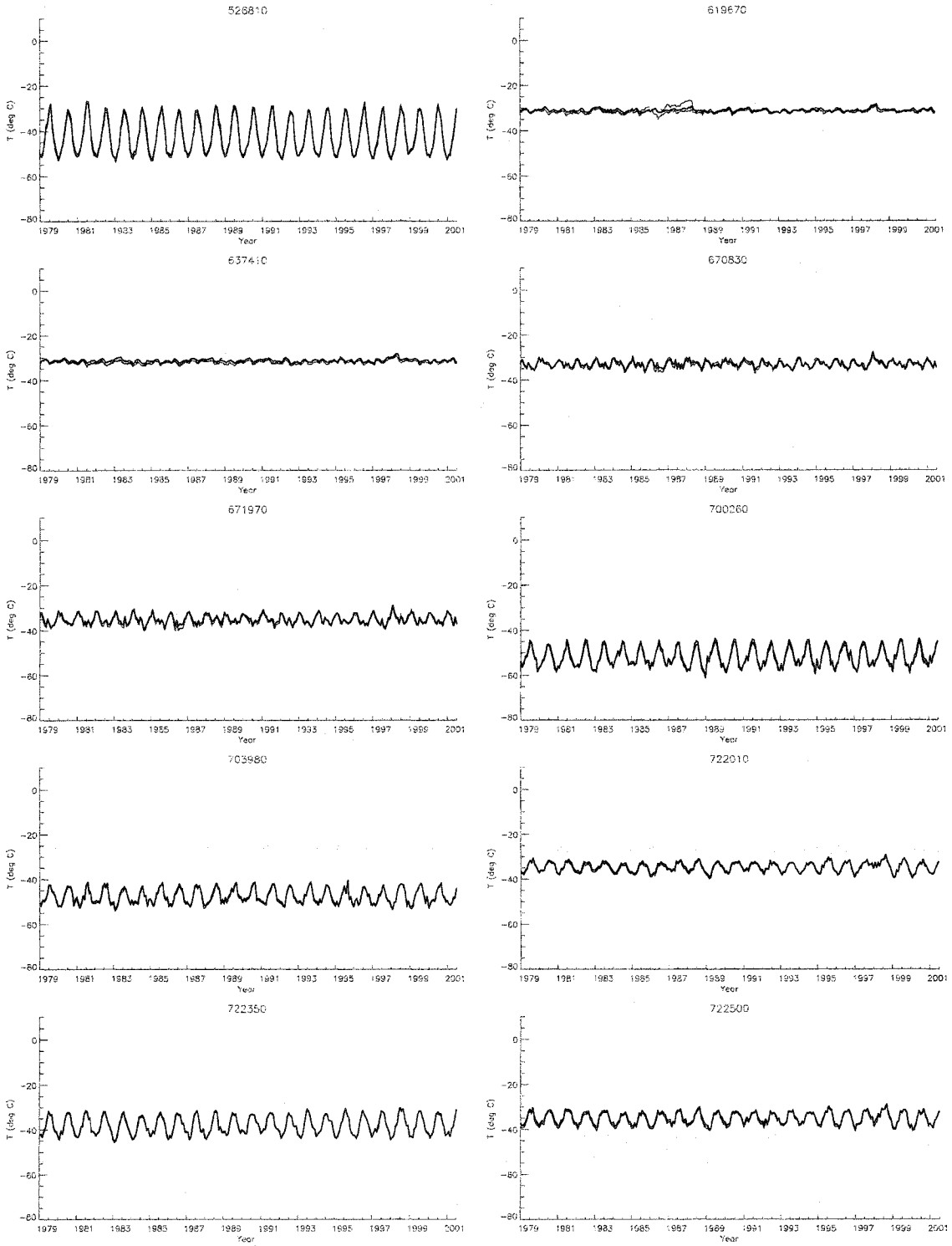

Figure C.4. Same as Figure C.1, but for 300 mb.

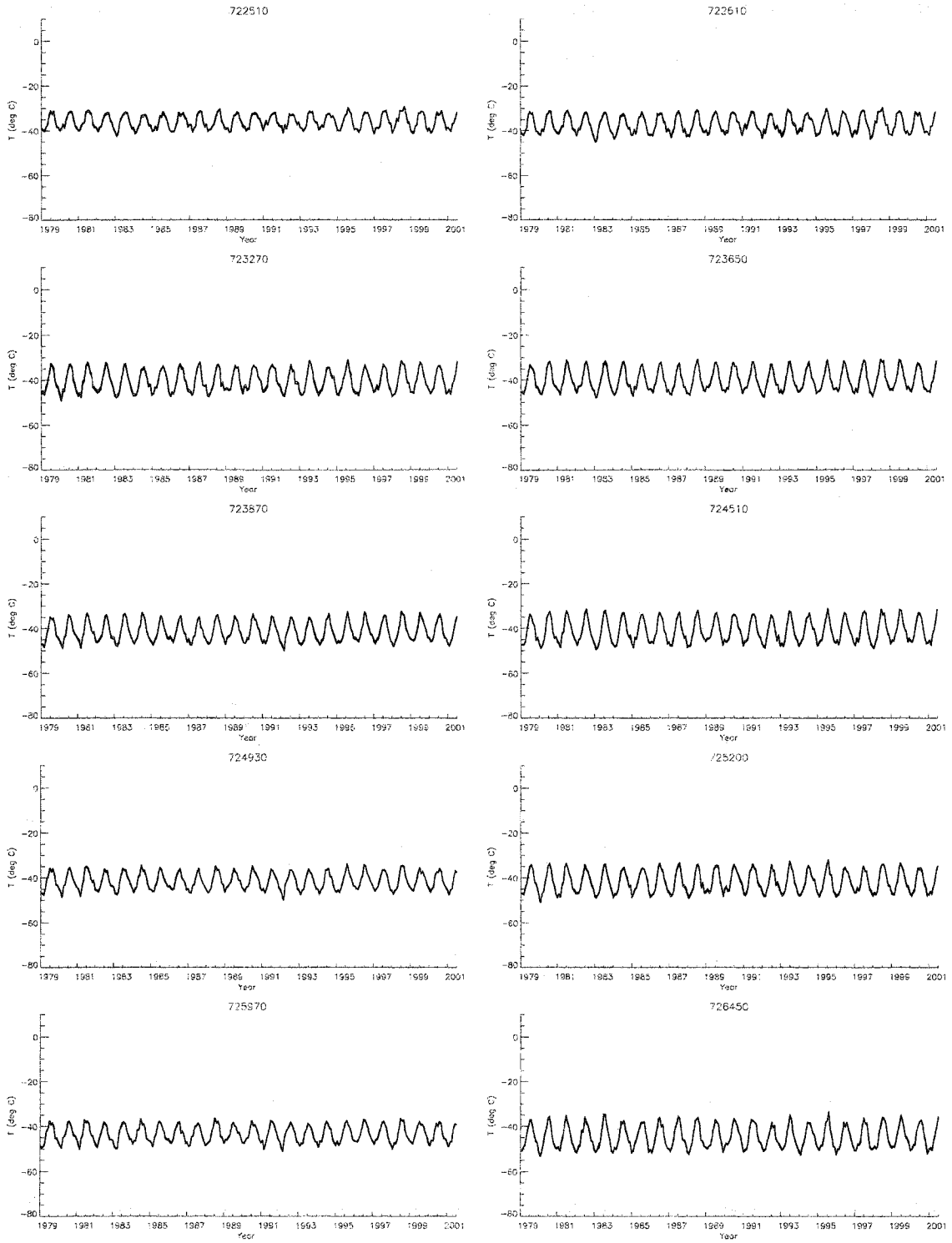

Figure C.4. (continued)

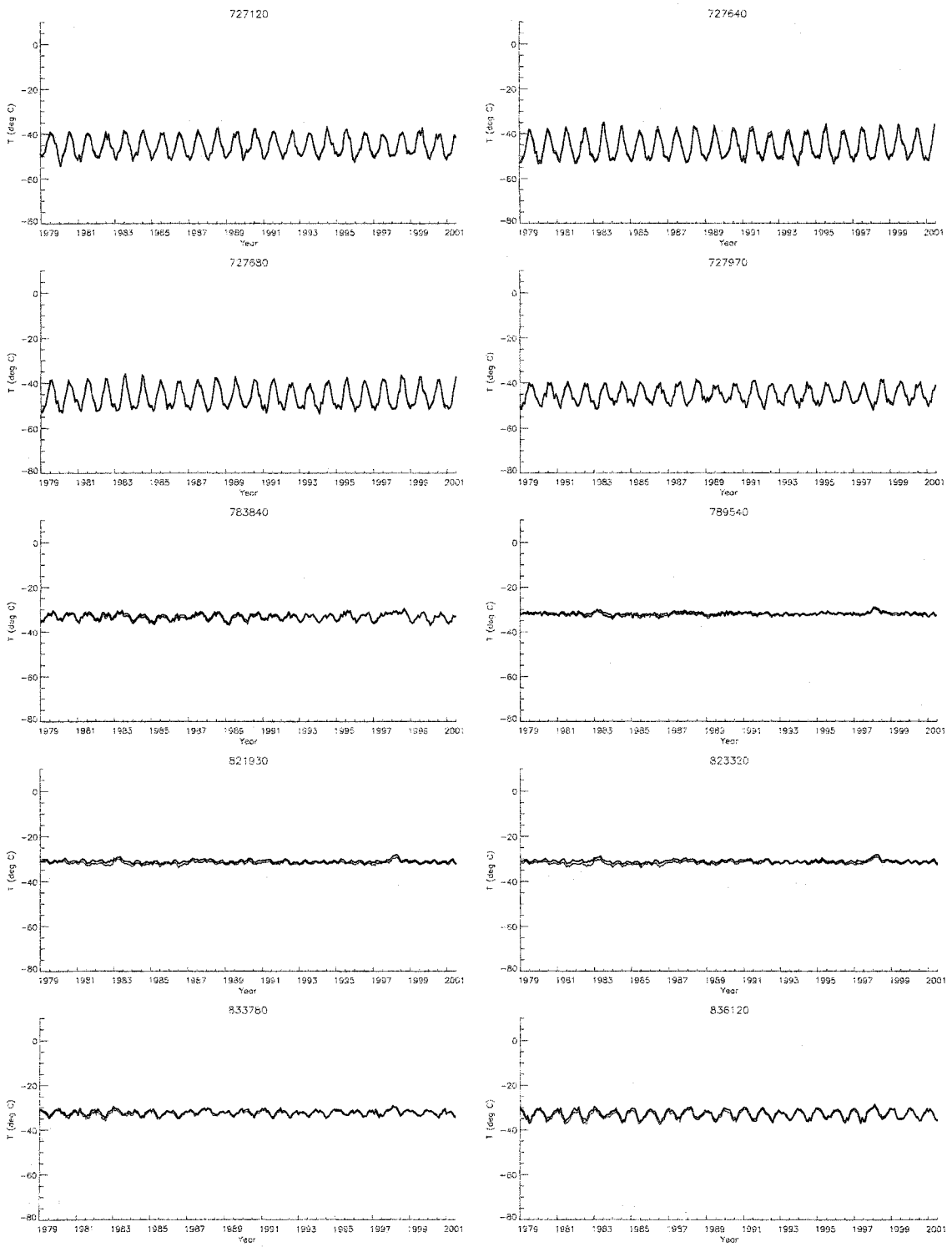

Figure C.4. (continued)

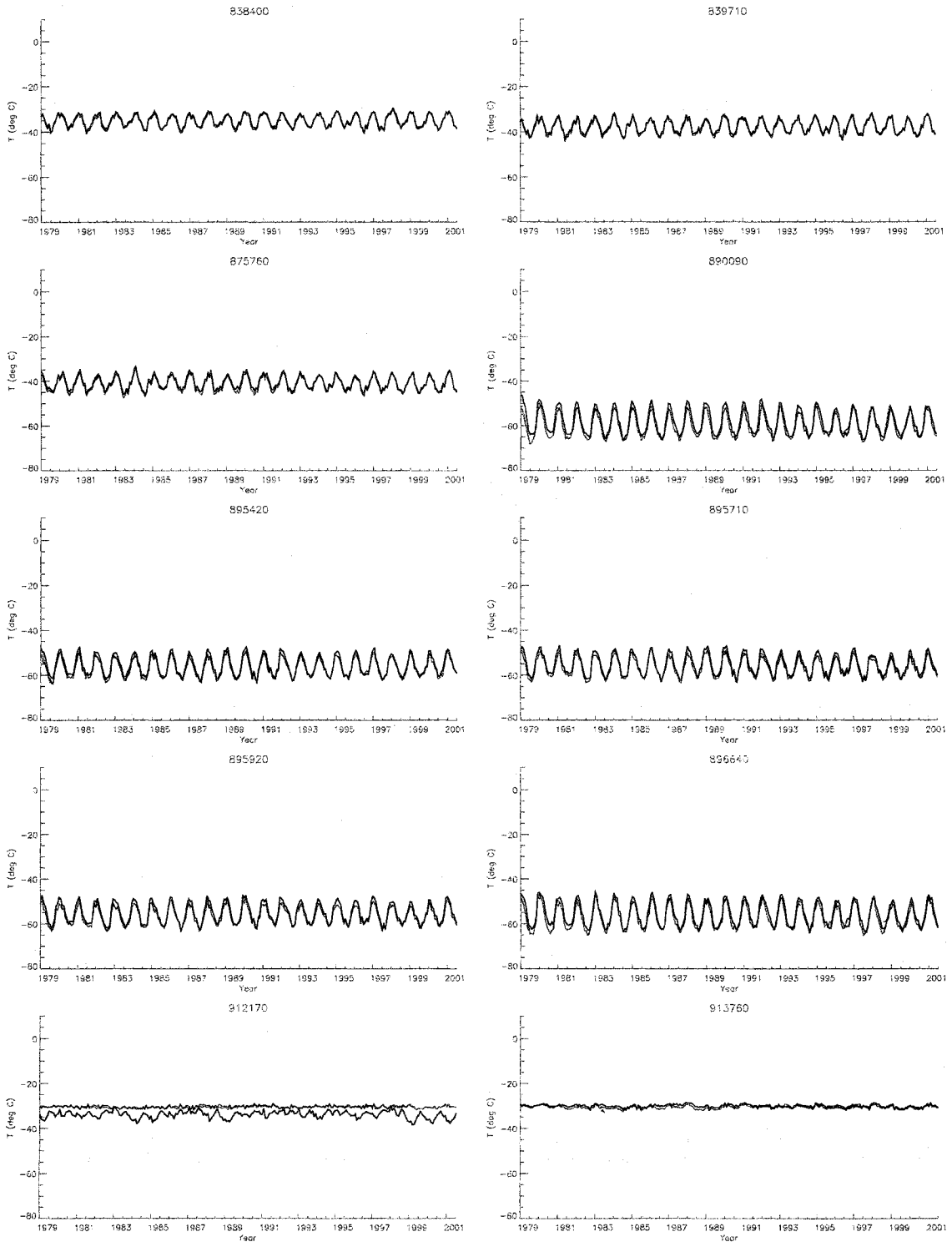

Figure C.4. (continued)

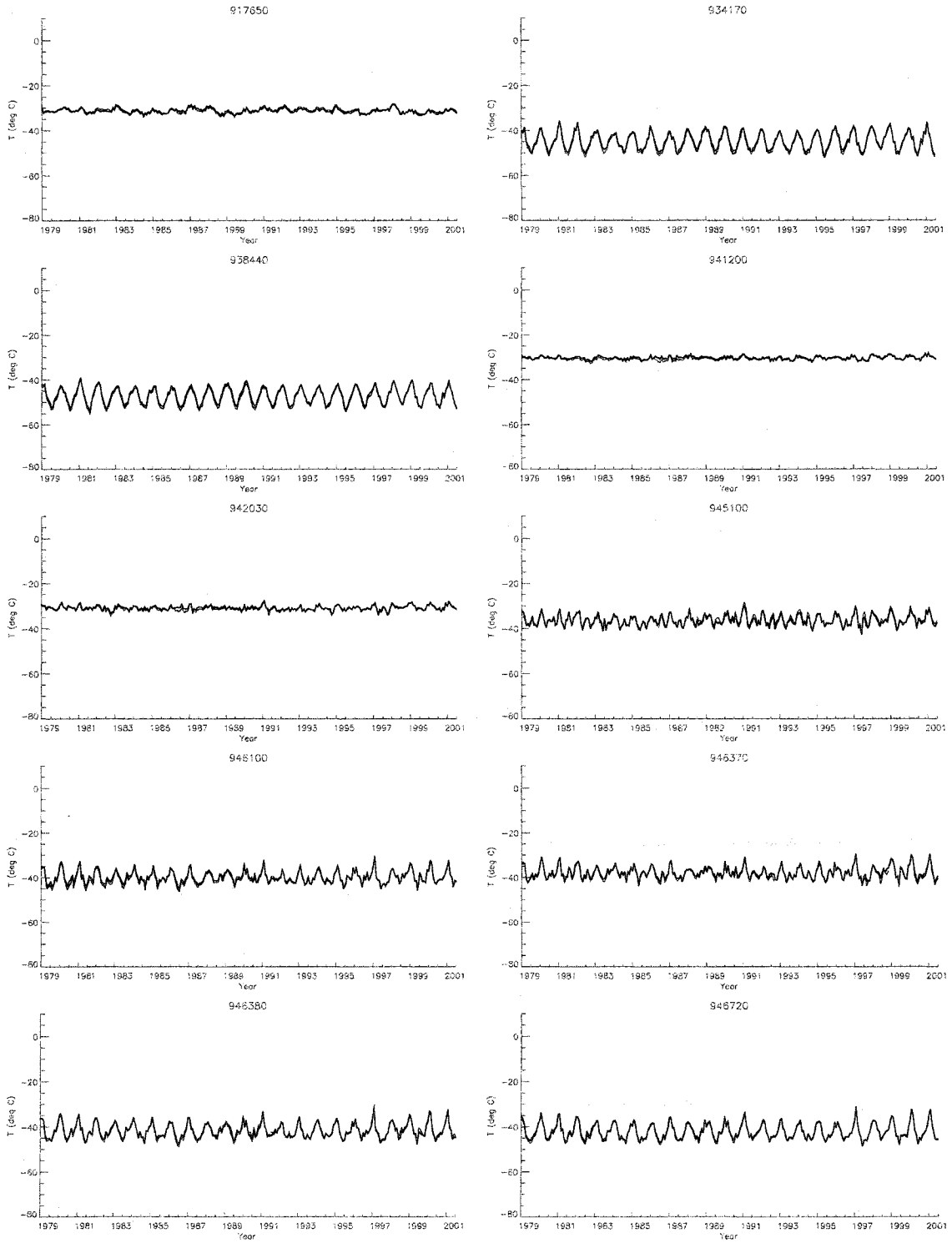

Figure C.4. (continued)

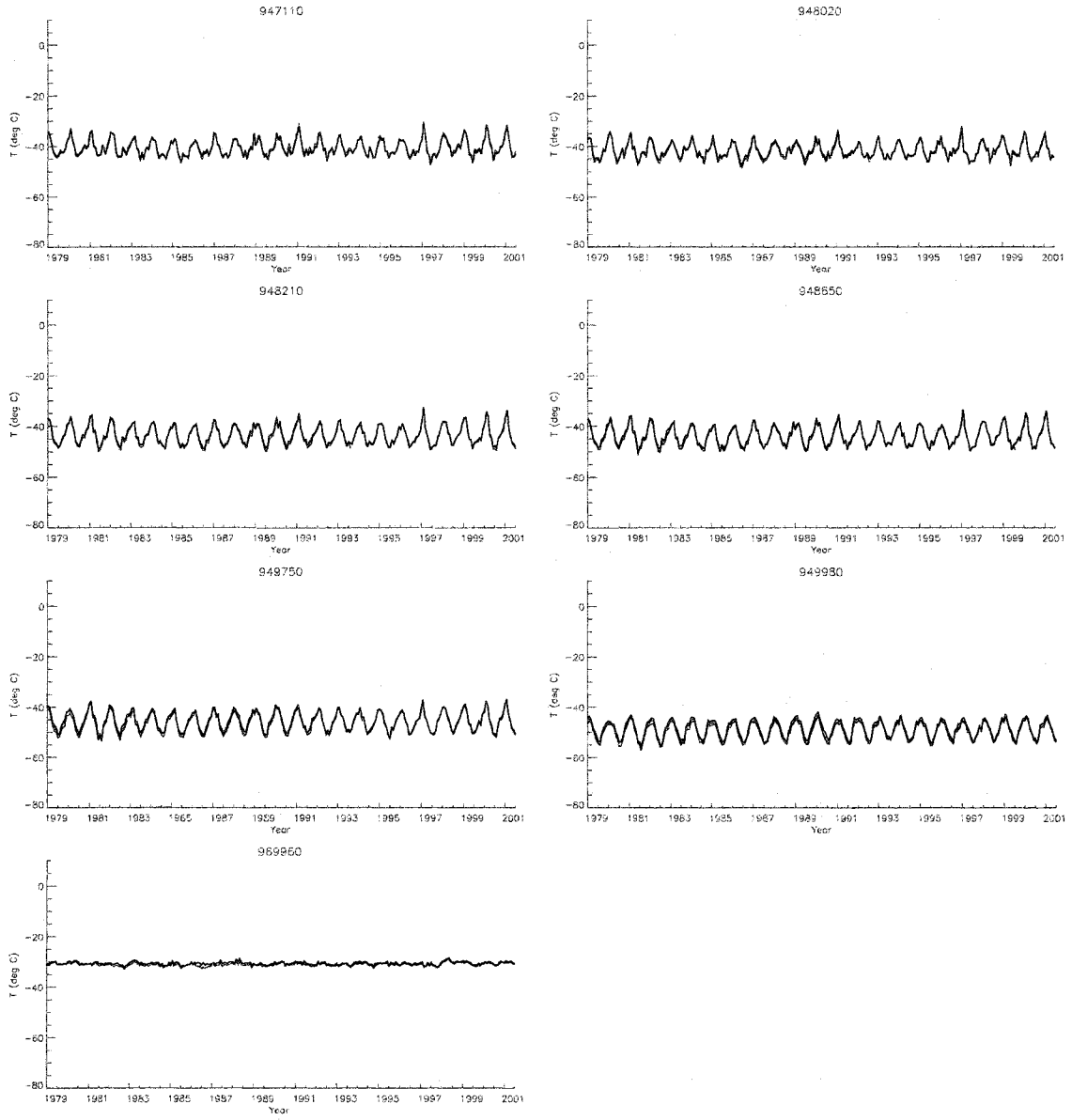

Figure C.4. (continued)

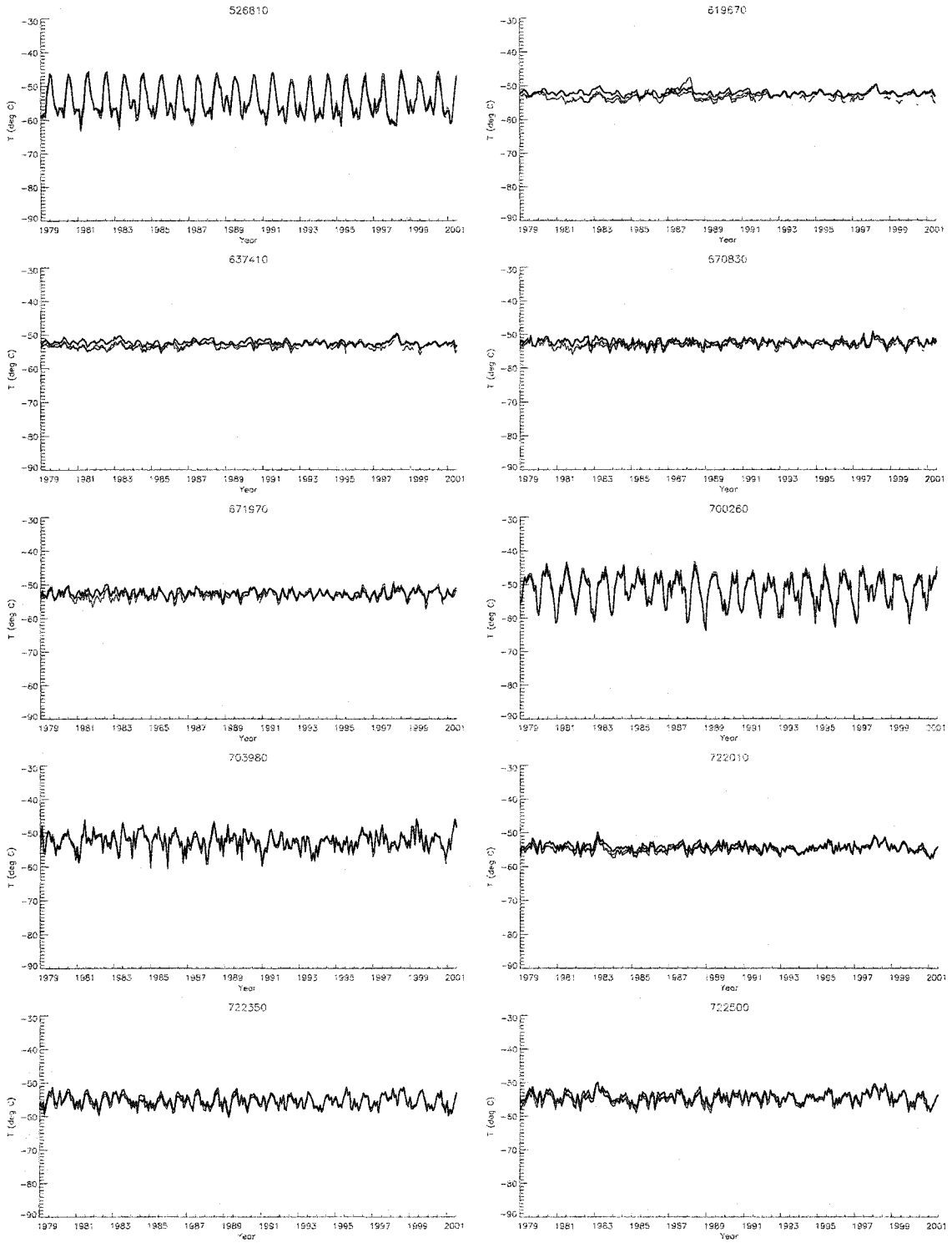

Figure C.5. Same as Figure C.1, but for 200 mb.

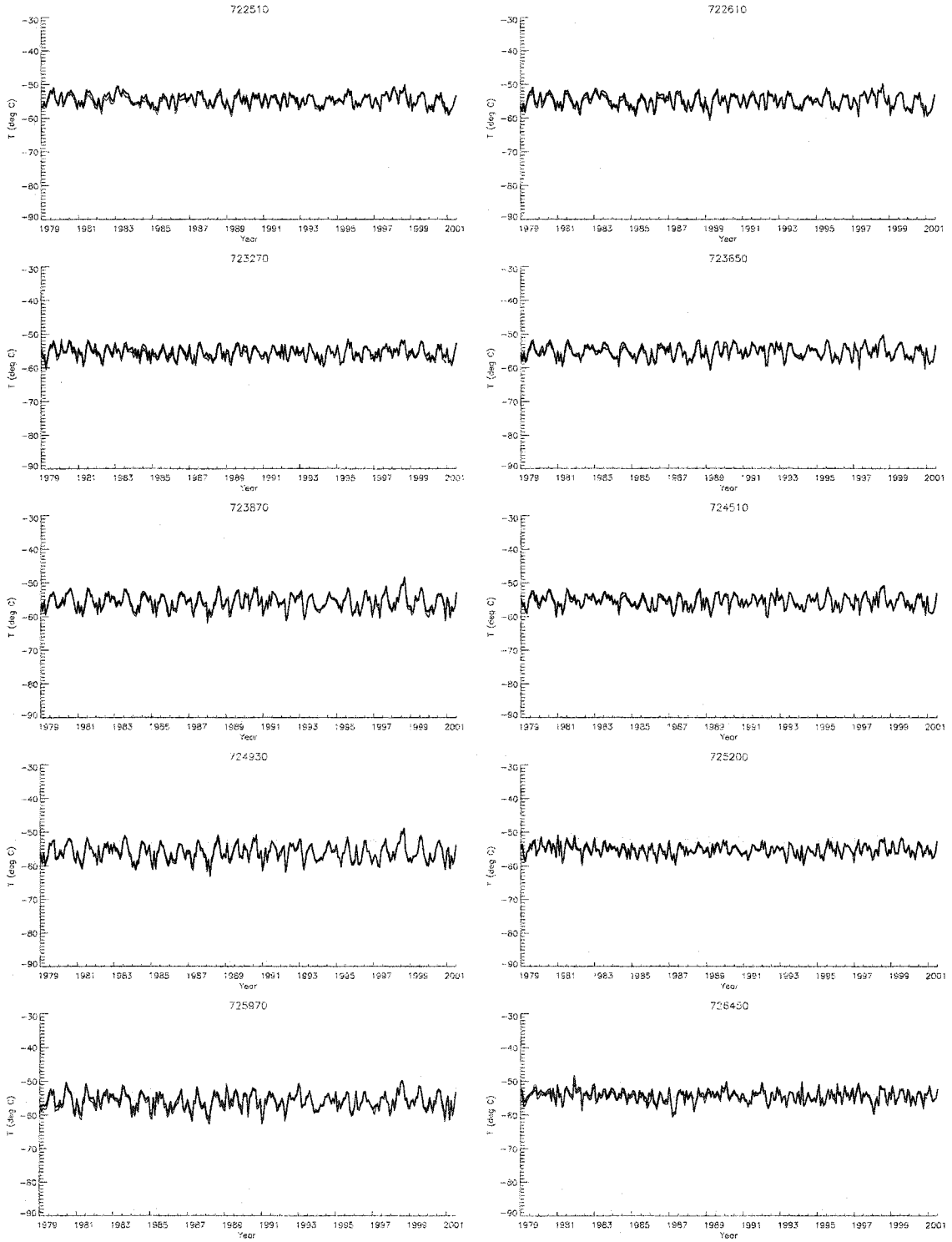

Figure C.5. (continued)

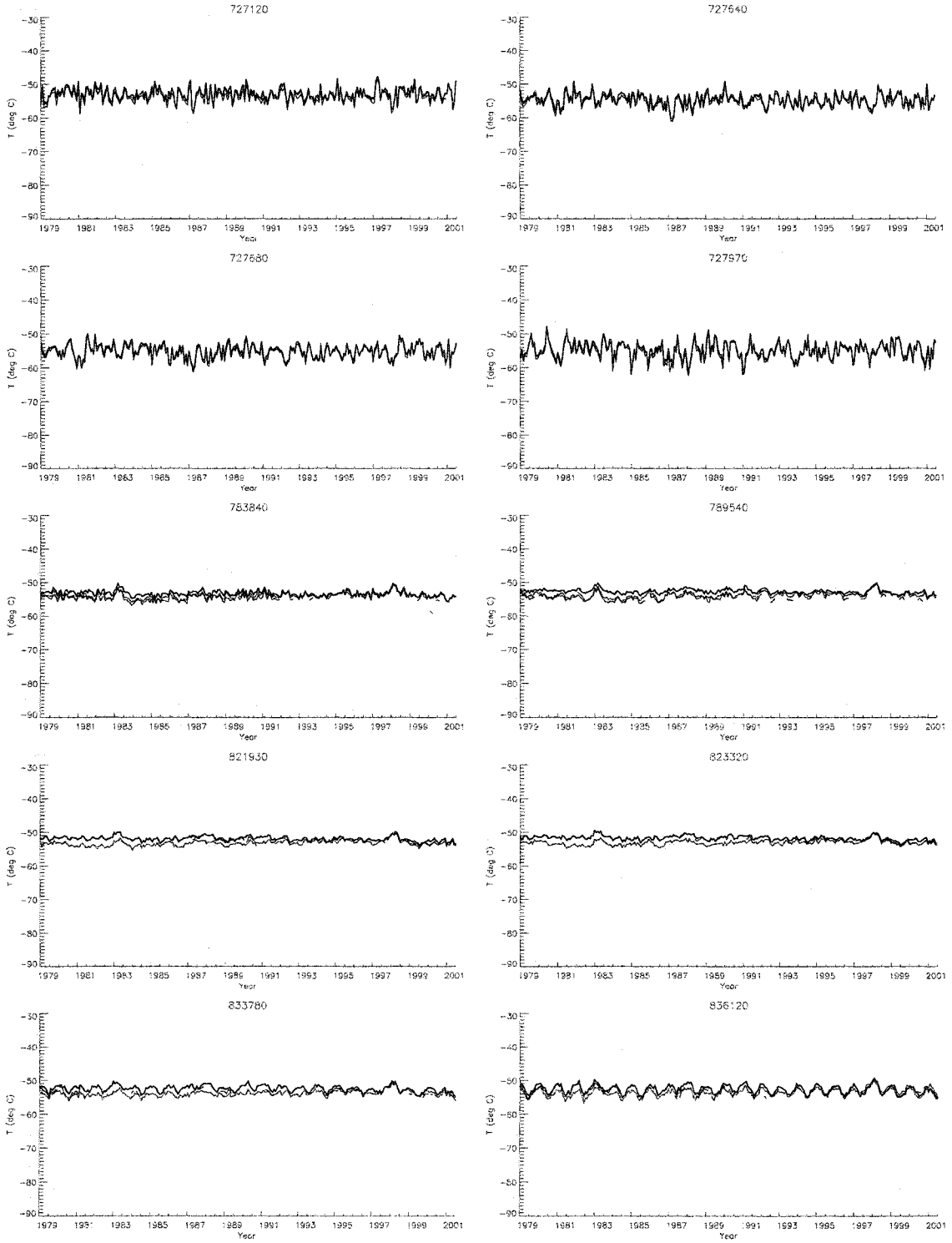

Figure C.5. (continued)

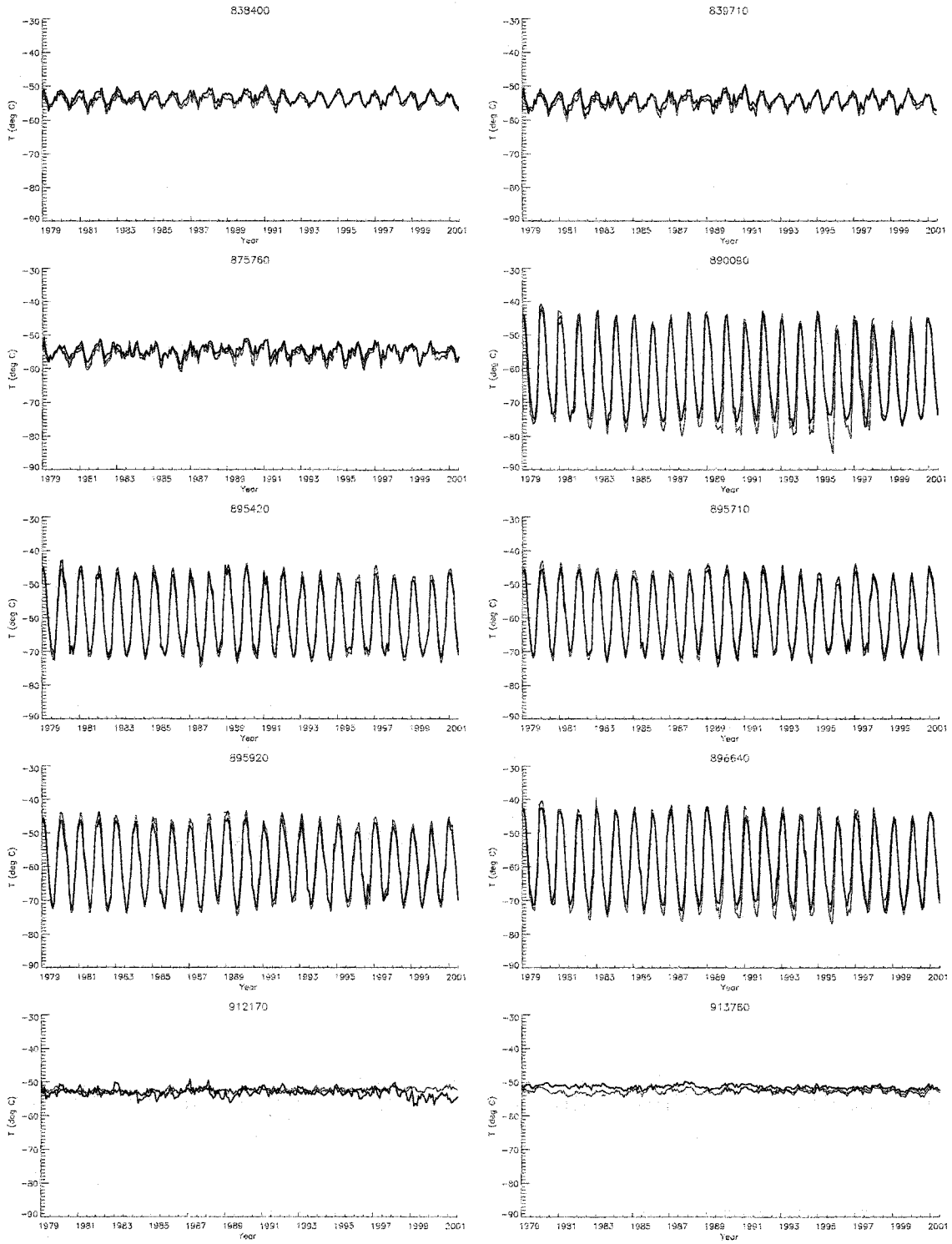

Figure C.5. (continued)

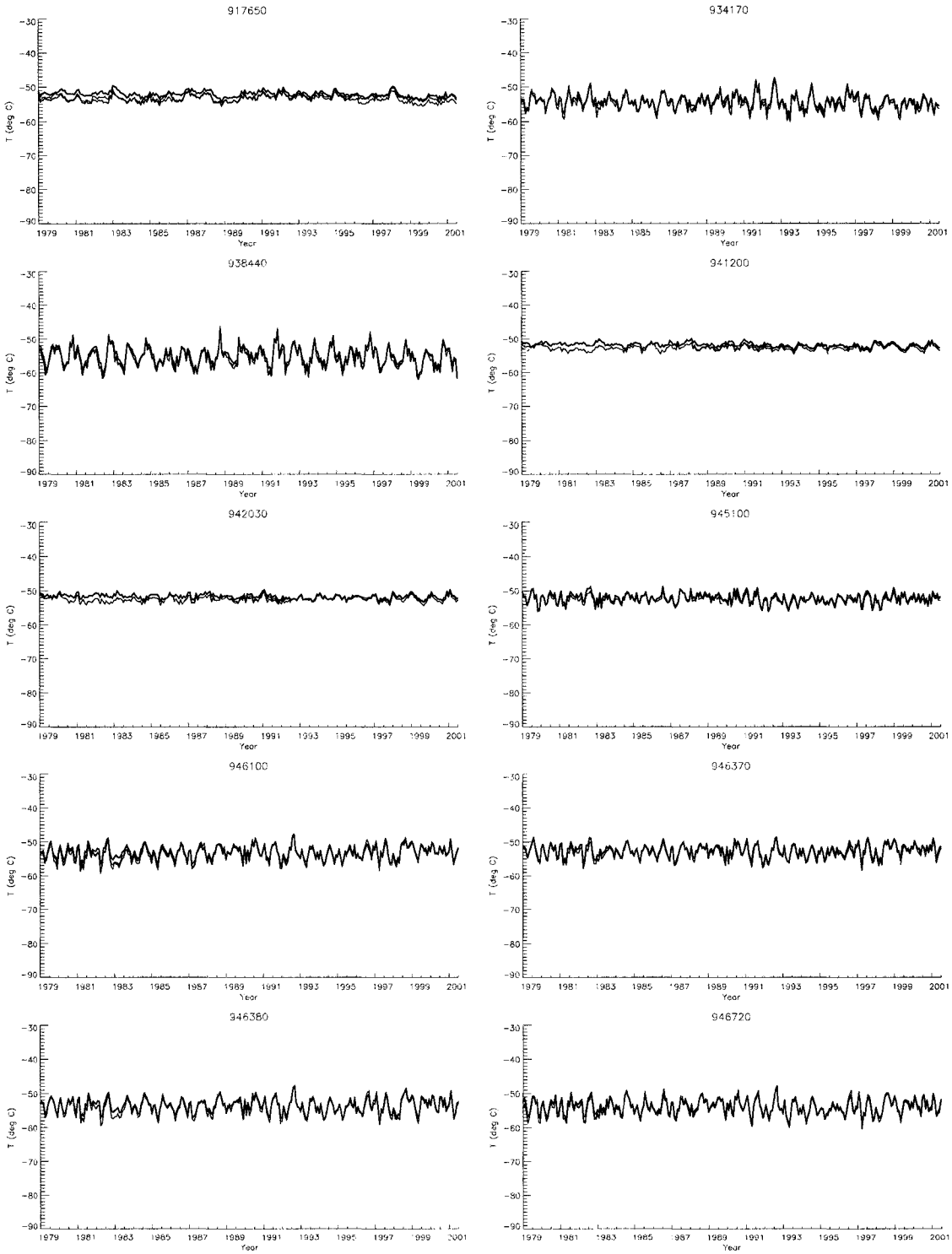

Figure C.5. (continued)

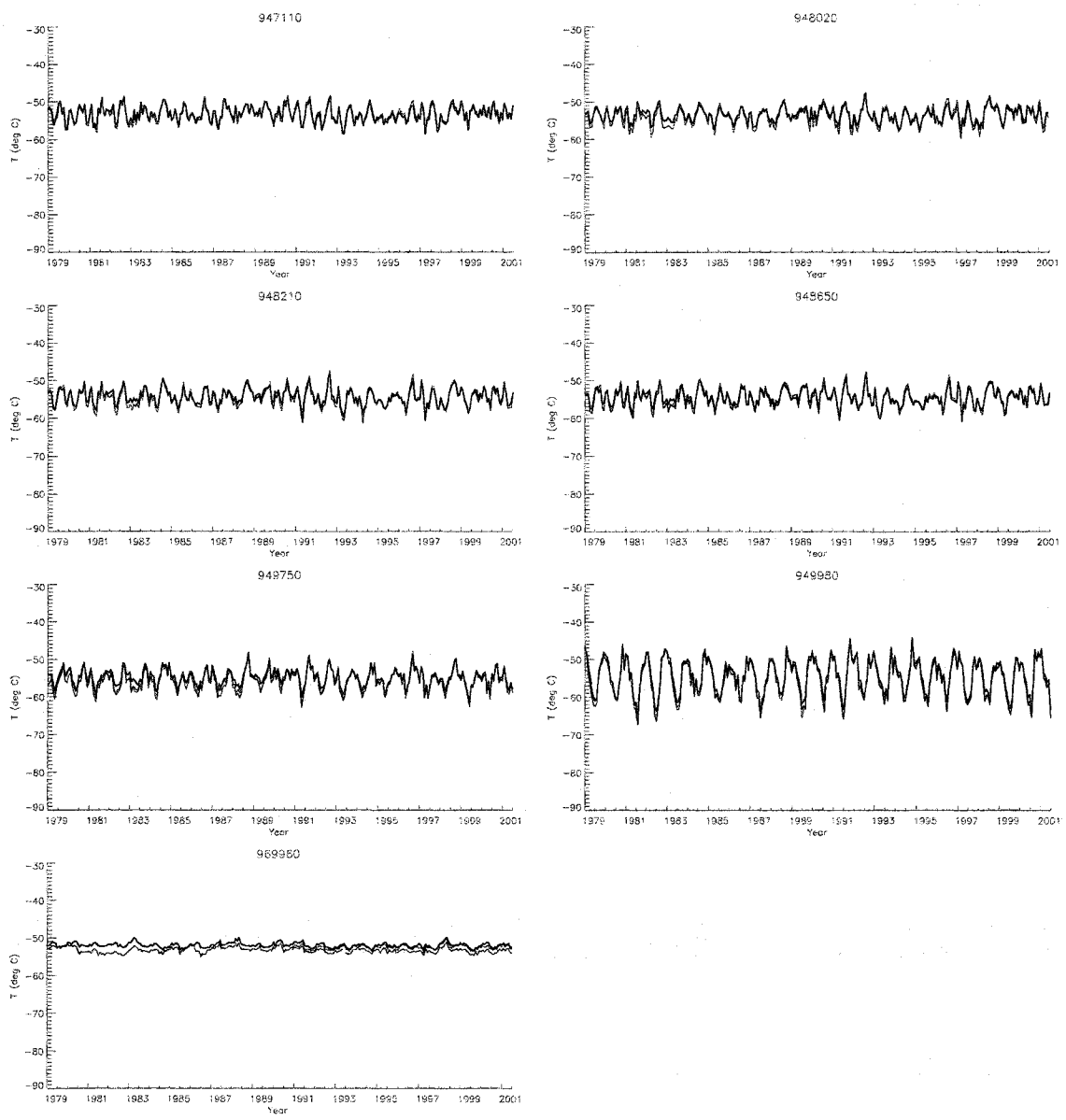

Figure C.5. (continued)

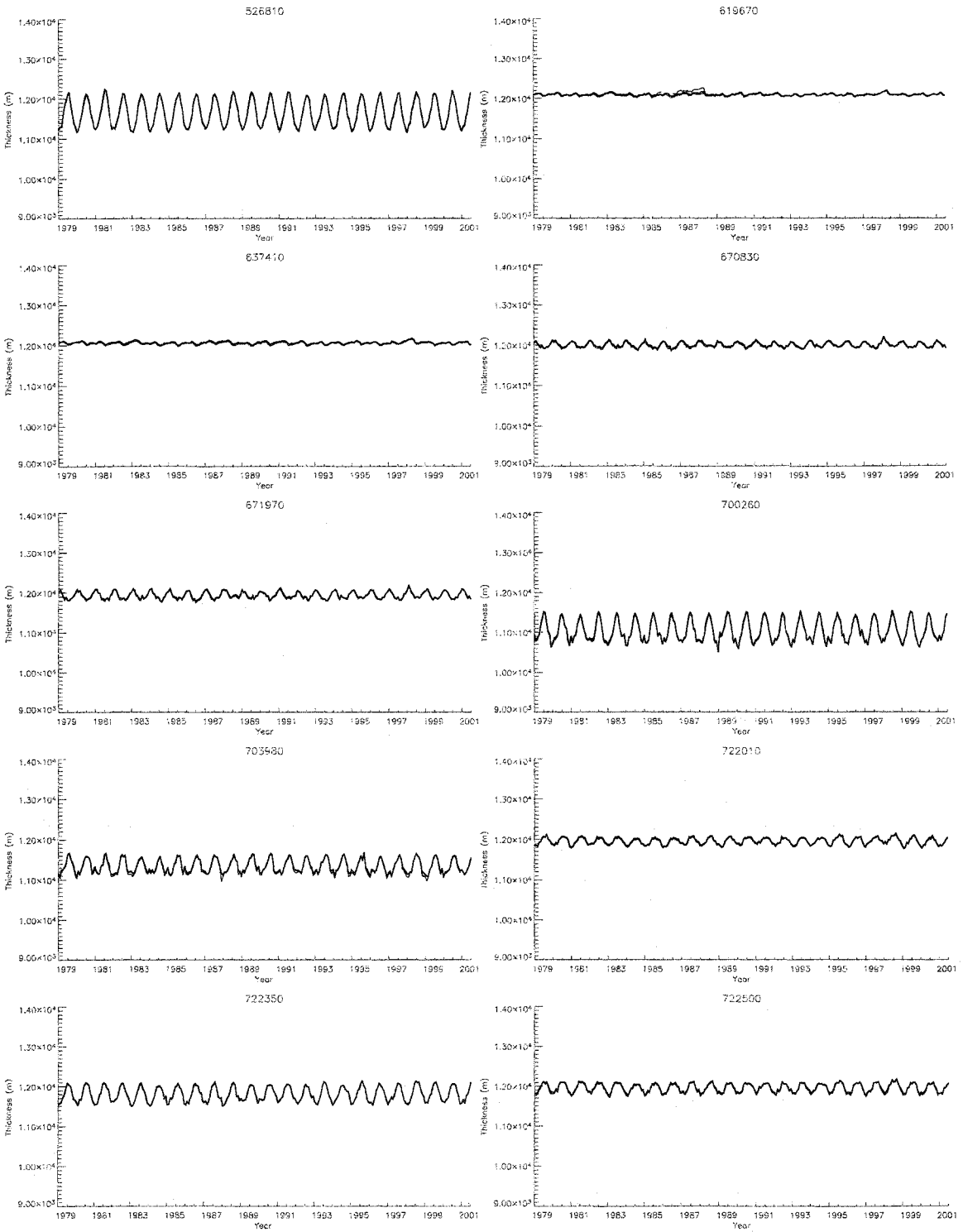

Figure C.6. 1979-2001 thickness time series for the 1000-200mb layer, for CARDS stations listed in Appendix B. ERA40 time series are shown in grey, NCEP time series are shown in thick black, and radiosonde time series are shown in thin black.

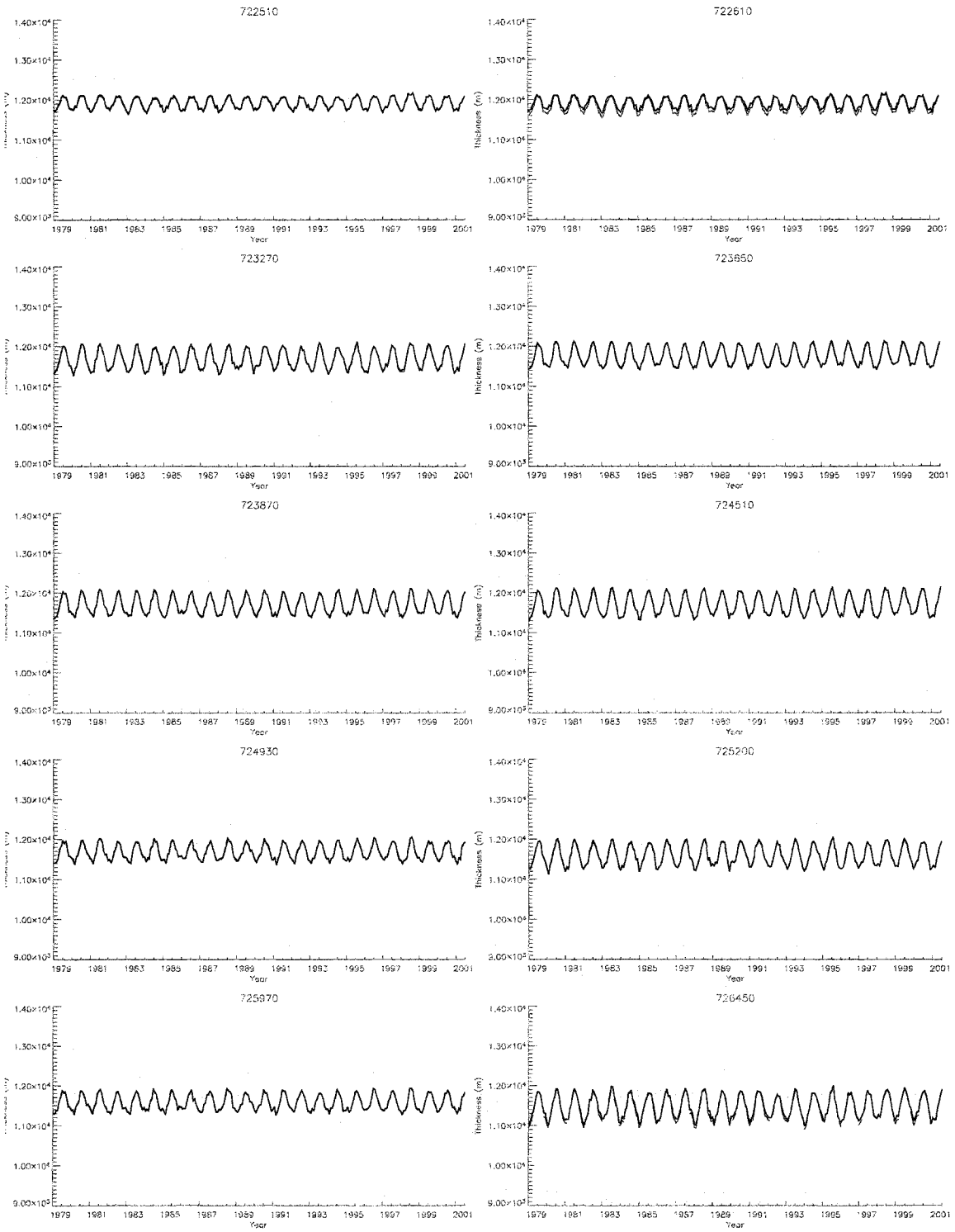

Figure C.6. (continued)

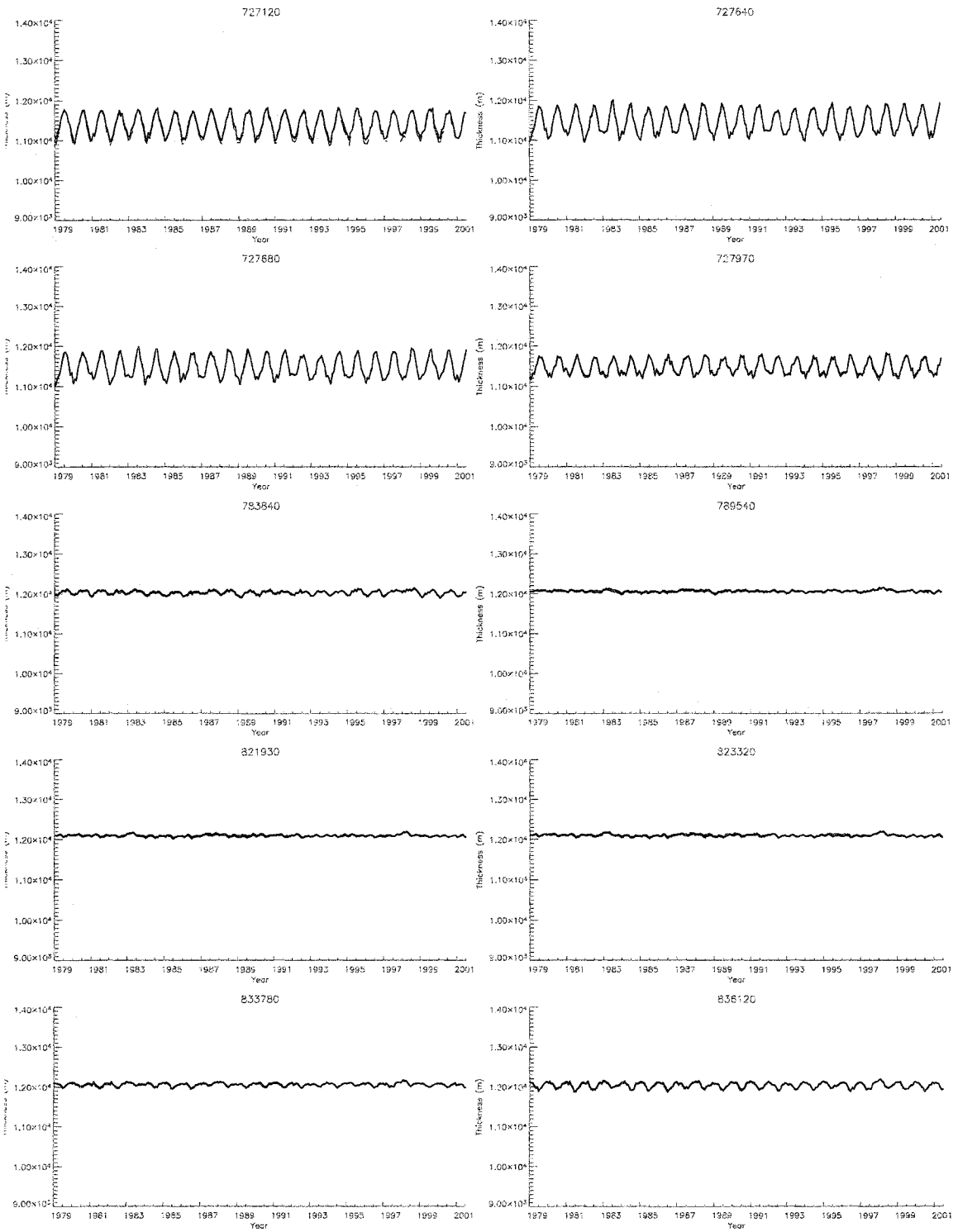

Figure C.6. (continued)

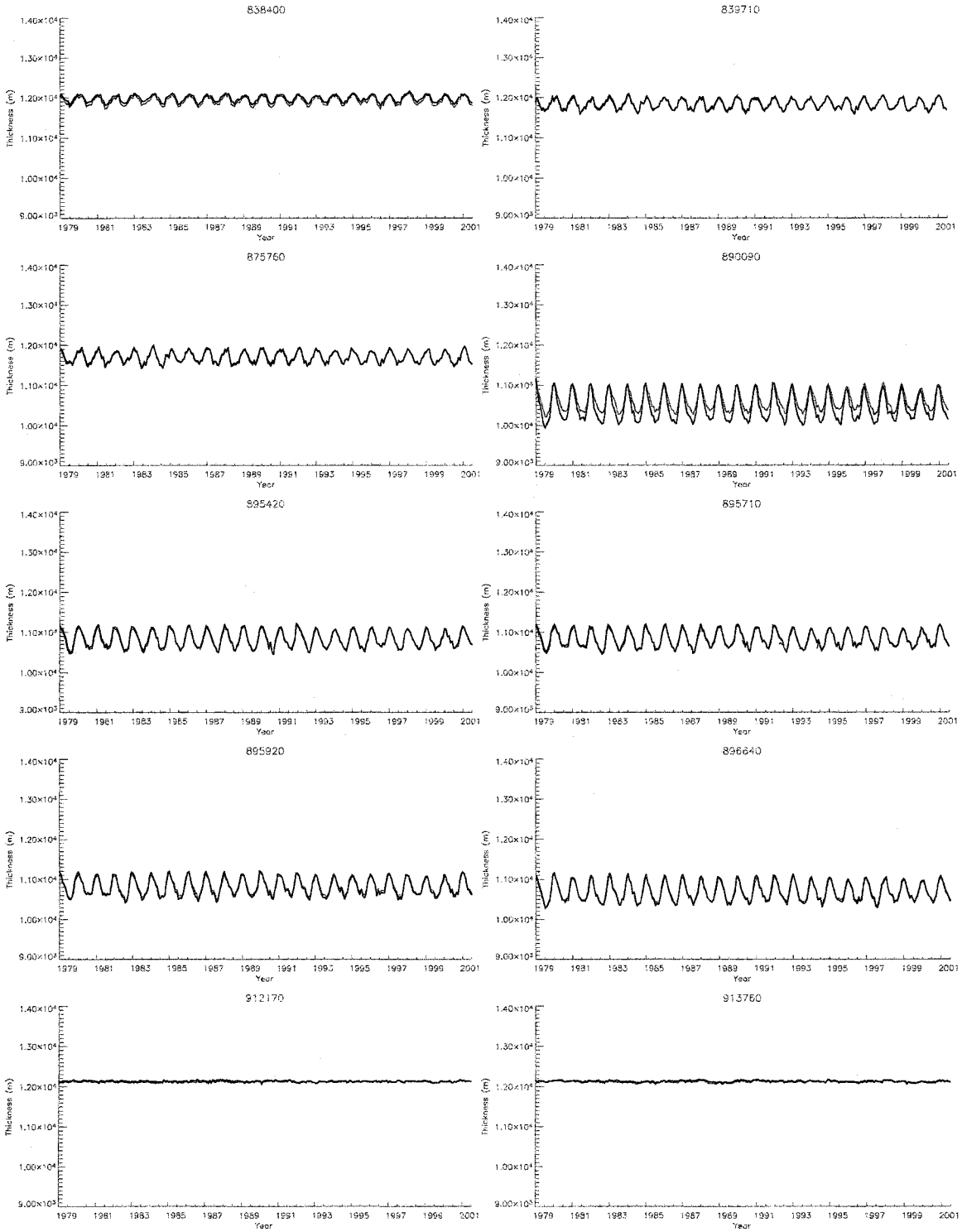

Figure C.6. (continued)

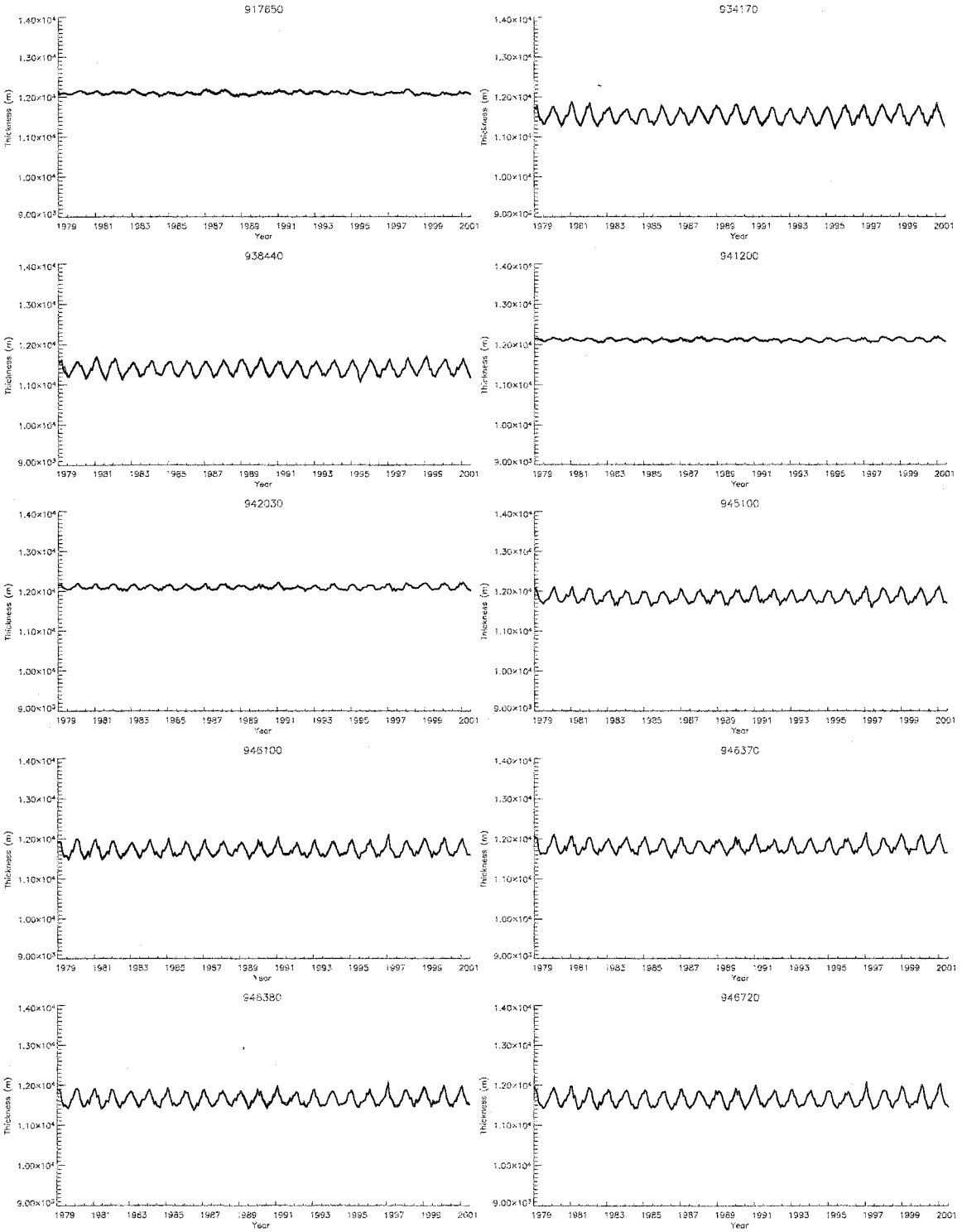

Figure C.6. (continued)

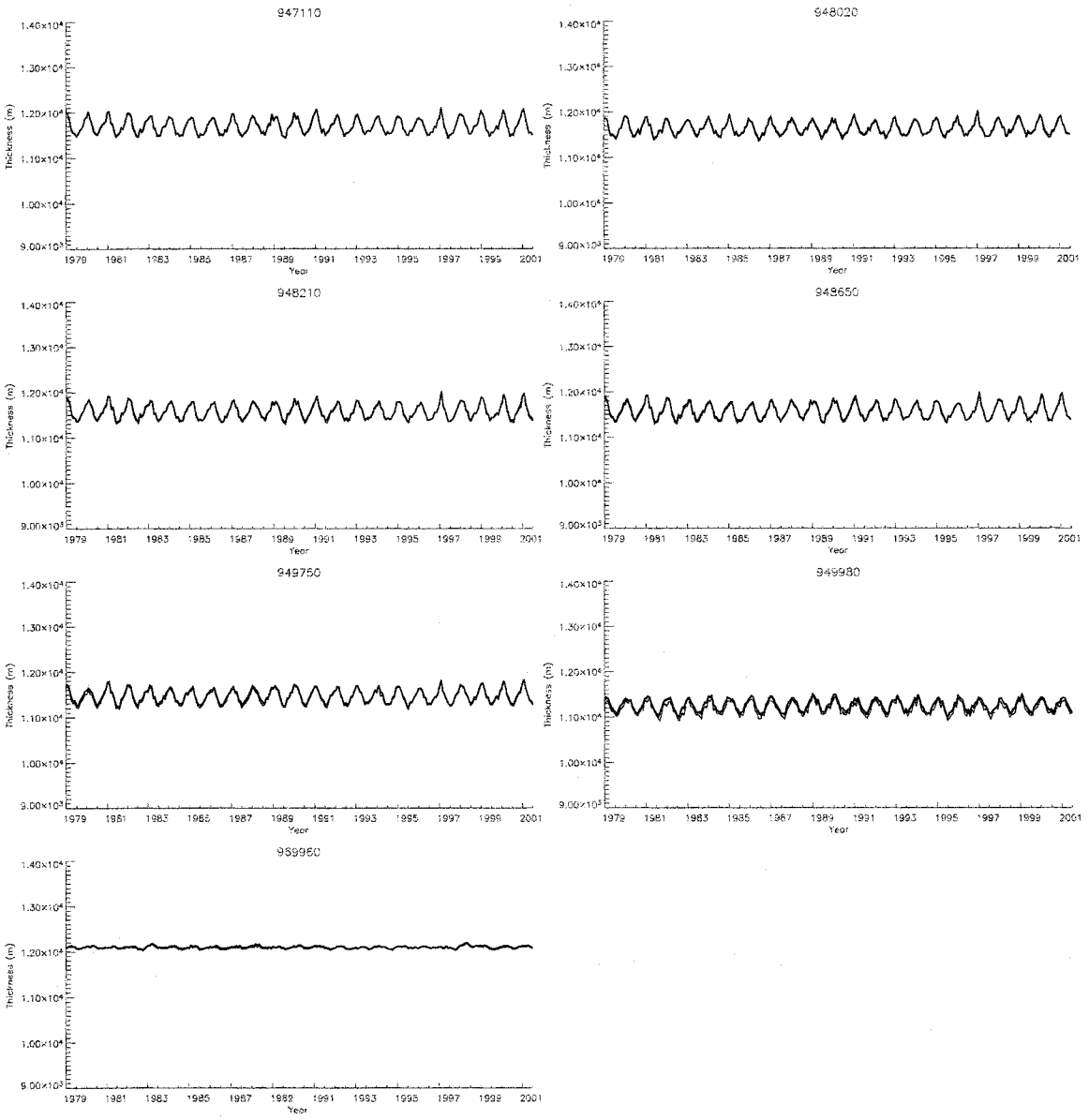

Figure C.6. (continued)

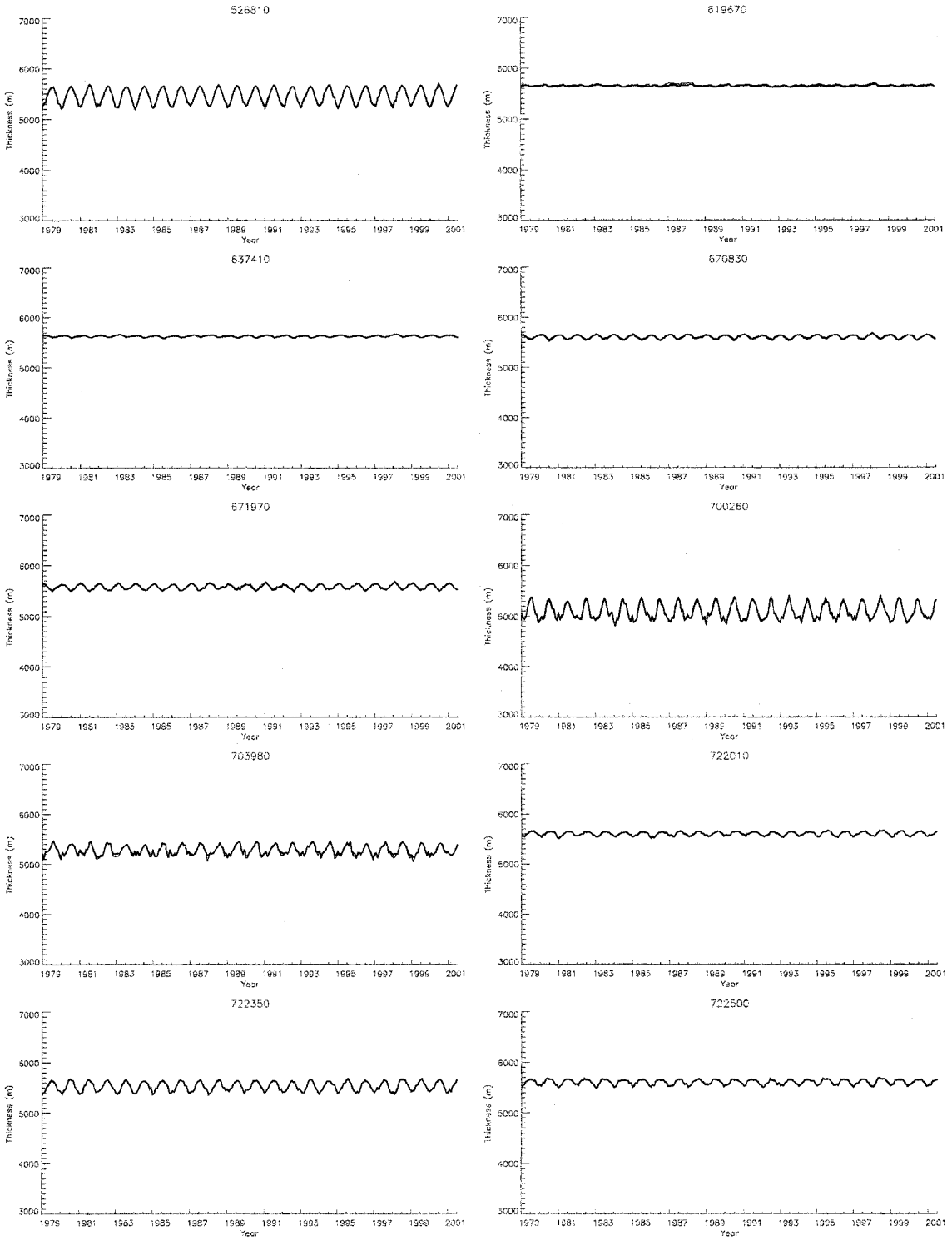

Figure C.7. Same as Figure C.6, but for the 1000-500mb layer.

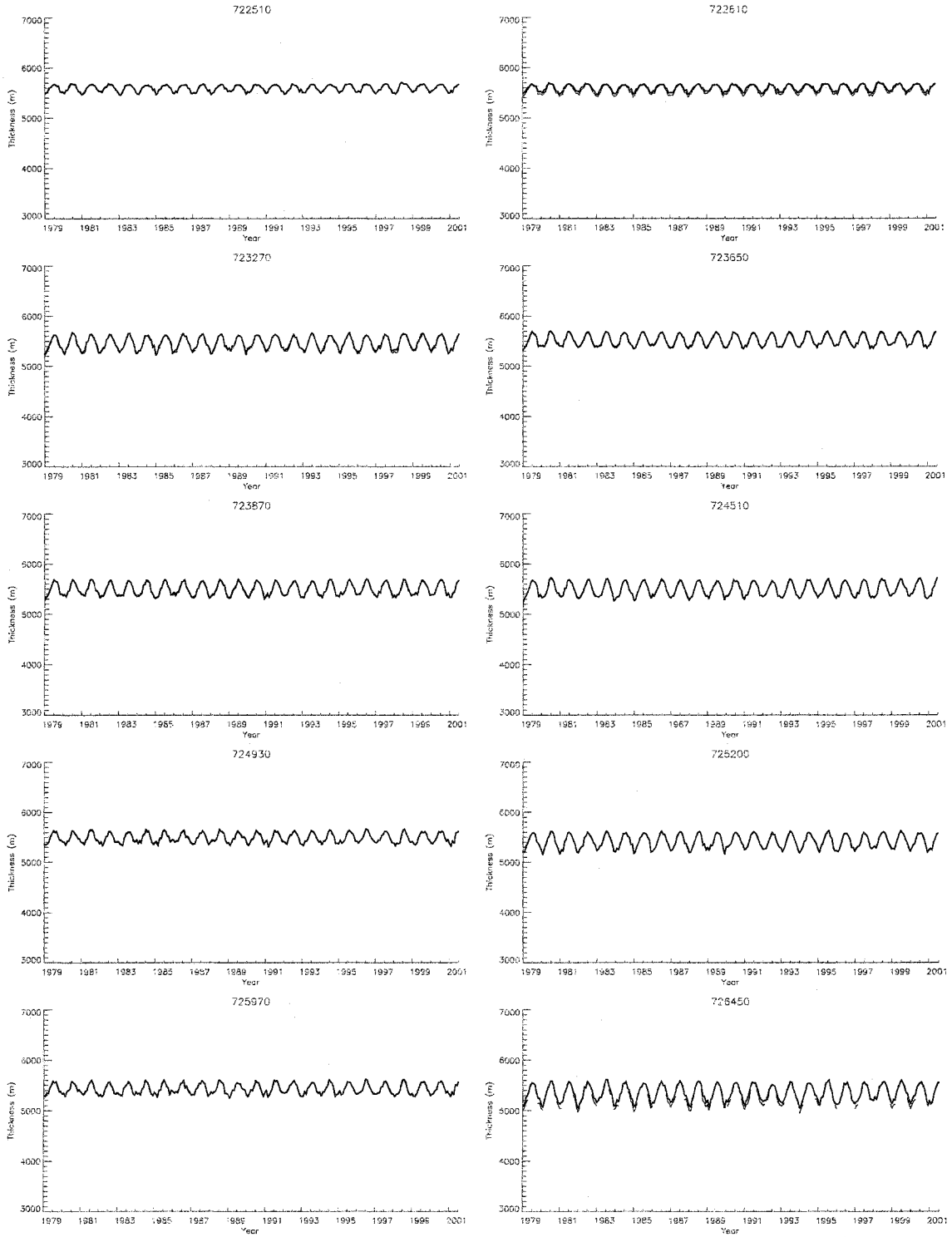

Figure C.7. (continued)

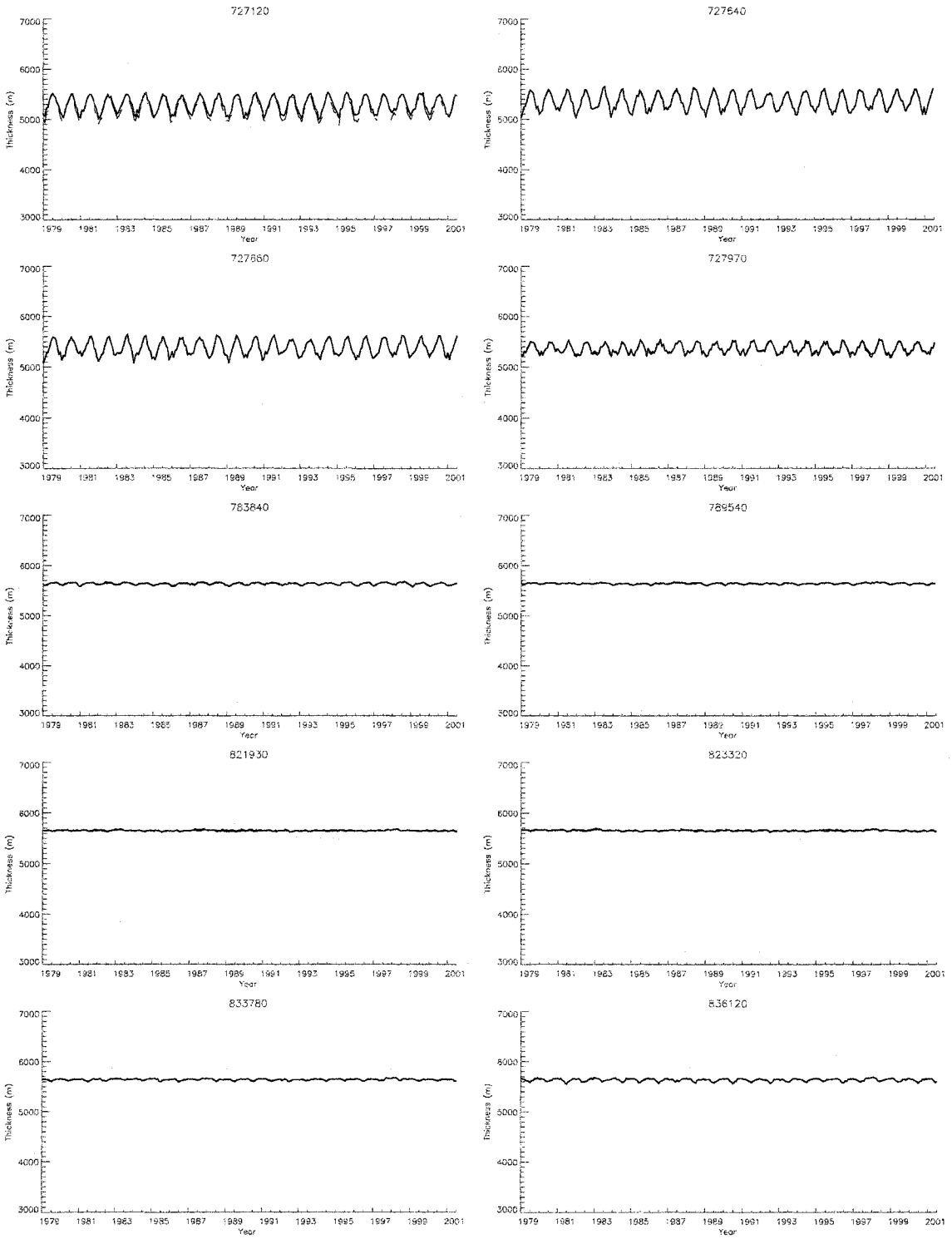

Figure C.7. (continued)

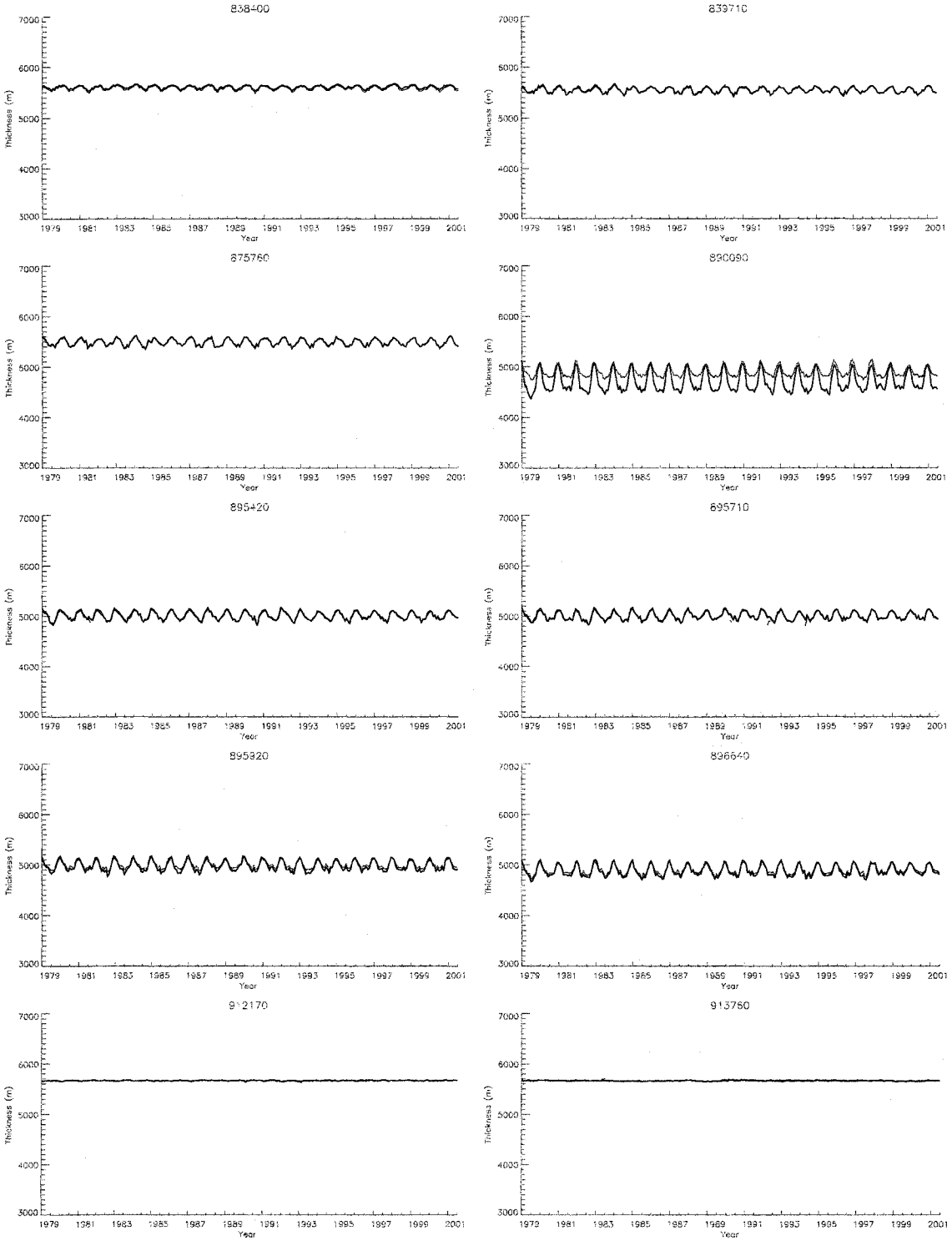

Figure C.7. (continued)

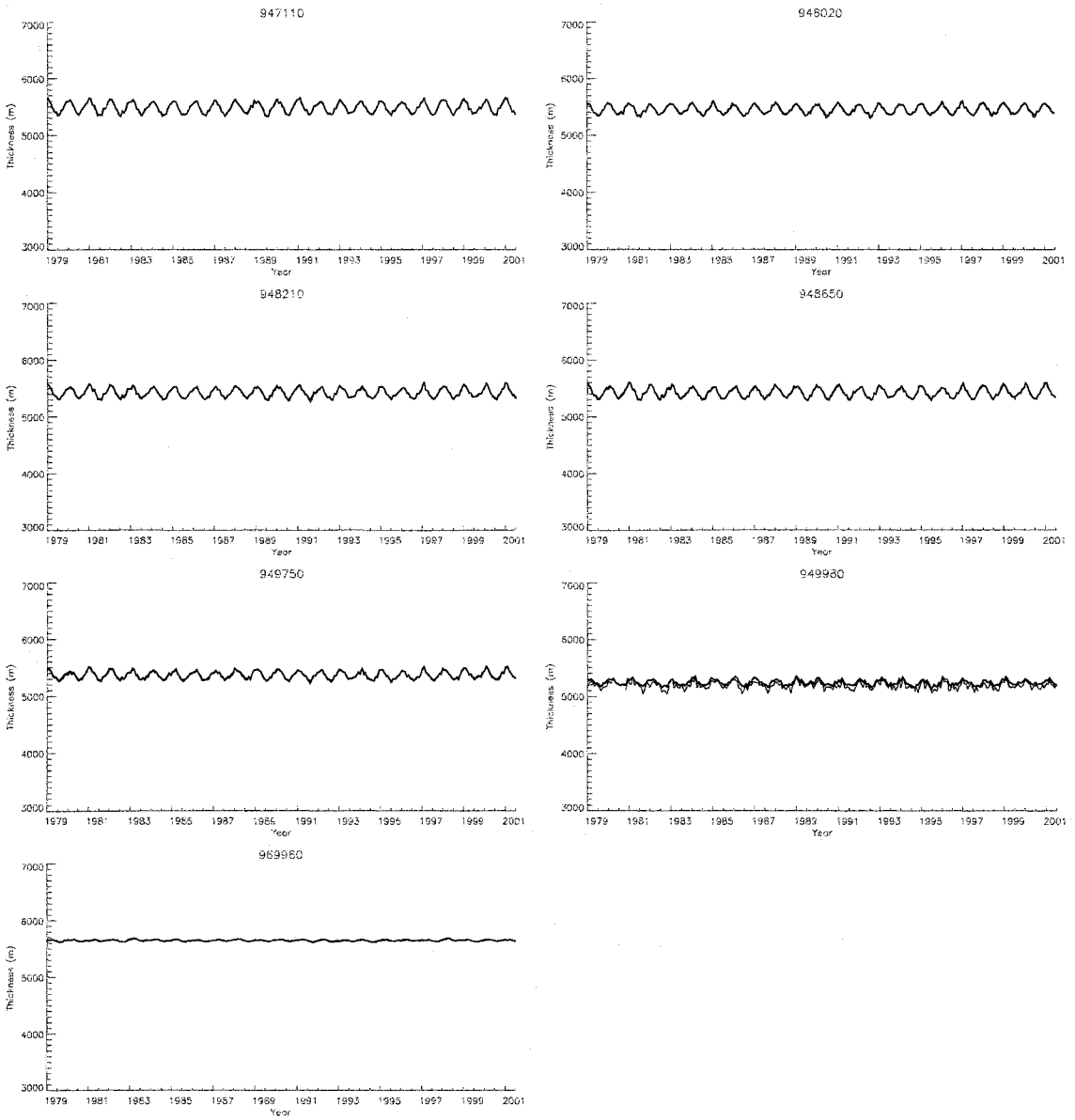

Figure C.7. (continued)

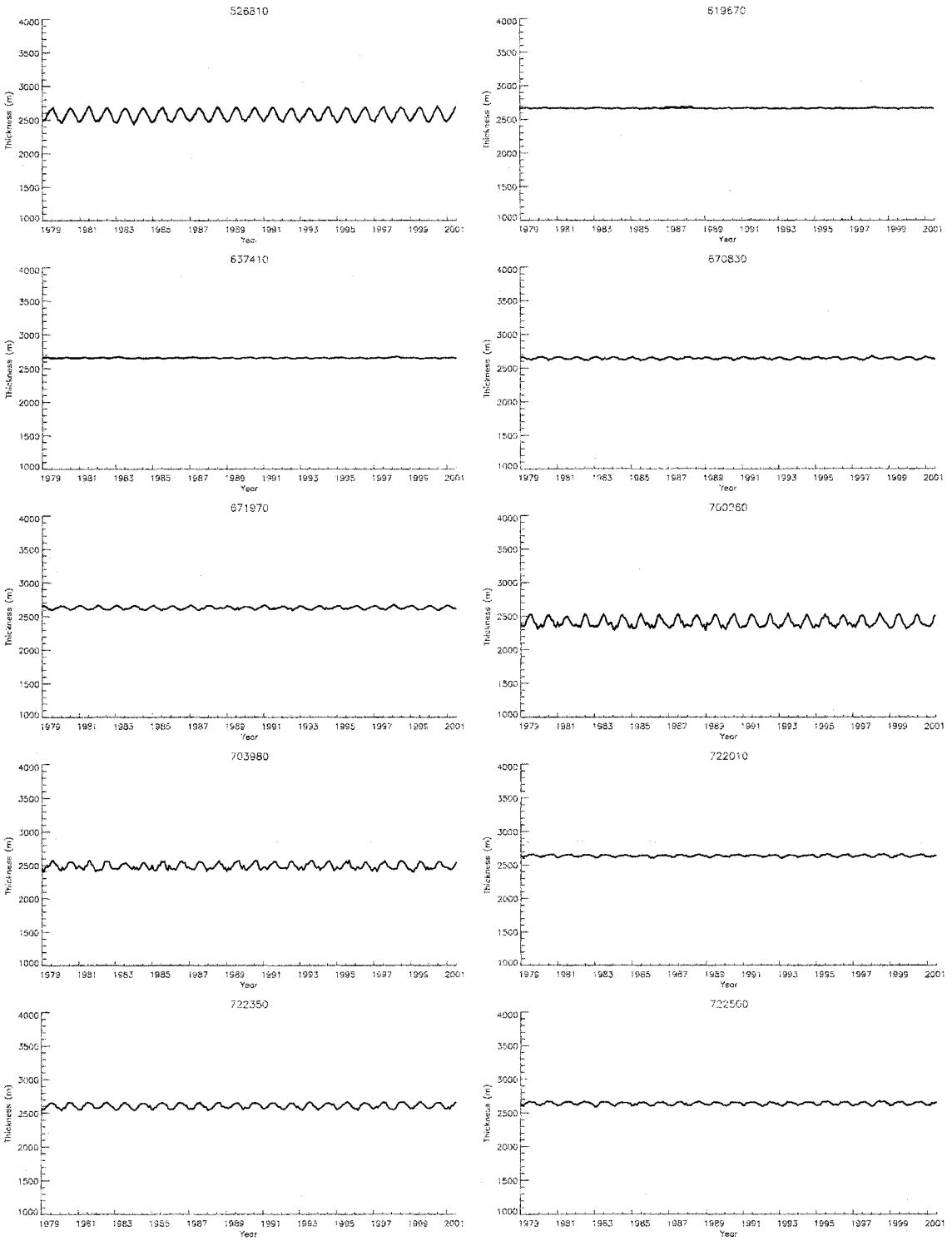

Figure C.8. Same as Figure C.6, but for the 700-500mb layer.

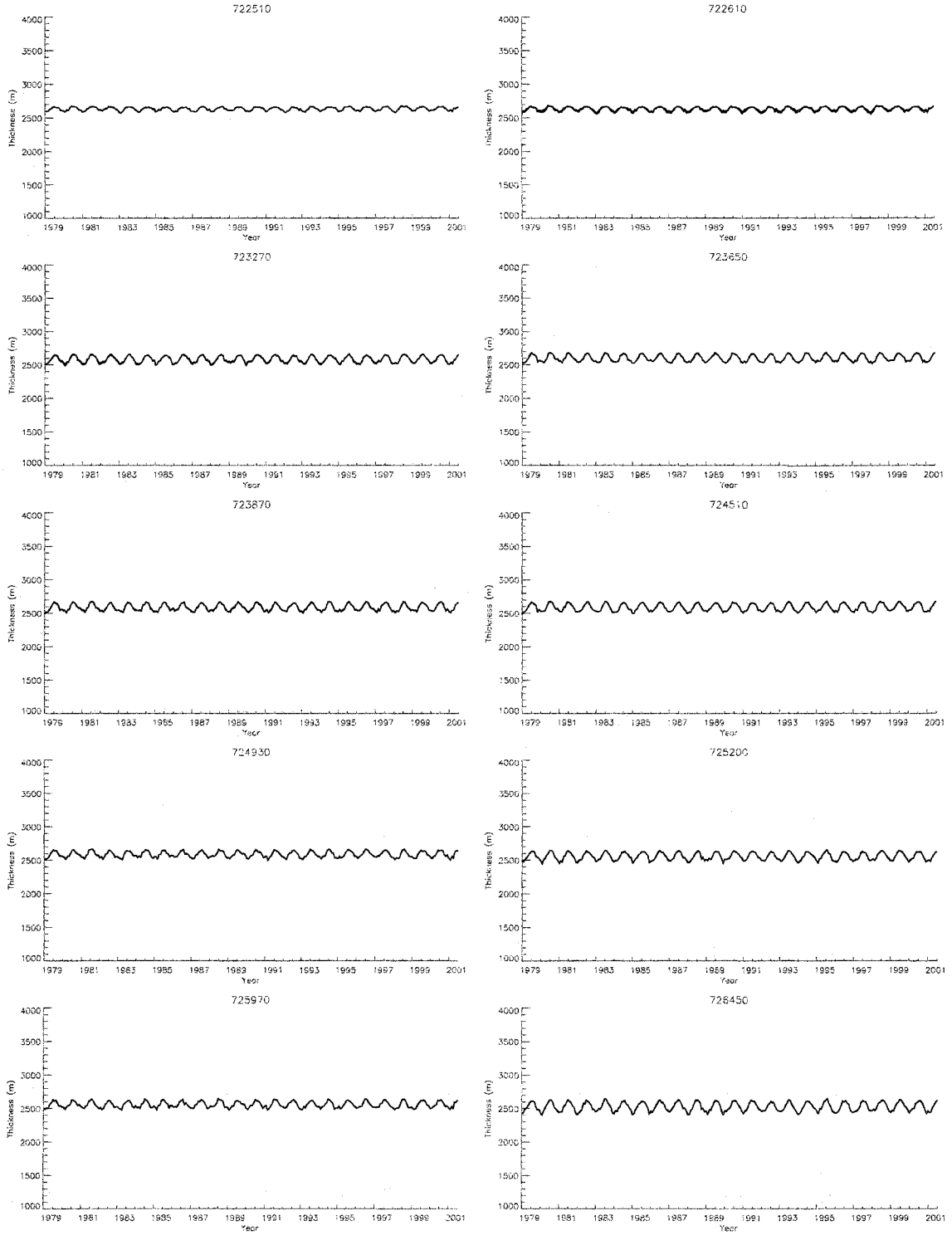

Figure C.8. (continued)

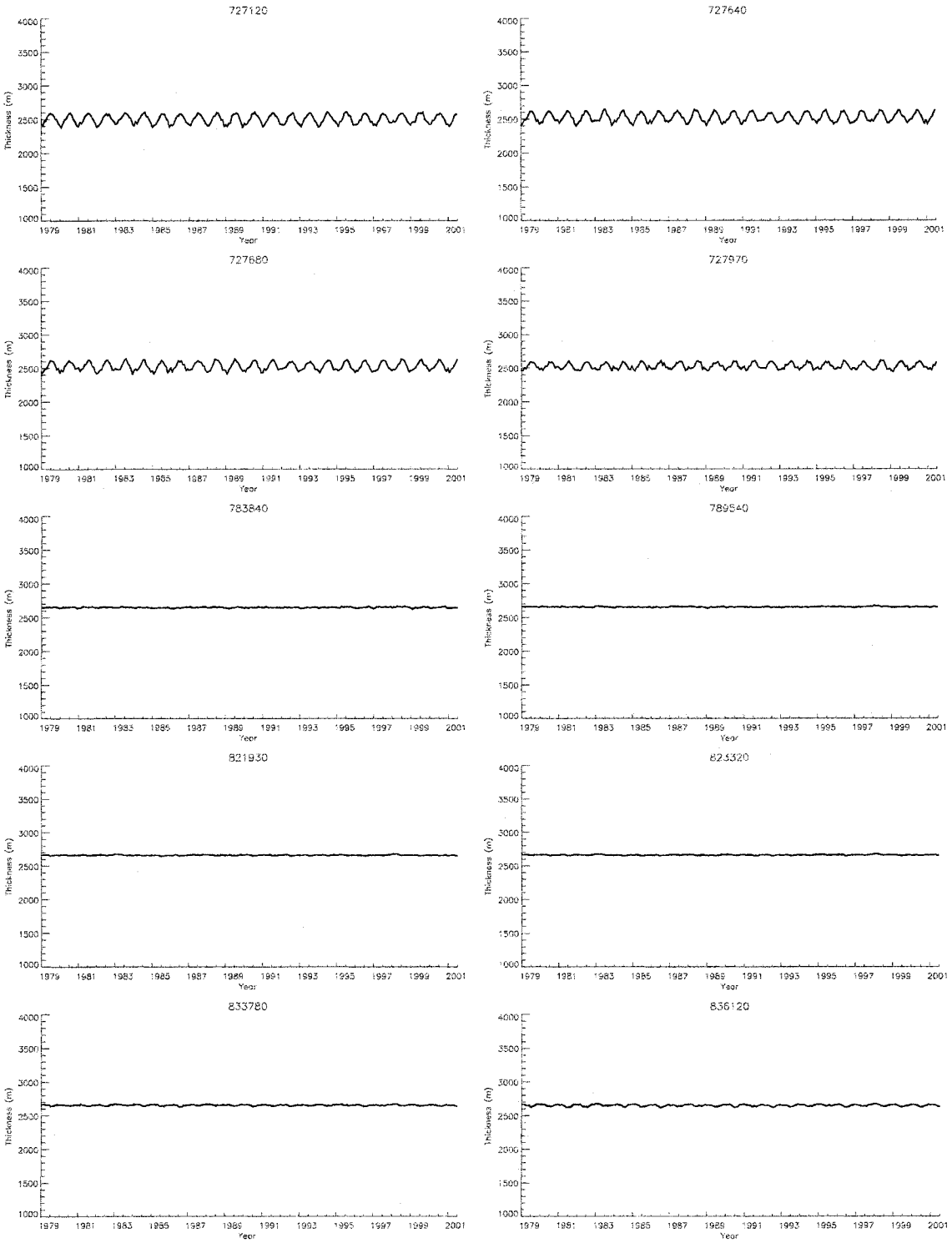

Figure C.8. (continued)

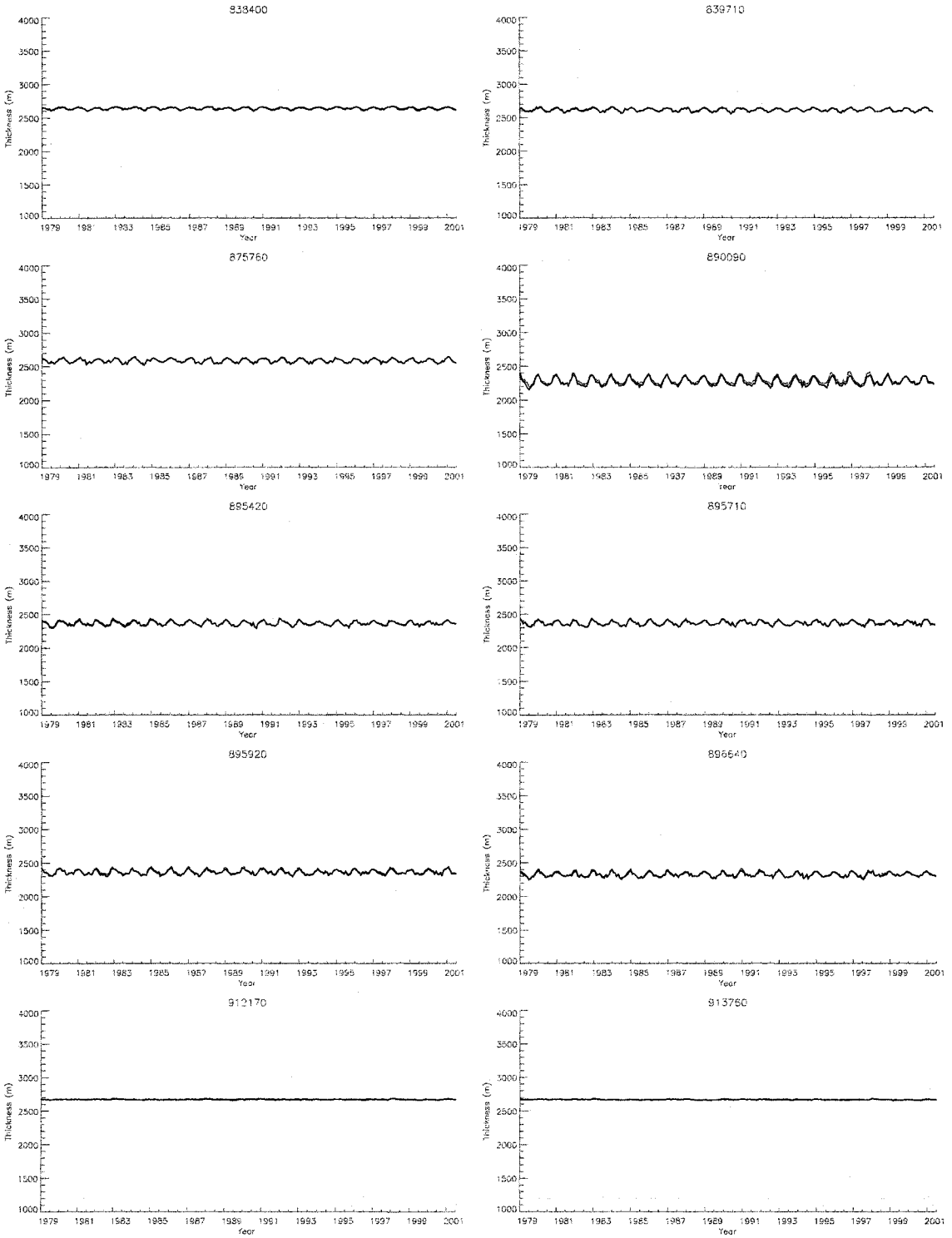

Figure C.8. (continued)

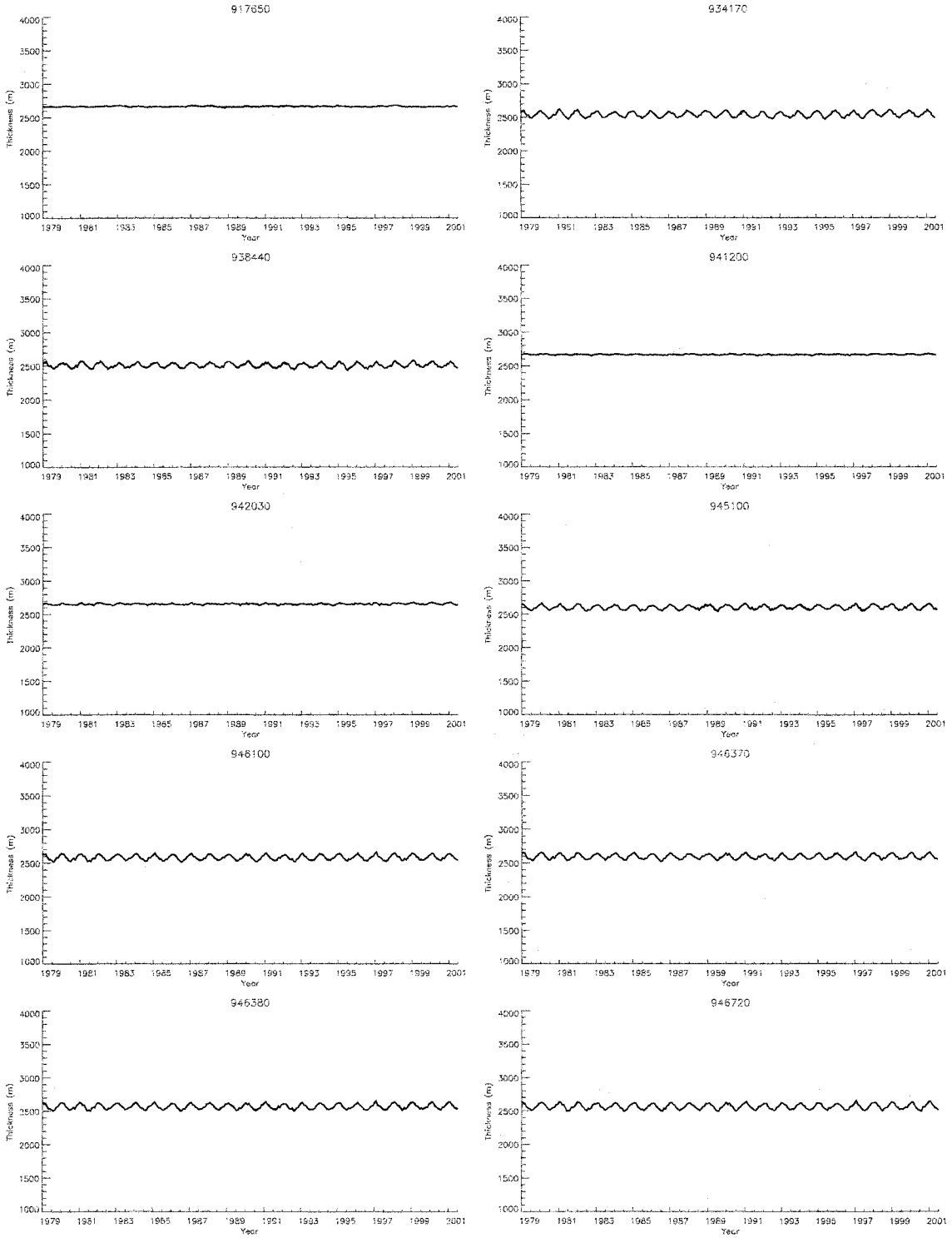

Figure C.8. (continued)

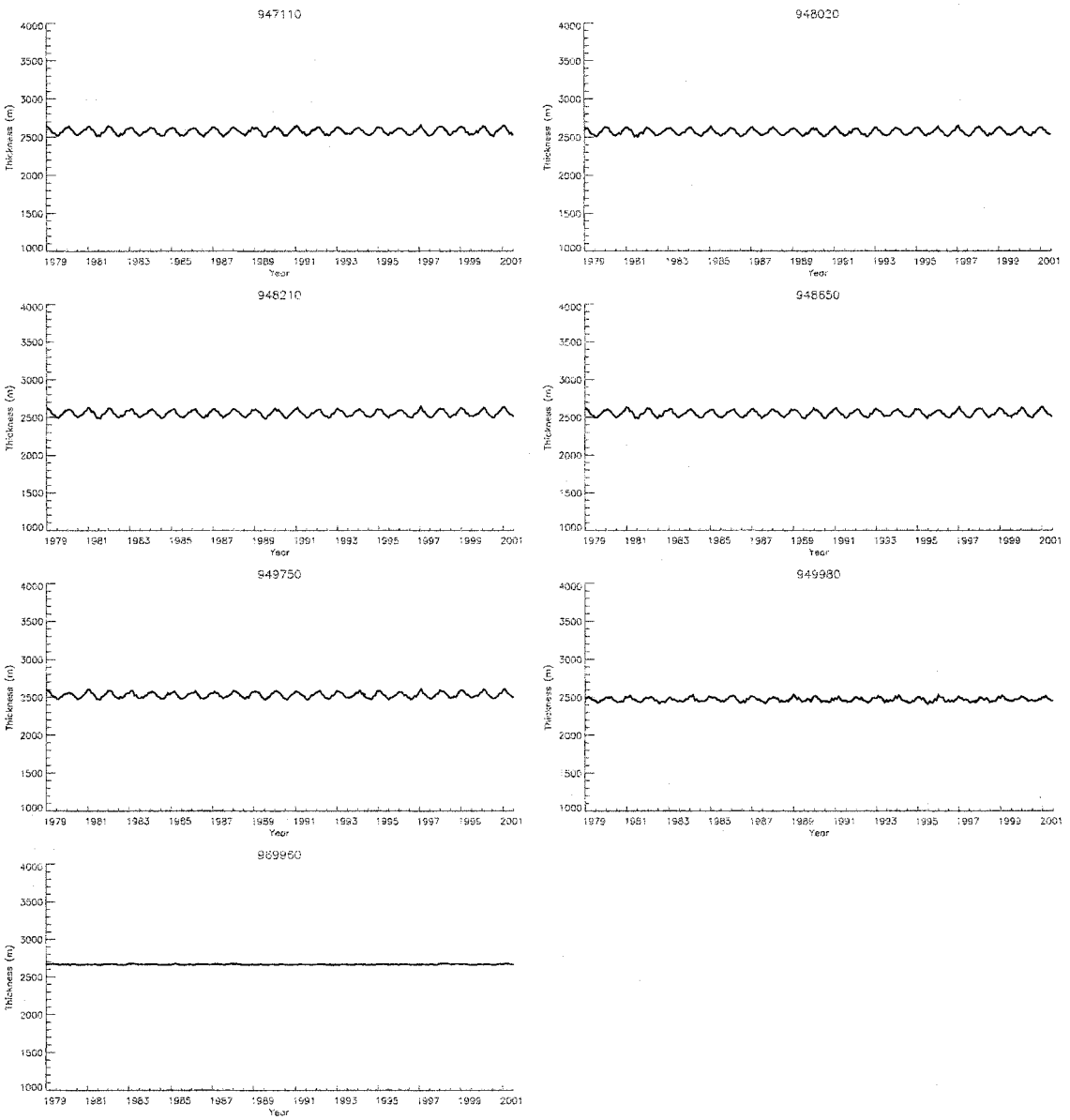

Figure C.8. (continued)